Development and application of advanced analytical strategies for understanding paracetamol metabolism and toxicity.

Thesis Submitted By:

Rebecca Dargue

For the Degree of Doctor of Philosophy of Imperial College London

Section of Integrative Systems Medicine and Digestive Diseases
Department of Surgery and Cancer
Imperial College London

Declaration of Originality

The author certifies that this thesis, and the research to which it refers are a product of their own work and that all else is appropriately referenced or acknowledged.

Copyright Declaration

The copyright of this thesis rests with the author. Unless otherwise indicated, its contents are licensed under a Creative Commons Attribution-Non-Commercial 4.0 International Licence (CC BY-NC).

Under this licence, you may copy and redistribute the material in any medium or format. You may also create and distribute modified versions of the work. This is on the condition that: you credit the author and do not use it, or any derivative works, for a commercial purpose.

When reusing or sharing this work, ensure you make the licence terms clear to others by naming the licence and linking to the licence text. Where a work has been adapted, you should indicate that the work has been changed and describe those changes.

Please seek permission from the copyright holder for uses of this work that are not included in this licence or permitted under UK Copyright Law.

Abstract

Paracetamol (*N-ac*etyl-*p*-aminophenol [APAP]) has been authorised in the United Kingdom as an analgesic and antipyretic therapy for over 60 years. When ingested at supratherapeutic doses, its hepatic metabolism is altered from a non-toxic route *via* conjugations, with sulfate or glucuronic acid, to an oxidative pathway of metabolism *via* cytochrome p450 (CYP) enzymes resulting in the formation of the reactive intermediate *N*-acetyl-*p*-benzoquinone imine (NAPQI). This reacts with glutathione (GSH), depleting this in the liver, causing APAP induced liver injury. APAP overdose is the largest cause of acute liver failure (ALF) in the UK and the second largest cause of liver transplantation world-wide. In England and Wales APAP overdose results in around 100 000 hospital admissions per year, of which 50% result in extended stays, and contributes to around 150 deaths. While improved treatments for APAP-induced liver injury are being developed, it is important to understand how to predict the severity of liver injury; to reduce unnecessary hospital stays and the number of deaths. The hypotheses for the work described below are that GSH depletion following APAP activation to NAPQI is a major route of APAP toxicity, and metabolites related to GSH biosynthesis, including 5-oxoproline (5-OP) and ophthalmic acid (OA), are circulating biomarkers for GSH depletion. In addition, APAP-glutathione conjugate (APAP-SG) and related metabolites, are predictive of liver injury. For the development of new therapies, animal models of APAP overdose are required. A detailed knowledge of the routes of APAP metabolism in these species is crucial for understanding their translation to human. Analytical methods have been developed and applied to samples from animal models and patients. Plasma/serum concentrations of 5-OP have been shown to be a promising biomarker across animal models and human patients, especially when used in combination with concentrations of alanine aminotransferase (ALT) and glutathione-derived APAP conjugates.

Acknowledgments

I would like to thank all of those involved in the supervision of my PhD for providing opportunities and advice, including Theo Dare, Andy Nicholls, Muireann Coen, and Ian Wilson.

For providing me with training and advice on LC-MS and method development, and for their invaluable contribution to the methods developed in this thesis, I would like to thank Leanne Nye and Isobelle Grant. I would also like to thank Nyasha Munjoma for his assistance with the LC-MS development.

I would like to thank ChungHo Lau and Sam Lodge for their help and assistance with ^{1}H-NMR spectroscopy, and ChungHo for his additional help with the data analysis. For her support during my time at GlaxoSmithKline, I would like to thank Tracy Walker who helped me to learn new skills in cell culture and working in an industrial environment.

For their contributions to the porcine study, I would like to thank Rabiya Zia and Hampus Andersson.

In addition, I would like to thank all of those who have been members of our 'Drug Metabolism' group who have provided support, advice and friendship; Kate, Pete, Marine, Nick, Aizat, Liza and Rabiya. (And of course, Toby Athersuch for his efforts in organising us!) And all the students on the 4th floor who have made my time at Imperial more enjoyable.

Finally, I would like to thank all my family, friends, and Matt for supporting me, and making the hard work worthwhile.

External Collaborators and Contribution of Others

The work presented in this Thesis would not have been possible without a number of external collaborators providing samples, data and expertise.

For providing the rat samples used in Chapter 2 of this Thesis for the development of the APAP method, I would like to thank Simone Stahl and the Drug Safety and Metabolism group at AstraZeneca UK.

For carrying out the animal work and collecting the clinical biochemistry and histopathology data for the research carried out in Chapter 4, I would like to thank Nathalie De-Bois Brilliant and the team at the University of Liverpool.

For the development of the Pig model described in Chapter 5, the collection of samples, data and initial help with the ^{1}H-NMR analysis, I would like to thank Karla Lee of the Royal Veterinary College. I would also like to thank Rajiv Jalan for his supervision of this study, and his team at University College London, Liver and Digestive Diseases department, The Royal Free Hospital.

Finally, for providing me with samples from the Markers and Paracetamol Poisoning study I would like to thank Nathalie, Dan Antoine, and James Dear from The University of Edinburgh.

Funding

I would like to thank the Biotechnology and Biological Sciences Research Council and GlaxoSmithKline for providing funding for this research through an iCASE studentship, and for providing the opportunity to undertake a placement with GlaxoSmithKline during the course of this research.

Contents

Abstract 3
1 Introduction 22
1.1 Aims and methods 23
1.2 APAP metabolism 23
1.2.1 APAP metabolism overview 23
1.2.2 APAP metabolism and toxicity 25
1.2.3 Species and individual differences in APAP metabolism and toxicity 27
1.3 GSH related metabolism 30
1.3.1 GSH biosynthesis and the γ-glutamyl cycle 30
1.3.2 The methionine cycle and the trans-sulfuration pathway 32
1.4 Biomarkers for APAP induced liver injury and general hepatic GSH depletion 36
1.4.1 Current biomarkers 36
1.4.2 New biomarkers for APAP induced liver injury 37
1.4.3 5-Oxoproline and ophthalmic acid as potential biomarkers 38
1.5 Methodology 39
1.5.1 NMR spectroscopy 39
1.5.2 UHPLC-MS/MS 40
1.6 Summary 43
2 Development of a UHPLC-MS/MS method for the analysis of paracetamol and seven metabolites in rat, pig, mouse and human plasma or serum. 45
2.1 Introduction 46
2.1.1 Hypothesis 46
2.1.2 Rationale and aims 46
2.1.3 Background 46
2.2 Methods 48
2.2.1 Chemicals and reagents used throughout experiment 48
2.2.2 Chromatography 49
2.2.3 Mass spectrometry 50
2.2.4 Method validation 51
2.2.5 Method validation in rat plasma 54
2.2.6 Addition of PAP-G and alterations for method application to porcine plasma 60
2.2.7 Cross validation to human plasma 63
2.2.8 Cross validation to mouse serum 63
2.3 Results 66
2.3.1 Rat plasma validation results 66

2.3.2 Porcine plasma validation results 75
2.3.3 Mouse serum validation results 78
2.3.4 Human plasma validation results 80
2.3.5 Determination of paracetamol and metabolites in plasma following oral administration to the rat 82
2.4 Discussion 87
2.4.1 Conclusions 89
3 A UHPLC-MS/MS method for quantifying and semi-quantifying glutathione biosynthesis related metabolites. 90
3.1 Introduction 91
3.1.1 Hypothesis 91
3.1.2 Aims 91
3.1.3 Background and rationale 92
3.2 Materials and methods 95
3.2.1 Materials 95
3.2.2 Mass spectrometry 96
3.2.3 Chromatography 98
3.2.4 Preparation of samples for mouse serum validation 99
3.3 Cross validation to human serum 102
3.3.1 Preparation of QCs for matrix factor and recovery determination 103
3.4 Results 106
3.4.1 Chromatography of IS in mouse serum validation 106
3.4.2 Matrix factor, recovery and sample preparation effects in mouse serum. 109
3.4.3 Chromatography in human serum 114
3.4.4 Matrix factor and extraction recovery in human serum 116
3.5 Discussion 121
3.5.1 Results summary 121
3.5.2 Discussion of results 125
3.5.3 Conclusions and future work 127
4 Application of UHPLC-MS/MS assays to mouse serum and liver samples in order to determine APAP metabolism and changes in glutathione metabolism. 128
4.1 Introduction 129
4.1.1 Hypotheses 129
4.1.2 Aims 129
4.1.3 Background 130
4.2 Materials and methods 133

4.2.1 Contribution of others 133
4.2.2 Mouse study 133
4.2.3 Preparation of tissue samples for UHPLC-MS/MS 133
4.2.4 Glutathione pathway UHPLC-MS/MS assay 134
4.2.5 GSH assay sample preparation in serum 137
4.2.6 APAP method sample preparation. 140
4.2.7 Data analysis and run acceptance 144
4.2.8 Statistical analysis 145
4.3 Results 146
4.3.1 Clinical chemistry and biomarkers 146
4.3.2 Circulating metabolites 148
4.3.3 Hepatic metabolism 158
4.4 Discussion 171
4.4.1 Key findings 171
4.4.2 Summary of results 172
4.4.3 GSH assay discussion 174
4.4.4 APAP metabolism discussion 175
4.4.5 Conclusions and future work 176
5 APAP metabolism and related toxicity in a porcine model of acute liver failure 178
5.1 Introduction 179
5.1.1 Hypotheses 179
5.1.2 Aims 179
5.1.3 Background and rationale 179
5.2 Materials and methods 181
5.2.1 Animal model and study design 181
5.2.2 ^{1}H-NMR spectroscopy of aqueous tissue extracts, plasma and urine 184
5.2.3 ^{1}H-NMR spectral data processing 186
5.2.4 APAP UHPLC-MS/MS method analysis of plasma 188
5.2.5 Glutathione pathway UHPLC-MS/MS method analysis of plasma 190
5.2.6 Univariate statistical analysis 192
5.3 Results 192
5.3.1 Survival, histopathological and biochemical characterisation of the model 192
5.3.2 APAP metabolism 203
5.3.3 Endogenous metabolism changes 204
5.3.4 UHPLC-MS/MS analysis of plasma samples 212
5.4 Discussion 217

5.4.1 Endogenous metabolite changes measured by NMR spectroscopy 217
5.4.2 GSH metabolism changes measured by UHPL-MS/MS 218
5.4.3 APAP metabolism and its relation to toxicity in the pig 219
5.4.4 Conclusions 223
6 Application of UHPLC-MS/MS assays to serum from APAP overdose patients for identification of circulating biomarkers of glutathione depletion 224
6.1 Introduction 225
6.1.1 Hypothesis 225
6.1.2 Aims 225
6.1.3 Background and rationale 226
6.2 Methods 227
6.2.1 Study design and group selection 227
6.2.2 Materials for UHPLC-MS/MS 231
6.2.3 GSH UHPLC-MS/MS method and sample preparation 231
6.2.4 APAP UHPLC-MS/MS method and sample preparation 233
6.2.5 Statistics 233
6.3 Results 233
6.3.1 GSH method overview 233
6.3.2 APAP method overview 236
6.3.3 APAP metabolism 237
6.3.4 Predictivity of suggested biomarkers 241
6.4 Discussion 242
6.4.1 GSH metabolism changes summary 242
6.4.2 APAP metabolism changes summary 242
6.4.3 Discussion of results 243
6.4.4 Conclusions, limitations and future directions 244
7 Conclusions 247
7.1 Key hypotheses and aims 248
7.2 Summary of key findings 249
7.3 Study Limitations 250
7.3.1 Methodological limitations 250
7.3.2 Study design and sample collection 251
7.4 Future Work 252
7.4.1 Method development and validation 252
7.4.2 Understanding APAP toxicity and sulfur depletion more broadly 252
7.5 Conclusions 254

8 References and bibliography 255

List of Figures

Figure 1.1 Overview of the analytical strategies developed and their application to animal models or clinical samples listed by chapter. 23
Figure 1.2 overview of some of the major routes of APAP metabolism in humans and preclinical species. 27
Figure 1.3 The γ-glutamyl cycle 30
Figure 1.4 Summary of cysteine biosynthesis from methionine via the methionine cycle and trans-sulfuration pathway. 34
Figure 1.5 Summary of the hepatic biosynthesis of taurine from cysteine. 36
Figure 1.6 Overview of key events in APAP metabolism and toxicity, and the approach of the research presented in this Thesis to find potential biomarkers of APAP induced liver injury 44
Figure 2.1 A reconstructed ion chromatogram for all standards following spiking into plasma, extracted with MeOH (+ 0.1% FA), and diluted with H_2O (+ 0.1% FA) obtained using the optimised chromatographic system, all normalised to the highest peak. 50
Figure 2.2 Summary of sample preparation for all sample types including the double blank, standard curve and QC samples, the single blank used for the standard curve containing only the internal standards.[a]35µL added to standard/QC; 85 µL added to single blank and samples; 95 µL added to double blank. Abbreviations: DB: double blank; FA: formic acid; IS: internal standard; SB: single blank; QC: quality control 59
Figure 2.3 Plasma concentration data for APAP, APAP-G and APAP-S, obtained pre-dose and at various time points post-dose up to 24 h, for rats administered APAP at either 500 or 1500 mg/kg (based on the analysis of 5 µL of sample). Each point represents an individual animal, boxes represent the median and interquartile range and whiskers show the full range. 84
Figure 2.4 Plasma concentration data for the APAP-C (upper), APAP-NAC (middle) and APAP-SG (lower) conjugates, at various time points post-dose, in samples obtained from rats administered APAP at either 500 or 1500 mg/kg(based on analysis of 5 µL of sample.) Each point represents data from one animal, boxes represent the median and interquartile range. Abbreviations: APAP-C: paracetamol cysteinyl conjugate; APAP-NAC: paracetamol n-acetyl-cysteine conjugate; APAP-SG: paracetamol glutathione conjugate. 85
Figure 2.5 A) Representative chromatograms for samples from the 500mg/kg APAP dose group 1 hr post dose or B) 24hr post dose. Some chromatographic peaks have been increased in intensity in some cases for clarity (as indicated by the numbers in parenthesis above the peaks.) All chromatographic peak intensities are relative to APAP in Figure 2.5A. 86
Figure 3.1 The key components of metabolites related to glutathione metabolism, including the components of the methionine cycle, trans-sulfuration pathway and gamma-glutamyl cycle. The metabolites highlighted in red are included in the method. 95
Figure 3.2 Summary of total ion chromatograms for standards measured in matrix free samples, normalised to the highest peak. 99
Figure 3.3 Flow chart to show how each of the 4 sample types for the mouse serum validation was prepared. 101
Figure 3.4 Flow chart of preparation of samples for human serum matrix effects and recovery calculations 103
Figure 3.5 Total ion chromatogram normalised to the highest peak in each figure, of each of the IS's spiked into a sample at the HQC concentration measured in A) a matrix free sample and B) a mouse serum sample, spiked before extraction 107

Figure 3.6. Relative total ion chromatograms of choline-d4 in High quality control sample 1, all normalised to the highest peak (3). 108
Figure 3.7 Total ion chromatogram normalised to the highest peak in each figure, of each IS measured in A) a matrix free sample at the HQC concentration level and B) spiked into human serum samples before extraction. 115
Figure 4.1 Overview of study design and summary of sample types and techniques applied in this chapter. 132
Figure 4.2 Clinical chemistry measurements analysed by One-way ANOVA, FDR corrected p values (q), q<0.03 (*), q<0.002 (**), q<0.0002 (***), q<0.0001 (****) 148
Figure 4.3. Concentrations of APAP and metabolites measured in serum samples from mice treated with APAP at 300mg/kg i.p. or with APAP followed by NAC. Analysed by Kruskal-Wallis of three groups followed by FDR correction, adjusted p values 0.03 (*), 0.002 (**), 0.0002 152
Figure 4.4 GSH-related metabolites measured in serum from mice treated with APAP, Vehicle or APAP+ NAC and sacrificed at time points from 3 to 96 hours post APAP treatment. Analysed by one-way ANOVA followed by FDR correction, adjusted p (q) values, adjusted p values 0.03 (*), 0.002 (**), 0.0002 (***), <0.0001 (****). Abbreviations: APAP: paracetamol; GSH: reduced glutathione; NAC: n-acetylcysteine. 156
Figure 4.5. Concentrations of APAP and metabolites measured in dried hepatic extracts from mice treated with APAP at 300mg/kg ip or with APAP followed by NAC. 160
Figure 4.6. Concentrations of A) Pooled QCs and B) Over-spiked QCs for analytes measured against the “High” curve, which were analysed at regular intervals throughout the run (n=6) 164
Figure 4.7. Concentrations of A) Pooled QCs and B) Over-spiked QCs for analytes measured against the “Mid” curve, which were analysed at regular intervals throughout the run (n=6) 165
Figure 4.8. Concentrations of A) Pooled QCs and B) Over-spiked QCs for analytes measured against the “low” curve, which were analysed at regular intervals throughout the run (n=6) 166
Figure 4.9. Metabolites measured in liver extracts from mice treated with APAP, Vehicle or APAP + NAC and sacrificed at time points from 3 to 96 hours post treatment. Time-points with 2 groups analysed by one-way ANOVA followed by FDR correction, adjusted p values 0.03 (*), 0.002 (**), 0.0002 (***), <0.0001 (****). Abbreviations: APAP: paracetamol; γ-glu-cys: gamma-glutamyl cysteine; GSH: reduced glutathione; NAC: n-acetylcysteine. 169
Figure 4.10. Each point on the plots A & C represents a mouse and is coloured according to treatment and labelled with the time point of sampling, each point on plots B & D represents a metabolite. A) PCA scores plot and B) Loadings plot for all metabolites measured in liver extracts. C) PCA scores plot and B) Loadings plot for all metabolites measured in hepatic extracts at 3 and 6 hours only. 170
Figure 4.11. Overview of the GSH metabolism pathway and the metabolism changes seen following APAP treatment at early time points (3-6h.) 175
Figure 5.1 Overview of study design, timings and sampling as undertaken by external collaborators at University College London, prior to sample shipping to Imperial College London for analysis. 183
Figure 5.2 Overview of sample preparation and analysis for 1H-NMR spectroscopy. 184
Figure 5.3 Representative figure of STOCSY driven from PAP-G labelled above 187
Figure 5.4 Overlaid spectra of a plasma sample analysed before and after addition of PAP-G standard. Original spectrum in red, PAP-G-spiked plasma represented by blue spectrum. 187
Figure 5.5 Summary of parameters measured to characterise the ALF model. 195
Figure 5.6 Representative 1H-NMR spectra of porcine plasma at the ALF timepoint in an APAP treated and Control animal with key endogenous and drug metabolite resonances labelled. 197
Figure 5.7 Representative 1H-NMR spectra of porcine urine at the ALF timepoint in an APAP treated and Control animal with key endogenous and drug metabolite resonances labelled. 198

Figure 5.8 Representative 1H-NMR spectra of porcine liver at the ALF timepoint in an APAP treated and Control animal with key endogenous and drug metabolite resonances labelled. 199
Figure 5.9 Representative 1H-NMR spectra of porcine kidney extracts at the ALF timepoint in an APAP treated and Control animal with key endogenous and drug metabolite resonances labelled. Abbreviations: ALF: acute liver failure; APAP: paracetamol; APAP-G: paracetamol glucuronide; NMR: nuclear magnetic resonance; PAP-G: p-aminophenol glucuronide; ppm: parts per million; TMAO; trimethylamine N-oxide. 200
Figure 5.10 APAP and metabolites measured by ^{1}H-NMR spectroscopy in biofluids and tissue extracts. A) Plasma: median concentration and interquartile range of APAP and 2 metabolites identified in plasma over the time course of the experiment (n=18). 204
Figure 5.11 Endogenous metabolism changes in plasma. Kruskal-Wallis with FDR corrected multiple comparisons. * q<0.05. Abbreviations: ALF: acute liver failure; APAP: paracetamol; AU: arbitrary units; FDR: false discovery rate. 206
Figure 5.12 Endogenous metabolism changes in urine. Kruskal-Wallis with FDR corrected multiple comparisons. * q<0.05. Red colour represents final time point for that animal prior to ALF or prior to death. Abbreviations: ALF: acute liver failure; APAP: paracetamol; AU: arbitrary units; FDR: false discovery rate; TMAO: trimethylamine N-oxide. 208
Figure 5.13 Endogenous metabolism changes in liver extracts from pigs treated with paracetamol, at 0 h, 12 h and post-mortem. Kruskal-Wallis with FDR corrected multiple comparisons. * q<0.05. Abbreviations: AU: arbitrary units; FDR: false discovery rate; PM: post-mortem. 209
Figure 5.14 Significant changes to endogenous metabolites in kidney extracts from pigs treated with paracetamol, at 0 h and post-mortem. Mann-Whitney **p<0.01 ***p<0.001 Abbreviations: APAP: paracetamol; AU: arbitrary units; PM: post-mortem; TMAO: trimethylamine N-oxide. 210
Figure 5.15 Representative total ion chromatogram of APAP metabolites in porcine plasma after 4 hours of dosing. Abbreviations: APAP: paracetamol; APAP-C: paracetamol cysteinyl conjugate; APAP-G: paracetamol glucuronide; APAP-S: paracetamol sulfate; APAP-SG: paracetamol glutathione conjugate; PAP-G: p-aminophenol glucuronide. 212
Figure 5.16 Metabolites quantified in plasma using the UHPLC-MS/MS method. 213
Figure 5.17 GSH metabolites measured in porcine plasma. Data were log transformed and analysed by One-Way ANOVA with FDR corrected multiple comparisons. q<0.03(*), q<0.002 (**), q<0.0001 (***), q<0.0001(****). Abbreviations: ALF: acute liver failure; APAP: paracetamol; FDR: false discovery rate; 5-OP: 5-oxoproline; SAM: s-adenosyl methionine. 216
Figure 5.18 Diagram showing the key components of the TCA cycle within the mitochondria some of which were seen to change in one or more of the matrices and biofluids we investigated, including plasma, urine, liver and kidney extracts. The TCA cycle components have been colour coded to show in which of the matrices these components were increased in as per the key within the figure. Abbreviations: TCA: tricarboxylic acid. 218
Figure 5.19 Proposed mechanism of APAP metabolism in the pig including the formation of PAP-G from PAP and the potential mechanism of metHb formation by PAP in red blood cells, and the formation of a PAP-GSH conjugate which may have a role in nephrotoxicity. Abbreviations: APAP: paracetamol; APAP-C: paracetamol cysteinyl conjugate; APAP-G: paracetamol glucuronide conjugate ; APAP-NAC: paracetamol n-acetyl-cysteine conjugate; APAP-OMe: 3-methoxy paracetamol; APAP-S : paracetamol sulfate conjugate; APAP-SG: Paracetamol glutathione conjugate; BQI: benzoquinone imine; CES: Carboxyl esterase; CYP: Cytochrome p-450; MetHb: methaemoglobin; NAPQI: n-acetyl-p-benzoquinone imine; NAT: n-acetyl transferase; PAP: p-aminophenol; PAP-G: p-aminophenol glucuronide; PAP-SG: p-aminophenol glutathione conjugate; SULTs: sulfotransferase enzymes; UGT: UDP-glucuronosyl transferase 220

Figure 6.1 Summary of definitions for groups of patients in the sub-set of patients sampled for application of the paracetamol and glutathione pathway assays. Abbreviations: ALT: alanine aminotransferase; INR: international normalised ratio; NAC: n-acetylcysteine. 229
Figure 6.2 A) differences in 5-OP concentrations in groups 1-3. Analysed using ANOVA and FDR multiple comparisons, **=p<0.002. B) Scatter plot of 5-OP vs. Peak ALT with fitted linear regression. 237
Figure 6.3 Differences in log transformed APAP metabolite concentrations in Groups 1-3. Analysed using ANOVA and FDR multiple comparisons p<0.03 (*), p<0.002 (**), p<0.0002 (***), p<0.0001 (****) 238
Figure 6.4 Differences in log transformed APAP metabolite concentrations as a proportion of total metabolites in Groups 1-3. Analysed using ANOVA and FDR multiple comparisons p<0.03 (*), p<0.002 (**), p<0.0002 (***), p<0.0001 (****) 239
Figure 6.5 Differences in log transformed APAP-C and total APAP-CYP as a proportion of APAP-S in Groups 1-3. Analysed using Kruskal-Wallis and FDR multiple comparisons p<0.03 (*), p<0.002 (**), p<0.0002 (***), p<0.0001 (****) Abbreviations: ANOVA: Analysis of variance; APAP-C: paracetamol-cysteinyl conjugate; APAP-CYP: paracetamol conjugates formed by cytochrome p450 metabolism; APAP-S: paracetamol sulfate FDR: false discovery rate. 240
Figure 6.6 Scatter plots of A) APAP-CYP as a proportion of Total APAP and B) APAP-C as a proportion of APAP-S, with Peak ALT, fitted with a linear regression. Abbreviations: ALT: alanine aminotransferase; APAP-C: paracetamol-cysteinyl conjugate; APAP-CYP: paracetamol conjugates formed by cytochrome p450 metabolism; APAP-S: paracetamol sulfate. 241

List of Tables

Table 2.1 Salt Conversion Factors for analytical standards and internal standards. 48
Table 2.2 Chromatographic gradient for separation of metabolites 49
Table 2.3 Mass spectrometry and liquid chromatography data for APAP and metabolites quantified 51
Table 2.4 Preparation of stock solutions A and B for rat plasma validation. 56
Table 2.5. Preparation of calibration curve standard solutions through serial dilution of stock solution B for rat plasma validation. 56
Table 2.6 Preparation of QC standard stock solutions through serial dilution of stock solution B 57
Table 2.7 Preparation of internal standard stock solution for rat plasma validation 58
Table 2.8 Calibration curve concentrations for the standards used for the analysis of APAP and metabolites in rat plasma by UHPLC-MS/MS[a] 60
Table 2.9 Concentrations of quality control samples for the analysis of APAP and metabolites in rat plasma by UHPLC-MS/MS[a] 60
Table 2.10 Preparation of standard stock solutions A and B for porcine plasma cross-validation. 62
Table 2.11 The final calibration range for all analytes for porcine plasma cross-validation. 62
Table 2.12 The final concentration of quality control samples for porcine plasma cross-validation 63
Table 2.13 Preparation of standard stock solutions A and B for mouse serum cross-validation. 64
Table 2.14 Calibration ranges used for mouse serum cross-validation 64
Table 2.15 Quality control concentration levels for mouse serum cross-validation 65
Table 2.16 Internal standard stock solution preparation for mouse serum validation 65
Table 2.17 Linearity of the standard curves for each compound for each day of the validation in rat plasma. 66
Table 2.18 Summary of the inter-day coefficient of variance for rat plasma validation 67
Table 2.19 Summary of the inter-day mean bias for rat plasma validation 67
Table 2.20 Summary of the intra-day coefficient of variance of the quality control samples in the rat plasma validation[a] 68
Table 2.21 Summary of the intra-day mean bias of the quality control samples in the rat plasma validation[a] 68
Table 2.22 Carryover for all analytes measured during validation for rat plasma. 69
Table 2.23 Carryover for all internal standards measured during validation for rat plasma. 69
Table 2.24 Mean matrix factor determined for the LQC and HQC Samples in rat plasma validation 70
Table 2.25 Mean percentage recovery for all analytes at HQC measured in rat plasma validation 71
Table 2.26 Mean peak areas of analytes before and after up to six freeze-thaw cycles. 72
Table 2.27 Mean percentage bias from original peak area and CV of peak areas after six freeze-thaw cycles (n=6) 73
Table 2.28 Mean areas of MQC before and after 4 hours on the benchtop and at ambient temperature and CV and mean % bias from original concentration. (n=6) 73
Table 2.29 Autosampler stability: mean initial and 36 Hour QC Concentrations. 74
Table 2.30 Autosampler stability: percentage bias from initial concentration after 36 hours at 5°C. 74
Table 2.31 Autosampler stability: CV of concentrations after 36 hours at 5°C. 74
Table 2.32 Dilution Integrity nominal and mean measured concentration, CV and % bias of QC sample measured after dilution. 75
Table 2.33 Porcine Plasma Cross Validation: Range of calibration curve for PAP-G showing CV and Bias of measured curve from nominal concentration. 76
Table 2.34 Summary of Results for Porcine Plasma Cross Validation 77
Table 2.35 Summary of validation data for mouse serum 79

Table 2.36. Summary of cross- validation for human serum 81
Table 3.1 Mass spectrometric and chromatographic properties for each standard in the GSH method. 97
Table 3.2 Mass spectrometric and chromatographic properties for each internal standard in the GSH method 98
Table 3.3 Chromatographic gradient used for glutathione method 99
Table 3.4 Volumes of IS standard stock solutions mixed to form the IS top stock solutions, with concentrations for each of the three concentration ranges, mouse serum validation. 101
Table 3.5 Concentration of each internal standard in the IS top stock solution before dilution to produce LQC and HQC IS stock solutions, mouse serum validation. 102
Table 3.6 Preparation of HQC and LQC internal standard stock solutions, mouse serum validation.. 102
Table 3.7 Preparation of the internal standard stock solutions, human serum validation[a] 104
Table 3.8 Concentration of each IS in the IS top stock solution before dilution to produce LQC and HQC IS stock solutions, human serum validation 105
Table 3.9 Preparation of HQC and LQC IS stock solutions from the IS top stock solution B, human serum validation 105
Table 3.10 Final concentration of the IS stock solutions 105
Table 3.11 Retention time ranges of peaks after elution of internal standards, from internal standards spiked into samples either containing or not containing mouse serum. 109
Table 3.12 Mean peak areas of each of the internal standards at the LQC measured in the four samples types, with CV. 110
Table 3.13 Mean peak areas of each of the internal standards at the HQC measured in the four samples types, with CV. 111
Table 3.14 Comparison of peak areas of samples prepared with internal standards spiked before extraction, and the sample prepared to reflect actual sample preparation, “normal preparation”. 112
Table 3.15 Extraction recoveries of the internal standard stock solutions when comparing peak areas of the HQC or LQC IS solutions were spiked into mouse serum, either before or after protein precipitation. 113
Table 3.16 Matrix factor measured by spiking IS stock solutions into in mouse serum or water at the LQC and HQC concentrations. 114
Table 3.17 Mean peak areas of each of the IS standards at the LQC measured in the four samples types, with CV. 116
Table 3.18 Mean peak areas of each of the IS standards at the HQC measured in the 4 samples types, with CV. 117
Table 3.19 Extraction recoveries of the IS stock solutions when comparing peak areas of the IS spiked into human serum either before or after protein precipitation. 118
Table 3.20 Percentage recoveries of the IS stock solutions when comparing peak areas of the IS spiked into matrix samples after extraction, with or without drying under nitrogen. 119
Table 3.21 Matrix factor measured by spiking IS stock solutions into human serum or water the LQC and HQC concentrations. 120
Table 3.22 Summary of results for mouse serum comparisons between sample preparation, recovery and matrix factors 122
Table 3.23 Summary of CVs for mouse serum comparisons between sample preparation, recovery and matrix factors. 123
Table 3.24 Summary of results for human serum comparisons between sample preparation, recovery and matrix factors. 124

Table 3.25 Summary of CVs for human serum comparisons between sample preparation, recovery and matrix factors. Green=CV≤20%, amber=30%<CV>20%, red=CV>50%. 124
Table 4.1 Concentration of each IS standard in the top IS stock solution for application of the glutathione pathway assay to mouse liver extracts. 135
Table 4.2 Concentrations of top stock solutions for the glutathione pathway assay ULOQ QC and standard curves in mouse liver extracts.[a] 136
Table 4.3 The preparation of the calibration curve for the application of the glutathione pathway assay to mouse liver extracts. 136
Table 4.4 The preparation of the quality control samples for the application of the glutathione pathway assay to mouse liver extracts. 137
Table 4.5 Concentration of each IS added to the top IS stock solution for application of the glutathione pathway to mouse serum. 138
Table 4.6 Concentrations of top stock solutions for the glutathione pathway assay ULOQ QC and standard curve in application to mouse serum.[a] 139
Table 4.7 The preparation of the calibration curve for the application of the glutathione pathway assay to mouse serum. 139
Table 4.8 The preparation of the QC stock solutions for application of the glutathione pathway assay to mouse serum. 140
Table 4.9 Final concentration of the ULOQ of each of the APAP standards, and the concentration of IS used for each, for application of the assay to tissue extracts, not accounting for salt factors. 141
Table 4.10 Concentration ranges of the analytes in calibration curve for the application of the APAP method to mouse liver extracts. 142
Table 4.11 QC concentrations for application of the APAP method to mouse liver extracts, taking into account salt factors. 142
Table 4.12 Calibration curve range for APAP method application to mouse serum. 144
Table 4.13 QC Concentrations for APAP method application to mouse serum. 144
Table 4.14 Biochemistry and hepatocyte damage scores for C57/BL-6 mice treated with 300 mg/kg paracetamol. 147
Table 4.15 Summary of APAP method application to mouse serum: concentrated sample preparation method 150
Table 4.16 Summary of matrix effects and recovery at LQC and HQC when APAP method was applied to mouse serum: concentrated sample preparation. 151
Table 4.17 The linearity and percentage meeting acceptance criteria for calibration curves, QCs at each level and, the total percentage of QCs meeting acceptance criteria, for glutathione pathway assay applied to mouse serum. 153
Table 4.18 Pearson correlation coefficients for metabolites measured in serum with key biomarkers, only metabolites with at least 1 significant correlation and r>0.45 are included in the table. 157
Table 4.19 Summary of linearity displayed as r2 value of calibration curve and number of acceptable points on curve, the CV of the QCs and mean % bias form the expected concentration. 158
Table 4.20 Mean concentration of pooled QCs and pooled QCs over-spiked with the HQC. 159
Table 4.21 Effectiveness of the assay when applied to mouse hepatic extracts, including linearity (r2), the percentage of calibration curve points and QCs meeting acceptance criteria, the actual range over which analyte were present in the tissue extracts and the accurate range of the method, and the range of retention times in the run. Red highlighting indicates analytes did not meet acceptance criteria and/or all concentrations were outside analytical range, orange indicates a truncated range was used, and/or some results were outside the acceptable analytical range. Abbreviations: 2-AB: 2-amino butyrate; bld: below limit of detection; cys-gly: cysteinyl-glycine; y-glu-cys: gamma glutamyl cysteine; GSH: glutathione; GSSG: oxidised glutathione; HQC: high quality

control; LLOQ: lower limit of quantification; LQC: low quality control; MQC: mid quality control; na: not applicable; OA: ophthalmic acid; 5-OP: 5-oxoproline; QC: quality control; RT: retention time; SAH: s-adenosyl homocysteine; SAMe: s-adenosyl methionine; ULOQ: upper limit of quantification. 162
Table 4.22 Mean areas of pooled QCs and over-spiked QCs with CVs, and the mean difference between the pooled and over-spiked QC and the percentage difference from the concentration of standard added in application of glutathione pathway assay to mouse tissue. 163
Table 4.23 Summary of changes in both hepatic extracts and serum in APAP and APAP + NAC treated mice compared to controls. 173
Table 5.1 Concentration ranges for APAP and metabolites in application of APAP method to porcine plasma. 188
Table 5.2 Final QC concentrations for APAP and metabolites in application of APAP method to porcine plasma. 189
Table 5.3 Final measured concentrations of each deuterated internal standard in porcine sample analysis. 189
Table 5.4 UHPLC-MS/MS conditions for analytes and internal standards measured for the APAP assay in porcine plasma. 190
Table 5.5 Standard ULOQ and IS concentration for the three curves concentration levels which were prepared and mixed for sample analysis 191
Table 5.6 Calibration range used for standards in the “low”, “mid” and “high” QC ranges. 191
Table 5.7 Final concentration of the QCs at the for each high, mid and low curve calibration curves 192
Table 5.8 Results of clinical chemistry tests on serum taken from pigs at 4 hours intervals up to ALF, and 4 hourly intervals from ALF until death. 193
Table 5.9 Histopathology scores for liver and kidney for individual animals. 194
Table 5.10 Assigned representative resonances for endogenous and APAP metabolites in plasma, with multiplicity and functional group of proton represented 201
Table 5.11 Assigned resonances for endogenous and APAP metabolites in urine, with multiplicity and functional group of proton represented. 201
Table 5.12 Assigned resonances for endogenous and APAP metabolites in soluble aqueous liver extracts, with multiplicity and functional group of proton represented. 202
Table 5.13 Assigned resonances for endogenous and APAP metabolites in soluble aqueous liver extracts, with multiplicity and functional group of proton represented. 202
Table 5.14 Summary of endogenous metabolism changes in the pig pre- and post- paracetamol induced ALF, as measured by 1H-NMR spectroscopy, across all matrices. 211
Table 5.15 Linearity and percentage of curves and QCs which met acceptance criteria for application of the glutathione method to porcine plasma 214
Table 5.16 Mean concentrations and CVs of pooled QCs and QCs over-spiked with 50% of the HQC, plus the mean percentage bias of the over-spiked concentration from the nominal concentration, for application of glutathione pathway assay to porcine plasma. 215
Table 6.1 Overview of patient metadata from collaborators including patient information, APAP dose and timing and traditional biomarkers measured in the clinic. 230
Table 6.2 Standards and IS for the “low”, “mid” and “high” calibration curves, with the ULOQ concentration and the concentration of IS in the samples. 232
Table 6.3 Calibration range used for standards in the “low”, “mid” and “high” QC ranges. 232
Table 6.4 Final concentration of the QCs at the for each “high”, “mid” and “low” curve calibration curves 232
Table 6.5 Overview of the effectiveness of the GSH assay in human serum. 234

Table 6.6 Summary of pooled QCs reproducibility and the % difference between over-spiked QC concentration and expected concentration. 235
Table 6.7 Overview of linearity and number of points on the curve and QCs which meet acceptance criteria, for application of APAP method to MAPP samples. 236
Table 6.8 Exclusions made from analysis due to all, or the majority of, APAP metabolites being under the limit of quantification, or due to no metabolites being detected due to an analytical issue. 237
Table 6.9 Summary of ROC-analysis comparing traditionally measured biomarkers with APAP concentration and APAP-CYP metabolism as a proportion of total metabolites, and APAP-C as a proportion of APAP-S. Sensitivity is given for 90% specificity. 242

Abbreviations

^{1}H-NMR	proton nuclear magnetic resonance
5-OP	5-oxoproline, pyroglutamic acid
5-oxoprolinase	5-OPase
ALF	acute liver failure
ALP	Alkaline phosphatase
ALT	Alanine aminotransferase
ANOVA	Analysis of variance
AP-1	Activator protein 1
APAP	Acetaminophen, paracetamol, *n*-acetyl-*p*-aminophenol
APAP-C	Paracetamol cysteine conjugate
APAP-CYP	Paracetamol Cytochrome p-450 related conjugates
APAP-G	Paracetamol glucuronide conjugate
APAP-NAC	Paracetamol n-acetyl-cysteine conjugate
APAP-OMe	3-methoxy paracetamol
APAP-S	Paracetamol sulfate conjugate
APAP-SG	Paracetamol glutathione conjugate
AST	aspartate aminotransferase
AUC	Area under the curve
BEH	Ethylene bridged hybrid
BHMT	betaine homocysteine methyl transferase
CBS	cystathionine-β-synthase
CDO	Cysteine dioxygenase
CDO	Cysteine dioxygenase
CE	Capillary electrophoresis
CES	Carboxyl esterase
CPMG	Carr-Purcell-Meiboom-Gill
CSE	Cystathionine-γ-lyase
CV	Coefficient of variance
CYP	Cytochrome p-450
Cys-gly	Cysteinyl-glycine
dcSAMe	De-carboxylated s-adenosyl methionine
DILI	Drug induced liver injury
DIQC	Dilution integrity quality control
DP	Dipeptidase
ESI	Electrospray ionisation
FA	Formic Acid
FDA	Food and Drug Administration
FDR	False discovery rate
GC	Gas Chromatography
GCL	Gamma-glutamyl cysteine ligase
GCLc	Gamma-glutamyl cysteine ligase catalytic subunit
GCLm	Gamma-glutamyl cysteine ligase modifier subunit
GGC	Gamma-glutamyl cyclotransferase
GGT	Gamma-glutamyl transpeptidase
GS	Glutathione synthetase
GSH	Reduced glutathione
GSH-AA	GSH-amino acid conjugate
GSSG	Glutathione disulfide

HILIC	Hydrophobic interaction liquid chromatography
HMGB1	High mobility group box 1 protein
HQC	High quality control
ICP	Intracranial pressure
INR	International normalised ratio
I.p.	intraperitoneal
IS	Internal Standard
JRES	J-resolved Spectroscopy
LC	Liquid chromatography
LLOQ	Lower limits of quantification
LQC	Low quality control
MetHb	Methaemoglobin
miR-122	Micro ribonucleic acid 122
MTHF	5-methyltetrahydrofolate
MRM	Multiple reaction monitoring
γ-glu-cys	Gamma-glutamyl-cysteine
MAPP	Markers and Paracetamol Poisoning
MAT	Methionine adenosyl transferase
MS	Mass spectrometry
MS	Methionine synthase
MQC	Mid quality control
NAT	n-acetyl transferase
NAC	*n*-acetylcysteine
NAPQI	*n*-acetyl-*p*-benzoquinone imine
NFκB	nuclear factor kappa-light-chain-enhancer of activated B cells
NOESY	Nuclear Overhouser Effect Spectroscopy
Nrf-2	Nuclear factor erythroid 2–related factor 2
OA	Ophthalmic acid
PAP-G	*p*-aminophenol glucuronide conjugate
PAP	*P*-aminophenol, 4-aminophenol
PAPS	3-phosphoadenosyl-5-phosphosulfate
PCA	Principal components analysis
PPG	Propargylglycine
QC	quality control
ROC	Receiver operating characteristic
RT	Retention time
RP	Reversed-phase
SAH	s-adenosyl-homocysteine
SAMe	s-adenosyl-methionine
SULTs	sulfotransferase enzymes
STOCSY	Statistical TOtal Correlation Spectroscopy
TBil	Total bilirubin
TCA	Tri-carboxylic acid.
TMAO	trimethylamine N-oxide
TQ	Triple quadrupole
UGT	uridine diphosphate-glucuronosyl transferase
UHPLC	Ultra-High-Performance Liquid Chromatography
UV	Ultra-violet detector
UV scaling	Unit variance scaling
ULOQ	Upper limit of quantification
UDP	uridine diphosphate

1 Introduction

1.1 Aims and methods

- To understand paracetamol (*N-ac*etyl-*p*-aminophenol [APAP]) metabolism and associated toxicity in animal models and clinical APAP overdose patients, with an emphasis on APAP metabolite and sulfur amino acid and glutathione (GSH) related metabolism.
- To develop and apply "targeted" analytical methods to produce quantitative metabolite concentrations, and to confirm results gained through "untargeted" metabolic profiling.
- To understand whether 5-oxoproline (5-OP) and ophthalmic acid (OA) represent putative biomarkers of APAP-induced liver injury and of general hepatic GSH depletion.

A general layout of the contents of the Thesis, giving a brief overview of the contents of each chapter is provided below in Figure 1.1

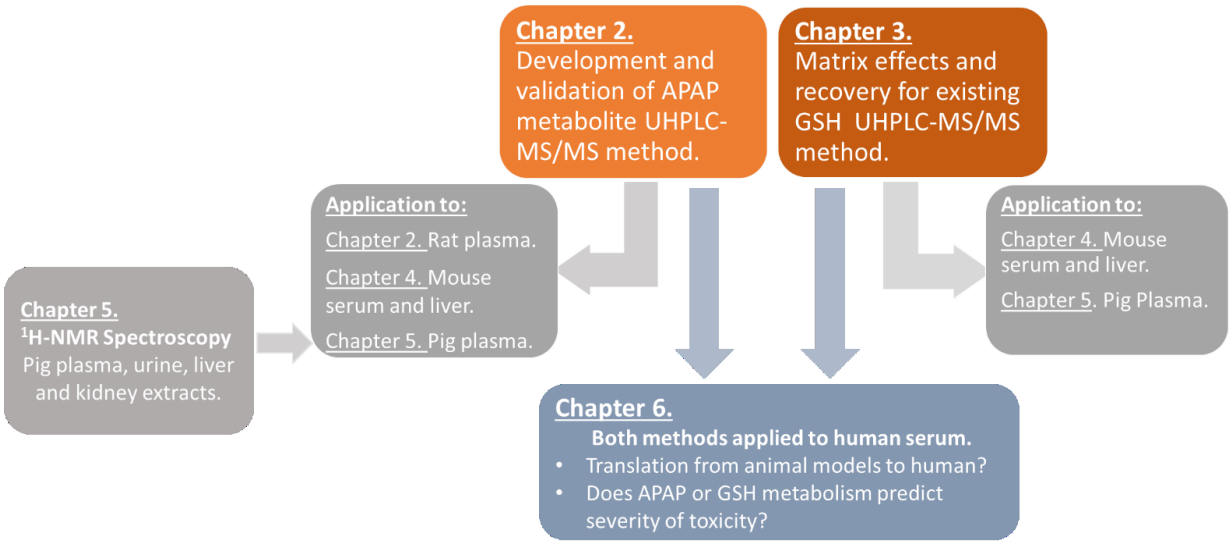


Figure 1.1 Overview of the analytical strategies developed and their application to animal models or clinical samples listed by chapter.
Abbreviations: ^{1}H-NMR: proton nuclear magnetic resonance; APAP: paracetamol; GSH: glutathione; UHPLC-MS/MS: ultra-high-performance liquid chromatography coupled mass spectrometry

1.2 APAP metabolism

1.2.1 APAP metabolism overview

Although usually safe at the therapeutic dose, APAP is toxic in overdose and is the leading cause of acute liver failure ALF in developed countries (Lee 2012a; Lee 2012b; Makin et al. 1995; Ostapowicz et al. 2002; Perkins 2006). The primary routes of hepatic APAP metabolism in humans, and many

animal species, are glucuronidation and sulfation, these conjugation reactions occur at the para-hydroxyl group of APAP. Glucuronidation occurs *via* the transfer of uridine diphosphate glucuronic acid in a reaction catalysed by a UDP-glucuronosyl transferase (UGT) enzyme (Mackenzie et al. 2005). Sulfation occurs by formation of a sulfate ester; the most common sulfate donor is 3-phosphoadenosyl-5-phosphosulfate (PAPS) and this reaction is catalysed by sulfotransferase enzymes (SULTs) in the cytosol (McGill and Jaeschke 2013). At therapeutic doses, 5-15% of APAP is metabolised by oxidative metabolism *via* CYP enzymes to the reactive metabolite NAPQI, which is then detoxified by conjugation with GSH to form APAP-SG. Oxidative metabolism involves a number of CYP enzymes, however, the evidence suggests the most important of these is CYP2E1 (and CYP1A2/3A4) in humans and rodents (Dahlin et al. 1984; Patten et al. 1993; Thummel et al. 1993). APAP-SG is excreted in the bile or can be metabolised to produce the cysteinyl (APAP-C) and *N*-acetylcysteinyl (APAP-NAC) conjugates. Initially APAP-SG loses the glutamyl residue in a reaction catalysed by γ-glutamyl-transpeptidase (GGT) followed by glycine *via* cysteinylglycinase, leaving the cysteinyl conjugate. The amino group of cysteine is then acetylated by *N*-acetyltransferase (NAT), using acetyl-coenzyme A as the donor, to produce the *N*-acetylcysteine-APAP (APAP-NAC) conjugate (Mitchell et al. 1973b). There are a number of other routes of metabolism of APAP including de-acetylation to form *p*-aminophenol (PAP). This has been observed in the Fischer rat (Newton et al. 1985), but this appears to be a minor route in man (ca. 1%) and is generally followed by rapid re-acetylation (Nicholls et al. 1997). Major pathways of APAP metabolism are displayed in Figure 1.2.The arachidonic acid conjugate of PAP, shown to be formed by fatty acid amide hydrolase in rodent models, is thought to be linked to its therapeutic mechanism of action (Hogestatt et al. 2005). Other minor routes of metabolism include a non-toxic route of CYP related metabolism to form 3-hydroxy-APAP and subsequently 3-methoxy APAP conjugates, and further metabolites have been identified including methoxy-APAP-glucuronide, amongst others (Chen et al. 2008; Chen et al. 1998; Forte et al. 1984).

1.2.2 APAP metabolism and toxicity

In humans and rodents, following an overdose of APAP, the reactive metabolite NAPQI depletes hepatic glutathione stores, after which it reacts with cellular macromolecules, leading to centrilobular hepatic necrosis (McGill and Jaeschke 2013; Mitchell et al. 1973a; Prescott 1980). NAPQI is able to bind to sulfhydryl groups and reacts with GSH either by a simple chemical reaction or enzymatically *via* glutathione-S-transferases; it can also oxidise GSH to GSSG and at high doses of APAP, and GSH is quickly depleted (James et al. 2003; Potter et al. 1973). Evidence that the oxidative pathway of APAP metabolism *via* CYP enzymes is crucial for the toxic consequences of APAP overdose was provided through CYP genetic knock-out models. CYP2E1 null mice were more resistant to APAP toxicity, particularly at doses up to 400mg/kg, although at 600mg/kg some toxicity was seen in the knock-out mice (Lee et al. 1996). Mice which were both CYP2E1 and CYP1A2 null were resistant to liver enzyme increases, liver necrosis and protein covalent binding following a large APAP dose (800mg/kg) (Zaher et al. 1998). In addition, the APAP sulfation reaction, a high-affinity but low-capacity conjugation reaction, becomes saturated at high doses of APAP. This is because of limited availability of the active sulfate donor, PAPS, the supply of which is, in turn, limited by the availability of its precursor, inorganic sulfate. This leads to decreased APAP-S synthesis relative to APAP-G (Bales et al. 1988; Liu and Klaassen 1996). Early investigation into APAP toxicity using metabolic profiling found that in clinical overdose cases the APAP-G/APAP-S ratio, APAP-C and APAP-NAC were all increased, reflecting the saturation of sulfation and switch to CYP related metabolism (Bales et al. 1988)

GSH is an intracellular store of cysteine, therefore depletion of GSH may affect the amounts sulfur containing amino acids methionine and cysteine available for other biochemical needs, and decrease protein synthesis (Lu 2013; Mast et al. 2018) In early reports it was found that chronic APAP feeding in the rat led to weight loss, which was not seen when diets were supplemented with methionine (McLean et al. 1989). A major mechanism of APAP toxicity is thought to be covalent binding to proteins by NAPQI (Gibson et al. 1996). NAPQI can also oxidise free -SH groups on cysteinyl residues of proteins, forming protein disulfide-bridges (Bessems and Vermeulen 2001; Heard et al. 2011; Vermeulen et al.

1992). A key event in APAP toxicity appears to be mitochondrial dysfunction due to either targeted protein binding or reaction with mitochondrial proteins, and oxidative stress. This can lead to the mitochondrial permeability transition pore opening, leading to increased mitochondrial DNA fragment being present in the blood, and to hepatocyte nuclear DNA fragmentation and necrosis (McGill et al. 2012a). Previous metabonomic investigations in the mouse have shown that mitochondrial oxidative stress leading to energy metabolism perturbations and the formation of "mega-mitochondria" followed APAP treatment in mice (Coen et al. 2003; Coen et al. 2004). The main mechanisms of APAP induced liver injury therefore appear to be a combination of hepatic mitochondrial dysfunction due to oxidative stress, GSH depletion, and covalent binding to and oxidation of sulfur residues on mitochondrial proteins (Jaeschke and McGill 2015; McGill and Jaeschke 2013). The focus of the research presented in this thesis is the impact of GSH depletion in APAP toxicity, as described in more detail below.

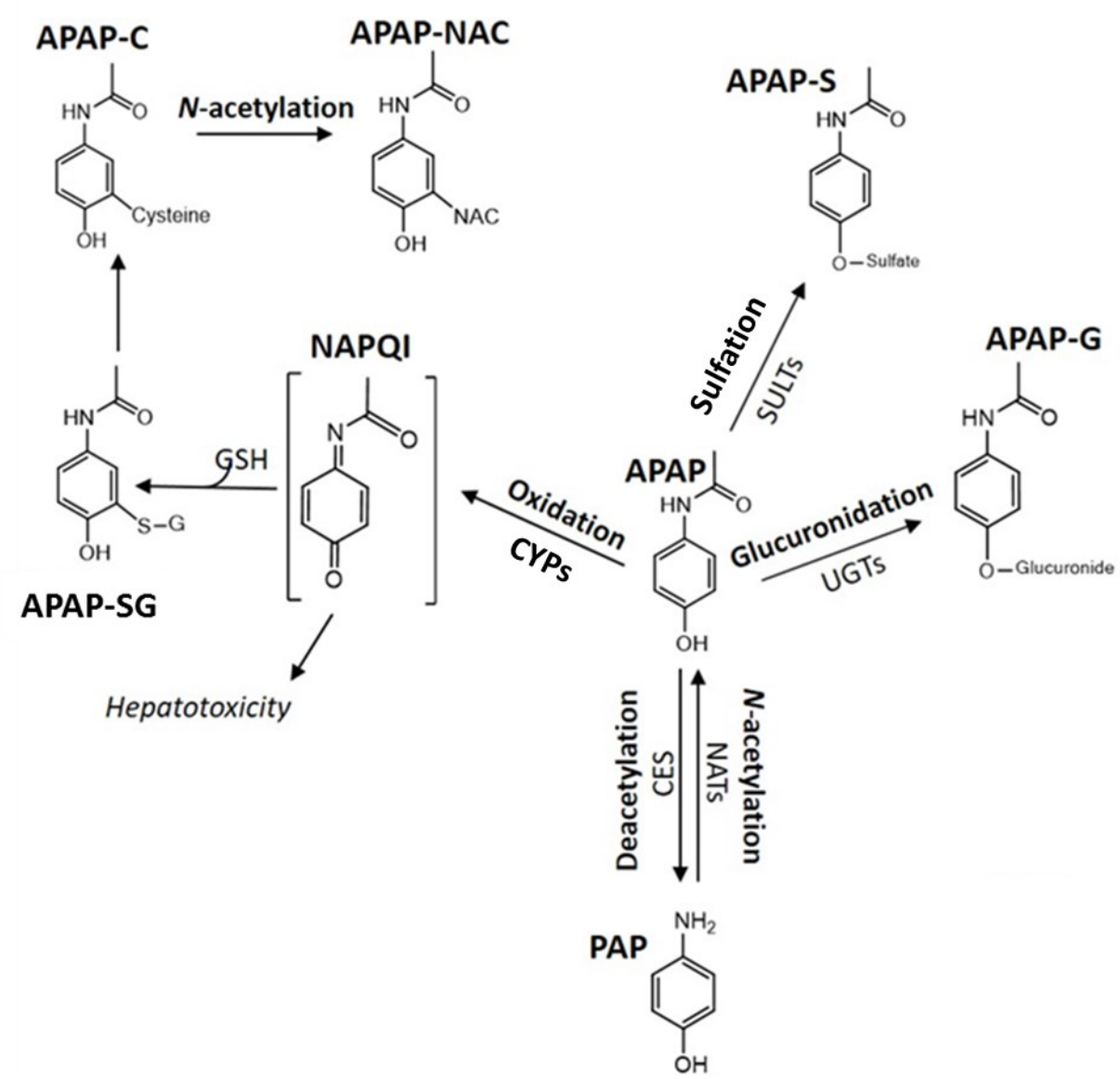


Figure 1.2 overview of some of the major routes of APAP metabolism in humans and preclinical species.
Abbreviations: APAP: paracetamol; APAP-C: paracetamol cysteinyl conjugate; APAP-G: paracetamol glucuronide conjugate ; APAP-NAC: paracetamol n-acetyl-cysteine conjugate; APAP-OMe: 3-methoxy paracetamol; APAP-S : paracetamol sulfate conjugate; APAP-SG: paracetamol glutathione conjugate; CES: Carboxyl esterase; CYP: Cytochrome p-450; NAPQI: n-acetyl-p-benzoquinone imine; NAT: n-acetyl transferase; PAP: p-aminophenol; SULTs: sulfotransferase enzymes; UGT: UDP-glucuronosyl transferase

1.2.3 Species and individual differences in APAP metabolism and toxicity

APAP metabolism is known to differ between animal models and between individuals, and as oxidative metabolism is so closely linked with the toxicity of APAP, understanding these differences is of key importance. This is true for both the development of suitable animal models for testing treatments for ALF or APAP overdose, and for clinical decision making.

Previous investigations have determined that between rodent models there are differing metabolism profiles and related toxicity. Early investigations with isolated hepatocytes found that hamster and mouse hepatocytes were more sensitive to APAP toxicity than rat or human hepatocytes, and that there was significantly lower GSH depletion in rat hepatocytes compared to hamster (Tee et al. 1987). Similarly, in a more recent study with primary human rat and mouse hepatocytes, human hepatocytes were shown to be most resistant to APAP and mouse least resistant. Interestingly, these results did not correlate with CYP2E1 activities (Jemnitz et al. 2008). *In vivo* investigations using mice and rats have shown that rats are more resistant to oxidative stress and mitochondrial dysfunction than mice and are therefore less suitable for modelling human toxicity (McGill et al. 2012b). There are also differences in sensitivity between animal strains, for example Fischer-344 rats seem to be more sensitive to APAP toxicity than other strains (McGill et al. 2012b), and there are sensitivity differences between different strains of mice, with C57BL/6 being the most widely used (Harrill et al. 2009). Other species which are known to metabolise APAP differently to human are cat and dog, which are both sensitive to APAP toxicity. Cats are extremely sensitive to APAP as they have a very low glucuronidation capacity due to no expression of major UGTs (Court and Greenblatt 2000), and do not express NAT2 and therefore cannot re-acetylate PAP to APAP which results in methaemoglobinemia (Trepanier et al. 1998). Dogs, which are a commonly used preclinical species, do not express either NAT1 or NAT2 enzymes and similarly suffer with methaemoglobinemia in response to APAP administration (McConkey et al. 2009; Trepanier et al. 1997). Methaemoglobinemia is not a common toxic event in clinical APAP overdose, although some cases have been reported (Abdelghani et al. 2015; Queiros et al. 2017), and one of these cases was in an elderly female patient already receiving treatment for kidney injury, so the mechanism of methaemoglobin formation may have been complicated beyond simple APAP toxicity (Queiros et al. 2017). A commonly used non-human primate model species, cynomolgus monkey, was also shown to be very resistant to APAP dosing due to efficient glucuronidation combined with minimal oxidative metabolism, and clearly represents a poor model for human (Yu et al. 2015). Pigs have also been suggested as a second line model toxicology

species in drug development and are being used in the development of APAP overdose therapies, however sulfation capacity has been found to be low in the pig, and APAP has been shown to cause methaemoglobinaemia in these animals (Capel et al. 1972; Newsome et al. 2010; Thiel et al. 2011).

Considering the variation in APAP metabolism and associated toxicity in species and strains of animals, and the importance of oxidative metabolism in the toxic effects of APAP, the inter-individual differences between humans in APAP sensitivity due to metabolic differences may also be significant. In addition to factors such as underlying metabolism such could affect APAP metabolism and toxicity, for example *p*-cresol was correlated with an increased APAP-G/APAP-S ratio in the urine of human subjects treated with APAP (Clayton et al. 2009). Ethnicity may also have some impact on APAP metabolism and toxicity (Court et al. 2017; Critchley et al. 1986; Lee et al. 1992). In addition, there are known polymorphisms in the genes encoding key enzymes involved in APAP metabolism, with polymorphisms in the UGT enzymes leading to increased APAP-protein adduct formation, while CYP2E1 polymorphisms reduce oxidative metabolism (Court et al. 2017), and there is evidence that gene expression differences in UGTs correlate with differential APAP metabolism (Fisher et al. 2000). In addition, there are known gender differences in APAP metabolism and toxicity in C57BL/6 mice (Botta et al. 2006; Du et al. 2014; McConnachie et al. 2007), and CD-1 mice (Masubuchi et al. 2011), where females are more resistant to APAP induced toxicity and GSH depletion. The translation of these findings to humans is unclear as more cases of APAP induced ALF are reported in women, but whether this is due to increased susceptibility or higher prevalence of overdose and co-ingestions of other medications is unclear (Rubin et al. 2018). There have previously been reports gender differences in the APAP metabolism including a higher APAP-G/APAP-S ratio seen in male subjects and male liver microsomes compared to females (Court et al. 2001; Critchley et al. 1986).

The current best practice treatment for APAP overdose is intravenous N-acetyl cysteine (NAC), and the decision to treat is currently based on a nomogram of APAP plasma/serum concentration and time since overdose (Bateman 2015; Bateman et al. 2014; Rumack et al. 1981). However, the differences in metabolism and related toxicity mean that some patients are likely to develop liver injury despite

relatively low doses, while other patients will be treated with NAC unnecessarily. As discussed above, differences in APAP metabolism are also prevalent in animal models, of APAP toxicity. Therefore, it is important to understand APAP metabolite profiles of the various animal models of APAP induced liver injury, and of individual patients when making treatment decisions. This is especially important as the proportion of CYP metabolism related APAP metabolites in circulation have been shown to be correlated to the degree of liver injury severity in human overdose situations (Vliegenthart et al. 2017).

1.3 GSH related metabolism

1.3.1 GSH biosynthesis and the γ-glutamyl cycle

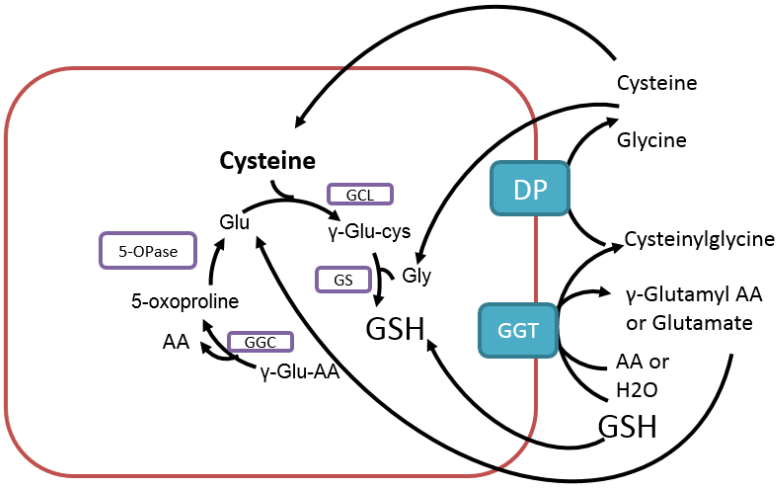


Figure 1.3 The γ-glutamyl cycle
Abbreviations: GCL: glutamyl cysteine synthase, GS: Glutathione synthetase, GGT: γ-glutamyl transpeptidase, DP: Dipeptidase, GGC: γ-glutamyl cyclotransferase, 5-OPase: 5-oxoprolinase

GSH is a sulfur containing tripeptide and has a number of functions that make it crucial to cell survival including reduction of oxidative species, maintaining redox homeostasis, conjugation with reactive xenobiotics, mitochondrial bioenergetics, and cell cycle progression and cell survival (Lu 2013). GSH is synthesised from the sulfur-containing amino acid cysteine in a continuous cycle known as the γ-glutamyl cycle, summarised in Figure 1.3. The rate limiting stage in the γ-glutamyl cycle is the addition of the γ-glutamyl group to cysteine via the enzyme glutamate cysteine ligase (GCL); made up of a catalytic (GCLc) and modifier (GCLm) subunit (Griffith and Meister 1979). Under normal cellular conditions GSH can be transported out of the cell where it reacts with an amino acid via γ-glutamyl-transpeptidase (GGT) to form a GSH-amino acid (GSH-AA) conjugate and cysteinyl-glycine (cys-gly).

Cys-gly is broken down to its constituent amino acids *via* a transpeptidase, the resultant amino acids are transported back into the cell. Cysteine can then either be used as a substrate in the γ-glutamyl cycle, incorporated into protein, or metabolised into other sulfur-containing molecules such as taurine and inorganic sulfate. The GSH-AA conjugate is also transported back into the cell where it is converted to 5-OP by γ-glutamyl cyclotransferase (GGC) which is further metabolised to glutamate *via* 5-OP. GSH then acts upon GCL in a negative feedback loop when concentrations are sufficiently high (Griffith and Meister 1979).

In rodents, altering GSH synthesis using genetic modifications has demonstrated the importance of GCL expression and GSH biosynthesis in survival and APAP sensitivity. Overexpression of GCL in transgenic mice has been shown to protect against APAP induced liver injury (Botta et al. 2006) and GCLc knockout is embryonic-lethal in mice (Dalton et al. 2000). Mice with inducible GLCc knockout failed to survive to adolescence due to liver failure with signs of steatosis, mitochondrial damage and increased lipid peroxidation (Chen et al. 2007). GCLm knock-out mice have increased susceptibility to APAP induced liver injury where there is no response to NAC treatment (Dalton et al. 2000) (McConnachie et al. 2007). In addition to its role in GSH biosynthesis, GCL can use 2-amino-butyrate as a substrate in the biosynthesis of γ-glutamyl-2-amino-butyrate, to which glycine is added to in a reaction catalysed by GS to produce ophthalmic acid (OA). OA concentrations therefore often alter with GSH depletion. For example, OA concentrations have been shown to increase in mouse liver and plasma in response to fasting where GSH is decreased (Kobayashi et al. 2017) and OA concentrations are increased in mice in response to APAP dosing (Soga et al. 2006). The mechanisms for this may be due to increased activity of the GCL enzyme as a response to oxidative stress, or simply due to the removal of the negative feedback loop upon the enzyme as GSH is quickly depleted, therefore, increased OA concentration could be a biomarker of hepatic GSH depletion. (Geenen et al. 2013; Soga et al. 2006).

GSH synthesis has potential roles in a number of human diseases (including inborn errors of metabolism such as 5-oxoprolinuria). Polymorphisms in GLC genes leading to loss of function have been linked to coronary disease and myocardial infarction, diabetes mellitus, cancer and cystic fibrosis (de Lima Marson et al. 2014; Eksi et al. 2014; Huang et al. 2001; Katakami et al. 2014; Kawabata et al. 2011; Nakamura et al. 2003). However, it should be noted that there is limited mechanistic evidence for these disease-related correlations, and results may differ between human populations. GCL is transcriptionally regulated by transcription factor Nrf-2 and members of the AP-1 and NFκB family in response to oxidative stress, binding to the antioxidant response element (Lu 2009) (Kensler et al. 2007). It has recently been shown that under stress GSH is synthesised directly from methionine via the trans-sulfuration pathway preferentially to uptake of extracellular cystine (Eriksson et al. 2015). GSH depletion therefore could have wide ranging effects on other sulfur containing products of cysteine and compounds related to the methionine cycle and trans-sulfuration pathway (Jung et al. 2008)

1.3.2 The methionine cycle and the trans-sulfuration pathway

The main source of mammalian sulfur is the essential amino acid methionine, which unlike cysteine must be obtained from the diet. In addition to its use in protein synthesis, methionine is metabolised *via* the trans-sulfuration pathway to form cysteine or is recycled back to methionine as part of the methionine cycle. The methionine cycle has roles in important biological functions, for example biological methylations, polyamine synthesis and one carbon metabolism. The first stage in the metabolism of methionine is catalysed by the enzyme methionine adenosyl transferase (MAT) in an ATP-dependent reaction forming S-adenosylmethionine (SAMe), of the three MAT isozymes, (MATI, II and III), MATI and MATIII are liver-specific and allow the liver to increase SAMe production when methionine concentrations levels are increased, showing the importance of this reaction in the liver (Chou 2000; Kotb and Geller 1993). SAMe is responsible for most biological methylations, and is therefore critical to cellular function, during the process of methylation S-adenosylhomocysteine (SAH) is formed (Grillo and Colombatto 2008). Alternatively, SAMe can be decarboxylated to form

SAMe decarboxylase (dcSAMe). During polyamine synthesis putrescine and dcSAMe combine to form spermidine *via* spermidine synthase, subsequently forming spermine in a reaction catalysed by spermine synthase (Pegg 2009; Wallace et al. 2003). SAH is hydrolysed to homocysteine which is re-methylated to form methionine and complete the methionine cycle by two mechanisms. These re-methylation reactions require either betaine or 5-methyltetrahydrofolate (MTHF) as the methyl donor and the enzymes betaine homocysteine methyl transferase (BHMT) or methionine synthase (MS) respectively (Stipanuk 2004).

Homocysteine can also form cysteine *via* the trans-sulfuration pathway. Thus, cystathionine-β-synthase (CBS) catalyses the formation of cystathionine from homocysteine and serine, which is then hydrolysed by cystathionine-γ-lyase (CSE) to form cysteine, α-ketobutyrate and ammonia (Stipanuk and Ueki 2011). Cysteine is then catabolised by a number of pathways, including the γ-glutamyl cycle. Alternatively, cysteine can form cysteine sulfinate which is broken down to end products including taurine, sulfates, pyruvate and H_2S (Stipanuk and Ueki 2011). Figure 1.4 summarises some reactions in the trans-sulfuration pathway.

In order to study the trans-sulfuration pathway, transgenic mice either null or heterozygous for the two key trans-sulfuration enzymes cystathionine-β-synthase (CBS) and cystathionine-γ-lyase (CSE) and have been developed. CBS null mice fail to survive (Watanabe et al. 1995), however CBS heterozygotes and CSE null and heterozygous mice reach maturity and may provide useful models. These animals have decreased hepatic GSH concentrations and increased susceptibility to APAP toxicity (Hagiya et al. 2015). CSE deficient mice were particularly susceptible to APAP toxicity and there were changes to GCL which included increased activity and increased affinity for both cysteine and glutamate (Hagiya et al. 2015).

Drugs which deplete GSH by two different mechanisms, BSO which inhibits GCL to prevent GSH synthesis and phorone which depletes GSH by conjugation, have been shown to alter the concentrations of sulfur-containing metabolites and the activity of key TSP enzymes (Jung et al. 2008).

BSO treatment led to decreased hepatic concentrations of methionine, SAMe, cysteine and GSH, with an initial decrease in GCL and MAT activity which then recovered quickly. There was also an increase in cysteine dioxygenase (CDO) activity at 2 hours, therefore leading to increased taurine and hypotaurine concentrations. Phorone on the other hand increased SAMe concentrations and gave a larger initial increase in GSH and cysteine concentrations, with no change to those of methionine and decreases in taurine and hypotaurine concentrations. Phorone treatment caused increased activity of MAT, CBS, CSE and GCL with a decrease in CDO activity (Jung et al. 2008).

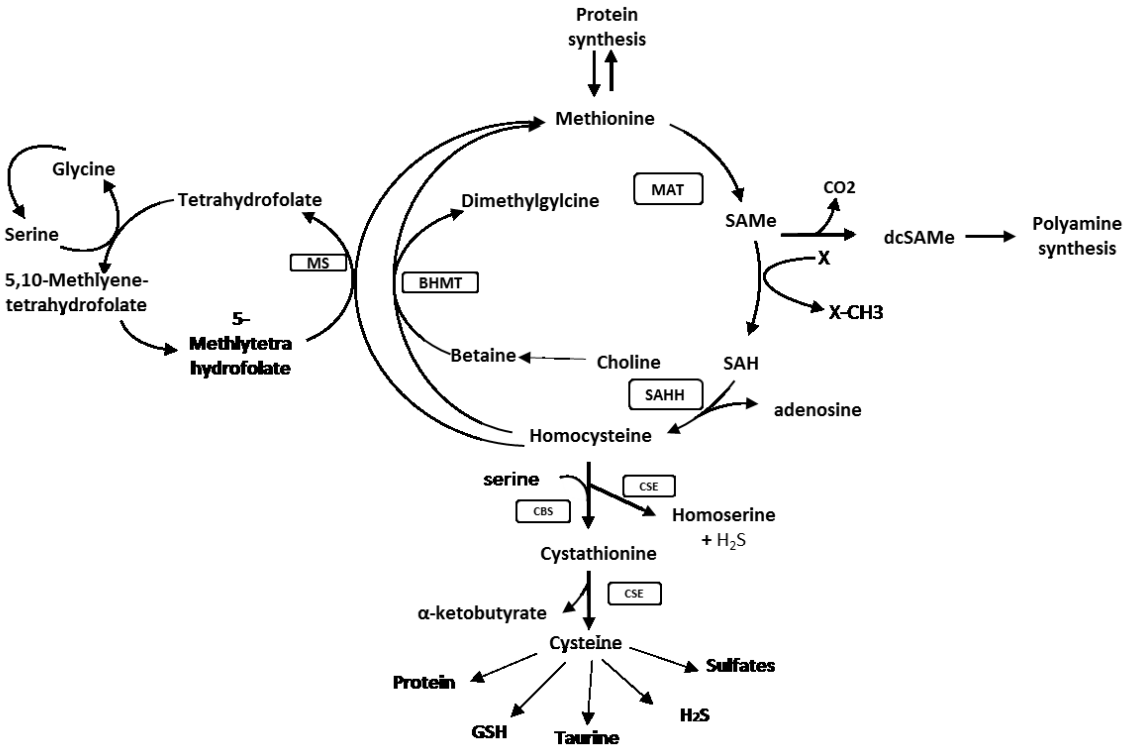


Figure 1.4 Summary of cysteine biosynthesis from methionine via the methionine cycle and trans-sulfuration pathway.
Abbreviations: BHMT: Betaine homocysteine methyl transferase; CBS=cystathionine beta synthase; CSE: cystathionine gamma lyase; dcSAMe: decarboxylated s-adenosyl methionine; MAT: methionine adenosyl transferase; MS: methionine synthase; SAHH:S-adenosyl homocysteine hydrolase; SAMe: s-adenosyl methionine

Taurine is a product of cysteine which is predominantly synthesised in humans by the oxygenation of cysteine to cysteine sulfinate by cysteine dioxygenase, followed by decarboxylation to hypotaurine *via* cysteine sulfinate decarboxylase and dehydrogenation to taurine *via* taurine dehydrogenase (Hayes

and Sturman 1981; Jurkowska et al. 2015). Taurine can also be synthesised *via* cysteamine in a reaction involving the breakdown of coenzyme A, which is then oxidized to hypotaurine (E. Dominy et al. 2007). Alternatively, taurine can be synthesised by decarboxylation of cysteic acid in a pathway not including hypotaurine (Hayes and Sturman 1981), as shown in Figure 1.5. Mammals are unable to metabolise taurine significantly, so it is excreted *via* conjugation with bile acids or in urine *via* the kidney (Hayes and Sturman 1981). Primary bile acids are conjugated with either glycine or taurine *via* the enzyme bile acid Coenzyme A: amino acid *N*-transferase (Yamazaki et al. 2013). In rats, where taurine-conjugated bile acids are favoured due to a high abundance of taurine, the ratio of taurine to glycine-conjugated bile acids has been shown to be altered in response to hepatotoxins and appears to be related to changes in taurine and glutathione concentrations. (Yamazaki et al. 2013). Taurine also has a number of other functions in the cell including maintaining membrane potentials, improving mitochondrial function, antioxidant properties, detoxification and links to obesity and type 2 diabetes (Lambert et al. 2015; Rosa et al. 2014). Taurine concentrations may alter methionine metabolism and the trans-sulfuration pathway, whilst taurine supplementation has been shown to alter concentrations of methionine, cysteine, taurine, hypotaurine, SAH, SAMe and GSH in rats after chronic ethanol treatment compared to ethanol alone (Yang et al. 2009). Cysteine dioxygenase (CDO) knockout mice have also been shown to have significantly altered cysteine metabolism, with hypotaurine concentrations being significantly decreased by CDO knock while those of cysteine and H_2S were significantly increased (Roman et al. 2013). A recent study found that the synthesis of both taurine and hypotaurine was inhibited by the cystathionine-γ-lyase inhibitor propargylglycine (PPG) (Jurkowska et al. 2015). There was a significant decrease in taurine and hypotaurine concentrations in wild type cells treated with PPG, and also in CDO knockout cells with and without PPG. As would be expected, there was accumulation of homocysteine and cystathionine which are upstream of the inhibition of PPG in the pathway (Jurkowska et al. 2015). Taurine and its related sulfur-containing metabolites downstream of cysteine are likely to be altered after APAP-induced GSH depletion and to have a toxic impact on the cells. Taurine supplementation has also been shown to protect against

APAP-induced hepatotoxicity in rodent models *in vivo* and *in vitro*, (Das et al. 2010; Waters et al. 2001) which is proposed to be due to increasing cysteine availability for GSH biosynthesis, and the antioxidant effects of taurine (Pushpakiran et al. 2004) (although the evidence for antioxidant nature of taurine is mixed (Aruoma et al. 1988)), and the potential inhibition of CYP2E1 by taurine-conjugated bile acids (Kerai et al. 1998). Hypotaurine concentrations have also been found to be reduced after APAP treatment in the mouse (Kyriakides 2016). Hypotaurine has been shown to have a protective effect in APAP overdose with similar efficacy to NAC (Acharya and Lau-Cam 2010) and is thought to have antioxidant properties (Aruoma et al. 1988).

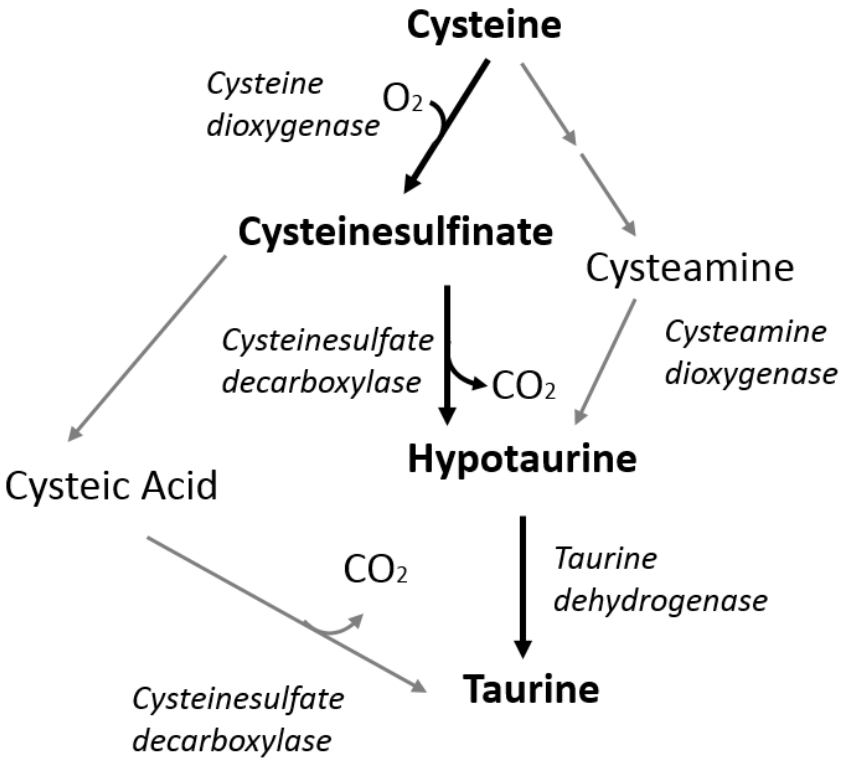


Figure 1.5 Summary of the hepatic biosynthesis of taurine from cysteine.

1.4 Biomarkers for APAP induced liver injury and general hepatic GSH depletion

1.4.1 Current biomarkers

In current clinical practice there are a few biomarkers which can be used to detect drug induced liver injury. To detect hepatocellular damage, the most commonly used markers were first discovered to be elevated in liver injury the 1950s and include the transaminases alanine aminotransferase (ALT)

and aspartate aminotransferase (AST) (Karmen et al. 1955). Both AST and ALT are abundant in the liver, and their increased presence in serum after liver injury is thought to be due to leakage from hepatocytes following cell death. This limits the value of ALT and AST as these biomarkers are only able to detect liver injury after cell death has already begun (Giannini et al. 2005; McGill 2016). Alkaline phosphatase (ALP) and total bilirubin (TBil) are used to detect bile clearance or bile duct injury (cholestasis) (Giannini et al. 2005), and ALT concentrations combined with TBil clearance are used to assess acute liver injury (Zimmerman 1968). Tests which are known as "liver function" tests are based on serum albumin concentrations and the prothrombin time, or international normalised ratio (INR). Increased INR means that the clotting time of the blood is increased due to reduced hepatic synthesis of blood clotting Factors II, V, VI, X. The synthesis of albumin is decreased following liver injury and in liver failure serum albumin concentrations are decreased (Giannini et al. 2005). ALT is the most commonly used of these biomarkers, however it is not organ specific for liver failure and, as indicated above, may be elevated only after liver injury has already occurred (Al-Hourani et al. 2013), reducing its value. The limited value of ALT means that and therefore new, prognostic, biomarkers are needed which are specific for drug induced liver injury (DILI), and which are sensitive to early changes in response to toxicity (Clarke et al. 2016)

1.4.2 New biomarkers for APAP induced liver injury

Due to the lack of biomarkers which are specific for liver injury, and even fewer that are specific for DILI, there has been much recent interest in a number of potential biomarkers which appear specific and sensitive at early time points. One such potential biomarker is micro RNA 122 (miR-122) which is a miRNA which is highly expressed and specific to the liver (Wang et al. 2009). MiR-122 has been found to correlate with ALT and has been suggested to be more sensitive at predicting liver injury than ALT (Antoine et al. 2013; Thulin et al. 2014). Other biomarkers which are currently undergoing investigation as mechanistic biomarkers for cell death include high mobility group box 1 (HMGB1) protein (Antoine et al. 2009), a chromatin binding protein which is released from cells during necrosis triggering the innate immune system (Scaffidi et al. 2002) and Keratin 18, which is released passively

during necrosis, or in a caspase-cleaved form during apoptosis (Wieckowska et al. 2006). These new biomarkers have been shown to correlate with ALT and to be increased in response to APAP induced liver injury (Antoine et al. 2013; Dear et al. 2018). However, these biomarkers are not specific to GSH depletion, instead providing information on the mode of cell death and immune system response. Biomarkers which are able to directly relate to GSH biosynthesis and APAP metabolism may provide information on APAP-induced liver injury, and that of molecules with a similar mechanism of toxicity, at early time points.

1.4.3 5-Oxoproline and ophthalmic acid as potential biomarkers

Previous investigations have found that 5-OP and OA may both be putative biomarkers of GSH depletion, and therefore of APAP toxicity. As previously discussed, OA is synthesised using the same enzymes as GSH, GCL and GS, and appears to increase during APAP toxicity in mice (Soga et al. 2006) and in a systems biology model based on human derived liver cells (Geenen et al. 2012; Geenen et al. 2013). Attempts to assess the utility of OA as a biomarker of APAP-induced liver injury can be translated to a clinical setting have not been entirely successful because of difficulties in measuring low concentrations of OA in plasma/serum. In a retrospective study of patients comparing APAP overdose survivors to non-survivors, the number of patients in which OA was detectable was compared between the two groups, and OA was detectable in more patients in the non-survival group compared to the survival group, and the concentrations in non-surviving patients were higher. However, OA gave no significant improvement over currently used biomarkers (Kaur et al. 2015). Similarly, 5-OP was suggested as a biomarker of GSH depletion by Geenen et al. (2012, 2013) and urinary 5-OP increases have previously been seen in the rat following APAP dosing (Ghauri et al. 1993). There is some evidence of 5-OP increases in cases of APAP overdose in patients, often linked to metabolic acidosis, (Alhourani et al. 2018; Armenian et al. 2012; Croal et al. 1998) and this topic has been systematically reviewed (Liss et al. 2013). Although some of these cases have been linked to in-born errors of metabolism or were cases where the patient was also receiving antibiotic treatment (Croal et al. 1998; Rolleman et al. 2008; Tailor et al. 2005). There is much evidence for 5-OP increases

following APAP overdose due to the number of cases reporting 5-oxoprolinurea. Some of these APAP-related cases showed elevated blood concentrations of 5-OP (Liss et al. 2013), with some cases found in blood from patients without metabolic acidosis. Further investigations in animal models seem warranted for this potential mechanistic biomarker of GSH depletion and APAP toxicity.

1.5 Methodology

A number of different analytical approaches were used to acquire data for use in the research described in this thesis. Predominately, the methods used for this research were "targeted", as either APAP metabolism or GSH pathway metabolites were being measured to satisfy pre-determined hypotheses. A proton nuclear magnetic resonance (^{1}H-NMR) spectroscopy-based "un-targeted" metabonomics approach was taken for the initial analysis of samples in the porcine model of APAP induced liver injury described in Chapter 5. Following the initial profiling, targeted techniques were then used to quantify particular metabolites of interest. The "targeted" analyses consisted of liquid chromatography (LC) coupled to tandem mass spectrometry (MS/MS). Specifically, the liquid chromatography employed was "Ultra(-High) Performance Liquid Chromatography" (UHPLC).

1.5.1 NMR spectroscopy

NMR spectroscopy is an analytical technique which can be applied to the profiling of biofluids, tissue extracts, and also even solid/semi-solid tissues through magic angle spinning NMR spectroscopy (Beckonert et al. 2010; Beckonert et al. 2007; Nicholson et al. 1995). NMR, particularly ^{1}H NMR, spectroscopy is able to provide structural information on a large number of metabolites and features simultaneously and is said to be "non-destructive" (Beckonert et al. 2007). The basic underlying basis of NMR spectroscopy is related to the "spin" that certain nuclei have, including ^{1}H and ^{13}C, which can be reversed upon the application of an external electromagnetic field and, as the nucleus return to its base state, energy is emitted at a radio frequency which is then detected. The resonance of a nucleus depends on factors such as shielding from surrounding nuclei in the molecule, which gives differing chemical shifts. For metabolic profiling pulse sequences are applied to the sample within the magnetic field and the Fourier transformed resonances with chemical shift in parts per million (ppm) are plotted

against the signal intensity (i.e. number of protons with identical chemical shift) to produce a spectrum. The spectrum is then integrated to give relative quantities of each resonance which can then be identified. The use of NMR spectroscopy, and particularly ^{1}H-NMR spectroscopy, for metabolic profiling in biological matrices is well described, as are the sample preparation techniques and pulse sequences which are used (Beckonert et al. 2007; Dona et al. 2014; Nicholson et al. 2002). For the work contained in this thesis, ^{1}H-NMR spectroscopy was applied to plasma, urine, liver and kidney extracts. For urine and tissue extracts a standard pulse sequence to suppress solvents, which is a 1-dimensional adaptation of Nuclear Overhouser Effect Spectroscopy (NOESY), NOESYpr1d sequence (Beckonert et al. 2007; McKay 2011) was used. For plasma the Carr-Purcell-Meiboom-Gill (CPMG) sequence was applied in order to reduce signals from lipoproteins and proteins (Carr and Purcell 1954; Meiboom and Gill 1958).

APAP metabolism and APAP-induced toxicity has been investigated using ^{1}H-NMR Spectroscopy in numerous studies previously (Bales et al. 1988; Bales et al. 1984; Coen et al. 2003; Coen et al. 2004; Ghauri et al. 1993; Kyriakides 2016; Nicholls et al. 1995; Nicholls et al. 1997)

1.5.2 UHPLC-MS/MS

LC-MS is a commonly used method for the separation and consists of a system where analytes of interested are separated on a stationary phase contained within a column which is generally packed with a silica-derived material. This “stationary phase” is modified in various ways in order to give different properties based on the analytes of interest and type of chromatography (Dettmer et al. 2007; Theodoridis et al. 2012). The mobile phase usually consists of an organic and aqueous solvent mixture. The solvent is pumped through the column using a high-pressure solvent delivery chromatography system. Samples containing the analytes of interest are injected into the system and are separated based on their ability to partition between the mobile and stationary. Elution is controlled by alterations the relative proportions of the organic modifier content of the mobile phase. Following separation and elution, analytes are ionised and detected using MS.

1.5.2.1 UHPLC

Advances in technologies for liquid chromatography instrumentation have allowed the development of UHPLC, a technique which improves the resolution of chromatography compared to previously used techniques (Wilson et al. 2005). UHPLC involves using a stationary phase with a sub-2 µM–particle diameter, which, whilst requiring much higher pressures than the previously used ca. 3 µM phases, enables the development of rapid, high resolution, methodologies for analyte separation.

For the purpose of this thesis, two types of chromatography were used. The methodology used for the APAP and metabolite-based assay was reversed-phased (RP) chromatography is a technique commonly used for both global and targeted metabolic profiling (Dettmer et al. 2007; Theodoridis et al. 2011; Theodoridis et al. 2012; Want et al. 2013). Reversed-phase chromatography was developed by "reversing" the phases of "normal phase" chromatography, which consisted of a polar stationary phase and a non-polar mobile phase, while reversed-phase chromatography consists of a non-polar stationary phase and a polar mobile phase. A better term for RPLC would be "partition chromatography, as this describes the mechanism whilst normal phase LC is more correctly adsorption chromatography. RPLC commonly uses a stationary phase such as a C18 derivatised silica and a mobile phase with a high proportion water and lower percentage of either acetonitrile (CH_3CN) or methanol (MeOH) content (Dettmer et al. 2007).

Hydrophobic interaction liquid chromatography (HILIC) was the second type of chromatography used for the research presented in this thesis. This was designed for the separation of highly polar analytes and was first employed in 1975 (Linden and Lawhead 1975). Columns contain very hydrophilic stationary phases; usually bare silica or silica chemically modified with hydrophilic groups such as amides; these can be coated with polymers. Alpert et al. (1990) suggested that water is attracted to the polar groups on the stationary phase which forms a water coating on the surface. Starting conditions for HILIC separations usually contain a high proportion (70% or more) of an organic solvent such as CH_3CN (Gama et al. 2012). Therefore polar/hydrophilic metabolites in the mobile phase partition into the aqueous layer on the stationary phase and are retained (Alpert 1990). The

interactions between analytes, mobile phase and stationary phases in HILIC are complex and include hydrogen bonding, dipole-dipole interactions and electrostatic interactions, and there is not a full consensus on the impact of these on retention, or the exact mechanisms of retention (Buszewski and Noga 2012). HILIC also has some draw backs including analyte drift and poor peak shapes (Buszewski and Noga 2012; Tang et al. 2016). HILIC has previously been used in targeted assays for the quantification of metabolites related to GSH metabolism (Lafaye et al. 2005) and was therefore the separation of choice for the development of the GSH assay. Other methodologies for quantifying polar metabolites rely on the derivatisation of these for subsequent RP analysis, which does not allow quantification of free thiols (Gray et al. 2017).

1.5.2.2 Mass Spectrometry

Mass spectrometry, as used in bioanalysis, is a technique that can detect the mass to charge ratio (m/z) of ions and can quantify these by measuring the signal intensity against a calibration curve covering a range of concentrations for the targeted analyte. It is commonly paired with separation techniques such as LC and capillary electrophoresis (CE), or gas chromatography (GC) for the detection of xenobiotics and endogenous compounds. To measure the desired analytes the metabolites separated by LC must first to be converted to ions in the gaseous phase which is done using various ionisation techniques. For the work of this thesis electrospray ionisation (ESI) was used. This consists of a highly charged needle with opposing charged plate, so as analytes dissolved in the mobile phase flow through the needle, this is charged by the electric field gradient and the opposite charge of the opposing plate draws the ions into the mass spectrometer (Kebarle and Verkerk 2009). All experiments undertaken for this thesis were performed using a “triple quadrupole” mass spectrometer (TQ-S). This spectrometer consists of a quadrupole (or mass analyser), a collision cell, followed by a second analyser. The quadrupole analysers create an electromagnetic charge which can separate ions by m/z values, or they can be used non-selectively in scanning mode. In the collision cell, parent ions collide with argon gas to form daughter ions by collision-induced dissociation (Maher et al. 2015). When developing targeted UHPLC-MS/MS assays, initially parent ions are detected by scanning at the first

analyser, after which the first quadrupole selects for the parent ion and the second quadrupole operates in scanning mode to detect the daughter ions. Following the selection of the daughter ions to be used for identification and quantification, and the selection of method parameters, the TQ-S is operated with both quadrupoles fixed so only ions of interest are detected (Maher et al. 2015), which is known as multiple reaction monitoring (MRM) mass spectrometry and provides sensitive and specific quantification of the ions of interest.

1.6 Summary

In order to understand APAP metabolism and GSH depletion, ultra-high-performance liquid chromatography tandem mass spectrometry (UHPLC-MS/MS) methods were developed. Initially a method to quantify APAP and its major metabolites in plasma was developed and validated to FDA standards and applied to a model of APAP administration to the rat. A second UHPLC-MS/MS method which had previously been partially developed was further investigated for matrix effects, and the sample preparation protocol further developed. These methods were applied to samples from a mouse model of APAP overdose, to identify the relationship between GSH depletion and metabolism, and the impact of NAC treatment on these. In addition, APAP and endogenous metabolism were investigated in a porcine model of acute liver failure using ^{1}H-NMR spectroscopy for the analysis of biofluids and tissue extracts. The circulating APAP and GSH metabolites were then determined by the application of these UHPLC-MS/MS methods. The same methods were then also applied to clinical samples to quantify APAP and GSH-related metabolites to understand their possible correlation with the severity of liver disease in patients. An overview of the progression of APAP overdose to liver injury, and how the work presented in this thesis will measure both endogenous and xenobiotic metabolites to form a picture of this toxicity, and to find evidence for potential biomarkers, is summarised in Figure 1.6 below.

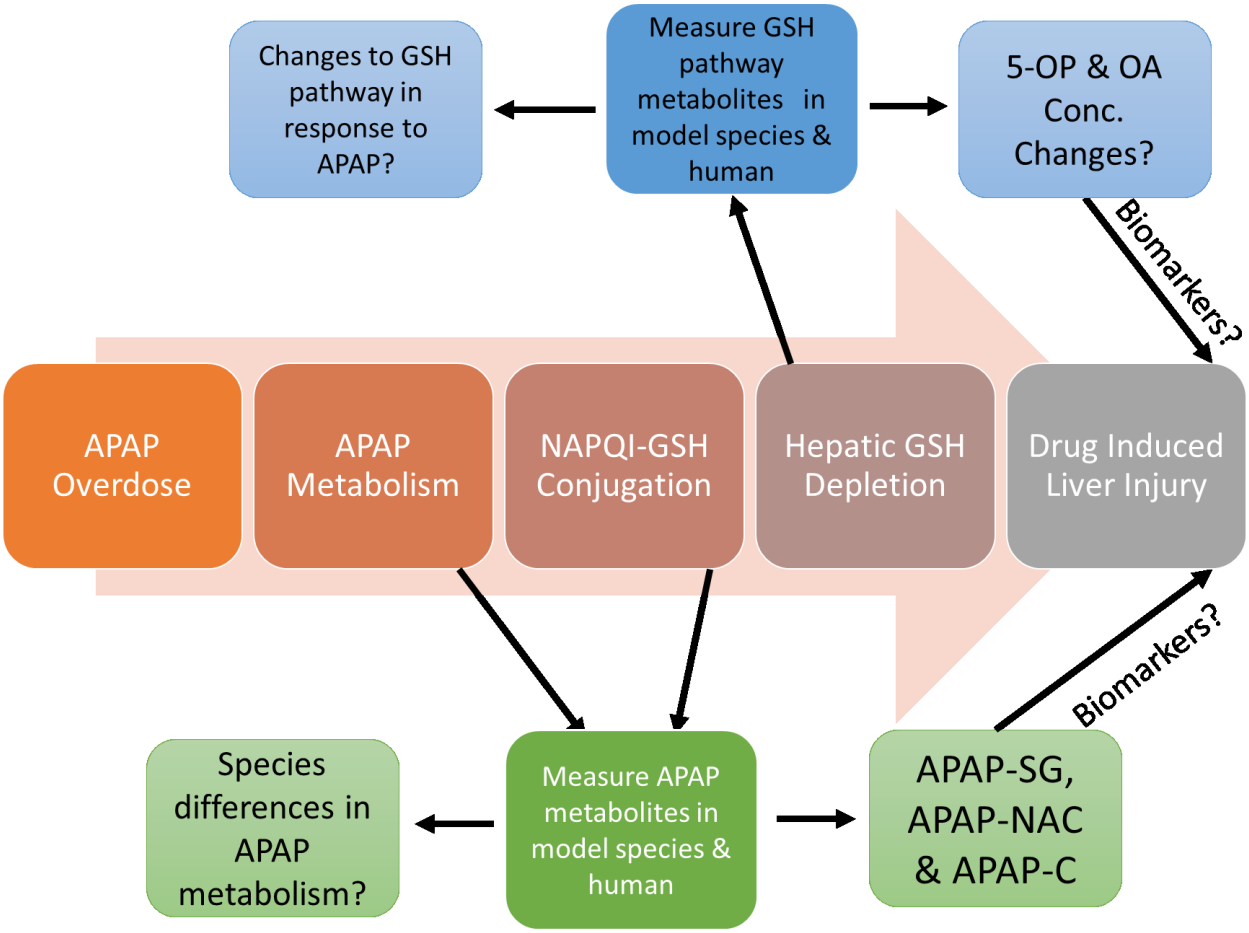


Figure 1.6 Overview of key events in APAP metabolism and toxicity, and the approach of the research presented in this Thesis to find potential biomarkers of APAP induced liver injury
Abbreviations: APAP: paracetamol; APAP-C: paracetamol cysteinyl conjugate; APAP-NAC: paracetamol n-acetyl-cysteine conjugate; APAP-S: paracetamol sulfate conjugate; APAP-SG: paracetamol glutathione conjugate GSH: glutathione; NAPQI: n-acetyl-p-benzoquinone imine; OA: ophthalmic acid; 5-OP: 5-oxoproline.

2 Development of a UHPLC-MS/MS method for the analysis of paracetamol and seven metabolites in rat, pig, mouse and human plasma or serum.

2.1 Introduction

2.1.1 Hypothesis

That a reproducible UHPLC-MS/MS assay could be developed that uses a lower quantity of sample and takes less time per injection than existing methods. That the method could be proved to be accurate and precise for measuring APAP and its metabolites in biofluids from various species.

2.1.2 Rationale and aims

Paracetamol metabolism varies between species and between individuals and may have significant effects on the differential toxicity seen between species, and outcomes of overdose in human patients. In order to investigate the effects of paracetamol toxicity across animal models and human paracetamol overdose, this method was developed to accurately quantify concentrations of circulating paracetamol and its major metabolites in a number of species. The method was originally developed and validated in rat plasma, with later cross-validation for applications in human, porcine and mouse plasma or serum. Although previous methods had been developed to measure these metabolites, this method was developed in order to use both a short chromatographic separation of 7.5 minutes, and a small sample size of 5 µL, with a simple sample preparation for rapid, high throughput analysis. In order to test the utility of the method for sample analysis, the method was then applied to samples from a single dose APAP administration in the rat, at 500 and 1500 mg/kg doses.

2.1.3 Background

As discussed in depth in Chapter 1, APAP overdose is a major cause of death in the United States and UK, causing half of all ALF cases (Makin et al. 1995; Ostapowicz et al. 2002; Perkins 2006). The overall mechanism responsible for the drug induced liver injury (DILI) produced following APAP overdose is known to be the result of the inability of the major metabolic pathways of detoxification (glucuronidation and sulfation) to fully metabolise the drug. Overdose of APAP results in the bioactivation of the drug, *via* oxidative metabolism by CYP enzymes, to the highly reactive intermediate NAPQI (Dahlin et al. 1984). Once formed, NAPQI is usually detoxified by reaction with hepatic GSH, but following GSH depletion, the metabolite will react with cellular macromolecules

eventually resulting in hepatic cell death (Dahlin et al. 1984). As an important model of reactive metabolite-induced drug induced liver injury, and due to the clinical impact of the number of hospital admissions and deaths relating to APAP overdose, understanding the relationship between APAP metabolism and toxicological outcome is an important area of research, and crucial to the work of this Thesis. Numerous assays for measuring APAP, in various biofluids, either alone or with metabolites, have been described to support both therapeutic monitoring and studies in animals, as detailed below. There remains the need for comprehensive, rapid and sensitive methods for the determination of the drug and its various conjugative and reactive-metabolite-derived metabolites. Providing sufficient sample is available, LC with UV detection, can be used to detect APAP and its metabolites (Di Girolamo et al. 1998; Jensen et al. 2004; Vertzoni et al. 2003), however the sensitivity and specificity of this approach is limited. As a result, a number of LC-MS-based methods have been developed that offer the opportunity to reduce sample size and improve specificity compared to LC-UV. For some of these methods, metabolite coverage was limited to the drug and its glucuronide and/or sulfate conjugates (Gicquel et al. 2013; Hewavitharana et al. 2008; Tan et al. 2012). However, other LC-MS-based methods also provide coverage of minor GSH-derived and other metabolites in both plasma and urine (Cook et al. 2015; An et al. 2012) Recently, two further methods have been described offering validated HPLC or UHPLC-MS/MS methods that enable the quantification of APAP, its glucuronide (APAP-G), sulfate (APAP-S), glutathione conjugate (APAP-GS), cysteinyl conjugate (APAP-C), N-acetylcysteinyl conjugate (APAP-NAC) (Flint et al. 2017; Lammers et al. 2017) and 3-methoxy conjugate (APAP-OMe) (Lammers et al. 2017) in human plasma. Chemical structures of the key APAP metabolites are shown in Figure 1.2.

In order to study the circulating APAP metabolites present in animal models, specifically the rat, a UHPLC-MS/MS method was required. Initially the method of An et al. (2012) was used as the basis for method development. Due to a lack of reproducibility of this method, and the need for a fast gradient and reduced sample volume, a new method was devised and validated. The method was initially validated in rat plasma and following the success of the assay it was further developed for use with

other biofluids, in order to provide quantitative APAP metabolism data for this Thesis. In this Chapter, the "fit for purpose" validation of the gradient reversed-phase UHPLC-MS/MS method for the quantification of APAP, APAP-S, APAP-G, APAP-C, APAP-NAC and APAP-SG metabolites, as well as the monitoring of the APAP-OMe and PAP-G is described.

2.2 Methods

2.2.1 Chemicals and reagents used throughout experiment

APAP, APAP-G (sodium salt) and the deuterated internal standard (IS) APAP-d_3 were purchased from Sigma Aldrich (Gillingham, UK). APAP-S (potassium salt), APAP-C (trifluoroacetic acid salt), APAP-NAC (disodium salt), glutathione APAP-SG (disodium salt) and 3- APAP-OMe conjugates and deuterated internal standards, APAP-S-d3 (potassium salt), APAP-G-d3 (sodium salt), APAP-C-d5 (trifluoroacetic salt) APAP-NAC-d5 (sodium salt) and APAP-SG-d_3 (disodium salt), were purchased from Toronto Research Chemicals (Toronto, Canada). PAP-G was purchased from SantaCruz Biotechnology (Dallas, Texas, USA). Optima grade water was obtained from Fisher Scientific (Leicester, UK), LC-MS grade solvents and formic acid (FA) were from Sigma Aldrich. Masses of each standard used in the development and validation of the method, with and without counter ions, and the conversion factor used are given in Table 2.1

Table 2.1 Salt Conversion Factors for analytical standards and internal standards.

Compound	Counter ion	Average Mass without salt	Average Mass with salt	Conversion factor[a]
APAP-G	Na	327.2867	349.2685	0.94
APAP-G-d3	Na	330.3052	350.2711	0.94
APAP-S	K	231.2258	269.3161	0.86
APAP-S-d3	K	234.2442	272.3346	0.86
APAP-C	TFA	254.3055	366.3129	0.69
APAP-C-d5	TFA	259.3363	371.3437	0.70
APAP-NAC	2xNa	312.3415	356.3052	0.88
APAP-NAC-d5	Na	317.3723	339.3542	0.94
APAP-SG	2 x Na	456.4702	500.4338	0.91
APAP-SG-d3	2 x Na	459.4886	503.4523	0.91

[a]Calculated as average mass without salt divided by the average mass with salt
Abbreviations: APAP: paracetamol; APAP-C: paracetamol cysteinyl conjugate; APAP-G: paracetamol glucuronide conjugate; APAP-NAC: paracetamol n-acetyl-cysteine conjugate; APAP-OMe: 3-methoxy paracetamol; APAP-S: paracetamol sulfate conjugate; APAP-SG: paracetamol glutathione conjugate.

2.2.2 Chromatography

The chromatographic separation was performed on an Acquity Chromatography (UHPLC) system using a 2.1 x 100 mm 1.8 µm 100A C18 Acquity HSS T3 column (Waters Corporation, Manchester, UK) with a multi-linear reversed-phase gradient with mobile phases consisting of water and 0.1% (v/v) FA (solvent A) and methanol and 0.1% (v/v) FA (solvent B). The gradient was performed over 7.5 minutes at a flow rate of 0.6 mL/min at 40°C. Starting conditions were set at 5% solvent B for 0.5 min, increasing linearly to 7% by 1.85 minutes then to 8% by 1.9 min, then 10% by 2.5 min, 16% by 4.0 min, 25% by 5 min increasing rapidly to 95% by 5.1 min to wash the column. The solvent composition was held at 95% B for 0.9 minutes before returning to 5% B at 6.1 min for re-equilibration (1.4 min). The resulting analysis time was 7.5 min/sample. In between samples the sample loop was subject to both weak and strong washes of 90:10 water/MeOH (v/v) and 100% isopropanol, respectively. The chromatography is detailed in Table 2.2 and the reconstructed total ion chromatogram for all metabolites is shown in Figure 2.1.

Table 2.2 Chromatographic gradient for separation of metabolites

Time (minutes)	% A (H_2O + 0.01% FA)	% B (MeOH + 0.01% FA)
0	95	5
0.5	95	5
1.85	93	7
1.9	92	8
2.5	90	10
4.0	84	16
5.0	75	25
5.1	5	95
6.1	95	5

Abbreviations: FA: formic acid

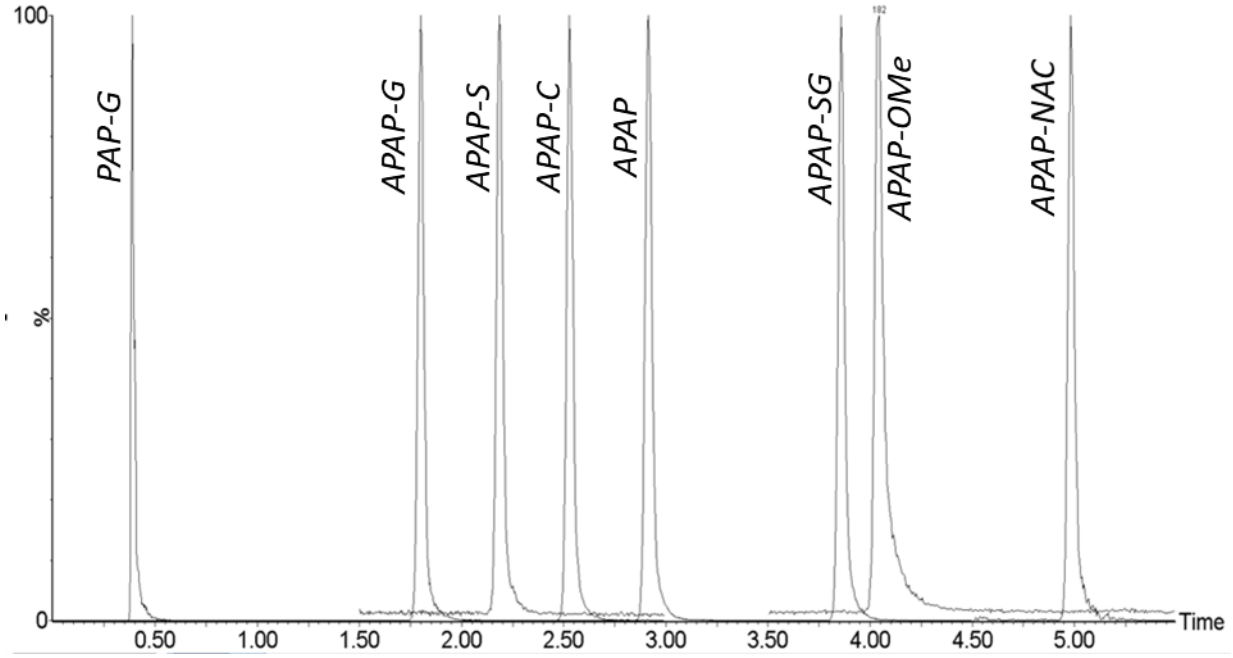


Figure 2.1 A reconstructed ion chromatogram for all standards following spiking into plasma, extracted with MeOH (+ 0.1% FA), and diluted with H_2O (+ 0.1% FA) obtained using the optimised chromatographic system, all normalised to the highest peak
Abbreviations: APAP: paracetamol; APAP-C: paracetamol cysteinyl conjugate; APAP-G: paracetamol glucuronide conjugate; APAP-NAC: paracetamol n-acetyl-cysteine conjugate; APAP-OMe: 3-methoxy paracetamol; APAP-S: paracetamol sulfate conjugate; APAP-SG: paracetamol glutathione conjugate; FA: formic acid; PAP-G: p*-aminophenol glucuronide.*

2.2.3 Mass spectrometry

MS/MS data were acquired using a Xevo tandem quadruple (TQ-S) mass spectrometer (Waters Corporation, Manchester, UK). MS/MS Detection was via ESI in positive ion mode using MRM for the quantification of each compound. MS conditions for each analyte were determined via direct infusion of individual analytes. Nitrogen was used as the desolvation gas and argon was used as the collision gas. The following generic source conditions were used: capillary voltage, 3 kV; source offset, 30 V; desolvation temperature, 500°C; source temperature, 150°C, desolvation gas flow, 1000 L/hr; cone gas flow, 150 L/hr; nebulizer gas, 7.0 bar; collision gas, 0.13 mL/min. See Table 2.3 for individual parameters for each compound used across all experiments.

Table 2.3 Mass spectrometry and liquid chromatography data for APAP and metabolites quantified

Compound	Parent ion (m/z)	Product ion for quantification (m/z)	Cone voltage (V)	Collision voltage (V)	RT (minutes)
APAP	152.1	110.1	30	16	2.91
APAP-d3	155.1	110.9	30	20	2.89
APAP-C	271.0	139.9	34	24	2.53
APAP-C-d5	276.2	142.8	34	26	2.50
APAP-S	232.1	110.1	30	22	2.17
APAP-S-d3	235.0	111.0	30	22	2.15
APAP-G	328.1	152.1	20	14	1.79
APAP-G-d5	353.2	177.1	42	16	1.77
APAP-NAC	335.1	152.0	6	16	4.98
APAP-NAC-d5	340.2	152.0	34	18	4.96
APAP-SG	457.2	139.9	30	36	3.85
APAP-SG-d3	460.2	331.1	32	14	3.81
PAP-G	308.3	199.05	2.0	12	0.37
APAP-OMe	182.2	108.08	16	20	4.04

Abbreviations: APAP: paracetamol; APAP-C: paracetamol cysteinyl conjugate; APAP-G: paracetamol glucuronide conjugate; APAP-NAC: paracetamol n-acetyl-cysteine conjugate; APAP-OMe: 3-methoxy paracetamol; APAP-S: paracetamol sulfate conjugate; APAP-SG: paracetamol glutathione conjugate; PAP-G: p*-aminophenol glucuronide; RT: retention time.*

2.2.4 Method validation

Method validation was based on the recommendations contained in the FDA "Guidance for industry" on Bioanalytical Methods (FDA 2018). A three-day validation was undertaken for rat plasma and the resulting method was then cross validated to human and pig plasma and mouse serum as described below.

2.2.4.1 Linearity

Linearity was determined from the evaluation of calibration curves generated from calibration standards with acceptable deviation (≤15% over the range of the standard curve and ≤20% at the lower limit of quantification) from their nominal values, using least squares linear regression with weighting 1/x or $1/x^2$ for APAP-SG. Linearity was assessed using the R^2 correlation coefficient, which was required to be >0.99 over the three days of the validation.

2.2.4.2 Precision and accuracy

Assay precision was determined using quality control samples (QCs) including low quality control (LQC), mid quality control (MQC), high quality control (HQC) and the lower limit of quantification (LLOQ) and upper limit of quantification (ULOQ) QCs. The nominal concentrations were decided based on the guidelines, to reflect potential sample concentrations across the range of the method. Six replicates at each of the concentrations of the LLOQ QC, LQC, MQC, HQC and ULOQ QC samples were analysed on all three days of the full validation for rat plasma and one day for each of the cross-validation studies. The intra-assay precision was determined using the coefficient of variance of the mean (CV) of the six replicates on one day. The inter-assay precision was determined as the CV of each set of QC samples over three batches (n=18) at each QC concentration. The inter-assay accuracy was described by the mean deviation of the QCs over three days (n=18) at each QC concentration. For both intra- and inter-assay assessments the acceptable CV was set at ≤15% for all QCs except the LLOQ QC which was set at ≤20%. A minimum of 66.7% of the QCs were required to fall within these limits for acceptance.

2.2.4.3 Carryover

Carryover was assessed with a double blank analysed immediately after an ULOQ calibration standard and was considered acceptable if the response for any of the analytes was ≤20% of the average response of the LLOQ standards. Carryover for the IS was deemed acceptable if the response for the double blank sample was ≤5% of the average response from the acceptable calibration standards (including the single blank).

2.2.4.4 Recovery

All analytes and internal standards were spiked into six individual lots of blank plasma (or five of serum) before and after protein precipitation at both the LQC and HQC concentrations. Peak areas of analytes at the LQC or HQC spiked in before extraction were compared to those from analytes spiked in after extraction, calculated as a percentage recovery.

2.2.4.5 Matrix effects

Matrix effects were assessed by spiking internal standards and standards for each analyte into six blank matrix samples of plasma (five of serum) after protein precipitation, with six replicates at the concentration of the LQC and six at the concentration of the HQC (referred to as over-spiked samples). Reference solutions were prepared by spiking internal standards and standards into water to reflect the LQC and HQC concentrations. Matrix effects were calculated by comparing the peak area for each standard or IS in the reference solution to the over-spiked samples. The IS normalised matrix factor was calculated by dividing the matrix factor calculated from the unlabelled standard by the matrix factor calculated from the labelled IS. To be acceptable the CV of the IS normalised matrix factor at each concentration was required to be ≤15% at LQC and HQC QC concentrations.

2.2.4.6 Selectivity and specificity

The method was evaluated for selectivity by assessing interference from the matrix in analyte free matrix (double blank samples), and for selectivity between analytes and internal standards by analysing blank matrix samples containing individual metabolites or IS only. Six double blanks containing none of the analytes were processed. Interference was defined as any response at the retention times of the analytes with a response ≥20% of the mean LLOQ response. For IS, interference was defined as a response at the retention time of the IS with a response ≥5% of the average IS response in the calibration curve. To determine IS and analyte selectivity, three aliquots of the same lot of blank plasma were spiked with IS only or individual analytes at the ULOQ only. Interference with another analyte was defined as any response at the retention time of the analyte with a peak area ≥20% of the average LLOQ response. Any responses at the retention time of an IS in the individual analyte samples were considered interference if found to be ≥5% of the average IS response for that IS.

2.2.4.7 Stability of samples and solutions

Freeze thaw stability was measured by freezing six 20 µL aliquots of the freeze-thaw MQC 'stock solution' plasma and freezing these at -20 ^{o}C for an hour, after which all aliquots were allowed to thaw on the bench for 20 minutes, before all but one were returned to the freezer to refreeze. The

remaining thawed sample was further aliquoted into six 5 µL samples which were then prepared as stated in methods. The area of each of the MQCs after a freeze-thaw cycle was compared to the peak area of the six MQC samples prepared prior to freeze-thaw cycles. A further six 5 µL aliquots of the MQC plasma were not frozen, but were left on the bench top at room temperature for 4 hours, and then prepared as previously stated, the peak area of these six benchtop stability samples were compared to the MQC samples prepared at Time 0.

To assess the stability of the analytes in prepared samples over the course of the LC-MS analysis, six replicates of each QC were analysed, then left for 36 hours in the autosampler at 5°C and then re-assayed against a fresh calibration curve and the CV and bias calculated.

2.2.4.8 Dilution integrity

A dilution integrity QC (DIQC) sample was prepared at three times the concentration of the ULOQ. This DIQC was then diluted 1 in 10 independently six times (100 µL DIQC into 900 µL water). The diluted DIQC samples were then analysed as part of the validation and quantified taking into account the 1 in 10 dilution of the IS. In order to be acceptable, at least four of the six DIQCs were required to be ≤±15% of the nominal concentration, with an overall CV for the six QC samples of ≤15%.

2.2.4.9 Data analysis

The raw LC-MS/MS data were processed by the TargetLynx application package within MassLynx software (Waters Corporation). The raw data were mean smoothed and peak integration was performed using the ApexTrak algorithm.

2.2.5 Method validation in rat plasma

2.2.5.1 Rat plasma sample collection

Rat plasma samples were obtained from collaborators at AstraZeneca UK. Following a single oral administration of APAP at doses of 0, 500 or 1500 mg/kg (in 0.5% methylcellulose) to male Wistar Han (Crl:WI(Han)) (300-350 g). Blood samples (ca. 800 µL) were collected (at the indicated time points from the tail vein (in-life) or vena cava (24 hours terminal) into tubes containing lithium heparin. The plasma samples (200 µL) were obtained from blood which was centrifuged at 1200 *g* (4°C), with the samples then frozen and stored at -70 °C, or lower, until analysis. Rats were housed 3–5 per cage in

polycarbonate solid bottom cages (Tecniplast, Kettering, UK) with Tapvei® Aspen Chips and Sizzle-Nest bedding and Tapvei® small Aspen bricks and polycarbonate tunnels as enrichment (all supplied by Datesand, Manchester, UK). Animals were fed with RM1 (E) SQC diet (Special Diets Service, Witham, UK) *ad libitum*, were not fasted before administration, and had free access to 0.2 µM filtered municipal water. Environmental controls were set to maintain conditions of 19–23 °C and 55 ± 15% relative humidity, with a 12-hour light/dark cycle. Animals were sacrificed using halothane at the end of the studies. The study was performed by Drug Safety and Metabolism, AstraZeneca UK (all experiments were conducted in compliance with UK home office licences issued under the UK Animals [Scientific Procedures] Act 1986 after review by the local Ethics Committee).

2.2.5.2 Standard Curve and QC stock solution preparation

Stock solutions for the preparation of calibration curves and QCs for APAP and APAP metabolite standards were prepared in MeOH. These were prepared initially by weighing out 1 mg of each standard or IS and diluting in 1 mL 50:50 MeOH:H_2O (v/v) to produce 1 mg/mL stock solutions, which were later converted to their final concentration using the salt conversion factors listed in Table 2.1, to account for the weight of the salts.

Final concentrations of standard stock solutions were 500 µg/mL for APAP, 93.7 µg/mL for APAP-G, 85.9 µg/mL for APAP-S, 18.2 µg/mL for APAP-SG, 17.5 µg/mL for APAP-NAC and 13.9 µg/mL for APAP-C. These were prepared by mixing the 1mg/mL stock solution together as listed in Table 2.4 below. The initial dilution produced a top stock solution of 500 µg/mL for APAP, 100 µg/mL for APAP-S and APAP-G, and 20 µg/mL for APAP-NAC, APAP-SG and APAP-C (including the counter ion). This was then further diluted 1 in 10 by diluting 100 µL stock solution A with 900 µL MeOH to produce stock solution B as reported below. Stock solution B was then serially diluted to produce eight calibration standard stock solutions, at 100 x the final concentration of the standard curve, as displayed in Table 2.5. Stock solution B was also serially diluted to produce QC stock solutions which would also be diluted 1 in 100 upon sample preparation, as shown in Table 2.6. Six stock solutions were produced, with two potential LLOQ concentrations, as it was predicted that there may be some issues with background interference

for the metabolites at the lowest concentration level. The inclusion of two LLOQ concentrations meant that in the case of difficulties with the validation of the LLOQ QC, a higher LLOQ value could be used in the calibration curve.

Table 2.4 Preparation of stock solutions A and B for rat plasma validation.

Standard added (concentration)[a]	**Volume of stock solution[b] (µL)**	**Concentration in stock solution A[c] (µg/ml)**	**Final standard concentration[d] (µg/ml)**
APAP (1 mg/mL)	500	500	50.0
APAP-S (1 mg/mL)	100	85.9	8.59
APAP-G (1 mg/mL)	100	93.7	9.37
APAP-C (1 mg/mL)	20	13.9	1.39
APAP-NAC (1 mg/mL)	20	17.5	1.75
APAP-SG (1 mg/mL)	20	18.2	1.82
MeOH added	*240*	-	
Total Volume Stock Solution A	***1000***	**-**	

[a]Standards were diluted together with MeOH to produce a top stock solution A, which was diluted 1 in 10 to produce stock solution B. [b] Volume of individual standard stock solutions added to make up to 1 mL total in MeOH. [c]Concentration of each standard in stock solution A. [d] Final concentration of each standard in stock solution B, after 1 in 10 dilution.
Abbreviations: APAP: paracetamol; APAP-C: paracetamol cysteinyl conjugate; APAP-G: paracetamol glucuronide conjugate; APAP-NAC: paracetamol n-acetyl-cysteine conjugate; APAP-S: paracetamol sulfate conjugate; APAP-SG: paracetamol glutathione conjugate.

Table 2.5. Preparation of calibration curve standard solutions through serial dilution of stock solution B for rat plasma validation.

Stock solution[a]	**Stock solution used[b]**	**Volume of stock solution (µL)**	**Volume MeOH (µL)**	**Final concentration of individual calibration stock solutions[c] (µg/mL)**					
				APAP	**APAP-G**	**APAP-S**	**APAP-C**	**APAP-SG**	**APAP-NAC**
1 (B)	1 (B)	600	0	50.0	9.37	8.59	1.39	1.82	1.75
2	1 (B)	300	300	25.0	4.69	4.29	0.69	0.91	0.88
3	2	300	200	15.0	2.81	2.58	0.42	0.55	0.53
4	3	300	200	9.00	1.69	1.55	0.25	0.33	0.32
5	4	300	150	6.00	1.12	1.03	0.17	0.22	0.21
6	5	300	150	4.00	0.75	0.69	0.11	0.15	0.14
7	6	300	200	2.40	0.45	0.41	0.07	0.09	0.08
8	7	200	100	1.60	0.30	0.28	0.04	0.06	0.06

[a]Calibration standard stock solutions were numbered from 1 to 8, with number 1 being the ULOQ (also referred to as stock solution B), and number 8 being the LLOQ. [b]The stock solution 1–8 which was diluted. [c]Prior to adding to plasma and further dilution.
Abbreviations: APAP: paracetamol; APAP-C: paracetamol cysteinyl conjugate; APAP-G: paracetamol glucuronide conjugate; APAP-NAC: paracetamol n-acetyl-cysteine conjugate; APAP-S: paracetamol sulfate conjugate; APAP-SG: paracetamol glutathione conjugate.

Table 2.6 Preparation of QC standard stock solutions through serial dilution of stock solution B

QC stock solution	Stock solution used[b]	Volume of stock solution (µL)	Volume MeOH (µL)	Final QC stock solution concentrations[c] (µg/mL)					
				APAP	APAP-G	APAP-S	APAP-C	APAP-SG	APAP-NAC
ULOQ (B)	ULOQ (B)	1000	0	50.0	9.37	8.59	1.39	1.82	1.75
High	ULOQ (B)	800	200	40.0	7.50	6.87	1.11	1.46	1.40
Mid	High	250	750	10.0	1.87	1.72	0.28	0.37	0.35
Low	Mid	480	520	4.80	0.90	0.82	0.13	0.18	0.17
LLOQ 2	Low	500	500	2.40	0.45	0.41	0.07	0.09	0.08
LLOQ 1	LLOQ 2	500	250	1.60	0.30	0.28	0.04	0.06	0.06

[a]Stock solutions were produced for each QC level through dilution of the ULOQ stock solution (also referred to as stock solution B). [b]The stock solution which was diluted with MeOH at each level to form the stock solution. [c]Prior to adding to plasma and further dilution
Abbreviations: APAP: paracetamol; APAP-C: paracetamol cysteinyl conjugate; APAP-G: paracetamol glucuronide conjugate; APAP-NAC: paracetamol n-acetyl-cysteine conjugate; APAP-S: paracetamol sulfate conjugate; APAP-SG: paracetamol glutathione conjugate; LLOQ: lower limit of quantification; ULOQ: upper limit of quantification.

An IS stock solution was also prepared at concentrations of 500 µg/ml for APAP-d3, 94.3 µg/ml for APAP-G-d3, 86.0 µg/ml for APAP-S-d3, 28.1 µg/ml for APAP-NAC-d5 and 21.0 µg/ml for APAP-C-d5. Individual IS solutions were prepared by diluting 1mg standard into 1mL 50:50 MeOH:H_2O (v:v). Standards were added together to make 1 mL of mixed IS stock solution A, which was then diluted further by adding 500µL stock solution to 2000 µL MeOH to produce the final IS stock solution, as displayed in Table 2.7. The IS stock solution was diluted 1 in 10 followed by 1 in 50 during sample preparation, 1 in 500 overall dilution, to give the concentrations displayed in Table 2.7

Table 2.7 Preparation of internal standard stock solution for rat plasma validation

IS added (concentration)[a]	Volume of IS stock solution[b] (µL)	concentration in IS stock solution A[c] (µg/ml)	Final IS stock solution concentration (µg/ml)	Final measured IS concentration[d] (ng/mL)
APAP-d3 (1 mg/mL)	500	500	100	200
APAP-S-d3 (1 mg/mL)	100	86.0	17.2	34.4
APAP-G-d3 (1 mg/mL)	100	94.3	18.9	37.7
APAP-C-d5 (1 mg/mL)	30	21.0	4.19	8.38
APAP-NAC-d5 (1 mg/mL)	30	28.1	5.61	11.2
MeOH	240	-	-	-
Total	**1000**	**-**	**-**	**-**

[a]IS were diluted together with MeOH to produce an IS top stock solution A, which was diluted 1 in 5 to produce the IS stock solution. [b] Volume of individual standard stock solutions added to make up to 1 mL total in MeOH. [c]Concentration of each IS in IS stock solution A. [d] Final concentration IS measured on the instrument, after 1 in 500 overall dilution.
Abbreviations: APAP: paracetamol; APAP-C: paracetamol cysteinyl conjugate; APAP-G: paracetamol glucuronide conjugate; APAP-NAC: paracetamol n-acetyl-cysteine conjugate; APAP-S: paracetamol sulfate conjugate; IS: internal standard.

2.2.5.3 Standard Curve and Quality Control sample preparation

For both calibration and QC samples, 5 µL of pooled blank rat plasma was mixed with 35 µL methanol, 10 µL IS stock solution and 50 µL of the relevant standard stock solution. For single blanks, 5 µL of plasma were mixed with 85 µL of MeOH and 10 µL of IS stock solution. Double blanks consisted of 5 µL blank matrix mixed with 95 µL of MeOH. All samples were kept at -20 °C for 20 min to precipitate proteins, and then centrifuged for 10 min at 10,000 *g*. A 20 µL aliquot of the clear supernatant from each sample was added to 980 µL of water in glass vials for analysis. A flow chart showing the sample preparation process for samples, QCs and standard curves is given in Figure 2.2**.** The final concentrations of the analytes in both calibration curves and QC samples following sample preparation in rat plasma are given in Table 2.8 and Table 2.9, respectively, and reflect the overall dilution of 1 in 1000 required to allow samples to be measured in the linear range of the mass spectrometer. For measurement of freeze-thaw and bench-top stability, a sample was prepared in plasma containing standard stock solutions at <5% total volume. Solutions were made of APAP 10

mg/mL, APAP-G 2.34 mg/mL, APAP-S 2.15 mg/mL, APAP-C 0.694 mg/mL, APAP-NAC 0.877 mg/mL and APAP-SG 0.912 mg/mL. 5 µL APAP solution, 4 µL each of APAP-S and APAP-G and 2 µL each of APAP-C, -NAC and –SG were added to plasma to create a total volume of 0.5 mL. This was then further diluted five-fold in plasma to produce a plasma stock solution sample. IS stock solution was prepared as stated previously then diluted 2.5 times in MeOH. The plasma stock solution sample was prepared by dilution with 40 µL MeOH and 5 µL IS solution, giving the prepared sample a concentration equivalent to the MQC.

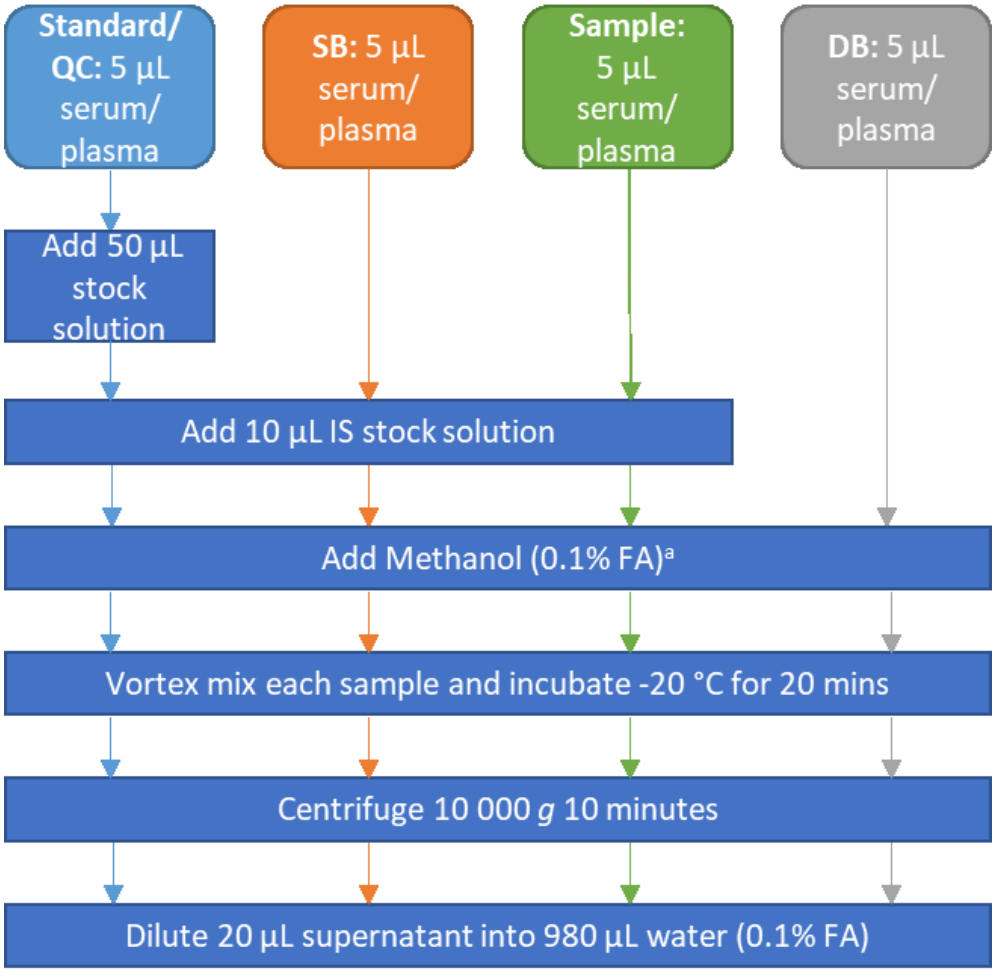


Figure 2.2 Summary of sample preparation for all sample types including the double blank, standard curve and QC samples, the single blank used for the standard curve containing only the internal standards.[a]35µL added to standard/QC; 85 µL added to single blank and samples; 95 µL added to double blank.
Abbreviations: DB: double blank; FA: formic acid; IS: internal standard; SB: single blank; QC: quality control

Table 2.8 Calibration curve concentrations for the standards used for the analysis of APAP and metabolites in rat plasma by UHPLC-MS/MS[a]

Calibration curve ranges (ng/mL)					
APAP	**APAP-G**	**APAP-S**	**APAP-C**	**APAP-SG**	**APAP-NAC**
16	3.00	2.75	0.44	0.58	-
24	4.50	4.12	0.67	0.88	0.84
40	7.50	6.87	1.11	1.46	1.40
60	11.2	10.3	1.67	2.19	2.10
90	16.9	15.5	2.50	3.28	3.16
150	28.1	25.8	4.173	5.47	5.26
250	46.9	42.9	6.94	9.12	8.77
500	93.7	85.9	13.9	18.2	17.5

[a]The concentrations given in this table are those in the final samples following sample preparation for analysis which results in a 1000-fold dilution compared to the original sample.
Abbreviations: APAP: paracetamol; APAP-C: paracetamol cysteinyl conjugate; APAP-G: paracetamol glucuronide conjugate; APAP-NAC: paracetamol n-acetyl-cysteine conjugate; APAP-S: paracetamol sulfate conjugate; APAP-SG: paracetamol glutathione conjugate; LLOQ: lower limit of quantification; UHPLC-MS/MS: ultra-high-performance liquid chromatography coupled tandem mass spectrometry.

Table 2.9 Concentrations of quality control samples for the analysis of APAP and metabolites in rat plasma by UHPLC-MS/MS[a]

QC concentrations / ng/mL						
QC	**APAP**	**APAP-G**	**APAP-S**	**APAP-C**	**APAP-SG**	**APAP-NAC**
ULOQ	500	93.7	85.9	13.9	18.2	17.5
High	400	75.0	68.7	11.1	14.6	14.0
Mid	100	18.7	17.2	2.78	3.65	3.51
Low	48	9.00	8.24	1.33	1.75	1.68
LLOQ	16	3.00	2.75	0.44	0.58	0.84

[a]The concentrations given in this table are those in the final samples following sample preparation for analysis which results in a 1000-fold dilution compared to the original sample.
Abbreviations: APAP: paracetamol; APAP-C: paracetamol cysteinyl conjugate; APAP-G: paracetamol glucuronide conjugate; APAP-NAC: paracetamol n-acetyl-cysteine conjugate; APAP-S: paracetamol sulfate conjugate; APAP-SG: paracetamol glutathione conjugate; LLOQ: lower limit of quantification; UHPLC-MS/MS: ultra-high-performance liquid chromatography coupled tandem mass spectrometry; ULOQ: upper limit of quantification.

2.2.6 Addition of PAP-G and alterations for method application to porcine plasma

Initial evaluation of porcine plasma samples by ^{1}H-NMR spectroscopy identified PAP-G as a major metabolite of APAP in the pig. These data also confirmed very low levels of sulfation plus relatively high concentrations of APAP-G. As such, some changes were made for the cross validation of the method for porcine plasma. A one day fit for purpose validation was carried out in this matrix, where the accuracy and precision of the QCs, matrix factor and recovery were measured.

2.2.6.1 Sample Collection

Porcine plasma samples from female Landrace Cross Large White Pigs were obtained from the Royal Veterinary College, UK, as described in full in Chapter 5 and previous publication (Lee et al. 2013)

2.2.6.2 Standard Curve and QC preparation

Stock solutions for the preparation of calibration curves and QC samples for APAP and APAP metabolite standards were prepared as stated previously, with the following exceptions: APAP-G concentration was increased in this species due to very high concentrations in samples and added to the stock solution at 0.7 mg/mL. PAP-G was added to stock solutions at a concentration of 0.5 mg/mL. The stock solution was prepared as per Table 2.10, APAP-S was in a stock solution of 2.5 mg/mL and the stock solution was made up to 1000 µL total volume, at 500 times the final concentration of the standards, and was diluted by 1 in 5 to produce stock solution A as shown in Table 2.10, before being serially diluted as per Table 2.5 and Table 2.6, to give the standard curve and QC concentrations shown below in Table 2.11 and Table 2.12. A full validation was not performed for this compound as no isotopically labelled IS was available. Samples were prepared as described for rat validation. Final concentrations of the IS were; APAP and APAP-G: 200 ng/mL, APAP-S: 40 ng/mL and APAP-NAC and APAP-C: 12 ng/mL. For PAP-G an external standard curve over the range 16 to 500 ng/mL was prepared to enable semi-quantification.

Table 2.10 Preparation of standard stock solutions A and B for porcine plasma cross-validation.

Standard added (concentration)[a]	**Volume of stock solution[b] (µL)**	**concentration in stock solution A[c] (µg/mL)**	**Final standard concentration[d] (µg/mL)**
APAP (1mg/mL)	250	250	50.0
APAP-S (2.5mg/mL)	20	43	8.59
APAP-G (1mg/mL)	375	351	70.3
APAP-C (1mg/mL)	10	6.95	1.39
APAP-NAC (1mg/mL)	10	8.75	1.75
APAP-SG (1mg/mL)	10	9.1	1.82
PAP-G (1mg/mL)	250	250	50.0
MeOH added	*75*	*240*	
Total Volume Stock Solution A	***1000***	**-**	

[a]Standards were diluted together with MeOH to produce a top stock solution A, which was diluted 1 in 5 to produce stock solution B. [b] Volume of individual standard stock solutions added to make up to 1 mL total in MeOH. [c]Concentration of each standard in stock solution A. [d] Final concentration of each standard in stock solution B, after 1 in 5 dilution.
Abbreviations: APAP: paracetamol; APAP-C: paracetamol cysteinyl conjugate; APAP-G: paracetamol glucuronide conjugate; APAP-NAC: paracetamol n-acetyl-cysteine conjugate; APAP-S: paracetamol sulfate conjugate; APAP-SG: paracetamol glutathione conjugate; PAP-G: p-aminophenol glucuronide.

Table 2.11 The final calibration range for all analytes for porcine plasma cross-validation.

Calibration curve ranges[a] (ng/mL)					
APAP, PAP-G	**APAP-G**	**APAP-S**	**APAP-C**	**APAP-SG**	**APAP-NAC**
16	22.5	2.75	0.44	0.58	-
24	33.8	4.12	0.67	0.88	0.84
40	56.3	6.87	1.11	1.46	1.40
60	84	10.3	1.67	2.19	2.10
90	127	15.5	2.50	3.28	3.16
150	211	25.8	4.173	5.47	5.26
250	352	42.9	6.94	9.12	8.77
500	703	85.9	13.9	18.2	17.5

[a]The concentrations given in this table are those in the final samples following sample preparation for analysis which results in a 1000-fold dilution compared to the original sample.
Abbreviations: APAP: paracetamol; APAP-C: paracetamol cysteinyl conjugate; APAP-G: paracetamol glucuronide conjugate; APAP-NAC: paracetamol n-acetyl-cysteine conjugate; APAP-S: paracetamol sulfate conjugate; APAP-SG: paracetamol glutathione conjugate; PAP-G: p-aminophenol glucuronide.

Table 2.12 The final concentration of quality control samples for porcine plasma cross-validation.

Quality control sample concentrations[a] (ng/ml)						
QC	**APAP-G**	**APAP, PAP-G**	**APAP-S**	**APAP-SG**	**APAP-C**	**APAP-NAC**
ULOQ	703	500	85.9	18.2	13.9	17.5
High	562	400	68.7	14.6	11.1	14.0
Mid	141	100	17.2	3.65	2.78	3.51
Low	67.5	48	8.24	1.75	1.33	1.68
LLOQ	22.5	16	2.75	0.58	0.44	0.84

[a]The concentrations given in this table are those in the final samples following sample preparation for analysis which results in a 1000-fold dilution compared to the original sample.
Abbreviations: APAP: paracetamol; APAP-C: paracetamol cysteinyl conjugate; APAP-G: paracetamol glucuronide conjugate; APAP-NAC: paracetamol n-acetyl-cysteine conjugate; APAP-S: paracetamol sulfate conjugate; APAP-SG: paracetamol glutathione conjugate; LLOQ: lower limit of quantification; PAP-G: p-aminophenol glucuronide; ULOQ: upper limit of quantification; QC: quality control.

2.2.7 Cross validation to human plasma

Samples were prepared as per the rat validation. A one day fit for purpose validation was carried out including accuracy and precision of QCs, matrix factor, recovery and dilution integrity. Human plasma, lithium heparin, non-filtered, and serum, was purchased from seralabs (BioreclamationIVT, West Sussex, UK).

2.2.8 Cross validation to mouse serum

For cross validation of the method to mouse serum and plasma, a new IS for APAP-SG had become available, APAP-SG-d_3. An analytical standard for APAP-OMe was also purchased and added to the standard curve for monitoring, at a range of 0.64-20.0 ng/mL. Standard curve and QC stock solutions were prepared as per the rat validation, with the exception of the addition to the new standard to the top stock solution A as shown in Table 2.13 below. Following this the stock solutions underwent the same serial dilution as in Table 2.5 and Table 2.6 above to produce final curve and QC ranges listed in Table 2.14 and Table 2.15 below. The IS was prepared as per Table 2.16 with the addition of APAP-SG-d_3 to the top stock solution. This was then treated the same as IS stock solution A in the rat validation, as per Table 2.7, giving a final concentration of 10.9 ng/mL for APAP-SG-d_3 in samples following conversion for salt factor. QC and calibration curve samples were prepared using these stock solutions

as per the rat validation. The cross validation included measuring the intra-day accuracy and precision of curves and QCs, investigating the matrix effects and recovery and the dilution integrity.

Table 2.13 Preparation of standard stock solutions A and B for mouse serum cross-validation.

Standard added (concentration)[a]	Volume of stock solution[b] (µL)	concentration in stock solution A[c] (µg/ml)	Final standard concentration[d] (µg/ml)
APAP (1mg/mL)	500	500	50.0
APAP-S (1mg/mL)	100	85.9	8.59
APAP-G (1mg/mL)	100	93.7	9.37
APAP-C (1mg/mL)	20	13.9	1.39
APAP-NAC (1mg/mL)	20	17.5	1.75
APAP-SG (1mg/mL)	20	18.2	1.82
APAP-OMe	20	20.0	2.0
MeOH added	*220*	-	
Total Volume Stock solution A	***1000***	**-**	

[a]Standards were diluted together with MeOH to produce a top stock solution A, which was diluted 1 in 10 to produce stock solution B. [b] Volume of individual standard stock solutions added to make up to 1 mL total in MeOH. [c]Concentration of each standard in stock solution A. [d] Final concentration of each standard in stock solution B, after 1 in 10 dilution.
Abbreviations: APAP: paracetamol; APAP-C: paracetamol cysteinyl conjugate; APAP-G: paracetamol glucuronide conjugate; APAP-NAC: paracetamol n-acetyl-cysteine conjugate; APAP-OMe: 3-methoxy paracetamol conjugate; APAP-S: paracetamol sulfate conjugate; APAP-SG: paracetamol glutathione conjugate.

Table 2.14 Calibration ranges used for mouse serum cross-validation

Calibration curve ranges[a] (ng/ml)							
APAP	**APAP-G**	**APAP-S**	**APAP-C**	**APAP-SG**	**APAP-NAC**	**APAP-OMe**	**APAP**
16	3.00	2.75	0.44	0.58	-	0.64	16
24	4.50	4.12	0.67	0.88	0.84	0.96	24
40	7.50	6.87	1.11	1.46	1.40	1.6	40
60	11.2	10.3	1.67	2.19	2.10	2.4	60
90	16.9	15.5	2.50	3.28	3.16	3.6	90
150	28.1	25.8	4.173	5.47	5.26	6.0	150
250	46.9	42.9	6.94	9.12	8.77	10	250
500	93.7	85.9	13.9	18.2	17.5	20	500

[a]The concentrations given in this table are those in the final samples following sample preparation for analysis which results in a 1000-fold dilution compared to the original sample.
Abbreviations: APAP: paracetamol; APAP-C: paracetamol cysteinyl conjugate; APAP-G: paracetamol glucuronide conjugate; APAP-NAC: paracetamol n-acetyl-cysteine conjugate; APAP-OMe: 3-methoxy paracetamol conjugate; APAP-S: paracetamol sulfate conjugate; APAP-SG: paracetamol glutathione conjugate.

Table 2.15 Quality control concentration levels for mouse serum cross-validation

Quality control sample concentrations[a] (ng/ml)							
QC	**APAP**	**APAP-S**	**APAP-G**	**APAP-SG**	**APAP-C**	**APAP-OMe**	**APAP-NAC**
ULOQ	500	85.9	93.7	18.2	13.9	20.0	17.5
High	400	68.7	75.0	14.6	11.1	16.0	14.0
Mid	100	17.2	18.7	3.65	2.78	4.00	3.51
Low	48.0	8.24	9.00	1.75	1.33	1.92	1.68
LLOQ	16.0	2.75	3.00	0.58	0.44	0.64	0.84

[a]The concentrations given in this table are those in the final samples following sample preparation for analysis which results in a 1000-fold dilution compared to the original sample.
Abbreviations: APAP: paracetamol; APAP-C: paracetamol cysteinyl conjugate; APAP-G: paracetamol glucuronide conjugate; APAP-NAC: paracetamol n-acetyl-cysteine conjugate; APAP-OMe: 3-methoxy paracetamol conjugate; APAP-S: paracetamol sulfate conjugate; APAP-SG: paracetamol glutathione conjugate; LLOQ: lower limit of quantification; QC: quality control; ULOQ: upper limit of quantification.

Table 2.16 Internal standard stock solution preparation for mouse serum validation

IS added (concentration)[a]	**Volume of IS stock solution[b] (µL)**	**concentration in IS stock solution A[c] (µg/ml)**	**Final IS stock solution concentration (µg/ml)**	**Final measured IS concentration[d] (ng/mL)**
APAP-d3 (1mg/mL)	500	500	100	200
APAP-S-d3 (1 mg/mL)	100	86.0	17.2	34.4
APAP-G-d3 (1 mg/mL)	100	94.3	18.9	37.7
APAP-C-d5 (1 mg/mL)	30	21.0	4.19	8.38
APAP-NAC-d5 (1 mg/mL)	30	28.1	5.61	11.2
APAP-SG-d3 (1 mg/mL)	30	27.3	5.46	10.9
MeOH	*210*	-	-	-
Total	***1000***	**-**	**-**	**-**

[a]IS were diluted together with MeOH to produce an IS top stock solution A, which was diluted 1 in 5 to produce the IS stock solution. [b] Volume of individual standard stock solutions added to make up to 1 mL total in MeOH. [c]Concentration of each IS in IS stock solution A. [d] Final concentration IS measured on the instrument, after 1 in 500 overall dilution.
Abbreviations: APAP: paracetamol; APAP-C: paracetamol cysteinyl conjugate; APAP-G: paracetamol glucuronide conjugate; APAP-NAC: paracetamol n-acetyl-cysteine conjugate; APAP-S: paracetamol sulfate conjugate; APAP-SG: paracetamol glutathione conjugate.

2.3 Results

2.3.1 Rat plasma validation results

The results of the validation in rat plasma including linearity, accuracy and precision, selectivity and specificity, matrix interference, stability and dilution integrity are displayed below.

2.3.1.1 Linearity

Over the three days of the inter-day validation the method was found to be linear over the concentration ranges measured for all of the analytes with all r^2 values above 0.99, as shown in Table 2.17.

Table 2.17 Linearity of the standard curves for each compound for each day of the validation in rat plasma.

Compound	Day 1		Day 2		Day 3	
	R^2	Line Equation	R^2	Line Equation	R^2	Line Equation
APAP	0.992	2.26x+4.26	0.997	2.26x+8.48	0.998	2.52x-0.323
APAP-S	0.996	0.261x+0.0289	0.998	0.199x+0.0447	0.997	0.217x-0.0959
APAP-G	0.995	0.381x+0.204	0.995	0.441x-0.0726	0.995	0.501x-0.204
APAP-C	0.994	1.752x+0.0735	0.997	1.629x+0.0725	0.997	1.874x-0.144
APAP-NAC	0.994	0.790x+0.114	0.997	0.803x+0.0659	0.992	0.871x+0.118
APAP-SG	0.993	2960x-61.2	0.995	2560x+52.8	0.995	2880x-190

Abbreviations: APAP: paracetamol; APAP-C: paracetamol cysteinyl conjugate; APAP-G: paracetamol glucuronide conjugate; APAP-NAC: paracetamol n-acetyl-cysteine conjugate; APAP-S: paracetamol sulfate conjugate; APAP-SG: paracetamol glutathione conjugate

2.3.1.2 Precision and accuracy

For each day, and across all three days, the CV and bias data for QCs met the acceptance criteria outlined in the methods section. The lowest LLOQ QC was chosen as it met these criteria for all compounds except APAP-NAC, where the higher LLOQ was chosen due to background interference reducing the precision and accuracy of the results for this compound (data not shown) The resulting LLOQs (back calculated to undiluted plasma samples) of 16 µg/mL (APAP), 3.00 µg/mL (APAP-G), 2.75 µg/mL (APAP-S), 0.84 µg/mL (APAP-NAC), 0.58 µg/ml (APAP-SG) and 0.44 µg/mL (APAP-C); and ULOQs of 500 µg/mL (APAP), 93.7 µg/mL (APAP-G), 85.9 µg/mL (APAP-S), 18.2 µg/mL (APAP-SG), 17.5 µg/mL (APAP-NAC) and 13.9 µg/mL (APAP-C) were considered suitable for the analysis of the drug and its metabolites in samples.

The inter-day precision and accuracy are shown in Table 2.18 and Table 2.19, respectively. The CV calculated form the mean and standard deviation of all 18 QC samples at each level from the third day of experimentation are shown in Table 2.18, whilst Table 2.19 shows the mean percentage difference from the nominal concentration of all 18 QCs. For intra-day precision and accuracy, Table 2.20 shows the CV of each of 6 QC samples at each QC level, which were below the acceptance level of 15% (20% LLOQ) for each analyte. Table 2.21 shows the percentage difference between the nominal concentration and actual concentration calculated from the standard curve for each of the six QCs at each QC level on each day.

Table 2.18 Summary of the inter-day coefficient of variance for rat plasma validation

Analyte	Coefficient of Variance (%)				
	LLOQ	LQC	MQC	HQC	ULOQ
APAP	6.8	10.0	8.5	4.9	5.3
APAP-S	17.5	12.8	10.2	5.8	6.9
APAP-G	15.9	8.7	8.8	6.7	8.3
APAP-C	11.1	8.2	7.5	5.8	5.6
APAP- NAC	12.5	11.3	9.6	7.8	7.6
APAP-SG	8.7	7.5	9.5	8.3	5.9

Abbreviations: APAP: paracetamol; APAP-C: paracetamol cysteinyl conjugate; APAP-G: paracetamol glucuronide conjugate; APAP-NAC: paracetamol n-acetyl-cysteine conjugate; APAP-S: paracetamol sulfate conjugate; APAP-SG: paracetamol glutathione conjugate

Table 2.19 Summary of the inter-day mean bias for rat plasma validation

Analyte	Mean Bias (%)				
	LLOQ	LQC	MQC	HQC	ULOQ
APAP	1.8	0.9	-3.4	1.4	1.7
APAP-S	-8.6	-1.8	-0.3	-0.8	-2.3
APAP-G	0.6	8.6	6.0	6.8	6.6
APAP-C	-1.1	-1.2	-0.4	-2.9	-4.9
APAP-NAC	-1.1	3.3	0.6	1.4	0.9
APAP-SG	-7.5	-0.5	-0.6	-5.0	-6.1

Abbreviations: APAP: paracetamol; APAP-C: paracetamol cysteinyl conjugate; APAP-G: paracetamol glucuronide conjugate; APAP-NAC: paracetamol n-acetyl-cysteine conjugate; APAP-S: paracetamol sulfate conjugate; APAP-SG: paracetamol glutathione conjugate; HQC: high quality control; LLOQ: lower limit of quantification; LQC: low quality control; HQC: high quality control; ULOQ: upper limit of quantification.

Table 2.20 Summary of the intra-day coefficient of variance of the quality control samples in the rat plasma validation[a]

Analyte	Coefficient of Variance (%)														
	Day 1					Day 2					Day 3				
	1	2	3	4	5	1	2	3	4	5	1	2	3	4	5
APAP	4.8	12.2	8.7	4.9	5.6	7.9	1.6	7.6	4.3	1.2	4.4	3.4	3.0	2.7	2.6
APAP-S	13.4	7.5	10.0	3.4	7.1	16.4	10.9	6.8	4.8	2.7	15.4	3.9	3.6	3.6	3.8
APAP-G	7.4	11.8	8.7	5.0	5.6	11.3	5.9	4.3	3.5	3.8	4.6	2.6	4.3	3.4	2.4
APAP-C	7.1	6.2	8.8	3.7	6.8	8.2	2.3	3.5	3.1	3.9	6.4	2.6	3.0	3.0	3.1
APAP-NAC	8.8	10.4	7.4	6.8	6.6	7.3	5.8	3.8	5.5	3.3	10.9	7.5	4.1	6.8	2.5
APAP-SG	6.2	6.1	8.2	9.0	3.7	5.2	3.7	6.0	6.3	4.1	7.7	5.7	3.8	6.5	5.2

[a] n=6 per day at each level
Abbreviations: APAP: paracetamol; APAP-C: paracetamol cysteinyl conjugate; APAP-G: paracetamol glucuronide conjugate; APAP-NAC: paracetamol n-acetyl-cysteine conjugate; APAP-S: paracetamol sulfate conjugate; APAP-SG: paracetamol glutathione conjugate.

Table 2.21 Summary of the intra-day mean bias of the quality control samples in the rat plasma validation[a]

Analyte	Mean Bias (%)														
	Day 1					Day 2					Day 3				
	1	2	3	4	5	1	2	3	4	5	1	2	3	4	5
APAP	0.1	-5.9	4.3	0.7	3.3	2.1	9.5	9.3	0.2	-3.7	-6.9	-4.9	-2.9	-5.3	-5.1
APAP-S	2.6	0.6	3.6	3.4	6.8	18.2	13.4	5.4	4.0	3.6	3.6	-7.5	-8.4	-4.5	-3.6
APAP-G	-13.5	-12.2	0.3	-1	1.9	-4.7	-8.5	-11.9	-8.2	-10.0	16.7	-4.9	-6.7	-11.8	-12.1
APAP-C	4.2	-2.1	-2.5	1.5	6.3	9.4	12.0	6.7	9.2	6.3	-8.9	-4.5	-2.5	-1.6	1.8
APAP-NAC	5.9	-2.1	2.1	-0.9	5.7	9.4	8.5	7.5	3.6	-2.5	-9.7	-13.2	-8.7	-6.5	-6.4
APAP-SG	9.4	-3.6	-5.8	0.3	1.9	12.0	6.8	9.6	11.4	11.6	1.6	-1.9	-0.8	3.9	5.8

[a] n=6 per day at each level
Abbreviations: APAP: paracetamol; APAP-C: paracetamol cysteinyl conjugate; APAP-G: paracetamol glucuronide conjugate; APAP-NAC: paracetamol n-acetyl-cysteine conjugate; APAP-S: paracetamol sulfate conjugate; APAP-SG: paracetamol glutathione conjugate.

2.3.1.3 Carryover, Selectivity and Specificity

Carryover and IS carryover were calculated by comparing any responses in the double blank measured directly after the ULOQ to the average response or IS response in the calibration curve. Carryover was low, and within the acceptance criteria with responses at the retention times of the individual compounds below 20% of the LLOQ for all analytes as shown in Table 2.22, and 5% of the IS responses as shown in Table 2.23**.** Selectivity and specificity were calculated by comparing the responses of any analytes or IS at the retention time of another. All were well within the acceptance criteria for all analytes and IS (data not shown).

Table 2.22 Carryover for all analytes measured during validation for rat plasma.

Compound	Average LLOQ Response	Carryover Response 1	Carryover (%)	Carryover Response 2	Carryover (%)
APAP	142220	3163	2.22	3469	2.44
APAP-S	1123	0	0	40.5	3.61
APAP-G	578	0.71	0.12	0.49	0.09
APAP-C	2126	20.5	0.97	14.7	0.69
APAP-NAC	138	14	10.1	1.87	1.35
APAP-SG	1866	11.4	0.11	0.251	0.014

Abbreviations: APAP: paracetamol; APAP-C: paracetamol cysteinyl conjugate; APAP-G: paracetamol glucuronide conjugate; APAP-NAC: paracetamol n-acetyl-cysteine conjugate; APAP-S: paracetamol sulfate conjugate; APAP-SG: paracetamol glutathione conjugate; LLOQ: lower limit of quantification.

Table 2.23 Carryover for all internal standards measured during validation for rat plasma.

Compound	Average IS Response	Carryover Response 1	Carryover (%)	Carryover Response 2	Carryover (%)
APAP-d3	513818	129	0.09	87.0	0.06
APAP-S-d3	61293	0.00	0.00	0.00	0.00
APAP-G-d3	15428	7.60	1.32	0.74	0.13
APAP-C-d5	14812	15.6	0.74	0.00	0.00
APAP-NAC-d5	1233	12.3	8.89	0.00	0.00

Abbreviations: APAP: paracetamol; APAP-C: paracetamol cysteinyl conjugate; APAP-G: paracetamol glucuronide conjugate; APAP-NAC: paracetamol n-acetyl-cysteine conjugate; APAP-S: paracetamol sulfate conjugate; IS: internal standard.

2.3.1.4 Matrix Interference and Recovery

Matrix factor was calculated by comparing the peak area of six lots of the LQC and HQC spiked into water compared with six lots of the LQC and HQC spiked into post extraction blank matrix. The results obtained for the determination of the matrix factors for the various analytes were all acceptable, with CVs below 15%. Recoveries were calculated by comparing peak areas of QCs spiked with analytes before and after extraction. Recoveries were over 80% for all analytes except APAP-NAC for the LQC, where the mean recovery was 78.7%, with CVs generally below 10%. The recovery and matrix factor data for each of the analytes are summarised in Table 2.24 and Table 2.25, respectively.

Table 2.24 Mean matrix factor determined for the LQC and HQC Samples in rat plasma validation

QC level	Analyte	Mean MF (%)	Mean IS normalised MF (%)	CV (N=6)
HQC	APAP	9	-7	3.11
	APAP-S	4	-6	5.59
	APAP-G	7	-11	3.89
	APAP-C	9	-5	2.26
	APAP-NAC	11	-10	6.92
	APAP-SG	10	-	-
LQC	APAP	7	-1	2.47
	APAP-S	12	2	4.08
	APAP-G	11	1	6.14
	APAP-C	5	-1	5.13
	APAP-NAC	15	10	4.73
	APAP-SG	5	-	

Abbreviations: APAP: paracetamol; APAP-C: paracetamol cysteinyl conjugate; APAP-G: paracetamol glucuronide conjugate; APAP-NAC: paracetamol n-acetyl-cysteine conjugate; APAP-S: paracetamol sulfate conjugate; APAP-SG: paracetamol glutathione conjugate; CV: coefficient of variance; HQC: high quality control; LQC: low quality control; MF: matrix factor; QC: quality control.

Table 2.25 Mean percentage recovery for all analytes at HQC measured in rat plasma validation

QC level	Analyte	% Recovery	CV (N=6)
HQC	APAP	88.0	9.59
	APAP-S	86.4	7.80
	APAP-G	82.6	10.6
	APAP-C	88.7	5.72
	APAP-NAC	81.4	4.23
	APAP-SG	81.5	5.57
LQC	APAP	94.6	2.76
	APAP-S	90.8	8.02
	APAP-G	87.8	8.56
	APAP-C	88.3	14.3
	APAP-NAC	78.7	17.5
	APAP-SG	86.5	11.4

Abbreviations: APAP: paracetamol; APAP-C: paracetamol cysteinyl conjugate; APAP-G: paracetamol glucuronide conjugate; APAP-NAC: paracetamol n-acetyl-cysteine conjugate; APAP-S: paracetamol sulfate conjugate; APAP-SG: paracetamol glutathione conjugate; CV: coefficient of variance; HQC: high quality control; LQC: low quality control; QC: quality control.

2.3.1.5 Stability

Previous studies have reported varying results for stability, with some reports showing all analytes to be stable in the autosampler for up to 48 hours (An et al. 2012; Lammers et al. 2017), while another report found that APAP-SG was only stable for up to 24 hours, whereas the other analytes remained stable for up to 48 hrs (Flint et al. 2017). Another study found all metabolites to be stable in the autosampler for up to 73 hours (but also stated that APAP-SG degraded to APAP-C in human plasma) (Cook et al. 2015).

Analyte stability was investigated in a number of ways, including bench top stability, 36-hour autosampler stability and freeze-thaw stability as described in methods. Table 2.26 displays the results of peak areas after up to six freeze-thaw cycles, these results also include APAP-OMe as this was added to the investigation outside of the original three-day validation. Table 2.27 shows the percentage bias and CV of the mean of the six QC samples run after each freeze-thaw compared to initial peak area. There was some decline in peak area after a number of freeze-thaw cycles, but generally under 25–30%, and precision did not greatly decline. Table 2.28 shows benchtop stability. The peak areas and precision stayed relatively stable after 4 hours on the bench top at room temperature for all analytes.

QC samples kept in the autosampler for 36 hours (at 5°C) and analysed against a freshly prepared standard curve, indicated a small overall decrease in response for all of the analytes, as shown in Table 2.29. The CVs were all within the predefined acceptance criteria of less than 15% with the exception of the LQC for APAP-G with a CV of 15.5%. The percentage decline (bias) was generally below 15%, with a limited number for APAP-S, APAP-G and APAP-NAC between 15-20% (See Table 2.30 and Table 2.31)

Table 2.26 Mean peak areas of analytes before and after up to six freeze-thaw cycles.

Metabolite	Mean peak area (n=6)						
	0 FT	**1FT**	**2 FT**	**3 FT**	**4 FT**	**5 FT**	**6 FT**
APAP	253388	217498	197631	223733	233769	220896	181740
APAP-S	16688	13653	14465	16326	16903	15979	12799
APAP-G	3851	3404	3377	3862	4105	3885	3166
APAP-C	16283	14532	15332	16974	18518	17252	14499
APAP-NAC	387	331	362	406	433	413	344
APAP-SG	10289	8692	9237	10060	10901	10416	8845
APAP-OMe	11214	8465	8831	10296	10721	10290	8110

Abbreviations: APAP: paracetamol; APAP-C: paracetamol cysteinyl conjugate; APAP-G: paracetamol glucuronide conjugate; APAP-NAC: paracetamol n-acetyl-cysteine conjugate; APAP-OMe: 3-methoxy paracetamol conjugate; APAP-S: paracetamol sulfate conjugate; APAP-SG: paracetamol glutathione conjugate; FT: freeze-thaw cycle.

Table 2.27 Mean percentage bias from original peak area and CV of peak areas after six freeze-thaw cycles (n=6)

Freeze-Thaw cycles		APAP	APAP-S	APAP-C	APAP-G	APAP-NAC	APAP-SG	APAP-Ome
1 FT	% Bias	-14.2	-18.2	-10.8	-11.6	-14.6	-24.5	-15.5
	CV	26.5	20.3	15.0	23.9	16.0	17.8	16.5
2 FT	% Bias	-22.0	-13.3	-5.84	-12.3	-6.56	-21.2	-10.2
	CV	18.7	16.1	16.1	18.7	15.6	17.9	15.2
3 FT	% Bias	-11.7	-2.17	4.24	0.27	4.94	-8.19	-2.23
	CV	20.0	20.1	18.4	21.5	19.1	22.6	18.5
4 FT	% Bias	-7.74	1.29	13.7	6.57	11.7	-4.39	5.95
	CV	15.4	15.1	14.2	14.4	17.3	15.5	14.3
5 FT	% Bias	-12.8	-4.25	5.95	0.88	6.74	-8.23	1.23
	CV	21.9	20.7	20.4	20.4	16.0	21.7	19.5
6 FT	% Bias	-28.3	-23.3	-11.0	-17.8	-11.1	-27.7	-14.0
	CV	25.2	21.0	24.2	26.2	23.4	26.9	26.3

Abbreviations: APAP: paracetamol; APAP-C: paracetamol cysteinyl conjugate; APAP-G: paracetamol glucuronide conjugate; APAP-NAC: paracetamol n-acetyl-cysteine conjugate; APAP-OMe: 3-methoxy paracetamol conjugate; APAP-S: paracetamol sulfate conjugate; APAP-SG: paracetamol glutathione conjugate; CV: coefficient of variance; FT: freeze-thaw cycle.

Table 2.28 Mean areas of MQC before and after 4 hours on the benchtop and at ambient temperature and CV and mean % bias from original concentration. (n=6)

Metabolite	Mean Area (0 h)	Mean area (4 h)	Mean % Bias	CV
APAP	253388	221484	-9.21	18.6
APAP-S	16688	16546	0.86	11.2
APAP-C	16283	18271	14.4	11.6
APAP-G	3851	3872	2.06	10.0
APAP-NAC	387	389	2.40	11.3
APAP-SG	10289	9024	-10.6	11.5
APAP-OMe	11214	10421	-5.87	10.4

Abbreviations: APAP: paracetamol; APAP-C: paracetamol cysteinyl conjugate; APAP-G: paracetamol glucuronide conjugate; APAP-NAC: paracetamol n-acetyl-cysteine conjugate; APAP-OMe: 3-methoxy paracetamol conjugate; APAP-S: paracetamol sulfate conjugate; APAP-SG: paracetamol glutathione conjugate; CV: coefficient of variance.

Table 2.29 Autosampler stability: mean initial and 36 Hour QC Concentrations.

Autosampler stability in rat plasma, values in ng/mL										
Analyte	**LLOQ**		**LQC**		**MQC**		**HQC**		**ULOQ**	
	Initial	**36 hrs**	**Initial**	**36 hrs**	**Initial**	**36 hrs**	**Initial**	**36 hrs**	**Initial**	**36 hrs**
APAP	14.9	13.6	45.7	38.9	97.1	81.5	379	322	474	403
APAP-S	2.85	2.64	7.62	6.59	15.7	13.5	65.6	54.3	82.8	67.2
APAP-G	2.86	3.00	8.23	6.61	16.5	15.0	68.8	57.9	84.4	73.7
APAP-C	0.40	0.43	1.27	1.13	2.71	2.40	11.0	9.58	14.2	12.4
APAP-NAC	0.76	0.64	1.46	1.36	3.20	2.88	13.1	11.3	16.4	14.6
APAP-SG	0.59	0.57	1.71	1.62	3.62	3.36	15.1	13.9	19.3	17.0

Abbreviations: APAP: paracetamol; APAP-C: paracetamol cysteinyl conjugate; APAP-G: paracetamol glucuronide conjugate; APAP-NAC: paracetamol n-acetyl-cysteine conjugate; APAP-S: paracetamol sulfate conjugate; APAP-SG: paracetamol glutathione conjugate; HQC: high quality control; LLOQ: lower limit of quantification; LQC: low quality control; QC: quality control; ULOQ: upper limit of quantification.

Table 2.30 Autosampler stability: percentage bias from initial concentration after 36 hours at 5°C.

Analyte	**LLOQ %**	**LQC %**	**MQC %**	**HQC %**	**ULOQ %**
APAP	-9.06	-14.8	-16.0	-14.9	-15.0
APAP-S	-7.54	-13.5	-14.5	-17.3	-18.8
APAP-G	4.92	-19.7	-9.18	-15.9	-12.6
APAP-C	5.71	-10.9	-11.5	-12.6	-12.0
APAP-NAC	-15.4	-7.00	-10.1	-13.7	-10.6
APAP-SG	-5.13	-5.31	-7.14	-8.63	-12.4

Abbreviations: APAP: paracetamol; APAP-C: paracetamol cysteinyl conjugate; APAP-G: paracetamol glucuronide conjugate; APAP-NAC: paracetamol n-acetyl-cysteine conjugate; APAP-S: paracetamol sulfate conjugate; APAP-SG: paracetamol glutathione conjugate; HQC: high quality control; LLOQ: lower limit of quantification; LQC: low quality control; QC: quality control; ULOQ: upper limit of quantification.

Table 2.31 Autosampler stability: CV of concentrations after 36 hours at 5°C.

Analyte	**LLOQ %**	**LQC %**	**MQC %**	**HQC %**	**ULOQ %**
APAP	6.71	11.3	12.3	11.4	11.5
APAP-S	5.54	10.2	11.0	13.4	14.7
APAP-G	3.39	15.5	6.8	12.2	9.48
APAP-C	3.93	8.16	8.66	9.50	8.99
APAP-NAC	11.8	5.13	7.48	10.4	7.91
APAP-SG	3.72	3.86	5.24	6.37	9.32

Abbreviations: APAP: paracetamol; APAP-C: paracetamol cysteinyl conjugate; APAP-G: paracetamol glucuronide conjugate; APAP-NAC: paracetamol n-acetyl-cysteine conjugate; APAP-S: paracetamol sulfate conjugate; APAP-SG: paracetamol glutathione conjugate; CV: coefficient of variance; HQC: high quality control; LLOQ: lower limit of quantification; LQC: low quality control; QC: quality control; ULOQ: upper limit of quantification.

2.3.1.6 Dilution Integrity

Dilution integrity was determined by quantification of the analytes following the 10-fold dilution of a DIQC sample prepared at three times the concentration of the ULOQ as described in the experimental methods section. The results of this analysis met the acceptance criteria of being within ±15% of the nominal concentration (with a CV of ≤15%) for all analytes with the exception of APAP-NAC. This is unlikely to present a problem in practice as concentrations of APAP-NAC are generally low in plasma and serum meaning the need for sample dilution is therefore unlikely. Results for the analyses of the DIQC integrity sample are summarised in Table 2.32.

Table 2.32 Dilution Integrity nominal and mean measured concentration, CV and % bias of QC sample measured after dilution.

Metabolite	Nominal Conc. (ng/mL)	Mean Measured Conc. (ng/mL)	CV % N=6	Bias % N=6
APAP	150	135	1.52	-10.3
APAP-S	25.8	22.3	5.94	-13.3
APAP-G	28.1	25.7	3.10	-8.67
APAP-C	4.17	3.73	6.84	-10.6
APAP-SG	5.47	6.14	4.37	12.2
APAP-NAC	5.26	4.53	21.0	-13.9
(APAP-NAC with no IS)	5.26	5.15	9.27	-1.9

Abbreviations: APAP: paracetamol; APAP-C: paracetamol cysteinyl conjugate; APAP-G: paracetamol glucuronide conjugate; APAP-NAC: paracetamol n-acetyl-cysteine conjugate; APAP-S: paracetamol sulfate conjugate; APAP-SG: paracetamol glutathione conjugate; CV: coefficient of variance; QC: quality control.

2.3.2 Porcine plasma validation results

The PAP-G standard curve was shown to be accurate and precise, with the CV of the two curves being below 15% at all points, and with less than 10% bias from the nominal concentration, as shown in Table 2.33. Linearity results are displayed in summary Table 2.34, and show that the curves had an r^2 value of approximately 0.99 for all compounds. Of the six QCs at each level from LLOQ QC to HQC, all were shown to be accurate and precise, (CV and bias below 15% [20% at the LLOQ]) ULOQ concentrations were precise but not accurate. Review of peak area in standard curve and in QCs shows peak areas as expected for standard curve, however peak area for compounds in the QC samples were double the expected area, hence the lack of accuracy is very likely due to an error in sample

preparation. Matrix factor, which was IS normalised, with the exception of APAP-SG, and recovery are displayed in Table 2.34. Matrix effects were all within acceptance criteria and were generally minimal. Recovery was good, and although there are no acceptance criteria for recovery, CVs were all ≤20.1%

Table 2.33 Porcine Plasma Cross Validation: Range of calibration curve for PAP-G showing CV and Bias of measured curve from nominal concentration.

Nominal conc. (ng/mL)	Mean measured conc. (ng/mL) (n=2)	CV	Bias %
0	0.9	0.0	0.9
16	16.2	1.3	0.9
24	23.5	6.9	-2.3
40	36.3	3.5	-9.3
60	56.7	6.5	-5.5
90	97.9	2.7	8.7
150	152.4	2.6	1.6
250	240.3	14.8	-3.9
500	506.9	3.8	1.4

Abbreviations: CV: coefficient of variance; PAP-G: p-aminophenol glucuronide.

Table 2.34 Summary of Results for Porcine Plasma Cross Validation

Parameter	QC Level		APAP	APAP-S	APAP-G	APAP-C	APAP-NAC	APAP-SG
Linearity R^2	-		0.988	0.991	0.989	0.99	0.986	0.996
Line equation	-		1.95x+2.31	0.639x+0.0247	0.0123x+0.0196	1.68x+0.0525	0.757x+0.115	1350x-73.8
Intra-Day Accuracy (Mean % Bias) N=6	*LLOQ*		6.98	5.21	0.35	17.2	9.38	2.42
	LQC		-4.51	-2.60	-5.32	3.30	2.43	2.43
	MQC		4.77	2.67	4.22	9.58	12.5	-5.00
	HQC		1.03	0.73	8.35	9.48	6.77	1.77
	ULOQ		**74.8**	**81.7**	**102**	**110**	**104**	**86.6**
Intra-Day Precision (CV) N=6	*LLOQ*		11.4	16.6	9.71	11.2	7.97	8.94
	LQC		11.1	9.56	12.2	10.3	11.0	7.66
	MQC		5.94	6.97	8.49	6.19	2.43	12.0
	HQC		5.30	6.04	5.88	4.11	7.53	9.27
	ULOQ		**6.26**	**5.81**	**8.88**	**10.6**	**12.0**	**12.9**
Matrix Factor N=6	*LQC*	*%*	-6.34	-7.37	-4.24	-5.09	-7.84	10.6[a]
		CV	2.3	6.94	3.87	3.01	9.27	9.0
	HQC	*%*	0.86	0.78	3.42	0.04	0.09	3.02[a]
		CV	3.98	5.55	4.17	3.63	2.34	9.63
Recovery N=6	*LQC*	*%*	96.1	86.6	86.8	84.6	86.1	80.9
		CV	20.1	13.8	11.7	13.4	18	9
	HQC	*%*	102	97.3	101	100	105	101
		CV	9.71	9.34	8.7	12.2	12.7	9.63

[a]*Matrix factor calculated without IS normalisation.*

Abbreviations: APAP: paracetamol; APAP-C: paracetamol cysteinyl conjugate; APAP-G: paracetamol glucuronide conjugate; APAP-NAC: paracetamol n-acetyl-cysteine conjugate; APAP-S: paracetamol sulfate conjugate; APAP-SG: paracetamol glutathione conjugate; CV: coefficient of variance; HQC: high quality control; LLOQ: lower limit of quantification; LQC: low quality control; QC: quality control; ULOQ: upper limit of quantification.

2.3.3 Mouse serum validation results

All cross-validation results are summarised in Table 2.35. All curves were shown to be linear with r^2 values above 0.99, including the added APAP-OMe which had an r^2 value of 0.993. The method was shown to be accurate and precise at all QC levels. Matrix factors were minimal and CVs were within acceptance criteria for all IS normalised matrix factors. Matrix factor for APAP-OMe at the HQC had a CV above 15%, but it was still below 20%, and is likely higher due to the lack of IS normalisation. Recoveries were all over 80%, and all CVs were below 17% for all analytes at LQC and HQC. CV and % bias met acceptance criteria for all analytes for the dilution integrity, as expected from previous results the % bias was higher for APAP-NAC than for the other compounds, however this was still below 15% and within acceptance criteria

Table 2.35 Summary of validation data for mouse serum

	QC level		APAP	APAP-S	APAP-G	APAP-C	APAP-NAC	APAP-SG	APAP-OMe
Linearity	-		0.995	0.995	0.995	0.997	0.996	0.995	0.993
Line Equation	-		0.00683x-0.0114	0.00738x-0.00525	0.0120x-0.00710	0.124x-0.00928	0.0966x+0.00200	0.0547x-0.00275	285x-1280
Intra-Day Accuracy (CV) N=6	*LLOQ*		18.7	15.9	15.0	13.0	19.0	14.0	12.0
	LQC		10.9	5.40	10.0	10.0	7.00	7.00	4.00
	MQC		7.50	2.80	6.70	3.30	0.30	2.30	-4.70
	HQC		3.00	-0.90	1.20	2.60	-4.40	-2.80	0.70
	ULOQ		4.30	4.90	1.10	6.20	2.60	1.70	-7.80
Intra-Day Precision (CV) N=6	*LLOQ*		3.00	10.1	5.90	7.30	19.1	7.00	4.80
	LQC		4.90	9.90	11.0	3.60	12.5	5.90	7.40
	MQC		8.70	7.90	10.0	6.20	8.10	7.50	6.10
	HQC		2.20	2.90	5.60	5.10	5.10	2.90	31.0
	ULOQ		8.40	6.90	10.0	5.00	9.30	10.3	11.0
Matrix Factor N=5	*LQC*	*%*	-12.9	-11.7	-9.60	-12.4	-13.5	-11.6	12.0[a]
		CV	8.30	5.90	5.90	4.30	10.5	2.80	6.40
	HQC	*%*	-14.0	-22.5	-10.0	-12.0	-13.0	-12.0	11.0[a]
		CV	4.20	5.07	4.77	2.89	4.21	2.98	16.4
Recovery N=5	*LQC*	*%*	92.5	88.0	88.0	88.0	96.0	91.0	88.0
		CV	11.2	16.6	13.9	12.1	16.2	10.6	15.7
	HQC	*%*	73.2	84.0	80.4	82.0	75.0	77.0	75.0
		CV	4.74	10.7	5.74	8.09	3.86	5.67	4.21
Dilution Integrity	**% Bias**		-7.90	-9.20	-1.90	-7.50	-13.6	-10.6	-7.50
	CV		3.70	4.10	7.10	3.70	7.90	1.00	3.20

[a]*Matrix factor not IS normalised.*

Abbreviations: APAP: paracetamol; APAP-C: paracetamol cysteinyl conjugate; APAP-G: paracetamol glucuronide conjugate; APAP-NAC: paracetamol n-acetyl-cysteine conjugate; APAP-OMe: 3-methoxy paracetamol; APAP-S: paracetamol sulfate conjugate; APAP-SG: paracetamol glutathione conjugate; CV: coefficient of variance; HQC: high quality control; LLOQ: lower limit of quantification; LQC: low quality control; QC: quality control; ULOQ: upper limit of quantification.

2.3.4 Human plasma validation results

All cross-validation results are summarised in Table 2.36**.** All curves were linear and had r^2 values above 0.99. The method was accurate and precise at all QC levels. The effect of the matrix on peak areas were minimal, with average peak areas within 11% above or below matrix free samples for all metabolites, and CVs were within acceptance criteria. Recoveries were good and higher than 88%, and all CVs were below 13% for all analytes at LQC and HQC. CV and percentage bias met acceptance criteria for all analytes for the dilution integrity except for APAP-NAC, as expected from previous results in rat plasma.

Table 2.36. Summary of cross- validation for human serum

Parameter	QC Level		APAP	APAP-S	APAP-G	APAP-C	APAP-NAC	APAP-SG
Linearity R2	-		0.997	0.996	0.996	0.995	0.994	0.990
Line equation	-		0.00812x-0.0242	0.00665x-0.00419	0.000831x-0.00387	0.235x-0.0452	0.136x-0.0105	2390x-566
Intra-Day Accuracy (Mean % Bias) N=6	**LLOQ**		13.2	6.80	12.3	12.0	-16.7	-8.90
	LQC		9.30	10.9	6.30	8.50	5.00	-6.20
	MQC		10.2	10.9	7.40	8.30	6.70	-13.3
	HQC		7.20	7.80	9.00	4.70	11.7	-2.60
	ULOQ		6.10	7.80	8.60	2.40	9.20	-2.10
Intra-Day Precision (CV) N=6	**LLOQ**		3.20	1.20	10.4	5.70	7.90	12.9
	LQC		4.90	4.30	7.50	5.60	3.70	9.30
	MQC		5.10	4.50	10.8	5.60	7.50	11.8
	HQC		5.80	5.10	4.70	5.50	9.10	5.40
	ULOQ		2.50	3.10	1.80	3.20	2.90	10.7
Matrix Factor (Mean %) N=6	**LQC**	**% Bias**	3.48	2.67	-0.62	0.04	10.8	8.51[a]
		CV	4.57	6.65	5.31	3.89	8.55	4.08
	HQC	**% Bias**	-3.86	-1.87	-3.47	-7.23	-3.32	-10.4[a]
		CV	2.78	2.89	4.82	4.09	3.86	5.95
Recovery (Mean %) N=6	**LQC**	**% Bias**	90.5	93.7	93.6	89.6	87.2	88.2
		CV	6.94	6.71	7.88	10.2	13.0	7.96
	HQC	**% Bias**	95.2	89.9	93.8	94.6	96.3	92.3
		CV	5.25	8.42	9.71	8.66	8.43	10.3
Dilution Integrity N=6	**Mean % Bias**		-0.40	2.20	-1.20	-5.60	14.2	4.20
	CV		1.80	3.80	8.30	7.70	25.6	1.80

[a]Matrix factor not IS normalised.

Abbreviations: APAP: paracetamol; APAP-C: paracetamol cysteinyl conjugate; APAP-G: paracetamol glucuronide conjugate; APAP-NAC: paracetamol n-acetyl-cysteine conjugate; APAP-S: paracetamol sulfate conjugate; APAP-SG: paracetamol glutathione conjugate; CV: coefficient of variance; HQC: high quality control; LLOQ: lower limit of quantification; LQC: low quality control; QC: quality control; ULOQ: upper limit of quantification.

2.3.5 Determination of paracetamol and metabolites in plasma following oral administration to the rat

The assay was applied to the analysis of APAP, APAP-S, APAP-G, APAP-C, APAP-NAC and APAP-SG in the plasma of rats receiving either a single oral administration of dose vehicle, or 500 or 1500 mg/kg of the drug. Neither APAP nor any of the targeted metabolites were detected in samples from pre-dose time points or from vehicle-dosed control animals. The highest plasma concentrations of APAP itself were detected in samples obtained for the 1 and 2 hr post-dose time points in both the 500 and 1500 mg/kg dose groups, with the concentrations measured falling between the upper and lower limits of quantification for all but one sample (from the 1500 mg/kg dose group).

Similarly, for APAP-S the mean peak observed concentrations were obtained at the 1 and 2 hour time points as seen with APAP itself, although several samples (at both 500 and 1500 mg/kg dose levels) were at, or above, the ULOQ (Figure 2.3 Plasma concentration data for APAP, APAP-G and APAP-S, obtained pre-dose and at various time points post-dose up to 24 h, for rats administered APAP at either 500 or 1500 mg/kg (based on the analysis of 5 µL of sample). Each point represents an individual animal, boxes represent the median and interquartile range and whiskers show the full range.). For APAP-G, the mean peak plasma concentrations were seen at 1 and 2 hr post-dose for the 500 mg/kg dose and slightly later, at the 2 and 4 hr post-dose time points, for the 1500 mg/kg dose level (where concentrations in several samples exceeded the ULOQ) (Figure 2.3). However, the high values for APAP and APAP-S, APAP-G were all within 150% of the value of the ULOQ and therefore could be extrapolated from the existing standard curve and are still quantitative.

The concentrations of the NAPQI-derived metabolites, APAP-C, APAP-NAC and APAP-SG were considerably lower than those of APAP and its phenolic sulfate and glucuronide conjugates. Both the APAP-C and APAP-NAC metabolites were detectable following APAP administration with peak observed concentrations seen at the 24 h time point at both doses. The concentrations of the APAP-C metabolite were often at, or just below, the LLOQ, at early time points for both 500 and 1500 mg/kg

dose levels (particularly for the 500 mg/kg dose group) (see Figure 2.4). Similarly, the APAP-NAC metabolite was generally detectable in all of the post-dose samples but only reliably above the LLOQ at the later time points. Likewise, the low concentrations of APAP-SG meant that the majority of the time points, apart from the 24-hour sample, whilst above the limit of detection of the method, fell below the LLOQ (Figure 2.4). The fact that these NAPQI-derived metabolites were detectable in the current analysis but were often at or below the LLOQ reflects the fact that the samples were diluted 1 in 1000 prior to analysis so that the more abundant analytes, such as APAP and the glucuronide and sulfate conjugates, were present in final concentrations within the linear range for their assay. In practice, if the 3 NAPQI-derived metabolites were the focus of the study their accurate quantification could be readily achieved by analysis of a less dilute sample. Reducing sample dilution would enable appropriate quantification of these NAPQI-derived metabolites (as we have shown for mouse serum in a recent application of the method (Triantafyllou et al. 2018)). The reconstructed ion chromatograms (Figure 2.5) for typical 1- and 24-hour plasma samples for the 500 mg/kg dose show the change in the balance of metabolites within the profile with time after dosing.

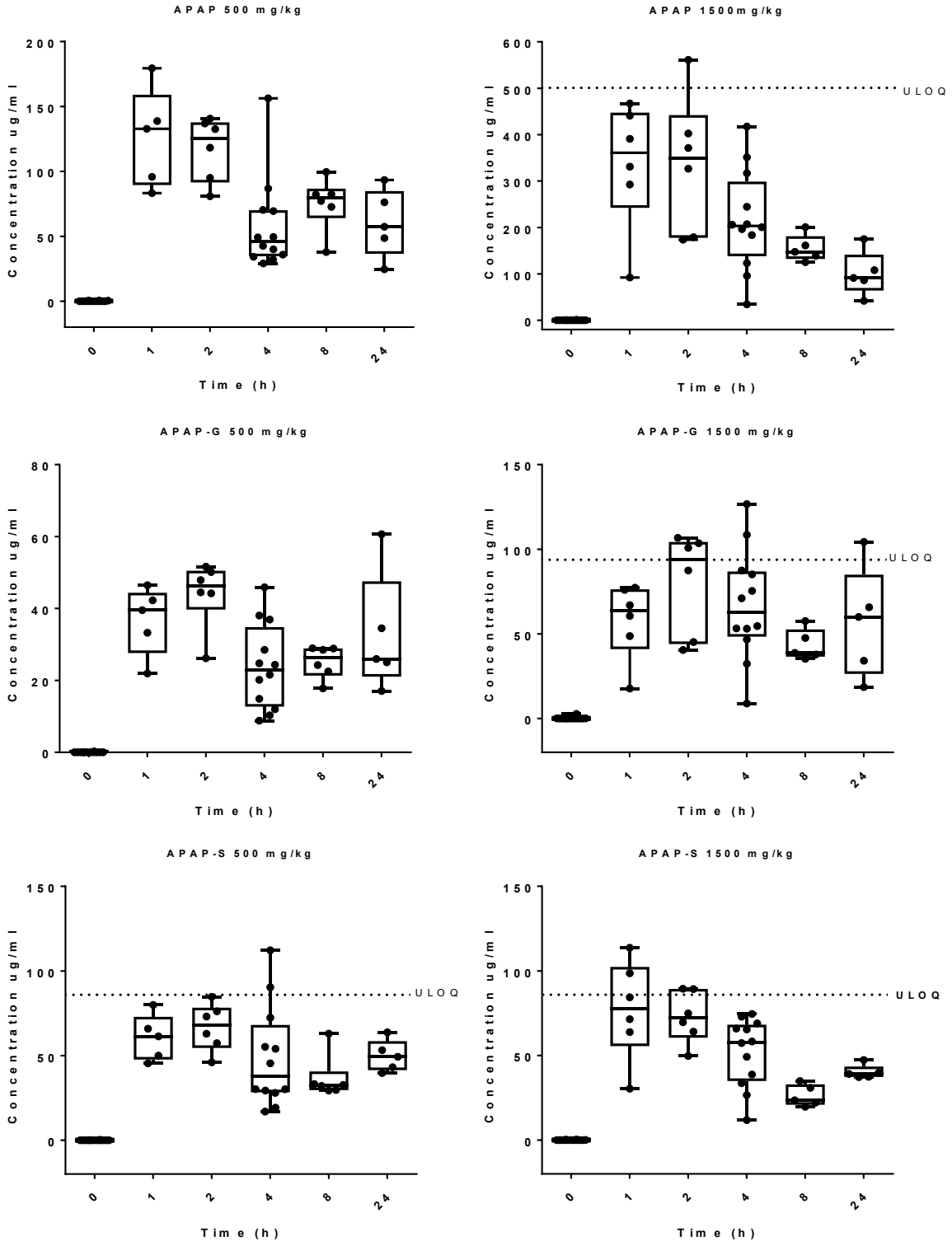


Figure 2.3 Plasma concentration data for APAP, APAP-G and APAP-S, obtained pre-dose and at various time points post-dose up to 24 h, for rats administered APAP at either 500 or 1500 mg/kg (based on the analysis of 5 µL of sample). Each point represents an individual animal, boxes represent the median and interquartile range and whiskers show the full range.
Abbreviations: APAP: paracetamol; APAP-G: paracetamol glucuronide conjugate; APAP-S: paracetamol sulfate conjugate.

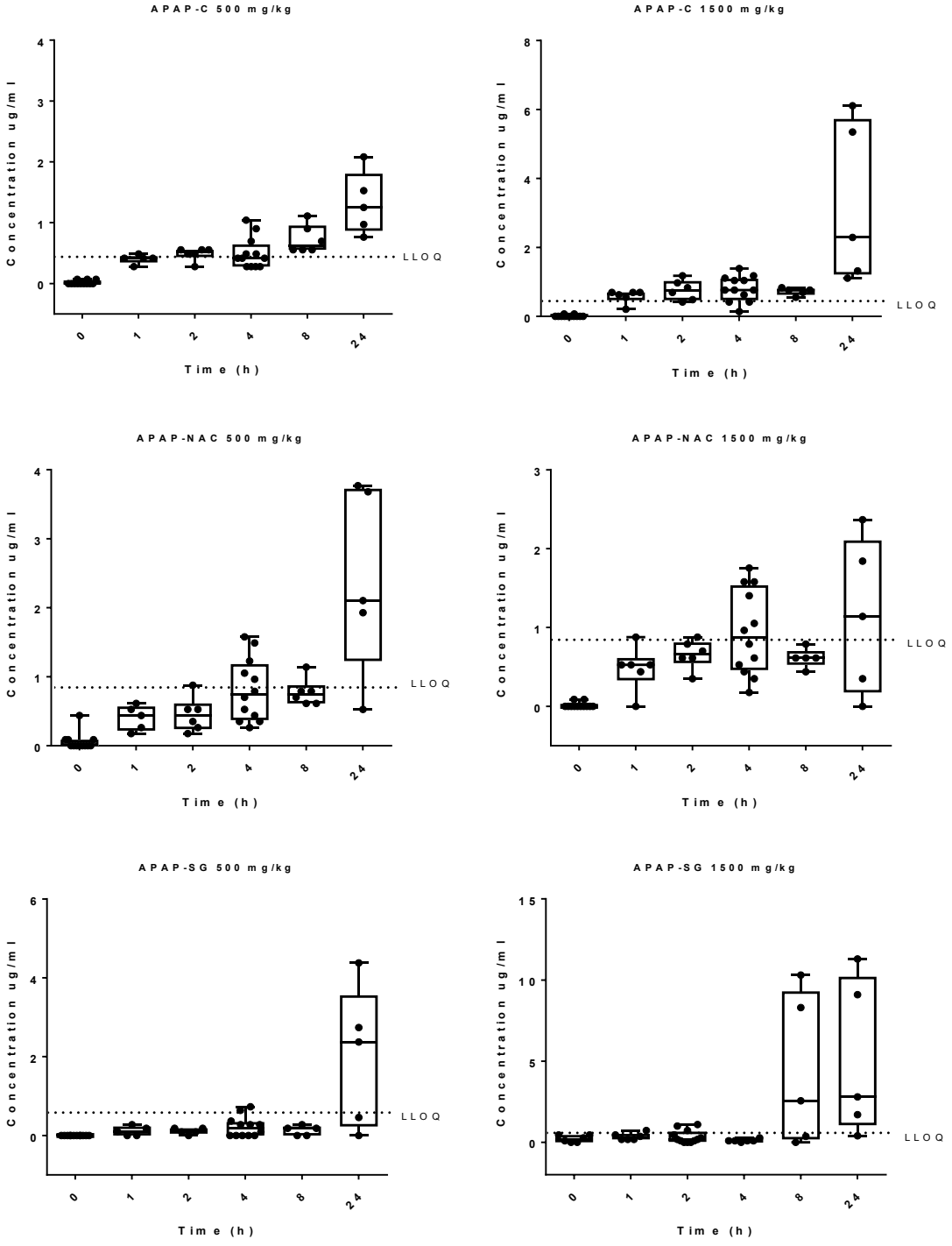


Figure 2.4 Plasma concentration data for the APAP-C (upper), APAP-NAC (middle) and APAP-SG (lower) conjugates, at various time points post-dose, in samples obtained from rats administered APAP at either 500 or 1500 mg/kg(based on analysis of 5 µL of sample.) Each point represents data from one animal, boxes represent the median and interquartile range.
Abbreviations: APAP-C: paracetamol cysteinyl conjugate; APAP-NAC: paracetamol n-acetyl-cysteine conjugate; APAP-SG: paracetamol glutathione conjugate

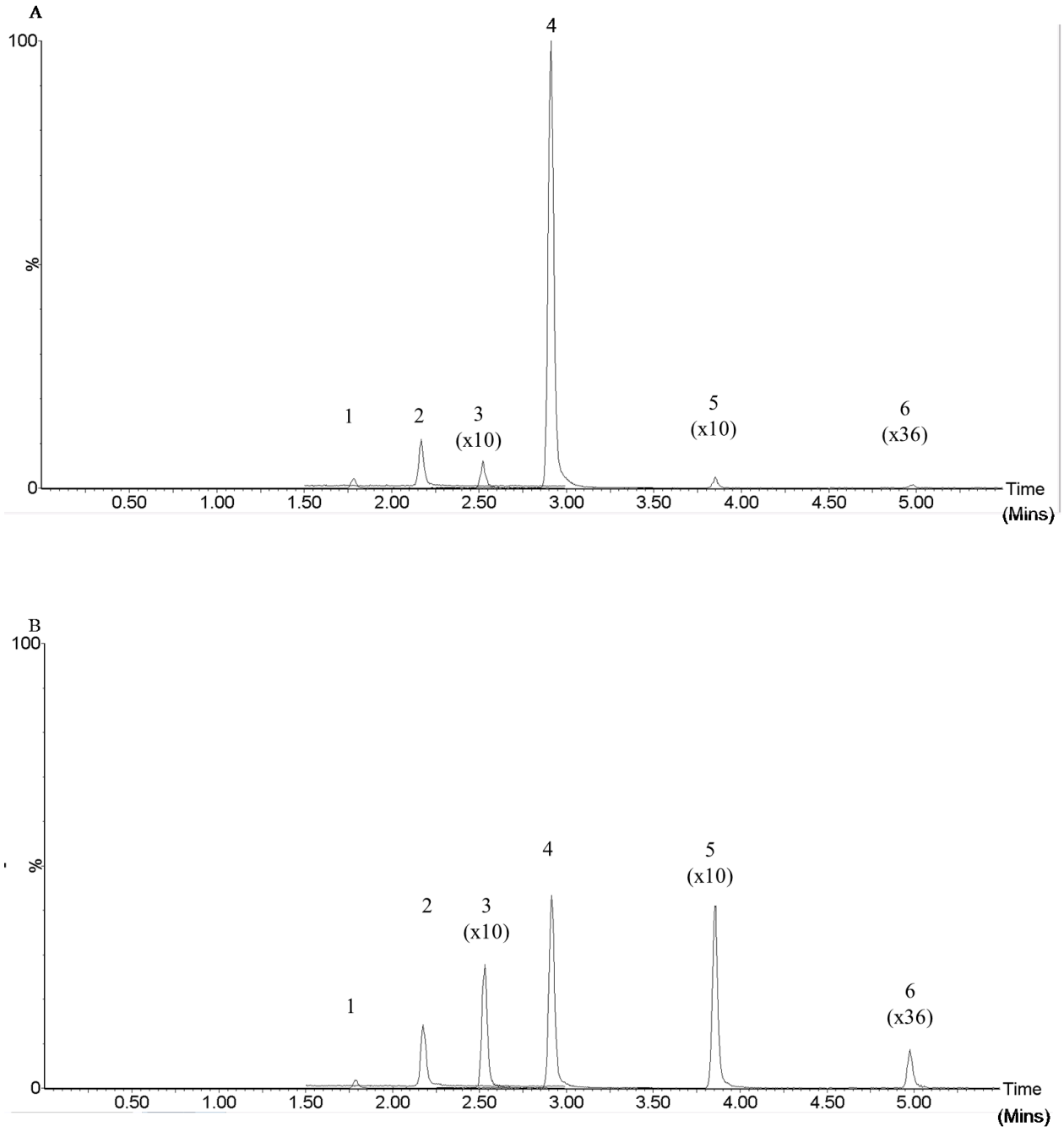


Figure 2.5 A) Representative chromatograms for samples from the 500mg/kg APAP dose group 1 hr post dose or B) 24hr post dose. Some chromatographic peaks have been increased in intensity in some cases for clarity (as indicated by the numbers in parenthesis above the peaks.) All chromatographic peak intensities are relative to APAP in Figure 2.5A.
1=paracetamol glucuronide, 2=paracetamol sulfate, 3=paracetamol cysteinyl conjugate, 4=APAP paracetamol, 5=paracetamol glutathione conjugate, 6=paracetamol n-acetylcysteinyl conjugate.

2.4 Discussion

The development of this UHPLC -MS-based method for the quantification of APAP and metabolites results in greater efficiency through the adoption of minimal sample preparation methods and shorter analysis times, as well as enabling the use of much smaller samples. As indicated previously, several LC-MS-based assays for APAP and (a variable number of) metabolites have been described for use in biofluids such as urine and blood derived samples. Some of these methods, such as that developed for mouse urine (Hewavitharana et al. 2008), are limited in their coverage to the determination of APAP and the major conjugated metabolites APAP-G and APAP-S. The method, which used the structural analogue of APAP 3-acetamidophenol as an internal standard, and employed an isocratic reversed-phase separation with a nominal run time of 10 min. However, with column washing and re-equilibration the analysis time per sample was 30 min. Subsequent methods enabled the determination of APAP and either APAP-G alone (Tan et al. 2012), or both APAP-G and APAP-S (Gicquel et al. 2013). The analysis of APAP and APAP-G used isocratic reversed-phase HPLC-MS/MS and was developed for the quantification of these analytes in human plasma and urine (Tan et al. 2012). Similarly an isocratic reversed-phase LC-MS/MS assay, used to determine APAP, APAP-G and APAP-S in mouse plasma (Gicquel et al. 2013), employed APAP-d4 as IS and had an overall analysis time of 10 min/sample (Gicquel et al. 2013). More recently methods have been described for the analysis of plasma or urine samples offering a more comprehensive coverage of APAP and its metabolites, including those resulting from the production of NAPQI (An et al. 2012; Cook et al. 2015; Flint et al. 2017; Lammers et al. 2017). The first of these methods allowed the determination of APAP and six metabolites (APAP-G, APAP-S, APAP-OMe, APAP-NAC, APAP-C and APAP-SG) in rat plasma using HPLC-MS/MS (An et al. 2012). This assay used deuterated APAP and APAP-G as internal standards and employed a reversed-phase gradient elution separation to give a run time of 16 min/sample. However, two runs were required to obtain the required data as the method employed positive ESI for APAP and 3-methoxy-APAP (APAP-OMe) and negative ESI for APAP-S, APAP-G, APAP-SG, APAP-NAC and APAP-C. The validated assay had an LLOQ of 100 ng/ml for APAP, APAP-S, APAP-G and for 10 ng/mL

APAP-SG, APP-NAC, APAP-Cys and APAP-OMe. Another multi-metabolite method, also based on gradient reversed-phase HPLC-MS/MS for the quantification of APAP, APAP-G, APAP-S, APAP-NAC, APAP-C and APAP-SG, and employing APAP-d4 and APAP-S-d3 as internal standards, was used to analyse 10 µL samples of both human urine and plasma (with an analysis time of 20 min/sample) (Cook et al 2015).

More recently a method based on reversed-phase gradient HPLC-MS/MS, with a total run time of 9 minutes, was developed to analyse APAP, APAP-G, APAP-S, APAP-OMe, APAP-SG, APAP-C, and APAP-NAC in 100µl of human plasma (Lammers et al. 2017). A feature of this method was the use of APAP-d4, APAP-G-d3, APAP-S-d3, APAP-C-d5, and APAP-NAC-d5 to monitor the assay, rather than a reliance on a more limited number of internal standards. A second method, this time based on UHPLC-MS also employed reversed-phase gradient chromatography, with a rapid (4.5 min) separation, to analyse APAP,APAP-G, APAP-S, APAP-C, APAP-SG and APAP-NAC (in addition protein-derived APAP-C formed via the reaction of NAPQI with protein) in 10µl of human plasma obtained from children taking part in a paediatric clinical study (Flint et al 2017). APAP-d3 was used as the IS for all analytes in this method.

The UHPLC -MS method described here has been validated for the analysis of small (5 µL) samples of rat, human and pig plasma and mouse serum, making it suitable for studies in animals or patients, where only limited quantities of plasma or serum are available, with minimal sample preparation. Unlike many earlier methods, the assay described here employs stable isotopically labelled internal standards for all of the analytes validated for quantitative analysis (APAP, APAP-G, APAP-S, APAP-C, APAP-SG and APAP-NAC). The method has a short analysis time (7.5 min/sample) and employs minimal sample preparation, offering the potential for efficient large-scale sample analysis. In addition to the quantification of APAP and the metabolites described above, the method can be used to monitor, and provide semi-quantitative data, for the minor APAP-OMe (for which no isotopically labelled IS was available) using an external standard curve. Similarly, the metabolite PAP-G (formed by the glucuronidation of *p*-aminophenol produced by the *N*-deacetylation of APAP and subsequent

O-glucuronidation) can also be monitored, and semi-quantified, in for example, porcine plasma using a similar approach.

2.4.1 Conclusions

A simple, rapid and sensitive UHPLC-MS/MS method for the quantitative analysis of acetaminophen and of its five metabolites (APAP-G, APAP-S, APAP-C, APAP-SG and APAP-NAC) using deuterated internal standards, has been developed for the analysis of plasma samples from rat, pig and human, and serum from mouse. In addition, a further two metabolites APAP-OMe and PAP-G can be monitored and semi-quantified using external standards. The method, which requires only 5 µL of sample, has been validated for use in human, rat and pig plasma, and mouse serum.

3 A UHPLC-MS/MS method for quantifying and semi-quantifying glutathione biosynthesis related metabolites.

3.1 Introduction

Hepatic glutathione is depleted during APAP overdose, and therefore there are changes to the concentrations of circulating metabolites associated with GSH biosynthesis and downstream sulfur containing metabolites. A robust analytical method for the simultaneous measurement of these metabolites in small biofluid volumes was required in order to quantify these metabolites for use in mathematical models, and for biomarker identification. A UHPLC-MS/MS method had previously been partially validated for measuring glutathione and related metabolites in serum. However, due to the fact that the analytes of interest are endogenous and present in serum and plasma it was difficult to obtain blank matrix for use in the validation, and so the original validation was performed in water. Considering that matrix effects are of increasing concern in bioanalysis, and particularly for HILIC based methods, it was important to evaluate this method for matrix effects and analyte recoveries in order to ascertain whether results could be considered quantitative. To further ensure the quality of the results provided by the method further validation experiments were undertaken to attempt to optimize the sample preparation protocol.

3.1.1 Hypothesis

It was hypothesised that there would be "matrix effects" on the measurement of the GSH biosynthesis-associated metabolites in serum that could affect the accuracy of their quantification, and in addition, that some metabolites from serum could be lost through the extraction process.

3.1.2 Aims

- To further develop and validate the UHPLC-MS/MS method for glutathione and biosynthetic pathway-related metabolites, which had previously been developed and partially validated, by optimizing metabolite extraction from serum and measuring matrix effects and extraction efficiencies (recovery).
- To make changes to the sample preparation protocol to allow the method to be successfully applied to human serum, in order to understand the effects of APAP overdose on GSH related metabolism.

3.1.3 Background and rationale

As discussed previously, APAP metabolism and toxicity has been studied extensively over the last 50 years. Following APAP overdose there is a metabolic switch from APAP metabolism by glucuronidation and sulfation, to oxidative metabolism, catalysed by CYP enzymes, to form the reactive intermediate NAPQI which depletes hepatic GSH (Dahlin et al. 1984; James et al. 2003; Mitchell et al. 1973a; Mitchell et al. 1973b; Potter et al. 1973). GSH depletion has toxicological consequences in APAP overdose, not only due to covalent binding to proteins of NAPQI and oxidative stress, but also due to the potential changes to the various metabolites involved in GSH biosynthesis, and downstream sulfur containing metabolites which are also synthesised from methionine and cysteine (as reviewed in (Lu 2013). In Figure 3.1, some of the key metabolic pathways in the methionine cycle, trans-sulfuration pathway and γ-glutamyl cycle, are summarized. APAP induced weight loss in the rat was not seen in animals fed a methionine enriched diet (McLean et al. 1989), suggesting that GSH depletion by APAP caused shifts in metabolic pathways relating to methionine and its downstream metabolites. Metabolites involved in GSH biosynthesis may also be potential biomarkers for GSH depletion in APAP toxicity and may be predictive of liver injury from APAP and other GSH depleting compounds. Concentrations of 5-OP and OA have been found to be potential biomarkers of GSH depletion in animal models (Ghauri et al. 1993; Soga et al. 2006) and in a systems biology model based on *in-vitro* data (Geenen et al. 2013).

There have previously been methods developed for the quantification of GSH and sulfur containing metabolites which use either GC, LC or CE separation coupled with UV or MS detection. However, none of these are able to cover the entire pathway. Methods have been described which rely on derivatisation of the free thiol groups, which means that compounds with and without free thiols cannot be simultaneously quantified (Guan et al. 2003; Hammermeister et al. 2000; Raggi et al. 1998; Stabler et al. 1987). A method which used HILIC without derivatisation has previously been developed, but the method was only able to cover cysteine, homocysteine, methionine, cystathionine, γ-glu-cys, GSH, GSSG and SAH (Lafaye et al. 2005). As key metabolites of interest for the work of this Thesis

include 5-OP and OA, a method that included these metabolites was required. There had also previously been a number of analytical methods for measurement and quantification of 5-OP, including an ion pairing method for quantification in cerebrospinal fluid (Eckstein et al. 2008), another method was developed for fermentation media (Qu et al. 2002). 5-OP has also been measured in rat plasma and cell extracts (Geenen et al. 2011a). More recently, a reversed phase LC-MS method was validated for 5-oxoproline plus glutamate, GSH and GSSG in a number of mouse biofluids and tissue extracts, which relied on derivatisation of GSH (Gil et al. 2018). Similarly, methods for the quantification of OA in rodent and human serum by LC-MS have been described (Geenen et al. 2011b; Kaur et al. 2015), and for the quantification of OA with GSSG and GSH (New and Chan 2008). However, none of these methods are able to simultaneously quantify metabolites including those in the methionine cycle, trans-sulfuration pathway, γ-glutamyl-cycle, taurine and related metabolites, and OA.

To investigate these metabolic shifts in response to GSH depletion by xenobiotics a UHPLC-MS/MS method was developed and was previously applied to rodent biofluids (Isobelle Grant PhD Thesis). This method is capable of quantifying or monitoring up to 24 metabolites relating to GSH biosynthesis and metabolism. In order to further investigate whether OA or 5-OP may be biomarkers for the severity of liver injury after a paracetamol overdose, it was important to further develop this method and to understand whether, taking into account extraction efficiencies and matrix effects, results from this assay could be described as quantitative and therefore used in mathematical models.

The matrix effects and recoveries were initially measured in mouse and human serum. There are two commonly used methodologies for assessment of matrix effects, which include the qualitative “post-column infusion method” which is a methodology involving adding compounds after the separation column and comparing these with standards spiked into blank matrix (Bonfiglio et al. 1999). However, this methodology is labour intensive compared to the “post-extraction addition” methodology, which is a quantitative assessment of matrix effects based on analysing standards when spiked into a blank

matrix sample post extraction, with standards in solvent (Matuszewski et al. 2003). As the UHPLC-MS/MS method described here involves the simultaneous quantification of numerous metabolites and is designed to be rapid, quantitative and simple, the “post-extraction addition” methodology was deemed the most appropriate approach. This methodology also allows recovery to be assessed by comparing the same post-extraction sample with a sample where standards are spiked into blank matrix before extraction. As all the analytes in this assay are present in serum, and so no blank matrix was available, matrix factors and recoveries were assessed, wherever possible, by spiking stable isotope labelled internal standards (IS) into the serum at the low- and high-quality control (QC) concentration levels. It was assumed that matrix effects and recovery of these IS would reflect the behaviour of the analytes

For this method a simple protein precipitation extraction method using acidified CH_3CN was used, with the addition of water to the extraction in order to help extraction efficiency of polar compounds following a comparison of different protocols (data not shown.) Changes were made to the extraction protocol in human serum to try to reduce some matrix effects and also increase extraction efficiency.

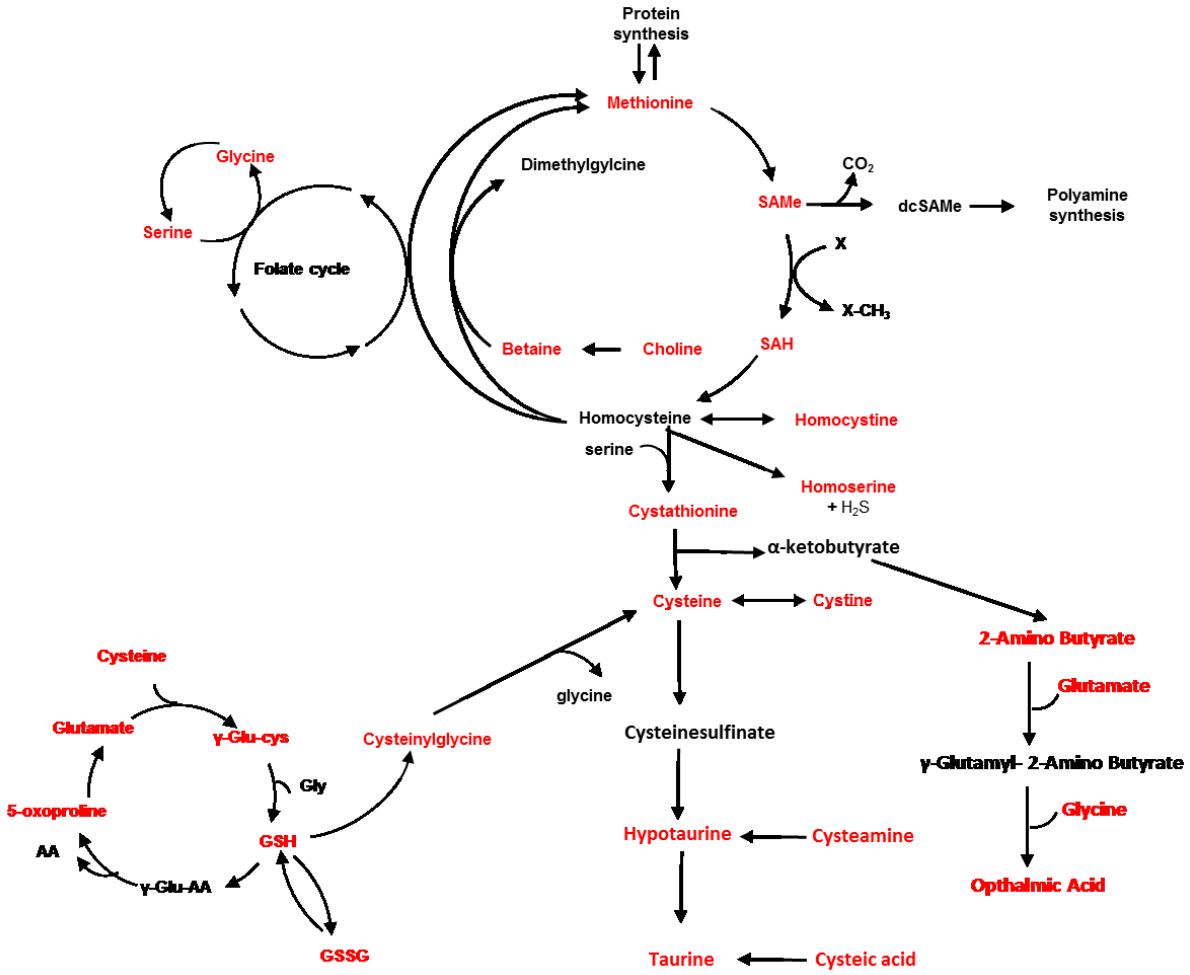


Figure 3.1 The key components of metabolites related to glutathione metabolism, including the components of the methionine cycle, trans-sulfuration pathway and gamma-glutamyl cycle. The metabolites highlighted in red are included in the method.
Abbreviations: dcSAMe: decarboxylated S-adenosyl methionine; γ-glu-AA: gamma-glutamyl amino acid; γ-glu-cys: gamma-glutamyl cysteine; GSH: glutathione; SAH: s-adenosyl methionine; SAMe: s-adenosyl methionine.

3.2 Materials and methods

3.2.1 Materials

All unlabelled standards were purchased from Sigma Aldrich (Gillingham, UK), with the exception of ophthalmic acid which was purchased from Bachem AG (Bubendorf, Switzerland). DL-glutamic acid-d_3, L-glutamine-d_5, DL-serine-d_3, were purchased from Cambridge Isotope Laboratories (MA, USA). DL-Methionine-$^{13}C^{15}N$ was purchased from QMX Laboratories (Essex, UK). Cysteine-$^{13}C_3{}^{15}N$, Choline-1,1,2,2-d_4 Bromide and 2-Aminoethane-d_4-sulfinic Acid (hypotaurine-d_4) were purchased from Qmx Laboratories Ltd, CND isotopes. Cystine-d_6, homocysteine-d_4, D,L-cystathionine-d_4, glutathione disulfide-$^{13}C_4$ $^{15}N_2$, 5-oxo-DL-proline-d_5, SAMe-d_3, L-homocysteine-d8 and taurine-d4 were from

Toronto Research Chemicals Inc. (Ontario, Canada). Human serum was purchased from Seralabs (Bioreclamation, IVT)

3.2.2 Mass spectrometry

The “targeted” UHPLC-MS/MS assay was performed on a Xevo (TQ)-S mass spectrometer (Waters Corporation, Manchester, UK). This was operated in ESI positive ion mode using nitrogen as the desolvation gas, and using MRM, argon was the collision gas. The source conditions were: capillary voltage, 3.0 kV; source offset, 50 V; desolvation temperature, 550°C; source temperature, 150 °C, desolvation gas flow, 1000 L/h; cone gas flow, 150 L/h; nebuliser gas, 7.0 bar; collision gas, 0.15 L/h. Cone Voltage and collision energies were individually determined for each standard during individual direct infusion using the “intellistart” function, with manual optimisation where required, and are given in Table 3.1 and for internal standards in Table 3.2**.** Dwell times were automatically determined by “masslynx” software based on the number of analytes. Also described in Table 3.1 and Table 3.2 , are the chromatographic properties of standards and IS including the retention time window used for acquisition, individual retention times are not displayed as these were not consistent between different matrices.

Table 3.1 Mass spectrometric and chromatographic properties for each standard in the GSH method.

Analyte	Parent (m/z)	Fragment (m/z) Quantification **Identification**	RT Window (min)	Dwell time (s)	CV (V)	CE (eV)
2-amino-butyric acid	103.866	57.892	1-2.5	0.004	50	12
Betaine	118.068	58.89 **42.16**	0.5-2.5	0.004	110 56	22 **74**
Choline	104.132	60.028 **5.002**	0-2	0.004	90 90	20 **16**
Cystathionine	223.077	134.01 **87.972**	5.5-7.5	0.013	40 40	12 **24**
Cysteic acid	169.937	105.981 **2.641**	5-7	0.013	30	18 **24**
Cysteine	122.192	75.984 **04.976**	1-3	0.004	24	12 **8**
Cysteinyl-glycine	178.987	75.952 **58.98**	0.5-2.5	0.004	22	14 **24**
Cystine	241.14	74.046 **52.049**	5.75-7.75	0.013	60	24 **12**
γ-glutamyl-cysteine	251.077	121.977 **84.008**	1.5-3.5	0.004	22	10 **22**
Glutamic acid	148.098	84.071 **102.032**	1.5-3.5	0.004	60	16 **12**
Glutamine	147.037	84.038 **56.074**	2.2-4.2	0.004	42	14 **22**
Glutathione, reduced	308.097	179.00 **75.991**	2-4	0.004	14	12 **24**
Glutathione, oxidised	613.287	355.054 **30.996**	6-14.7	0.013	40	22 **30**
Glycine	76.038	30.042 **48.078**	1-3	0.004	30	4 **6**
Homocystine	269.19	136.028 **87.97**	5-7	0.013	10	10 **30**
Homoserine	119.96	73.812 **55.863**	1.5-3.5	0.004	28	20 **25**
Hypotaurine	109.927	29.987 **45.077**	2.75-4.75	0.004	34	8 **14**
Methionine	150.05	104.048 **56.025**	0.3-2.3	0.004	50	10 **16**
Ophthalmic acid	290.13	58.102 **161.072**	2-4	0.004	10	16 **12**
5-Oxoproline	130.072	83.962 **55.992**	0-2	0.004	36	17 **20**
S-adenosyl-homocysteine	385.113	TIC (249.98) **87.97**	4.5-6	0.016	30	12 **40**
s-adenosyl-methionine	399.113	249.99 **135.955**	5.5-14.7	0.013	46	14 **32**
Serine	105.968	70.007 **42.102**	2.5-4.5	0.004	30	13 **17**
Taurine	126.054	44.079 **107.969**	1.75-3.75	0.004	42	30 **25**

Abbreviations: CE: collision energy; CV: cone voltage; RT: retention time.

Table 3.2 Mass spectrometric and chromatographic properties for each internal standard in the GSH method

Analyte	**Parent**	**Fragment** Quantification **Identification**	**RT Window (min)**	**Dwell time (s)**	**CV (V)**	**CE (eV)**
Choline-d_4	108.196	60.258 **49.079**	0-2	0.004	58	35
Cystathionine-d_4	227.013	137.836 **91.81**	5.5-7.5	0.013	4	14 **26**
Cysteine-$^{13}C_3{}^{15}N$	125.970	60.818 **78.834**	1.5-4	0.003	16	16 **10**
Cystine-d_6	246.949	122.837 **54.763**	5.75-7.75	0.013	20	40 **30**
DL-Glutamic acid-d_3	150.977	132.852 **104.892**	1.5-3.5	0.004	32	27 **33**
L-Glutamine-d_5	151.968	134.819 **88.119**	2.2-4.2	0.004	2	30 **40**
Glycine-$^{13}C^{15}N$	79.0181	32.023 **49.946**	1-3.5	0.003	22	6 **4**
GSSG -$^{13}C_4{}^{15}N_2$	619.377	TIC **231.059**	6-14.7	0.013	40	22 **30**
Homocysteine-d_4	140.118	58.963 **94.081**	1.25-2.75	0.003	16	14 **10**
Homocystine-d_8	277.113	91.858 **139.839**	5.25-6.75	0.011	4	28 **8**
Hypotaurine-d_4	114.132	32.135 **49.083**	2.75-4.75	0.004	38	10 **14**
DL-Methionine-$^{13}C^{15}N$	155.977	59.892 **108.854**	0.3-2.3	0.004	30	40 **35**
5-oxoproline-d_5	135.136	89.03 **61.06**	0-2	0.004	28	14 **22**
SAMe-d3	402.096	135.818 **49.851**	5.5-8	0.011	2	36 **16**
DL-Serine-d_3	108.95	62.842 **44.886**	2.5-4.5	0.004	32	10 **16**
Taurine-d_4	130.118	48.169	1.75-3.75	0.004	32	25

Abbreviations: CE: collision energy; CV: cone voltage; GSSG: oxidised glutathione; RT: retention time; SAMe: s-adenosyl methionine.

3.2.3 Chromatography

Analytes were separated using a HILIC methodology on a waters ACQUITY BEH amide 2.1 x 150 mm, 1.8 µm column over a 14.7-minute mobile phase gradient as shown in Table 3.3. Mobile phase A was 0.2% FA in water and mobile phase B was 0.2% FA in CH_3CN. A strong needle wash and seal wash of 95:5 H_2O:CH_3CN (v:v) was used, the weak needle wash was 100% CH_3CN. A summary of the chromatographic separation during method development with neat standards is shown in Figure 3.2**.**

Table 3.3 Chromatographic gradient used for glutathione method.

Time (min)	**Flow Rate (mL/min)**	**% Mobile phase A** H_20 + 0.2% FA	**% Mobile phase B** CH_3CN + 0.2% FA
0.0	0.6	16	84
4.0	0.6	16	84
8.0	0.6	60	40
10.0	0.6	60	40
10.1	0.6	16	84
14.7	0.6	16	84

Abbreviations: FA: formic acid.

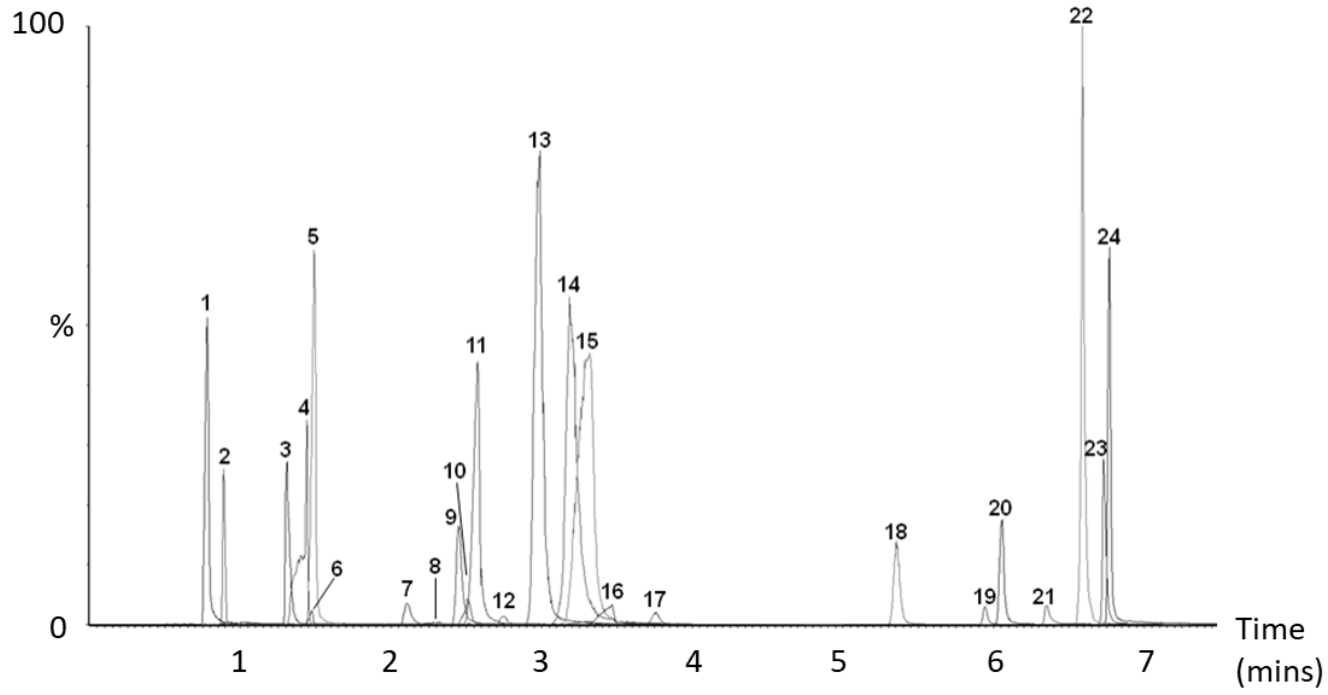


Figure 3.2 Summary of total ion chromatograms for standards measured in matrix free samples, normalised to the highest peak.
Key: 1. choline, 2. 5-oxoproline, 3. methionine, 4. cysteinyl-glycine, 5. betaine, 6 .2-amino butyrate, 7. cysteine, 8. glycine, 9. γ-glutamyl-cysteine, 10. homoserine, 11. glutamate, 12. taurine 13. ophthalmic acid, 14. reduced glutathione 15. glutamine 16. serine, 17. hypotaurine, 18. s-adenosyl-homocysteine, 19. cysteic acid, 20. homocystine, 21. s-adenosyl methionine, 22. cystathionine, 23. cystine, 24. Oxidised glutathione.

3.2.4 Preparation of samples for mouse serum validation

3.2.4.1 Validation Procedure

In order to assess matrix factor and extraction efficiency, three sets of six QC samples were prepared using the IS (where available) at the concentration of both the LQC and the HQC. IS were spiked into six individual samples of water +0.2% FA, into six individual serum samples which were then extracted in accordance with methods below or were spiked into six individual serum samples post extraction.

To calculate the matrix effects, the peak areas of IS when spiked into serum samples post extraction were compared to the areas of the IS in water. To calculate the extraction recovery, the peak area of IS were compared in samples spiked into serum before and after extraction. In Figure 3.3 a flow chart summarises how each of these standards were produced. The three types of sample which were prepared in order to measure matrix effects and recovery were the "IS Before Extraction," "IS After Extraction" and "Matrix Free" samples. As in this assay there is no secondary dilution step following protein precipitation, in order to produce the "IS Spiked After" and "Matrix Free" samples, IS solutions were spiked into samples after the protein precipitation step and before centrifugation. Because of this, the initial extraction is in a smaller volume of solvent with a lower water content than as samples are usually prepared i.e. "Normal Preparation". Therefore, to make the comparison between samples spiked before and after protein precipitation as similar as possible, 10 µL of water was also added to the "IS Before Extraction" samples after the protein precipitation step. As this sample preparation protocol does not exactly replicate that of real samples, another set of samples were prepared exactly as samples are usually prepared, with IS added before protein precipitation which will hereby be known as the "Normal Preparation" sample.

3.2.4.2 Preparation of Validation QCs

In order to produce stock solutions of the IS at the concentrations of the LQC and HQC of the standards they were used at, a new IS stock solution was produced as per Table 3.4in order to produce a stock solution with the concentrations listed in Table 3.5. This solution was then diluted to form an IS stock solution equivalent to the LQC and HQC concentrations for the standard for which it was an internal standard, as shown in Table 3.6**.** IS solutions were then spiked into samples of serum or matrix free samples following the samples preparation procedures set out in Figure 3.3**.**

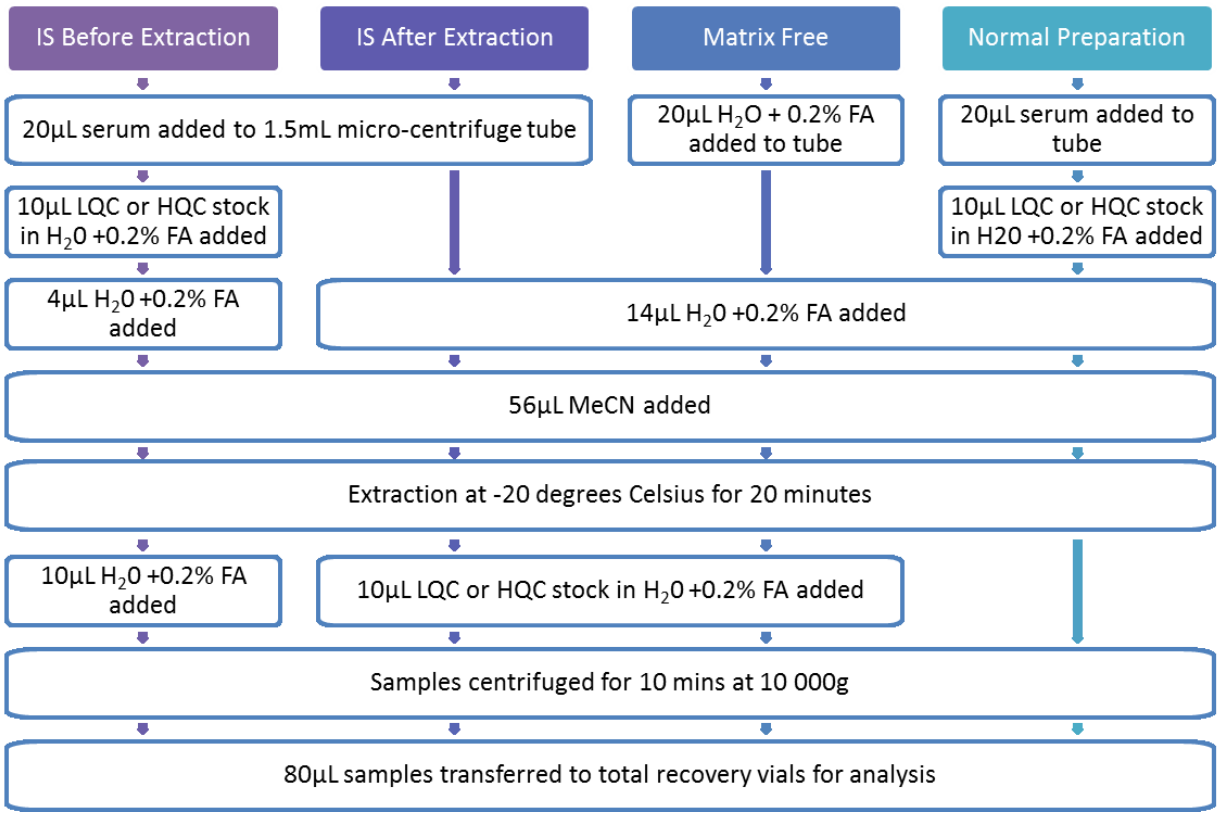


Figure 3.3 Flow chart to show how each of the 4 sample types for the mouse serum validation was prepared.
Abbreviations: FA: formic acid; HQC: high quality control; IS: internal standard; LQC: low quality control.

Table 3.4 Volumes of IS standard stock solutions mixed to form the IS top stock solutions, with concentrations for each of the three concentration ranges, mouse serum validation.

Stock solution component	Concentration (mg/mL)	Number of IS per group	Volume of each IS added (µL)	Total volumes µL in formation of IS stock solution 'A'
High concentration IS	1	5	50	250
Mid concentration IS	1	6	5	30
Low concentration IS	0.5	4	5	20
-	-	-	**H_2O+0.2% FA**	**200**
-	-	-	***Total***	***500***

Abbreviations: FA: formic acid; IS: internal standard.

Table 3.5 Concentration of each internal standard in the IS top stock solution before dilution to produce LQC and HQC IS stock solutions, mouse serum validation.

High concentration 100 µg/mL	Mid concentration 10 µg/mL	Low concentration 5 µg/mL
Glutamine-d_5	5-oxoproline-d_5	Cystathionine-d_4
Glycine-$^{13}C^{15}N$	Cystine-d_6	Choline-d_4
Serine-d_3	Glutamate-d_3	Homocysteine-d_4
Taurine-d_4	Hypotaurine-d_4	SAMe-d_3
GSSG-$^{13}C_4{}^{15}N_2$	Methionine -$^{13}C^{15}N$	Homocystine-d_8
	Cysteine-$^{13}C_3{}^{15}N$	

Abbreviations: GSSG: oxidised glutathione; SAMe: s-adenosyl methionine

Table 3.6 Preparation of HQC and LQC internal standard stock solutions, mouse serum validation.

IS Stock solution Soln.	Stock solution Soln. Conc. ng/mL		Final Conc. (1 in 10 dilution in prep) ng/mL	Volume IS 'Stock solution A' used	Volume H_2O + 0.2% FA added
HQC	High	80 000	8000	200µL	50µL
	Mid	8 000	800		
	Low	4 000	400		
LQC	High	6 000	600	30µL	470µL
	Mid	600	60		
	Low	300	30		

Abbreviations: FA: formic acid; HQC: high quality control; IS: internal standard; LQC: low quality control.

3.3 Cross validation to human serum

For application of the method to human serum, some changes were made to the original sample preparation protocol, in an attempt to reduce the matrix effects and improve extraction efficiency without the need to add further dilution steps to the preparation, the protocol was adapted to a two-stage extraction process with a drying stage. This allowed the initial extraction to take place in a larger volume of solvent, without including water, to allow extraction of the polar metabolites of interest in the samples, as water can adversely affect protein precipitation. Samples were originally extracted in MeOH + 0.2% FA (v/v), after which supernatants were dried at room temperature under a stream of nitrogen gas. The sample pellets were re-suspended in 16:84 H_20:CH3CN +0.2% (v/v) FA, to replicate the initial chromatographic gradient. The flow diagram shown in Figure 3.4summarises the human serum sample preparation protocol.

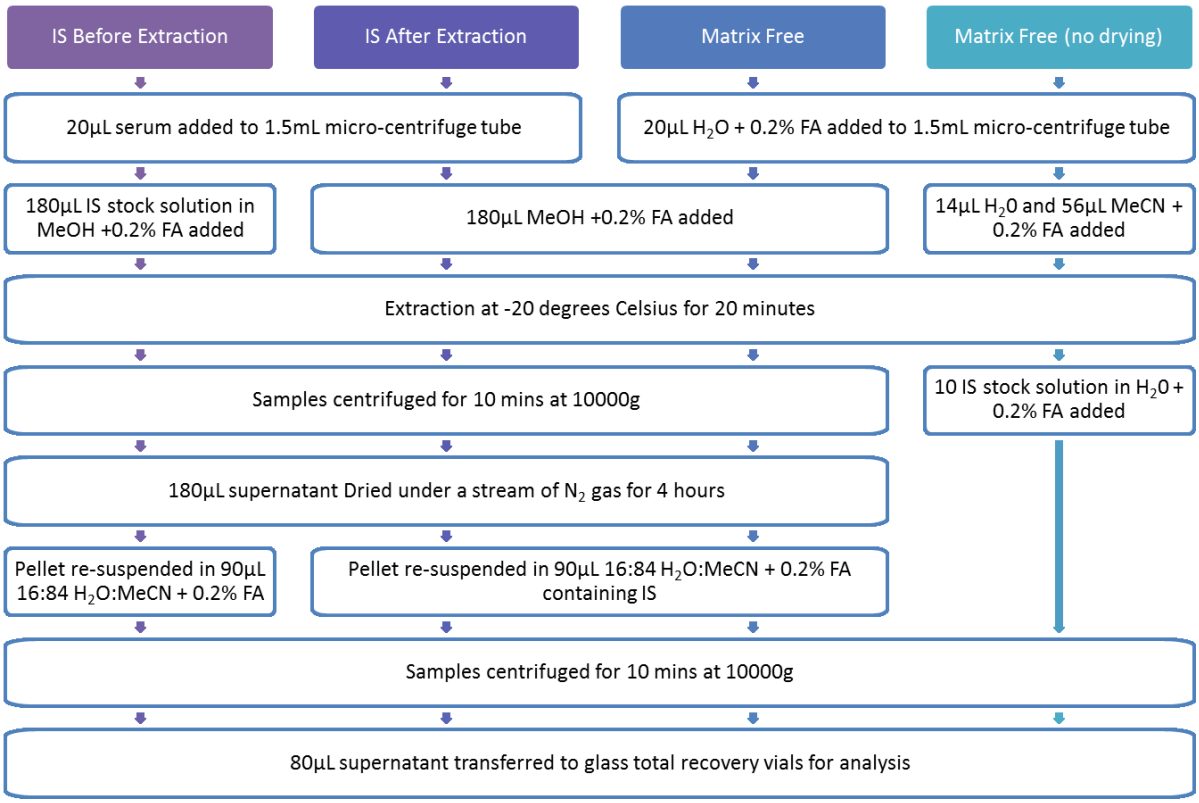


Figure 3.4 Flow chart of preparation of samples for human serum matrix effects and recovery calculations
Abbreviations: FA: formic acid; IS: internal standard.

3.3.1 Preparation of QCs for matrix factor and recovery determination

To produce the IS stock solutions, the concentrations of the top stock solutions were back calculated from the dilution and concentration steps in the sample preparation. The original IS solution was prepared so that upon addition to 20 µL of human serum, the concentration would be half of the final desired concentration, as 180 µL of this solution was then dried down and doubled in concentration. Some changes were made to the method including the removal of glycine and its IS from the method, as this could not be reproducibly measured. In order to test the efficiency of the sample preparation method for human serum by the new protocol, QCs were prepared with IS spiked in to serum in MeOH + 0.2% FA (v/v) before extraction and drying "IS Spiked Before", into 6 serum or matrix free samples after they have been extracted and dried the "IS Spiked After" and "Matrix Free" samples respectively, and one set of 6 samples prepared using the original protocol with IS added to H_20 and extraction in

H2O + 0.2% FA:Me_3CN + 0.2% FA 16:84 (v:v) which is referred to as "Matrix Free No Drying", summarised in Figure 3.4.

Top IS stock solution A was prepared as per Table 3.7in order to produce a stock solution containing IS at the concentrations below in Table 3.8**,**before being diluted to form HQC and LQC stock solutions as per Table 3.9. The LQC and HQC stock solutions were then added to 20 µL human serum which was dried and reconstituted in 50% volume of CH_3CN + 0.25 FA, to give the final concentrations shown in Table 3.10. For the samples spiked after extraction and for matrix free samples, the IS solutions were prepared in the same way with the exception that the 0.1:1.0 dilution step was with water and not human serum. This IS stock solution was then dried under nitrogen gas and reconstituted in 50% volume 84:16 CH_3CN + 0.2% FA:H_20 + 0.2% FA (v:v) and then 90 µL of this solution was used to reconstitute either the dried serum extract or matrix free sample 'extract'. For the "matrix free no drying" sample, the IS stock solution was prepared in H_2O in exactly the same process as in mouse serum above, with the exception of the removal of glycine IS and movement of GSSG to the "mid-range" curve. Samples were then extracted in H_2O and CH_3CN and the IS stock solution was added after extraction as summarised in Figure 3.4 above.

Table 3.7 Preparation of the internal standard stock solutions, human serum validation[a]

Stock solution component[b]	**Standard Concentration (µg/mL)**	**No. IS per group**	**Volume of each IS added (µL)**	**Total volume IS added (µL)**	**Final concentration in stock solution A (µg/mL)**	**Final concentration in stock solution B[c] (ng/mL)**
High concentration	1000	3	50	150	100	10000
Mid concentration	1000	7	5	35	10	1000
Low concentration	500	5	5	25	5	500
-	-	-	**MeOH + 0.2% FA**	**290**		
-	-	**-**	***Total***	***500***		

[a] Solutions of IS were mixed to form the IS top stock solution A, with concentrations for each of the three concentration ranges. [b]See Table 3.8 for list high, mid and low concentration IS. [c]Stock solution A was then diluted by a factor of 1 in 10 to give stock solution B concentration. Abbreviations: FA: formic acid; IS: internal standard.

Table 3.8 Concentration of each IS in the IS top stock solution before dilution to produce LQC and HQC IS stock solutions, human serum validation

High concentration 10 µg/mL	Mid concentration 1 µg/mL	Low concentration 0.5 µg/mL
Glutamine-d_5	5-oxoproline-d_5	Cystathionine-d_4
Serine-d_3	Cystine-d_6	Choline-d_4
Taurine-d_4	Glutamate-d_3	Homocysteine-d_4
	Hypotaurine-d_4	SAMe-d_3
	Methionine -$^{13}C^{15}N$	Homocystine-d_8
	Cysteine-$^{13}C_3{}^{15}N$	
	GSSG-$^{13}C_4{}^{15}N_2$	

Abbreviations: GSSG: oxidised glutathione; SAMe: s-adenosyl methionine

Table 3.9 Preparation of HQC and LQC IS stock solutions from the IS top stock solution B, human serum validation

Stock solution produced	Volume of stock solution B used (µL)	Volume of MeOH added (µL)
HQC stock solution	400	500
LQC stock solution	20	600

Abbreviations: HQC: high quality control; IS: internal standard; LQC: low quality control.

Table 3.10 Final concentration of the IS stock solutions

IS stock[a]	Final stock solution concentration (ng/mL)		Concentration in sample preparation (ng/mL)		Final concentration in measured samples (ng/mL)	
	HQC	LQC	HQC	LQC	HQC	LQC
High concentration	4444	333	4000	300	8000	600
Mid concentration	444	33.3	400	30	800	60
Low concentration	222	16.7	200	15	400	30

[a]See Table 3.8 for list high, mid and low concentration IS. [b]after 0.9:0.1 v:v dilution when 180 µL was added to 2 0µL serum or water.[c] following a 2x concentration of the samples following drying and resuspension.
Abbreviations: HQC: high quality control; IS: internal standard; LQC: low quality control.

3.4 Results

3.4.1 Chromatography of IS in mouse serum validation

In Figure 3.5A below, the total ion chromatograms of the HQC IS measured in the matrix free samples is shown, while Figure 3.5B displays the chromatogram traces for the IS spiked into mouse serum samples. In all cases the traces are normalised to the highest peak (GSSG-$^{13}C_4{}^{15}N_2$). It is clear from these images that there are effects on the IS retention times, peak areas, and peak shapes due to the extraction of samples and matrix effects. Peaks for homocysteine-d_4 and cysteine-$13C_3$15N have both shifted in retention to later times in the chromatographic gradient when measured in serum. Choline-d_4, cystathionine-d_4 and homocysteine-d_4 also have a much lower relative peak heights in the serum extracts compared to matrix free samples. There were no consistent peaks in terms of peak shape or retention time for either glycine-$^{13}C^{15}N$ or glutamate-d_3.

As choline was noted to have a reduced peak area in the samples containing serum compared to the matrix free samples in the Figure 3.5 chromatograms were compared in more detail across the 4 sample types measured, as shown in Figure 3.6. All the total ion chromatogram traces were normalised to the highest peak, and it is clear that the peak shape in the matrix free samples for choline-d_4 was much narrower and of higher peak intensity than when measured in samples containing serum extracts, where the peak was much broader. Matrix related shifts in retention or changes to peak shapes were also seen for other analytes, retention time ranges for samples containing serum and matrix free samples are summarised in Table 3.11. RTs were more variable in matrix containing samples, and there were large shifts in retention of up to a minute for homocysteine-d_4 and cysteine-$^{13}C_3{}^{15}N$.

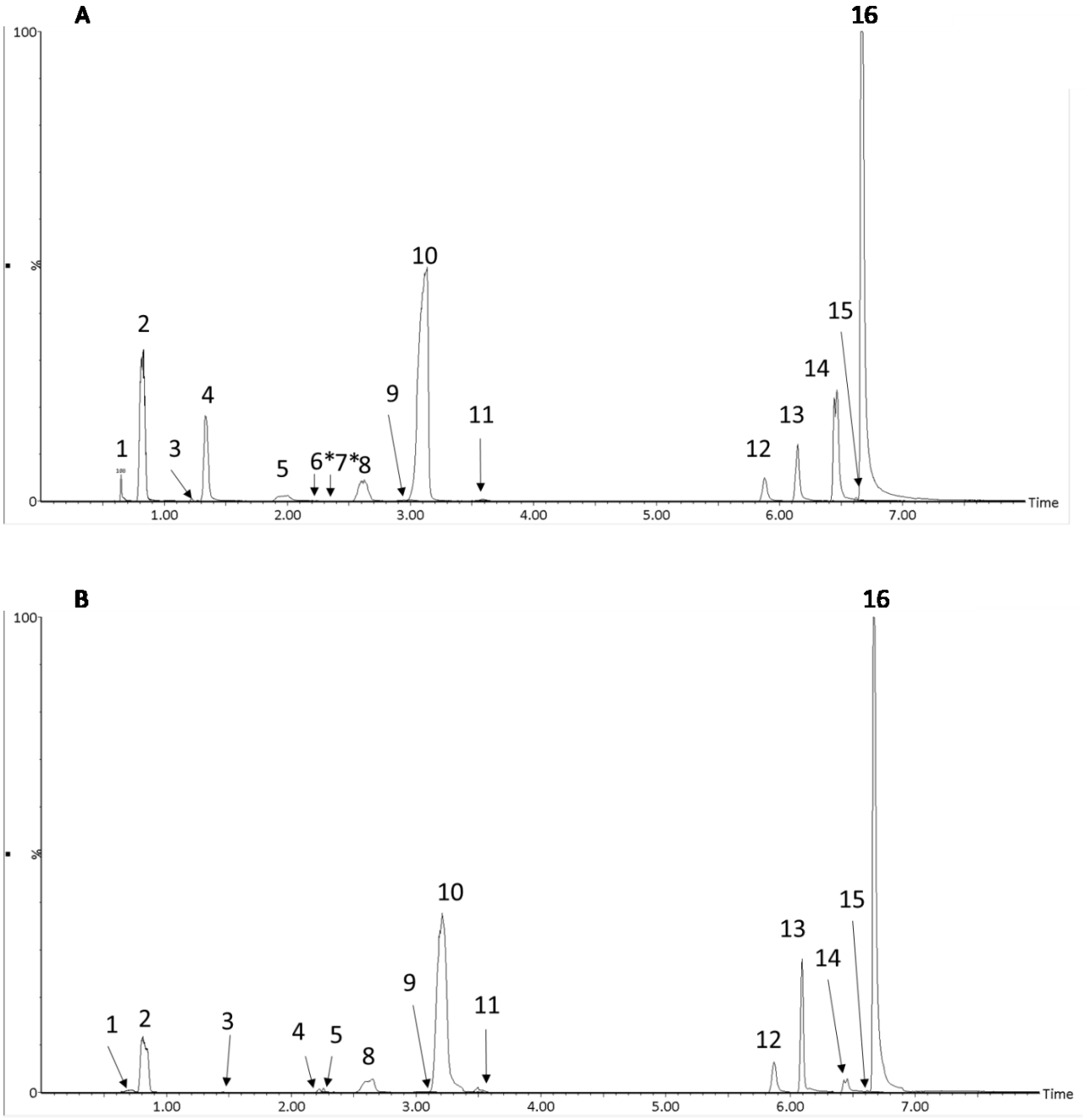


Figure 3.5 Total ion chromatogram normalised to the highest peak in each figure, of each of the IS's spiked into a sample at the HQC concentration measured in A) a matrix free sample and B) a mouse serum sample, spiked before extraction

*Key: 1. choline-d4 2. 5-oxoproline-d_5 3. methionine-$^{13}C_3{}^{15}N$ 4. homocysteine-d_4 5. cysteine-$^{13}C_3{}^{15}N$ 6. glycine-$^{13}C^{15}N$ 7. glutamate-d_3 8. taurine-d_4 9. glutamine-d_5 10. serine-d_3 11. hypotaurine-d_4 12. homocystine-d_8 13. S-adenosyl methionine-d_3 14. cystathionine-d_4 15. cystine-d_6 16. GSSG-$^{13}C_4{}^{15}N_2$. *: peak shape unacceptable or no consistent retention time/peak shape.*

Abbreviations: GSSG: oxidised glutathione; HQC: high quality control

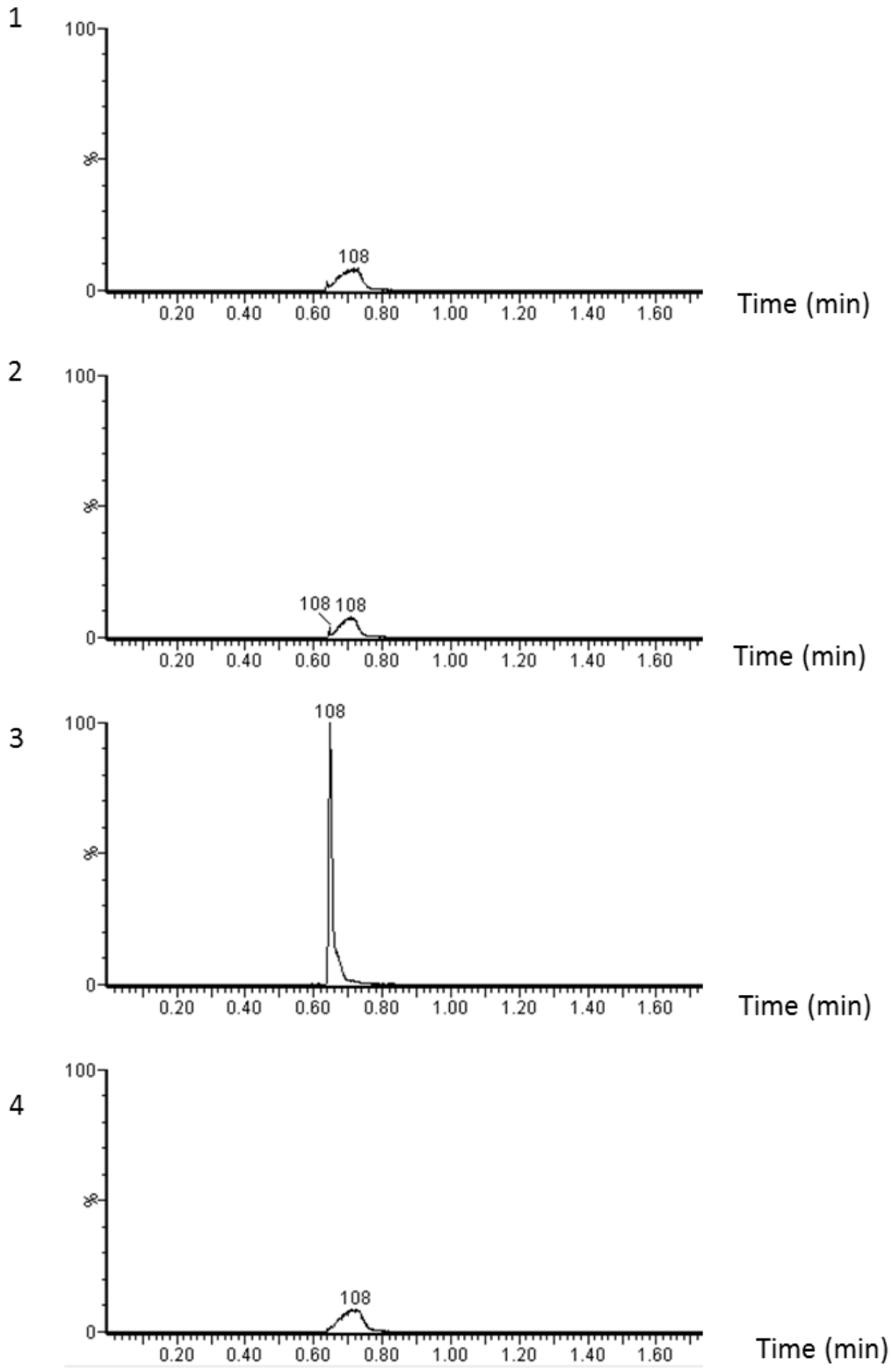


Figure 3.6. Relative total ion chromatograms of choline-d4 in High quality control sample 1, all normalised to the highest peak (3).
These peaks relate to 1) HQC 1 spiked before extraction into human serum 2) HQC1 spiked in human serum after extraction 3) HQC 1 spiked into matrix free solution and 4) HQC 1 prepared as a sample (i.e. spiked into human serum prior to extraction)
Abbreviations: HQC: High Quality Control

Table 3.11 Retention time ranges of peaks after elution of internal standards, from internal standards spiked into samples either containing or not containing mouse serum.

Analyte	Retention time (mins)	
	Matrix containing samples	Matrix free samples
choline-d_4	0.83-0.85	0.79
cystathionine-d_4	6.44-6.45	6.46
cysteine-$13C_3$15N	2.59-2.63	1.99-2.00
cystine-d_6	6.61-6.62	6.62-6.63
glutamine-d_5	3.01-3.18	2.98-3.00
GSSG-$13C_4$15N_2	6.67-6.69	6.68-6.69
homocysteine-d_4	2.15-2.34	1.34-1.35
homocystine-d_8	5.86-5.88	5.88
hypotaurine-d_4	3.49-3.57	3.59-3.60
methionine-$13C_3$15N	1.33-1.50	1.21-1.26
5-oxoproline-d_5	0.80-0.85	0.81-0.83
SAMe-d_3	6.06-6.13	6.15
serine-d_3	3.12-3.31	3.11-3.12
taurine-d_4	2.64-2.65	2.61

Abbreviations: GSSG: oxidised glutathione; SAMe: s-adenosyl methionine.

3.4.2 Matrix factor, recovery and sample preparation effects in mouse serum.

In Table 3.12**,** the mean peak areas with CV of IS at the concentrations of the LQC in all four sample types; serum samples spiked before and after extraction; the matrix free sample; and the "Normal Sample" are shown. Generally, the CVs in the LQC samples were highest, as analyte peak areas were the least consistent in the samples spiked before extraction, even compared to the "Normal Preparation" LQC samples which also contained IS spiked before extraction. The variability seen was however, both analyte and matrix dependent. For example, at the LQC homocysteine-d4 had the highest CV of any analyte in all sample types except the matrix free sample. Hypotaurine-d4, on the other hand, had a higher CV in samples spiked with IS before extraction. The CVs for cysteine-$^{13}C_3{}^{15}N$ and SAMe-d_3 spiked into matrix free samples were the highest for those analytes at over 50%. With the exception of LQC spiked before extraction, the CVs for the remaining analytes were all below 30%. In Table 3.13 the mean peak areas and CVs of IS at the concentrations of the HQC are shown for the four sample types. For the HQC samples the, CVs of the "Normal Preparation" samples were highest in general compared to samples spiked before or after the extraction and the matrix free samples. CVs were, as might be expected, (with the exceptions noted above) lowest in samples spiked after

extraction and in matrix free samples. CVs for Homocysteine-d_4 again had the highest CVs in all samples except matrix free, and hypotaurine-d_4 had higher CVs in samples which are spiked before samples extraction.

Table 3.12 Mean peak areas of each of the internal standards at the LQC measured in the four samples types, with CV.

Analyte	LQC spiked before extraction		LQC spiked after extraction		LQC matrix free		LQC normal sample preparation	
	Mean Peak Area	CV	Mean Peak Area	CV	Mean Peak Area	CV	Mean Peak Area	CV
choline-d_4	1394	25.5	1365	14.2	26310	8.94	1544	11.1
cystathionine-d_4	15737	35.6	14146	9.53	123081	4.83	16830	17.9
cysteine-$^{13}C_3{}^{15}N$	4669	34.9	6375	9.73	12834	53.1	7617	16.5
cystine-d_6	1621	36.6	1795	21.9	4078	5.18	2091	21.7
glutamine-d_5	2713	52.2	4530	13.7	11189	5.11	4901	21.3
GSSG-$^{13}C_4{}^{15}N_2$	91743	74.4	163277	12.1	172757	3.64	208876	20.8
homocysteine-d_4	4650	94.0	1882	41.1	118463	9.81	2597	69.5
homocystine-d_8	18656	64.9	28426	9.02	26561	4.22	32976	16.7
hypotaurine-d_4	5350	38.8	5483	17.5	1679	16.6	8269	40.3
methionine-$^{13}C_3{}^{15}N$	139	50.6	122	25.5	2726	26.4	140	20.4
5-oxoproline-d_5	80434	63.0	121116	18.3	275002	6.17	135408	27.3
SAMe-d_3	53327	62.7	99124	11.7	22985	56.5	123166	19.1
serine-d_3	485100	46.9	645172	15.9	294717	11.1	779814	22.2
taurine-d_4	52735	48.3	68458	11.8	194018	5.42	79534	20.0

Abbreviations: CV: coefficient of variance of the mean; GSSG: oxidised glutathione; LQC: low quality control; SAMe: s-adenosyl methionine.

Table 3.13 Mean peak areas of each of the internal standards at the HQC measured in the four samples types, with CV.

Analyte	HQC Spiked Before extraction		HQC Spiked After Extraction		HQC Matrix Free		HQC Normal Sample Preparation	
	Mean Peak Area	CV	Mean Peak Area	CV	Mean Peak Area	CV	Mean Peak Area	CV
choline-d_4	20804	16.5	21083	19.9	183162	3.62	22434	9.91
cystathionine-d_4	241373	10.9	220642	24.2	1889684	7.87	233888	24.9
cysteine-$^{13}C_3{}^{15}N$	6830	9.87	7177	12.2	317755	9.95	5346	36.6
cystine-d_6	29447	10.6	26842	17.5	67991	8.91	26131	28.2
glutamine-d_5	65944	18.5	58570	18.0	87780	5.35	53238	39.8
GSSG-$^{13}C_4{}^{15}N_2$	4797650	10.4	5181273	10.0	5028837	6.38	3941073	43.8
homocysteine-d_4	29230	65.7	25017	80.8	1890181	7.73	17370	105
homocystine-d_8	495833	18.5	459119	16.3	402703	7.71	443809	39.7
hypotaurine-d_4	117748	27.4	97521	37.7	49295	21.9	96318	60.3
Methionine-$^{13}C_3{}^{15}N$	3358	8.05	3276	13.4	30776	19.0	3373	21.6
5-oxoproline-d_5	1941792	26.7	1768331	12.9	4067436	4.70	1665773	41.0
SAMe-d_3	2012073	17.2	1835215	16.5	1024449	17.9	1800529	43.8
serine-d_3	8095633	14.5	7400429	16.2	11047299	2.33	6999646	39.7
taurine-d_4	819290	18.0	755978	16.2	1132228	4.36	670479	34.2

Abbreviations: CV: coefficient of variance of the mean; GSSG: oxidised glutathione; HQC: high quality control; SAMe: s-adenosyl methionine.

The peak areas of the IS in the "IS spiked before samples", and the "Normal Preparation" samples were compared to measure the effect of completing the protein precipitation step with different solvent volumes as in the "IS spiked before samples" 20 µL serum was extracted in 70 µL of solvent (14:56 H_20:Me_3CN v:v) with 10 µL water + 0.2% FA added after the protein precipitation stage, whereas in reality during sample extraction ("Normal Preparation"), 20 µL serum samples are extracted in 80 µL solvent (24:56 H_20:Me_3CN v:v). In Table 3.14, the area of the "before extraction" sample as a percentage of the "normal preparation" sample is shown. At the LQC all IS concentrations in "IS spiked before" samples were lower in concentration compared to the "normal sample" with the exception of homocysteine-d_4 which was 273% higher but had a standard deviation of CV of 111%. At the HQC level, IS peak mean areas the "IS spiked before" samples were generally similar to those in the "normal preparation" sample, with the exception of homocysteine-d4 which was over 200% higher, with a CV of over 50%. The CVs obtained at the LQC were variable, with the exception of choline-d4, with most CVs at over 30%. In the case of the HQC samples the %CVs were slightly

improved with the majority being under 35% with the exception of homocysteine-d_4 and hypotaurine-d_4.

Table 3.14 Comparison of peak areas of samples prepared with internal standards spiked before extraction, and the sample prepared to reflect actual sample preparation, "normal preparation".

Analyte	LQC % mean	Std Dev	CV	HQC % mean	Std Dev	CV
choline-d_4	88.5	19.1	21.6	88.3	29.0	32.9
cystathionine-d_4	96.0	33.4	29.8	111	27.0	24.3
cysteine-$^{13}C_3{}^{15}N$	39.2	24.5	34.6	99.6	29.3	29.4
cystine-d_6	78.0	27.1	34.8	104	30.2	29.1
glutamine-d_5	55.0	26.6	48.3	116	38.6	33.2
GSSG-$^{13}C_4{}^{15}N_2$	42.5	33.3	78.4	105	18.6	17.8
homocysteine-d_4	273	302	111	201	109	54.1
homocystine-d_8	55.3	32.2	58.3	98.9	24.7	25.0
hypotaurine-d_4	61.5	21.5	35.0	114	63.6	55.7
methionine-$^{13}C_3{}^{15}N$	99.4	48.3	48.6	98.0	29.6	30.2
5-oxoproline-d_5	57.7	29.8	51.7	105	26.5	25.2
SAMe-d_3	42.8	28.4	66.3	99.1	28.3	28.5
serine-d_3	61.2	18.7	30.5	105	33.5	31.9
taurine-d_4	65.7	25.5	38.9	112	37.1	33.0

Abbreviations: CV: coefficient of variance of the mean; GSSG: oxidised glutathione; HQC: high quality control; LQC: low quality control; SAMe: s-adenosyl methionine.

Recovery was measured in mouse serum samples and these data are displayed in Table 3.15. These recoveries were calculated by comparing at least five of the six samples prepared by spiking either the LQC or HQC IS stock solution into samples before extraction, with serum samples which were spiked with the IS stock solution only after extraction. There are no acceptance criteria for recovery however, it should be reproducible and ideally the CVs would be below 20%. Recovery is recorded as the peak area of the samples spiked with IS before extraction as a percentage of the area of those spiked after extraction. Glutamate and glycine were not included in the results due to the chromatographic problems discussed previously. At the HQC, the majority of recoveries were less than 20% above or below 100%, with the exception of homocysteine-d_4 and hypotaurine-d_4 which both had peak areas around 40% higher than the post extraction sample. CVs were below 30% for all except hypotaurine-d_4. At the LQC, extraction recoveries were generally lower with the majority at around 50-80% of the

nominal value. Homocysteine-d_4, a generally problematic analyte, had a mean peak area almost 300% of the post extraction sample, which was likely due to the variability between samples, and a CV of over 90%. CVs were generally higher at the LQC, with no CVs obtained that were below 20%.

Table 3.15 Extraction recoveries of the internal standard stock solutions when comparing peak areas of the HQC or LQC IS solutions were spiked into mouse serum, either before or after protein precipitation.

Analyte	LQC mean Recovery %	Std Dev	CV	HQC mean Recovery %	Std Dev	CV
choline-d_4	97.0	22.1	22.8	99.1	9.0	9.11
cystathionine-d_4	112	33.4	29.8	111	27.0	24.3
cysteine-$^{13}C_3{}^{15}N$	70.8	24.5	34.6	98.1	7.0	7.19
cystine-d_6	96.2	39.1	40.7	111	20.9	18.9
glutamine-d_5	57.5	24.5	42.6	108	16.5	15.2
GSSG-$^{13}C_4{}^{15}N_2$	54.5	38.4	70.4	88.3	9.7	11.0
homocysteine-d_4	274	253	92.6	141	37.5	26.5
homocystine-d_8	64.8	38.1	58.9	110	31.4	28.4
hypotaurine-d_4	98.7	54.4	55.2	137	68.4	49.9
methionine-$^{13}C_3{}^{15}N$	116	43.9	37.8	106	14.0	13.2
5-oxoproline-d_5	66.7	37.3	55.9	107	17.7	16.5
SAMe-d_3	53.1	31.8	59.9	113	27.8	24.6
serine-d_3	73.6	24.8	33.7	105	8.8	8.41
taurine-d_4	77.2	30.1	39.0	107	21.7	20.2

Abbreviations: CV: coefficient of variance of the mean; GSSG: oxidised glutathione; HQC: high quality control; IS: internal standard; LQC: low quality control; SAMe: s-adenosyl methionine.

The matrix factor was measured at both the LQC and HQC by comparing the IS peak areas from samples spiked with IS stock solutions post extraction into a matrix free sample with the areas from those spiked into samples containing mouse serum. Matrix factors are presented as the percentage difference between the matrix free and serum containing samples (Table 3.16). Matrix factors were very pronounced, and in some cases the peak areas in the matrix-containing samples were almost 100% lower than in the matrix free samples. For some analytes including GSSG$^{13}C_4{}^{15}N_2$, cysteine-$^{13}C_3{}^{15}N$ and homocystine-d_8 CVs were generally high, and peak shapes were not consistent. For hypotaurine-d4 and SAM-d3 the matrix effects led to increased peak area, particularly at the LQC. Choline-d4, cystathionine-d4, methionine-$^{13}C_3{}^{15}N$ and 5-OP-d5 consistently had a %CV under 20% at the LQC and HQC however, all except methionine-$^{13}C_3{}^{15}N$ had a matrix effects of greater than 85% reduction in peak area.

Table 3.16 Matrix factor measured by spiking IS stock solutions into in mouse serum or water at the LQC and HQC concentrations.

Analyte	LQC MF %	SD	CV	HQC MF %	SD	CV
choline-d_4	-94.7	0.52	-0.554	-87.9	9.71	-1.88
cystathionine-d_4	-88.9	0.01	-1.3	-88.1	0.03	-3.49
cysteine-$^{13}C_3{}^{15}N$	35.5	2.06	580	-97.9	0.00	-0.325
cystine-d_6	-56.8	0.12	-20.3	-61.0	0.07	-11.5
glutamine-d_5	-59.3	0.07	-12.5	-30.3	0.07	-23.1
GSSG-$^{13}C_4{}^{15}N_2$	-4.32	0.15	-357	6.27	0.14	215
homocysteine-d_4	-98.7	na	na	-99.0	0.01	-0.885
homocystine-d_8	4.68	0.13	276	14.6	0.20	135
hypotaurine-d_4	242	0.70	29.1	71	33.5	47.1
methionine-$^{13}C_3{}^{15}N$	-95.5	0.02	-1.9	-89.4	0.03	-3.09
5-oxoproline-d_5	-58.1	0.09	-14.9	-56.1	0.07	-11.7
SAMe-d_3	481	2.74	57.1	82.6	0.33	39.5
serine-d_3	107	0.33	30.3	-30.5	0.08	-25.6
taurine-d_4	-66.2	0.04	-6.7	-31.6	0.09	-30.0

Abbreviations: CV: coefficient of variance of the mean; GSSG: oxidised glutathione; HQC: high quality control; IS: internal standard; LQC: low quality control; MF: matrix factor; na: not applicable; SAMe: s-adenosyl methionine; SD: standard deviation.

3.4.3 Chromatography in human serum

In Figure 3.7A below, the total ion chromatograms of the HQC IS's, as measured in the matrix free samples, are shown, while Figure 3.7B shows the mass chromatogram traces for the IS's spiked into human serum samples. Traces are normalised to the highest peak which is cystathionine-d_4 in Figure 3.7A and serine-d_3 in Figure 3.7B. Similar to in mouse serum, there are effects on the IS retention times, peak areas, and peak shapes for sample extracts and matrix effects, such as retention time shift for homocysteine-d_4 and cysteine-$^{13}C_3{}^{15}N$. Glycine-$^{13}C^{15}N$ was not measured in human serum and glutamate-d_3 had low intensity and inconsistent peak shapes and retention times.

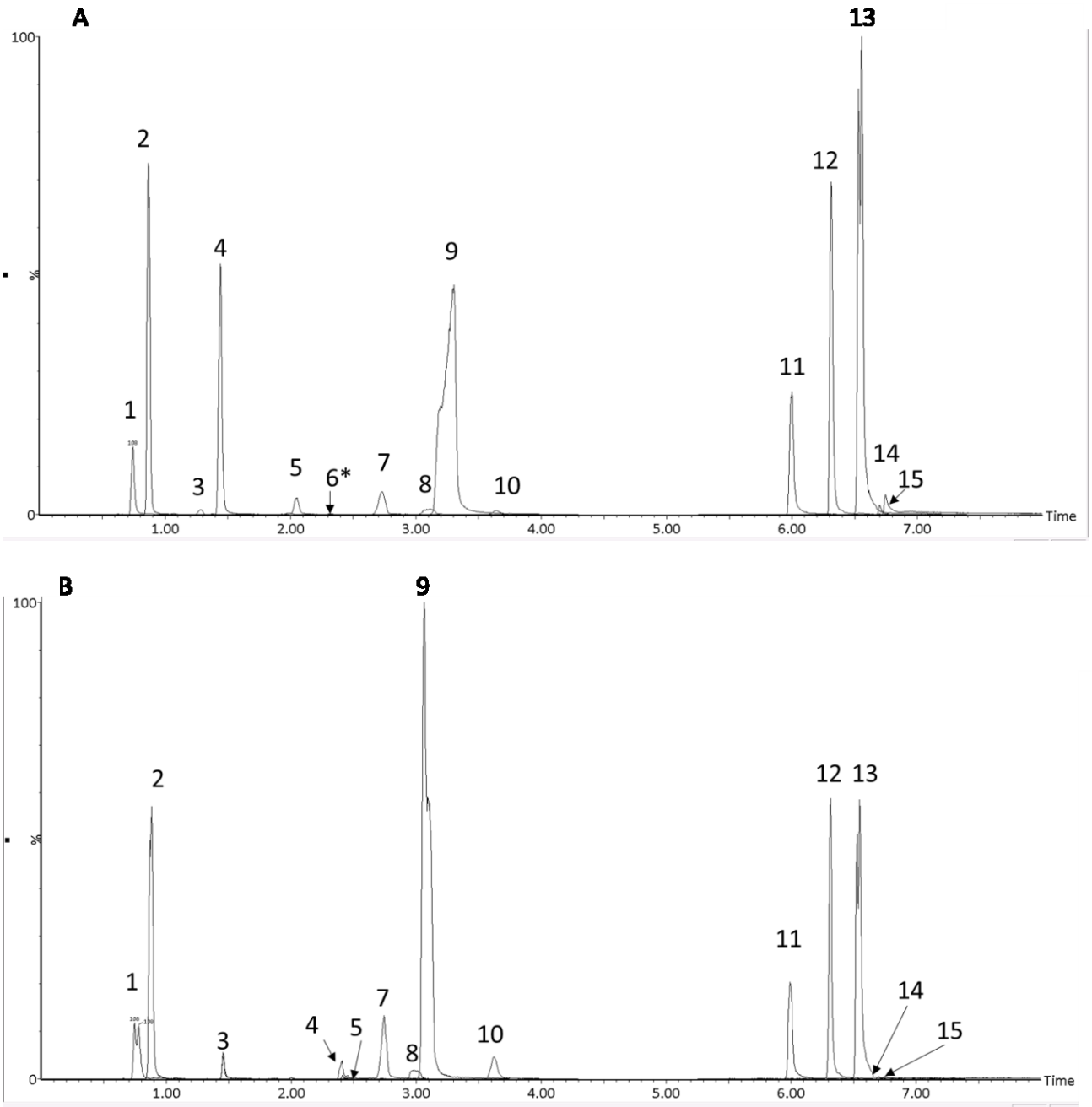


Figure 3.7 Total ion chromatogram normalised to the highest peak in each figure, of each IS measured in A) a matrix free sample at the HQC concentration level and B) spiked into human serum samples before extraction.
*Key: 1. choline-d4 2. 5-OP-d_5 3. methionine-$^{13}C_3{}^{15}N$ 4. homocysteine-d_4 5. cysteine-$^{13}C_3{}^{15}N$ 6. glutamate-d_3 7. taurine-d_4 8. glutamine-d_5 9. serine-d_3 10. hypotaurine-d_4 11. homocystine-d_8 12. SAMe-d_3 13. cystathionine-d_4 14. cystine-d_6 15. GSSG-$^{13}C_4{}^{15}N_2$. *= peak shape unacceptable or no consistent RT/peak shape.*
Abbreviations: GSSG: oxidised glutathione; HQC: high quality control; IS: internal standard; SAMe: s-adenosyl methionine.

3.4.4 Matrix factor and extraction recovery in human serum

In Table 3.17, the mean peak areas of IS at the LQC plus CV is shown for the four sample types compared in the human serum matrix and recovery assessment. In the LQC samples there were no peaks for cysteine-$^{13}C_3{}^{15}N$ and GSSG-$^{13}C_4{}^{15}N_2$ in the samples containing human serum. Glutamate-d_3 samples had no consistent peak shapes or retention times so it was not included in future analysis. The peak areas of cystine-d_6, homocysteine-d_4 and methionine-$^{13}C_3{}^{15}N$ were very low in both sample types containing matrix which were the "IS spiked before" and "IS spiked after".

Table 3.17 Mean peak areas of each of the IS standards at the LQC measured in the four samples types, with CV.

Analyte	IS LQC spiked before extraction		IS LQC spiked after extraction		IS LQC -matrix free		IS LQC -matrix free no drying	
	Mean Peak area	CV	Mean Peak area	CV	Mean Peak area	CV	Mean Peak area	CV
choline-d_4	9940	15.1	8262	26.1	31567	7.14	46023	24.4
cystathionine-d_4	14738	71.8	6662	53.6	82507	11.3	108896	17.8
cysteine-$^{13}C_3{}^{15}N$	0	na	0	na	27.9	33.3	608	79.3
cystine-d_6	219	45.2	136	56.9	1937	14.9	2489	18.5
glutamate-d3	0	na	0	na	0	na	26.7	70.7
glutamine-d_5	1765	27.8	1484	34.1	6778	8.74	8005	21.9
GSSG-$^{13}C_4{}^{15}N_2$	0	na	0	na	2150	21.5	3571	20.5
homocysteine-d_4	254	15.9	242	29.7	1207	120	3840	56.9
homocystine-d_8	5345	59.6	3174	41.5	24283	11.6	29649	20.8
hypotaurine-d_4	1412	23.0	1085	23.1	57.2	119	361	65.0
methionine-$^{13}C_3{}^{15}N$	524	24.0	576	32.0	611	53.4	972	40.8
5-oxoproline-d_5	9564	50.5	5778	29.1	82773	14.6	95606	26.0
SAMe-d_3	10328	56.0	4262	28.8	40284	12.4	54381	24.8
serine-d_3	103126	30.8	75789	22.9	314230	8.97	367065	23.4
taurine-d_4	9745	29.3	7743	20.1	25944	10.2	29691	21.8

Abbreviations: CV: coefficient of variance of the mean; GSSG: oxidised glutathione; IS: internal standard; LQC: low quality control; SAMe: s-adenosyl methionine.

The mean peak areas of IS In the four sample types and CVs at the HQC are reported in Table 3.18. The CVs of the IS areas were lower in the HQC samples, as peak areas were generally more consistent between replicates, however cysteine-$^{13}C_3{}^{15}N$ peaks were below the limit of detection in samples containing matrix. In general, peak areas were higher and CVs lower in the matrix free no drying group, with the exception of GSSG-$^{13}C_4{}^{15}N_2$. In the matrix-free group at the HQC, most CVs were below 25%, with the exception of cysteine-$^{13}C_3{}^{15}N$ and homocysteine-d_4. Serine-d_3, taurine-d_4, and methionine-

$^{13}C_3{}^{15}N$ had CVs below 30% across all sample types, and glutamine-d_5 had a CV of 30.1% in the sample spiked before extraction, but CVs of less than 30% for all other samples.

Table 3.18 Mean peak areas of each of the IS standards at the HQC measured in the 4 samples types, with CV.

Analyte	IS HQC spiked before extraction		IS HQC spiked after extraction		IS HQC matrix free		IS HQC matrix free no drying	
	Mean Peak Area	CV	Mean Peak area	CV	Mean Peak area	CV	Mean Peak area	CV
choline-d_4	134711	50.6	110609	10.5	213289	9.90	226775	12.7
cystathionine-d_4	242293	41.2	144491	45.0	1611699	4.67	3668940	3.30
cysteine-$^{13}C_3{}^{15}N$	0	na	0	na	35512	58.8	224074	11.6
cystine-d_6	2448	35.7	1647	44.0	33219	8.34	47511	12.1
glutamate-d3	150	48.8	78	28.7	327	17.8	180816	11.2
glutamine-d_5	31120	30.1	23649	18.4	85914	4.69	1280929	17.1
GSSG-$^{13}C_4{}^{15}N_2$	928	90.4	1722	128	74073	8.62	293	31.1
homocysteine-d_4	3876	21.9	4044	33.2	92425	72.3	76078	8.15
homocystine-d_8	104775	36.1	73872	36.7	462294	7.45	24942	5.87
hypotaurine-d_4	40843	40.7	28756	27.9	32636	24.9	1424818	5.12
methionine-$^{13}C_3{}^{15}N$	10482	10.8	9889	10.5	22795	25.0	33011	6.57
5-oxoproline-d_5	475966	65.9	248264	61.1	1498014	9.39	436133	12.6
SAMe-d_3	241985	40.9	158904	34.3	1049280	7.46	902191	11.1
serine-d_3	1134532	17.0	1015244	10.5	4224998	6.63	87683	17.2
taurine-d_4	128215	22.4	109953	14.2	241484	5.42	94614	6.09

Abbreviations: CV: coefficient of variance of the mean; GSSG: oxidised glutathione; HQC: high quality control; IS: internal standard; na: not applicable; SAMe: s-adenosyl methionine.

Analyte mean percentage recoveries are displayed in Table 3.19. CVs were generally higher for each analyte at the LQC than the HQC, with the exception of 5-OP-d5. For all analytes (except methionine-$^{13}C_3{}^{15}N$) where peaks could be detected and integrated at the LQC, recoveries exceeded 100% as peak areas in samples spiked before extraction were higher than in those spiked post extraction. All CVs were above 20%. This effect was more pronounced at the HQC and for all analytes which could be accurately measured, with peak areas of IS's spiked before extraction larger than those spiked after extraction and CVs were large and above 20% for all analytes except serine-d_3 and methionine-$^{13}C_3{}^{15}N$.

To measure the differences in matrix factor and recovery which may occur from dissolving IS in MeOH and reconstituting in CH3CN:H20 (84:16), the peak areas of the analytes in the matrix free samples were compared to matrix free samples prepared as per the original sample preparation

protocol, with IS in H2O being added to water and CH3CN and being analysed directly. At the LQC recoveries were generally good and above 70% for all analytes except for GSSG-13C415N2, and CVs were around or below 20% for all analytes except methionine-13C315N. At the HQC level, recoveries were generally within 80-120%. CVs were below 20% for all the IS, with the exception of cystine-d6, homocysteine-d4 and hypotaurine-d4 which all had recoveries of less than 70% and glutamine-d5 which had a higher peak area in the dried samples, with a recovery of 122%. The results were more imprecise for the analytes with higher or lower recoveries as shown in Table 3.20.

Table 3.19 Extraction recoveries of the IS stock solutions when comparing peak areas of the IS spiked into human serum either before or after protein precipitation.

Analyte	LQC mean Recovery %	SD	CV	HQC mean Recovery %	SD	CV
choline-d_4	125	30.3	24.2	124	67.6	54.5
cystathionine-d_4	327	331	101.2	187	93.8	50.2
cysteine-$^{13}C_3{}^{15}N$	0	na	na	0.0	na	na
cystine-d_6	267	239	89.7	169	89.3	53.0
glutamate-d3	na	na	na	246	243	99.0
glutamine-d_5	142	90.0	63.4	137	55.3	40.3
GSSG-$^{13}C_4{}^{15}N_2$	0	na	na	145	182	125
homocysteine-d_4	108	38.2	35.4	75.1	76.4	102
homocystine-d_8	220	192	87.1	159	88.6	55.6
hypotaurine-d_4	139	52.6	37.9	156	91.7	58.7
.methionine-$^{13}C_3{}^{15}N$	95.4	25.5	26.7	107	12.2	11.4
5-oxoproline-d_5	183	110	60.1	274	307	112
SAMe-d_3	269	170	63.2	169	94.2	55.6
serine-d_3	150	78.6	52.3	111	10.9	9.80
taurine-d_4	131	48.8	37.2	119	35.4	29.8

Abbreviations: CV: coefficient of variance of the mean; GSSG: oxidised glutathione; IS: internal standard; LQC: low quality control; na: not applicable; SAMe: s-adenosyl methionine; SD: standard deviation.

Table 3.20 Percentage recoveries of the IS stock solutions when comparing peak areas of the IS spiked into matrix samples after extraction, with or without drying under nitrogen.

Analyte	LQC mean % recovery drying	SD	CV	HQC mean % recovery drying	SD	CV
choline-d_4	70.8	11.1	15.7	94.5	6.59	6.60
cystathionine-d_4	77.3	13.8	17.8	113	8.16	7.04
cysteine-$^{13}C_3{}^{15}N$	79.9	18.1	22.7	101	12.1	11.1
cystine-d_6	0	0	na	36.8	20.9	31.6
glutamate-d3	86.7	11.9	13.7	113	6.71	5.93
glutamine-d_5	0	0	na	122	52.2	39.7
GSSG-$^{13}C_4{}^{15}N_2$	61.0	13.0	21.2	86.4	15.4	16.7
homocysteine-d_4	0	0	na	52.4	38.1	35.4
homocystine-d_8	84.1	16.9	20.1	107	11.4	9.90
hypotaurine-d_4	0	0	na	69.2	16.4	25.6
methionine-$^{13}C_3{}^{15}N$	72.4	43.3	59.8	91.7	23.6	18.3
5-oxoproline-d_5	88.8	11.7	13.2	118	10.6	8.51
SAMe-d_3	76.0	10.0	13.2	117	10.1	8.54
serine-d_3	87.8	11.6	13.2	115	8.41	7.30
taurine-d_4	89.3	11.3	12.6	109	9.53	8.88

Abbreviations: CV: coefficient of variance of the mean; GSSG: oxidised glutathione; HQC: high quality control; IS: internal standard; LQC: low quality control; na: not applicable; SAMe: s-adenosyl methionine; SD: standard deviation.

Matrix effects are displayed in Table 3.21 and are presented as the percentage difference between the matrix free and human serum-containing samples spiked after extraction. Matrix factors were very significant, and peak areas were on average 100% less than in matrix free samples for some analytes at the LQC where IS could not be detected in matrix-containing samples. Hypotaurine-d_4 had a peak area much higher than seen for the matrix free sample in the LQC and a relatively similar mean peak area to that of the HQC samples, but as demonstrated by their high CVs the peaks areas were variable amongst the replicates at both the LQC and HQC. At the LQC methionine-$^{13}C_3{}^{15}N$ had an enhancement of peak area in the serum-containing samples however, it also had a very high CV%. Homocysteine-d4 also had a variable response at the LQC. For all other analytes at the LQC matrix factors were substantial (over 70% reduction in peak area) but had consistent CVs of below 10%. For a number of analytes including cystathionine-d4, glutamine-d5, homocystine-d8, 5-oxoproline-d5, SAM-d3 and taurine-d4 matrix effects were lower at the HQC but the CVs exceeded 20%. For homocysteine-d4, at

the HQC matrix effects were more pronounced but data were more precise. Choline-d4, cystine-d6, GSSG-$^{13}C_4{}^{15}N_2$ and serine-d3 had CVs below 20% at both the LQC and HQC.

Table 3.21 Matrix factor measured by spiking IS stock solutions into human serum or water the LQC and HQC concentrations.

Analyte	LQC MF %	Std Dev	CV	HQC MF %	Std Dev	CV
choline-d_4	-74.0	5.74	-7.75	-46.5	3.5	-7.6
cystathionine-d_4	-92.0	4.00	-4.35	-74.8	34.4	-46.0
cysteine-$^{13}C_3{}^{15}N$	-100	0	na	-100	0	na
cystine-d_6	-93.0	3.91	-4.21	-90.4	9.49	-10.5
glutamine-d_5	-78.2	7.10	-9.09	-56.1	35.9	-64.0
GSSG-$^{13}C_4{}^{15}N_2$	-99.4	1.38	-1.39	-90.9	14.5	-15.9
homocysteine-d_4	-68.2	37.3	-54.7	-93.0	4.9	-5.3
homocystine-d_8	-87.3	4.03	-4.62	-70.9	28.0	-39.5
hypotaurine-d_4	6629	8099	122	-14.2	27.2	-192
methionine-$^{13}C_3{}^{15}N$	32.8	107	326	-57.6	15.6	-27.0
5-oxoproline-d_5	-93.0	1.81	-1.95	-65.6	41.6	-63.4
SAMe-d_3	-89.4	2.79	-3.12	-73.4	24.2	-33.0
serine-d_3	-75.9	5.10	-6.72	-73.3	6.7	-9.1
taurine-d_4	-70.1	5.55	-7.92	-39.3	32.8	-83.5

Abbreviations: CV: coefficient of variance of the mean; GSSG: oxidised glutathione; HQC: high quality control; IS: internal standard; LQC: low quality control; MF: matrix factor; na: not applicable; SAMe: s-adenosyl methionine; SD: standard deviation.

3.5 Discussion

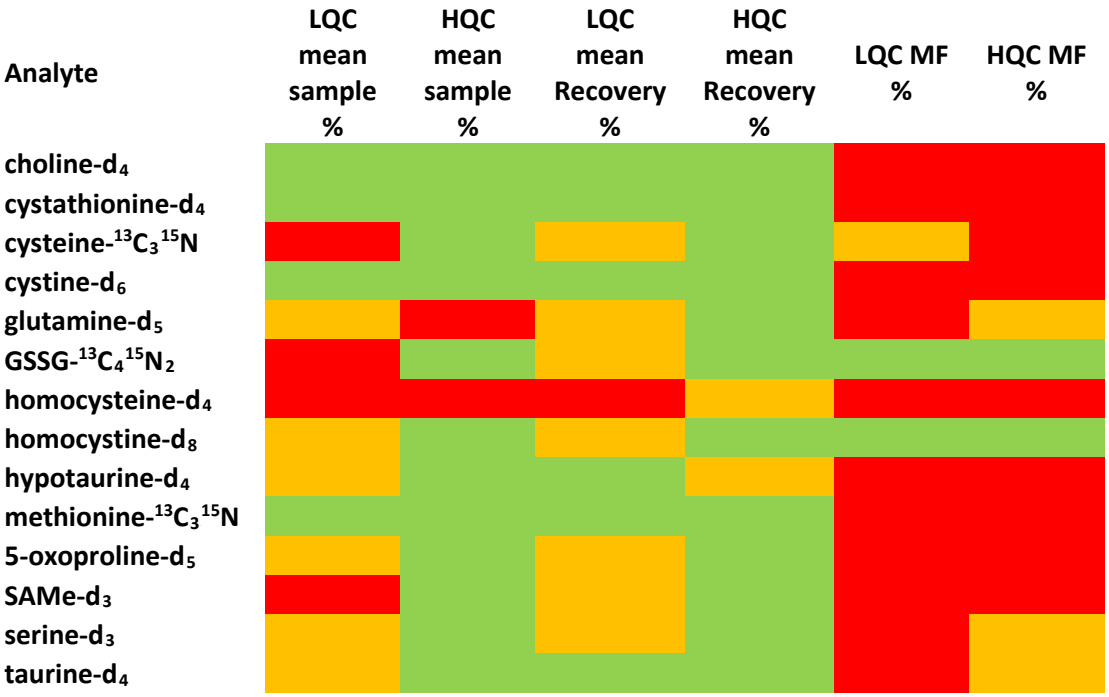
The aims of this work were to understand how sample extraction and sample matrix affected the precision and accuracy of LQC and HQC measurement in the GSH pathway assay in mouse and human serum. This was investigated using two different sample preparation protocols. For most metabolites, recovery appeared relatively poor, matrix effects were very significant, and results were generally imprecise, as summarised below in 3.5.1. However, it should be noted that in the application of this assay, the IS will account for the matrix effects and therefore for analytes with commercially available IS, it will still be possible to obtain quantitative results. For analytes for which no IS is available, results will be considered "semi-quantitative". In order to reduce these matrix effects, new sample preparation procedures should be employed.

3.5.1 Results summary

In the mouse samples, there were large differences in the peak areas when comparing the samples as prepared by the "normal" sample preparation procedure, and for those where water was added into the samples after the protein precipitation step and before centrifugation. This difference is likely due to there being a different volume of extraction solvent, and also due to water having an impact on the extraction efficiency of the analytes. Some analytes may be more soluble in water than in CH_3CN and therefore were extracted less efficiently using this sample preparation approach. There are also considerations to make regarding the effect of water on the amount of phospholipids present in the sample extract, as adding water to the extraction solvent is likely to have increased their concentrations in the extract. Therefore, it is likely that the assessment of matrix effects and recovery in mouse serum does not accurately reflect that seen using the "normal" sample preparation techniques. However, taking the results obtained experimentally it appears that recovery was generally good in mouse serum while matrix effects were very pronounced. Results were very imprecise at the LQC but less so at the HQC, this is likely due to interference from the matrix having a greater impact at lower concentrations. The matrix also affected the chromatography, and some large differences in peak areas and imprecision were due to varying retention times in samples containing

matrix, and also poor peak shapes. Some analytes appeared to have a lower peak area in matrix free samples, however this appeared to be due to broadening and interference on the peaks in the matrix. There was also matrix related ion enhancement for some analytes. The differences in chromatography and sample retention make it particularly difficult to accurately measure matrix effects on these samples, and as recovery was measured in matrix-containing samples, it may also have affected these results. Summary of bias of matrix factor and recoveries for mouse serum is shown in Table 3.22, and for CVs in Table 3.23.

Table 3.22 Summary of results for mouse serum comparisons between sample preparation, recovery and matrix factors



Key: Green: bias ≤25%; amber: 25%> bias <50%; red: bias ≥50%, from expected values.
Abbreviations: GSSG: oxidised glutathione; HQC: high quality control; LQC: low quality control; MF: matrix factor; SAMe: s-adenosyl methionine.

Table 3.23 Summary of CVs for mouse serum comparisons between sample preparation, recovery and matrix factors.

Analyte	LQC sample CV	HQC sample CV	LQC Recovery CV	HQC Recovery CV	LQC MF CV	HQC MF CV
choline-d_4						
cystathionine-d_4						
cysteine-$^{13}C_3{}^{15}N$						
cystine-d_6						
glutamine-d_5						
GSSG-$^{13}C_4{}^{15}N_2$						
homocysteine-d_4						
homocystine-d_8						
hypotaurine-d_4						
methionine-$^{13}C_3{}^{15}N$						
5-oxoproline-d_5						
SAMe-d_3						
serine-d_3						
taurine-d_4						

Key: Green: CV ≤25%; amber: 25%> CV <50%; red: CV ≥50%.
Abbreviations: CV: coefficient of variance of the mean; GSSG: oxidised glutathione; HQC: high quality control; LQC: low quality control; MF: matrix factor; SAMe: s-adenosyl methionine.

In the human samples, with the exception of analytes which could not be accurately measured at the LQC, preparing samples with IS solution made up in MeOH before drying did not give significantly different results to the matrix-free no drying samples. Recoveries were over 150% in most cases which may be due to the differences in sample preparation, or due to ion enhancements and suppression being different despite the serum being from the same individuals in this comparison. Matrix factors were considerable but generally reproducible, which is encouraging for application of the assay. The fact that recoveries were good and reproducible when comparing matrix-free samples with the matrix-free samples without drying, further supports the idea that in actual fact the poor recoveries were due primarily to matrix effects. Summary of bias of matrix factor and recoveries for human serum is shown in Table 3.24Table 3.22, and for CVs in Table 3.25.

Table 3.24 Summary of results for human serum comparisons between sample preparation, recovery and matrix factors.

Analyte	LQC mean % recovery drying	HQC mean % recovery drying	LQC mean recovery %	HQC mean recovery %	LQC MF %	HQC MF %
choline-d_4						
cystathionine-d_4						
cysteine-$^{13}C_3{}^{15}N$						
cystine-d_6						
glutamine-d_5						
GSSG-$^{13}C_4{}^{15}N_2$						
homocysteine-d_4						
homocystine-d_8						
hypotaurine-d_4						
methionine-$^{13}C_3{}^{15}N$						
5-oxoproline-d_5						
SAMe-d_3						
serine-d_3						
taurine-d_4						

Key: Green: bias ≤25%; amber: 25%> bias <50%; red: bias ≥50%, from expected values. Grey: no results reported.
Abbreviations: GSSG: oxidised glutathione; HQC: high quality control; LQC: low quality control; MF: matrix factor; SAMe: s-adenosyl methionine.

Table 3.25 Summary of CVs for human serum comparisons between sample preparation, recovery and matrix factors.

Analyte	LQC Rec. Drying CV	HQC Rec. Drying CV	LQC Recovery CV	HQC Recovery CV	LQC MF CV	HQC MF CV
choline-d_4						
cystathionine-d_4						
cysteine-$^{13}C_3{}^{15}N$						
cystine-d_6						
glutamine-d_5						
GSSG-$^{13}C_4{}^{15}N_2$						
homocysteine-d_4						
homocystine-d_8						
hypotaurine-d_4						
methionine-$^{13}C_3{}^{15}N$						
5-oxoproline-d_5						
SAMe-d_3						
serine-d_3						
taurine-d_4						

Key: Green: CV ≤25%; amber: 25%> CV <50%; red: CV ≥50%. Grey: no results reported.
Abbreviations: CV: coefficient of variance of the mean; GSSG: oxidised glutathione; HQC: high quality control; LQC: low quality control; MF: matrix factor; SAMe: s-adenosyl methionine.

3.5.2 Discussion of results

It is likely that the matrix effects from the human and mouse serum were responsible for the apparent poor recovery, plus the lack of reproducibility in peak areas, retention time and peak shapes, particularly at the LQC where the impact was most pronounced. Matrix effects can lead to either ion suppression or ion enhancement when measuring metabolites in extracted biofluids, and for this assay it seems plausible that matrix effects were caused by phospholipids which are abundant in plasma and serum (Myher et al. 1989). It is not entirely understood how phospholipids may cause these matrix effects, but it is thought that co-eluting phospholipids may prevent ionisation through competition for charge or through competition at the sprayed droplet phase for access to gas phase emission, or through binding to and co-precipitating with the analyte of interest (Furey et al. 2013). The matrix effects seen due phospholipids have been compared in previous studies using different extraction solvents and mobile phases, columns, reversed-phase chromatography (RPLC) and HILIC, UHPLC vs. traditional LC, pH, and different ionisation techniques (Chambers et al. 2007; Furey et al. 2013; Periat et al. 2016). For this assay a protein precipitation methodology was used for the extraction of samples. However, it may be necessary to evaluate different extraction techniques for further development of the assay, as protein precipitation has been found to be the least efficient method for removing phospholipids (Chambers et al. 2007). In one investigation, protein precipitation with CH_3CN was found to be very ineffective for phospholipid removal compared with solid phase extraction techniques for selected analytes when determined using a HILIC column; fewer than 15% of the analytes measured suffered no matrix effects (Periat et al. 2016). In addition, MeOH was found to be 40% less effective at the removal of phospholipids than CH_3CN when either were used for protein precipitation. The effects of poor phospholipid removal were also greater when a rapid gradient was used (Chambers et al. 2007). Therefore, as this method was developed in order to be a high throughput assay, with a rapid gradient and a simple sample preparation protocol, it may have reduced the quantitative nature of the assay and alternative sample preparation techniques may need to be investigated. Techniques such as using solid phase extraction plates for the removal of

phospholipids may decrease matrix effects and therefore increase the effectiveness of this assay (Furey et al. 2013).

Without altering the chromatography or sample preparation techniques, other options for decreasing the impact of matrix effects may be to increase the LLOQ for metabolites without internal standards, or to assume that results for these analytes can be used as fold change where QCs and curves meet acceptance criteria. Other options may be to use surrogate IS standards where a labelled standard is not available, but this approach risks false positive results where the analyte and the surrogate IS are affected differently by the matrix effects, have different recoveries and ionisation efficiencies and elute at different times in the chromatographic gradient. Another option would be to develop and synthesise deuterium labelled standards for use in the assay. When using IS for evaluation of matrix effects and recovery, the assumption that IS acts in the same way as the standards themselves is being made, and this may not be the case in reality. An alternative strategy for evaluating matrix effects and recovery is the "over spiking method", where standards are spiked into the matrix at increasing concentrations and the relative increases of standards are recorded and used to calculate concentrations (Ito and Tsukada 2002). However, this method is labour intensive and may not be effective where plasma or serum concentrations are naturally high and therefore over-spiking will lead to saturation. Another approach to try to measure matrix effects of endogenous compounds may be to perform this using matrix which has been stripped of endogenous compounds, which should have the same properties as plasma or serum but without containing the analytes of interest. One such matrix being a charcoal "stripped" matrix as was used in the validation by Huang et al (Huang et al. 2013). Other reports have investigated and reviewed other types of surrogate matrix (van de Merbel 2008), including the use of bovine serum albumin in phosphate buffered saline in a method to quantify GSH and related metabolites (Gil et al. 2018) This approach makes numerous assumptions about the similarity of any "stripped" matrix to plasma or serum, and assumes similar protein and phospholipid effects, which is unlikely to be accurate.

3.5.3 Conclusions and future work

There were significant matrix effects, which may be due to phospholipids, which interfered with the accurate quantification of analytes in this assay. The interference was concentration dependent and was greater at the LQC than the HQC. However, when this method is applied in practice IS should compensate for this, where they are available. In order to evaluate matrix effects and how quantitative metabolites without IS are, during application of the method pooled QC samples will be run alongside QCs made up of standards spiked into water, and pooled QCs spiked with standards at a known concentration. A future experiment may include analysing pooled serum over-spiked with a gradient of standards at increasing concentrations to assess matrix effects, which could potentially be used during analysis in order to back calculate concentrations, in combination with the current approach. In order to retain the properties of the assay in terms of using a rapid gradient over a HILIC column, it is clear that sample preparation techniques will need to be improved with the use of solid phase or mixed mode extraction protocols, and this will be the first step in future method development and matrix effect measurement.

4 Application of UHPLC-MS/MS assays to mouse serum and liver samples in order to determine APAP metabolism and changes in glutathione metabolism.

4.1 Introduction

As discussed in previous chapters, hepatic GSH is depleted following APAP overdose, as a result of generation of the electrophilic reactive intermediate, NAPQI, which is detoxified via conjugation with hepatocellular GSH. NAC is currently the best line of treatment for patients following APAP overdose. Measuring the GSH biosynthesis related metabolites in animal models treated with APAP, and APAP followed by NAC, may help to elucidate the effect of NAC on GSH metabolism. It may also provide further evidence about whether OA and 5-OP may be of value as circulating biomarkers of liver damage in APAP overdose. In addition, APAP metabolites may also be potential biomarkers for APAP-induced liver injury and severity of liver damage, and these were also quantified and compared with traditional biomarkers of liver injury. The UHPLC-MS/MS methods previously described in Chapters 2 and 3 were applied to liver extracts and serum from C57BL/6 mice treated with 300mg/kg APAP by intraperitoneal (i.p.) injection as an animal model of reactions in human from non-fatal APAP doses. This was the first time either method had been applied to hepatic extracts.

4.1.1 Hypotheses

The hypothesis for this work was that glutathione concentrations would be reduced in in the serum and livers of mice treated with APAP compared with untreated controls. This would lead to treatment-related changes in both hepatic and circulating key GSH-related metabolites including putative biomarkers 5-OP and OA, which would be correlated with the severity of liver injury. It was also hypothesised that APAP metabolites formed *via* CYP metabolism (APAP-C and APAP-NAC would be correlated with traditional biomarkers for liver injury.

4.1.2 Aims

- To determine the changes to GSH-related metabolism that happen in response to GSH depletion by APAP and after subsequent treatment with NAC.

- To identify potential biomarkers for hepatic GSH depletion and liver damage (hepatocyte damage scores and ALT) which can be measured in serum.
- To use the resulting data to better understand the consequences of APAP overdose on liver biochemistry in the mouse.

4.1.3 Background

The metabolic fate of paracetamol and resultant toxicity has been studied extensively in the mouse *in-vivo* (Antoine et al. 2009; Bray et al. 1992; Coen et al. 2003; Coen et al. 2004; Du et al. 2014; Kyriakides 2016; McGill et al. 2012b; Zwingmann and Bilodeau 2006). Data from these studies, and from other *in-vitro* studies and studies using compounds such as BSO and DEM to deplete GSH have suggested that changes in the concentrations of 5-OP and OA follow GSH depletion induced by APAP, and that these might be biomarkers for the severity of liver injury (Geenen et al. 2012; Geenen et al. 2013; Soga et al. 2006). OA is synthesised by the same enzymatic pathway as GSH, using the enzymes GCL and GS in its biosynthesis from 2-aminobutyrate (which replaces cysteine in the resulting tripeptide). It is assumed that increases in OA following APAP overdose could be due to either the upregulation of these enzymes, the removal of inhibition of GCL by GSH or a lack of cysteine as a substrate for GCL (Griffith and Meister 1979; Soga et al. 2006). Circulating 5-OP increases are thought to be due to upregulation of enzymes in the cycle in an attempt to increase GSH biosynthesis, and 5-OP accumulates due to the slower rate of reaction catalysed by 5-oxoprolinase, comparatively to other reactions in the cycle.(Meister 1991) There have also been reported changes to other sulfur containing metabolites measured following APAP dosing in the mouse, including decreases in hypotaurine and GSSG (Kyriakides 2016; Soga et al. 2006).

Previous literature has shown that in clinical paracetamol overdose, the concentration of the APAP metabolites, and the APAP conjugates formed following CYP mediated metabolism of APAP may be predictive of patient outcome and the severity of the liver injury (Vliegenthart et al. 2017). Therefore, this study aimed to apply the previously developed UHPLC-MS/MS methods (Chapters 2 and 3) to investigate whether, in the mouse, either paracetamol metabolites or sulfur-related metabolites were

indicative of liver injury as measured by ALT concentrations, and also to investigate how these metabolites changed in aqueous liver extracts.

NAC is used clinically as the antidote to APAP overdose (Antoine and Dear 2016; Bateman et al. 2014; Prescott et al. 1977). Its mechanism of action is presumed to be due to it being a precursor of cysteine (Corcoran et al. 1985; Corcoran and Wong 1986), a rate limiting step in GSH biosynthesis as a source of cellular sulfur. In one study, methionine was found to be less effective than NAC as an APAP antidote despite being a precursor of cysteine, which may be due to cysteine being a direct constituent of GSH for biosynthesis which may allow it to replete the cellular cysteine stores (Boobis et al. 1986). NAC has been used as the treatment of choice following its discovery (Prescott et al. 1980). However, it has also been suggested that NAC is not a superior therapy for treatment of APAP overdose, and that methionine is equal in efficacy and safety (Henry and Volans 1984). In addition, there have been reports that NAC leads to an increase in hypotaurine concentration and its effects may be due to reduction of oxidative stress independent of GSH repletion (Saito et al. 2010; Zwingmann and Bilodeau 2006). There have also been studies in the rat which have found that hypotaurine and taurine themselves can be used as antidotes for APAP overdose and can prevent increases in ALT and hepatic GSH depletion with equal effectiveness to NAC (Acharya and Lau-Cam 2010). Thereby, this study may provide evidence for how NAC treatment following APAP alters concentrations of various GSH related metabolites in the GSH biosynthesis pathway, and therefore whether it is likely that hypotaurine is increased following NAC treatment simply due to increased sulfur availability leading to metabolic pathways returning to a control state.

The mouse has been suggested as a more suitable model for understanding human paracetamol induced liver injury compared to other models, in particular the rat (McGill and Jaeschke 2014; McGill et al. 2012b). Therefore, the mouse was chosen as a species to test the UHPLC-MS/MS methods developed as described in Chapters 2 and 3, in order to try to better understand paracetamol metabolism and toxicity in man. A summary of the animal study design is provided in Figure 4.1.

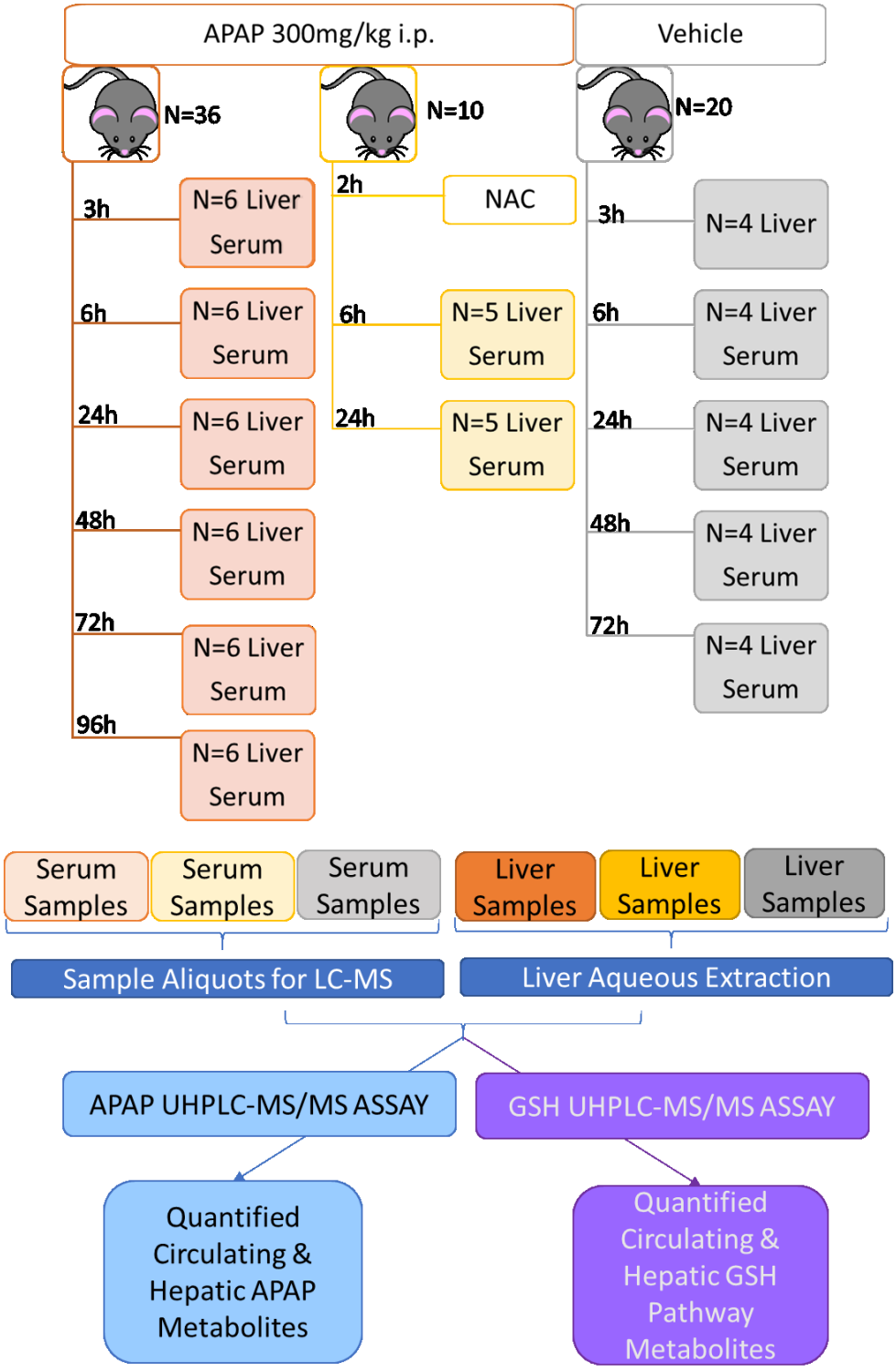


Figure 4.1 Overview of study design and summary of sample types and techniques applied in this chapter.
Abbreviations: APAP: paracetamol; GSH: glutathione; h: hour; i.p.: intraperitoneal injection; NAC: n-acetylcysteine; LC-MS: liquid chromatography coupled mass spectrometry; UHPLC-MS/MS: ultra-high-performance liquid chromatography coupled tandem mass spectrometry.

4.2 Materials and methods

4.2.1 Contribution of others

The *in-vivo* mouse work and measurement of biomarkers was completed by collaborators at the Department of Molecular & Clinical Pharmacology, MRC Centre for Drug Safety Science, Institute of Translational Medicine, University of Liverpool.

4.2.2 Mouse study

Male C57BL/6 mice aged 7-8 weeks and weighing 20-25 g were fasted overnight before being treated with paracetamol at 300 mg/kg i.p. or with water as a vehicle, at the University of Liverpool. A sub group of 10 animals were also treated with NAC at 2 hours post APAP dose. Animals were terminated at a series of time points after APAP dosing, ranging from 3 to 96 hours post APAP dose, where liver and serum samples were collected, and a number of biomarkers were measured in the blood samples, including ALT and total bilirubin (TBil). Liver samples were taken and were scored for hepatocyte damage, further liver samples were taken and homogenised in a GSH buffer of 6.3 mM EDTA and 143mM NaH_2PO_4. The supernatant of this sample was used to measure total hepatic GSH concentration and the pellet was retained to measure protein concentration using the Bradford assay (Bradford 1976).

4.2.3 Preparation of tissue samples for UHPLC-MS/MS

Liver samples of approximately 50-100 mg were taken and stored at -80 °C until they could be weighed more precisely over dry ice (mean weight 65.7 ± 12.5 g). Prior to analysis an "aqueous" extraction was carried out on these samples employing CH_3CN/MeOH/H_2O (40:40:20 v/v/v) at 100 µL/mg of tissue, with the volume adjusted for the weight of each individual sample. Tissues were extracted in 1.5 mL bead beater tubes containing glass beads of 1.1 mm diameter (Precellys). Samples were homogenised using a Precellys bead beater at 2 × 30s shaking cycles (6 500 hz), with a 20 second pause in between each cycle, and then centrifuged at 21,000 g at 4°C for 5 minutes. Two 10 µL aliquots were taken from each sample for analysis, and a further 10 µL aliquot was taken from each and combined to produce a pooled QC sample. Samples were dried down at 30°C in a rotary evaporator and stored at -80°C until

required. Dried samples were re-suspended in the relevant mobile phase, containing internal standards, for the relevant assay prior to analysis.

4.2.4 Glutathione pathway UHPLC-MS/MS assay

Chromatographic separation and mass spectrometry conditions for the GSH pathway assay are described in detail in Chapter 3. The concentration ranges of compounds were adapted to reflect the concentrations of analytes in samples, as ascertained through testing using the pooled QC samples (data not shown). Data acquisition and analysis were performed as per Chapter 3, however, the acquisition windows and TargetLynx methods were adapted to reflect any changes in retention time of analytes.

4.2.4.1 IS stock solution production for tissues

IS were split into three concentration groups equivalent to 50% of the ULOQ concentration of the analyte for which they were the internal standard, as indicated in Table 4.1, IS were made up in 1 mg/mL stock solutions, with the exception of the low concentration standards which were made up in solutions of 0.5 mg/mL. In order to make the top IS stock solution, 200 µL of the high concentration IS, and 20 µL each of the mid and low concentration IS solutions were mixed giving a final volume of 1040 µL, to which 960 µL H_20 + 0.2% FA was added to give a 2mL top stock solution. This stock solution was diluted 1:2.5 in H_2O + 0.2% FA to give a stock solution concentrations of 40 µg/mL, 4 µg/mL, 2 µg/mL, resulting in final concentration of 4 µg/mL, 0.4 µg/mL, 0.2 µg/mL for the high, mid and low concentration stock solutions respectively after a 1 in 10 dilution in sample preparation.

Table 4.1 Concentration of each IS standard in the top IS stock solution for application of the glutathione pathway assay to mouse liver extracts.

High stock solution concentration: 100 µg/mL	**Mid stock solution concentration: 10 µg/mL**	**Low stock solution concentration: 5 µg/mL**
Glutamine-d_5	5-Oxoproline-d_5	Cystathionine-d_4
Glycine-$^{13}C^{15}N$	Cystine-d_6	Choline-d_4
Serine-d_3	Glutamate-d_3	Homocysteine-d_4
Taurine-d_4	Hypotaurine-d_4	SAMe-d_3
	Methionine -$^{13}C^{15}N$	Homocystine-d_8
	Cysteine-$^{13}C_3{}^{15}N$	
	GSSG-$^{13}C_4{}^{15}N_2$	

Abbreviations: GSSG: oxidised glutathione; IS: internal standard; SAMe; s-adenosyl methionine

4.2.4.2 Standard stock solution preparation for tissue analysis

Standard curves were prepared in 84:16 CH_3CN:H_2O + 0.2% FA (v/v) and were split into three concentration levels for curves and QCs based on their relative concentrations when measured in tissues. Standards of 5-OP, cystathionine, cys-gly, cysteic acid, cysteine, homocysteine, glutamate, OA, hypotaurine, SAH, methionine, γ-glu-cys, homoserine, SAMe, cysteine, betaine, GSSG, choline, 2-amino-butyrate and homocysteine were made up in solutions of 1 mg/mL. GSH, glutamine, glycine, serine and taurine were made up in solutions of 5 mg/ml. For those forming the 'high standard curve', 20 µL of each analyte solution were mixed together with 10 µL of each analyte for the mid curve and 5 µL of each analyte forming the lower curve. This amounted to a 245 µL solution in total with all analytes mixed together, to which 155 µL of water was added to form the upper limit of quantification (ULOQ) stock solutions, concentrations of which are shown in Table 4.2. The standard curve stock solutions were produced by diluting the ULOQ stock solution, as stated in Table 4.3, to produce a series of standard stock solutions, while the QC standard stock solutions were produced by diluting the ULOQ standard as stated in Table 4.4.

Table 4.2 Concentrations of top stock solutions for the glutathione pathway assay ULOQ QC and standard curves in mouse liver extracts.[a]

High Concentration 200µg/mL	**Mid Concentration 20µg/mL**	**Low Concentration 10 µg/mL**
Glutamine	5-Oxoproline	Cystathionine
Glycine	Cys-gly	Cysteic acid
Serine	Cysteine	Homocystine
Taurine	Glutamate	Ophthalmic acid
GSH	Hypotaurine	SAH
	Methionine	γ-glu-cys
	Homoserine	SAMe
	Cystine	Betaine
	GSSG	Choline
		2-amino-butyrate
		Homocysteine

[a]Analytes were split into three curves based on their concentrations in tissue.
Abbreviations: Cys-gly: cysteinyl-glycine; γ-glu-cys: gamma-glutamyl-cysteine; GSSG: oxidised glutathione; GSH: reduced glutathione; QC: quality control; SAH: s-adenosyl homocysteine; SAMe: s-adenosyl methionine; ULOQ: upper limit of quantification.

Table 4.3 The preparation of the calibration curve for the application of the glutathione pathway assay to mouse liver extracts.

Standard Number	**Final concentration of calibration curve (µg/ml)**			**Concentration of standard stock solution (µg/ml)**			**Volume standard added (µL)**	**Standard used**	**Volume H_2O + 0.2% FA added (µL)**
	High	**Mid**	**Low**	**High**	**Mid**	**Low**			
7	20	2	1	200	20	10	-	-	-
6	10	1	0.5	100	10	5	250	7	250
5	5	0.5	0.2	50	5	2.5	100	7	300
4	2	0.2	0.2	20	2	1	50	7	450
3	1	0.2	0.05	10	1	0.5	50	6	450
2	0.5	0.05	0.02	5	0.5	0.25	50	5	450
1	0.2	0.02	0.01	2	0.2	0.1	50	4	450

[a]Final concentration of analytes in the each of the standard curves as measured by UHPLC-MS/MS after a 1 in 10 dilution in preparation.
Abbreviations: FA: formic acid; UHPLC-MS/MS: ultra-high-performance coupled tandem mass spectrometry.

Table 4.4 The preparation of the quality control samples for the application of the glutathione pathway assay to mouse liver extracts.

QC	Final QC concentration[a] (µg/mL)			Final concentration QC stock solution (µg/mL)			Volume QC stock solution added (µL)	QC stock solution used	Volume H_2O + 0.2% FA added (µL)
	High	Mid	Low	High	Mid	Low			
ULOQ	20	2	1	200	20	10	-	-	-
High	8	0.8	0.4	80	8	4	400	ULOQ	600
Mid	2	0.2	0.1	20	2	1	250	High	750
Low	0.6	0.06	0.03	6	0.6	0.3	300	Mid	700
LLOQ	0.2	0.02	0.01	2	0.2	0.1	300	Low	600

[a]Final concentration of each of the QC samples as measured by UHPLC-MS/MS after a 1 in 10 dilution in preparation.
Abbreviations: FA: formic acid; QC: quality control; UHPLC-MS/MS: ultra-high-performance liquid chromatography coupled tandem mass spectrometry.

4.2.4.3 Tissue sample preparation

QCs and Standard Curve samples were prepared by mixing 40 µL of QC or Curve stock solution and 40 µL IS stock solution (both in H_2O + 0.2% FA) with 320 µL CH_3CN + 0.2% FA. Pooled QCs were prepared from pooled aqueous liver extracts, which were prepared as described earlier. Extracted aliquots were suspended in 600µL of 80:20 Me_3CN:H_2O + 0.2% FA (v:v). From this solution, two 100 µl aliquots were taken and the following added: Pooled QC 1- 40µL IS stock solution, 20 µL H_20, 240 µL CH_3CN. Pooled QC 2: 40 µL IS stock solution + 20 µL standard stock solution at the concentration of the HQC and 240 µL CH_3CN (FA was present at 0.2% in all solutions).

For sample preparation, dried aqueous liver extracts were prepared as previously stated. Each extract was reconstituted with 40 µL IS stock solution, 40 µL H_2O + 0.2% FA and 320 µL CH_3CN + 0.2% FA. All samples and QCs were then centrifuged at 10000 x g for 10 minutes and 300 µL of the clear supernatant was transferred to glass vials for analysis.

4.2.5 GSH assay sample preparation in serum

4.2.5.1 IS solution preparation for serum

The IS stock solution, was produced as above to reflect the concentration of the analyte concentrations in serum, therefore GSSG$^{13}C_4{}^{15}N_2$ was placed in the 'high' concentration group. IS concentrations were as below in Table 4.5**.**

Table 4.5 Concentration of each IS added to the top IS stock solution for application of the glutathione pathway to mouse serum.

High stock solution concentration: 100 µg/mL	**Mid stock solution concentration: 10 µg/mL**	**Low stock solution concentration: 5 µg/mL**
Glutamine-d_5	5-oxoproline-d_5	Cystathionine-d_4
Glycine-$^{13}C^{15}N$	Cystine-d_6	Choline-d_4
Serine-d_3	Glutamate-d_3	Homocysteine-d_4
Taurine-d_4	Hypotaurine-d_4	SAMe-d_3
GSSG-$^{13}C_4{}^{15}N_2$	Methionine -$^{13}C^{15}N$	Homocystine-d_8
	Cysteine-$^{13}C_3{}^{15}N$	

Abbreviations: GSSG: oxidised glutathione; IS: internal standard; SAMe; s-adenosyl methionine

4.2.5.2 Standard curve and QC stock solution preparation.

Metabolites were split into three groups based on concentrations in samples as used for tissue analysis (Table 4.6) however for serum analysis, GSH was prepared in the "mid" curve and GSSG in the "high" curve. Standards were all diluted in H_2O containing 0.2% FA to form solutions of 1 mg/mL, with the exception of glutamine, GSSG, glycine, serine and taurine, which were prepared in solutions of 5 mg/ml. The ULOQ QC stock solution was prepared as in tissues by initially diluting the standard stock solutions together to form a sock solution of 245 µL to which 155µL water was added. The standard curve was then produced by diluting the ULOQ stock solution as stated in Table 4.6, to produce a series of standard stock solutions displayed in Table 4.7. The QCs were produced by diluting the ULOQ standard as stated in Table 4.8**,** producing a series of QC standard stock solutions.

Table 4.6 Concentrations of top stock solutions for the glutathione pathway assay ULOQ QC and standard curve in application to mouse serum.[a]

"High" stock solution: 100 µg/mL	**"Mid" Stock solution: 10 µg/mL**	**"Low" stock solution: 5 µg/mL**
Glutamine	5-Oxoproline	Cystathionine
Glycine	Cys-gly	Cysteic acid
Serine	Cysteine	Homocystine
Taurine	Glutamate	Ophthalmic acid
GSSG	Hypotaurine	SAH
	Methionine	γ-glu-cys
	Homoserine	GSH
	Cystine	SAMe
		Betaine
		Choline
		2-amino-butyrate
		Homocysteine

[a]Analytes were split into three curves based on their concentrations in serum.
Abbreviations: Cys-gly: cysteinyl-gycine; γ-glu-cys: gamma-glutamyl-cysteine; GSSG: oxidised glutathione; GSH: reduced glutathione; QC: quality control; SAH: s-adenosyl homocysteine; SAMe: s-adenosyl methionine; ULOQ: upper limit of quantification.

Table 4.7 The preparation of the calibration curve for the application of the glutathione pathway assay to mouse serum.

Standard Number	**Final concentration of calibration curve[a] (µg/ml)**			**Concentration of standard stock solution (µg/ml)**			**Volume standard added (µL)**	**Standard used**	**Volume H_2O + 0.2% FA added (µL)**
	High	**Mid**	**Low**	**High**	**Mid**	**Low**			
7	20	2	1	100	10	5	-	-	-
6	10	1	0.5	50	5	2.5	250	7	250
5	5	0.5	0.2	25	2.5	1	100	7	300
4	2	0.2	0.2	10	1	0.5	50	7	450
3	1	0.2	0.05	5	0.5	0.25	50	6	450
2	0.5	0.05	0.02	2.5	0.25	0.1	50	5	450
1	0.2	0.02	0.01	1	0.1	0.05	50	4	450

[a]The final concentrations of analytes in the each of the standard curves as measured by UHPLC-MS/MS after a 1 in 5 dilution in preparation.
Abbreviations: FA: formic acid; UHPLC-MS/MS: ultra-high-performance liquid chromatography coupled tandem mass spectrometry.

4.2.5.3 Serum sample preparation

Standard curves and QCs were produced from final stock solutions by mixing 20 µL of each relevant curve or QC stock solution with 10 µL of IS stock solution with 70 µL 80:20 MeCN:H_2O + 0.2% FA. Samples for analysis were prepared by mixing 20µL of serum with 10µL IS in H_2O+0.2%FA and 70 µL 80:20 MeCN:H_2O + 0.2% FA. These mixtures were kept at -20°C for 20 minutes to precipitate proteins and were then centrifuged at 10 000xg for 10 minutes, after which 80 µL of the solution was transferred to total recovery vials for analysis.

Table 4.8 The preparation of the QC stock solutions for application of the glutathione pathway assay to mouse serum.

QC	Final QC concentration[a] (µg/mL)			Final concentration QC stock solution (µg/mL)			Volume QC stock solution added (µL)	QC stock solution used	Volume H_2O + 0.2% FA added (µL)
	High	Mid	Low	High	Mid	Low			
ULOQ	20	2	1	100	10	5	-	-	-
High	8	0.8	0.4	40	4	2	400	ULOQ	600
Mid	2	0.2	0.1	10	1	0.5	250	High	750
Low	0.6	0.06	0.03	3	0.3	0.15	300	Mid	700
LLOQ	0.2	0.02	0.01	1	0.1	0.05	300	Low	600

[a]*The final concentration of the QC standard solutions for each curve level when measured after a 1 in 5 dilution in preparation.*

Abbreviations: FA: formic acid; LLOQ: lower limit of quantification; QC: quality control; ULOQ: upper limit of quantification.

4.2.6 APAP method sample preparation.

Chromatographic and mass spectrometry conditions for the APAP method were described in detail in Chapter 2. The method was applied to liver tissue extracts for the first time. Due to the low concentrations of APAP and its metabolites at the later time points of this study, the method was applied to serum samples twice using different dilution factors. Initially samples were diluted 1 in 1000 and then, in the second analysis, this was reduced to a 1 in 25 dilution.

4.2.6.1 Liver extract sample and IS and standard curve stock solution preparation

Each of the APAP metabolites was measured initially in a test tissue sample to determine the calibration range for each. The calibration range and QC concentration levels were kept the same as described in chapter in Chapter 2. (500-16 ng/mL, 100-3.2 ng/mL and 20-0.64 ng/mL) but the curve

for each analyte was changed to reflect actual sample concentrations, and the ULOQ for each analyte as determined by preliminary experiments is shown in Table 4.9. IS stock solutions were produced to give the final concentrations given in Table 4.9.

In order to produce standard and IS stock solutions, all standard and ISs were prepared in MeOH at a concentration of 0.1 mg/mL. For calibration curves and QC samples, calibration and QC stock solutions were diluted 1 in 2 with the IS stock solution. Therefore, standard and IS stock solutions were produced at 2 x the final required concentration. The IS stock solution was produced by mixing each individual IS, made up in 0.1mg/mL solutions, at the following volumes: 40 µL each of APAP-G-d3, APAP-GSH-d3 and APAP-NAC-d5; and 8 µL each of APAP-d3, APAP-S-d3, APAP-C-d5; this gave a total volume of 144µL to which 856µL of H_20 was added. This solution was then diluted 1 in 10, before undergoing a 1 in 2 dilution in sample preparation, to give the final concentration listed in Table 4.10.

Table 4.9 Final concentration of the ULOQ of each of the APAP standards, and the concentration of IS used for each, for application of the assay to tissue extracts, not accounting for salt factors.

500 ng/mL	200 ng/mL	100 ng/mL	40ng/mL	20 ng/mL
APAP-G	APAP-G-d_3	APAP	APAP-d_3	APAP-Ome
APAP-SG	APAP-SG-d_3	APAP-S	APAP-S-d_3	PAP-G
APAP-NAC	APAP-NAC-d_5	APAP-C	APAP-C-d_5	

Abbreviations: APAP: paracetamol; APAP-C: paracetamol-cysteinyl conjugate; APAP-G: paracetamol glucuronide; APAP-OMe: 3-methoxy paracetamol; APAP-NAC: paracetamol n-acetylcysteine conjugate; APAP-S: paracetamol sulfate; APAP-SG: paracetamol glutathione conjugate; PAP-G: p-aminophenol glucuronide.

Table 4.10 Concentration ranges of the analytes in calibration curve for the application of the APAP method to mouse liver extracts.

Standard	Concentration ranges in ng/mL							
	APAP	APAP-G	APAP-S	APAP-C	APAP-GSH	APAP-NAC	APAP-OMe	PAP-G
1	3.2	15	2.75	2.2	14.5	-	0.64	0.64
2	4.8	22.5	4.12	3.35	22	21	0.96	0.96
3	8	37.5	6.87	5.55	36.5	35	1.6	1.6
4	12	56	10.3	8.35	54.8	52.5	2.4	2.4
5	18	84.5	15.5	12.5	82	79	3.6	3.6
6	30	141	25.8	20.9	137	132	6.0	6.0
7	50	235	42.9	34.7	228	219	10	10
8	100	469	85.9	69.5	455	438	20	20

Abbreviations: APAP: paracetamol; APAP-C: paracetamol-cysteinyl conjugate; APAP-G: paracetamol glucuronide; APAP-OMe: 3-methoxy paracetamol; APAP-NAC: paracetamol n-acetylcysteine conjugate; APAP-S: paracetamol sulfate; APAP-SG: paracetamol glutathione conjugate; PAP-G: p-aminophenol glucuronide.

Table 4.11 QC concentrations for application of the APAP method to mouse liver extracts, taking into account salt factors.

QC Concentration in ng/ml								
QC	APAP	APAP-S	APAP-G	APAP-SG	APAP-C	APAP-OMe	APAP-NAC	PAP-G
HQC	80	68.7	375	365	55.5	16.0	350	16
MQC	20	17.2	93.5	91.3	13.9	4.00	87.8	4
LQC	9.6	8.24	45	43.8	6.65	1.92	42	1.92

Abbreviations: APAP: paracetamol; APAP-C: paracetamol-cysteinyl conjugate; APAP-G: paracetamol glucuronide; APAP-OMe: 3-methoxy paracetamol; APAP-NAC: paracetamol n-acetylcysteine conjugate; APAP-S: paracetamol sulfate; APAP-SG: paracetamol glutathione conjugate; HQC: high quality control; LQC: low quality control; MQC: mid quality control; PAP-G: p-aminophenol glucuronide; QC: quality control.

To produce the top analyte stock solutions, analytes made up at 0.1mg/mL were mixed as follows: 100 µL each of APAP-G, APAP-GSH and APAP-NAC; 20µL of APAP, APAP-C and APAP-S; and 4µL APAP-OMe and PAP-G; to give a final volume of 368 µL to which 632 µL H_2O was added. This solution was then diluted 1 in 10 in H_20 to give the final ULOQ stock solution. This was then serially diluted as per previously described in Chapter 2.0 in order to give stock solutions for the calibration curve (Table 4.10) and QCs (Table 4.11)

Dried hepatic extracts were prepared as described earlier and were reconstituted in 50 µL IS stock solution and 50 µL H_2O. These samples were then centrifuged at 10 000g for 5 minutes in order to remove any undissolved materials which might damage the column, and the supernatant was

transferred to total recovery vials for analysis. Pooled QC samples were prepared by reconstituting the hepatic extract with 50 µL IS stock solution and 50 µL of the HQC stock solution.

4.2.6.2 Serum sample and IS and curve stock solution preparation

For measurement of serum samples by the APAP method, samples were prepared and run in two batches based on the concentration of metabolites in the sample. The calibration curve and QC concentration ranges were kept the same for both runs, however these were prepared separately to reflect matrix effects in the more concentrated sample preparation. Calibration curves and QC ranges were as below in Table 4.12 and Table 4.13. For run 1 of samples at 3 and 6 hours post APAP treatment, samples were prepared exactly as described previously in Chapter 2. Concentrations of some metabolites were above the ULOQ in samples from the 3-hour time point, so these were further diluted 1 in 5 before being reanalysed and processed using 5x lower IS concentration. For run 2, which was for samples 6 hours to 96 hours, the standard curve and QC and IS top stock solutions were diluted by 1 in 80 before being serially diluted. Curves and QC samples were then prepared by adding 10 µL of curve or QC stock solutions in MeOH and 10 µL IS stock solution to 5 µL of serum (1 in 2.5 dilution) after which samples were stored at -20°C for 20 minutes to precipitate proteins and then were centrifuged at 10 000 g for 10 minutes. Then 10 µL of each of the clear supernatants were taken and diluted with 40 µL of H_2O to give an overall dilution of 12.5 for standard curve and QC stock solution preparation, following the original 1 in 80 dilution of the stock solution to give a 1 in 1000 overall dilution. Samples were prepared as above, except that 5 µL of serum was diluted with 10 µL of MeOH and 10 µL of IS solution before extraction and further dilution, giving samples an overall dilution of 1 in 25.

Table 4.12 Calibration curve range for APAP method application to mouse serum.

Calibration Curve Ranges in ng/ml							
Standard	**APAP**	**APAP-G**	**APAP-S**	**APAP-C**	**APAP-SG**	**APAP-NAC**	**APAP-OMe**
1	16	3.00	2.75	0.44	0.58	-	0.64
2	24	4.50	4.12	0.67	0.88	0.84	0.96
3	40	7.50	6.87	1.11	1.46	1.40	1.6
4	60	11.2	10.3	1.67	2.19	2.10	2.4
5	90	16.9	15.5	2.50	3.28	3.16	3.6
6	150	28.1	25.8	4.173	5.47	5.26	6.0
7	250	46.9	42.9	6.94	9.12	8.77	10
8	500	93.7	85.9	13.9	18.2	17.5	20

Abbreviations: APAP: paracetamol; APAP-C: paracetamol-cysteinyl conjugate; APAP-G: paracetamol glucuronide; APAP-OMe: 3-methoxy paracetamol; APAP-NAC: paracetamol n-acetylcysteine conjugate; APAP-S: paracetamol sulfate; APAP-SG: paracetamol glutathione conjugate; PAP-G: p-aminophenol glucuronide.

Table 4.13 QC Concentrations for APAP method application to mouse serum.

QC Concentration in ng/ml							
QC	**APAP**	**APAP-S**	**APAP-G**	**APAP-SG**	**APAP-C**	**APAP-OMe**	**APAP-NAC**
ULOQ	500	85.9	93.7	18.2	13.9	20.0	17.5
High	400	68.7	75.0	14.6	11.1	16.0	14.0
Mid	100	17.2	18.7	3.65	2.78	4.00	3.51
Low	48.0	8.24	9.00	1.75	1.33	1.92	1.68
LLOQ	16.0	2.75	3.00	0.58	0.44	0.64	0.84

Abbreviations: APAP: paracetamol; APAP-C: paracetamol-cysteinyl conjugate; APAP-G: paracetamol glucuronide; APAP-OMe: 3-methoxy paracetamol; APAP-NAC: paracetamol n-acetylcysteine conjugate; APAP-S: paracetamol sulfate; APAP-SG: paracetamol glutathione conjugate; LLOQ: lower limit of quantification; PAP-G: p-aminophenol glucuronide; QC: quality control; ULOQ: upper limit of quantification.

4.2.7 Data analysis and run acceptance

All UHPLC-MS/MS data were processed using Targetlynx software as previously described. For all metabolites, the acceptance criteria described below were individually applied to verify the accuracy and precision of the run for both APAP and GSH methods. The APAP assay method has previously been shown to be robust and reproducible (see Chapter 2), and for acceptance the percentage bias from expected values for six points on the curve and for 67% the QCs at each level, and 67% overall, was required to be 15-20%. For the GSH pathway assay, due to the complexity of this method and

difficulties in performing validation due to the endogenous nature of the metabolites, acceptance criteria for curve and QC bias was 20-30%. For the application of this assay to serum, a pragmatic approach was taken to acceptance of the method. If the standard curve points did not all meet acceptance criteria, points were excluded from the curve and results were acceptable if QCs throughout the run met acceptance criteria (bias of around 20% or less). In the case that not all curve points and/or QCs met acceptance criteria, but results were clustered at the lower or higher end of the curve, and only either the LQCs or HQCs respectively did not meet acceptance criteria, results in the new truncated range were used, providing 67% of the QCs within the new range met acceptance criteria. In some cases where internal standards were not present, the standard curves at the beginning or end of the run were linear independently but had shifted in absolute concentration. In these cases, only one curve was used to quantify the metabolite, provided 67% of the QCs throughout the run met acceptance criteria when measured against the single standard curve.

4.2.8 Statistical analysis

For Univariate analysis, all UHPLC-MS/MS data were exported from Target Lynx and further analysed in Microsoft Excel and Prism 8.0 (Graphpad, CA). For APAP metabolite analysis at 6 and 24 hours APAP and APAP + NAC results were compared using Mann-Whitney test. For 6 and 24 hours where there were 3 groups, (APAP, APAP + NAC and Control), Kruskal-Wallis tests with false discovery rate (FDR) corrected multiple comparisons were used using the “two-stage” step up method of Benjamini, Krieger and Yekutieli (Benjamini et al. 2006). For GSH metabolism analysis, results were $\log_{10}$ transformed prior to analysis with a one-way analysis of variance (ANOVA), with FDR corrected multiple comparisons. Clinical chemistry biomarkers were also $\log_{10}$ transformed and analysed using ANOVA, were analysed for relationships with $\log_{10}$ transformed circulating GSH and APAP metabolism data using a Pearson’s correlation coefficient. Multivariate modelling of hepatic data was carried out using SIMCA version 15 (Umetrics), all metabolite were $\log_{10}$ transformed with the addition of a constant, and unit variance (UV) scaled prior to principal components analysis (PCA) (van den Berg et al. 2006).

4.3 Results

4.3.1 Clinical chemistry and biomarkers

ALT, total bilirubin (TBil) and total hepatic GSH were measured by our collaborators at Liverpool, and liver tissues were scored for hepatocyte damage, results are displayed in Table 4.14. ALT was significantly higher in all APAP treated animals compared to time matched controls; ALT was significantly lower in NAC-treated mice than the time matched APAP-only treated mice. TBil was significantly higher compared to time matched controls at 3 and 6 hours post APAP treatment and at 48 hours, there were no significant differences between APAP + NAC samples and controls. Total hepatic GSH concentrations were significantly lower at 3 and 6 hours post APAP treatment compared to time matched controls. AT 24 hours, GSH concentrations were significantly higher in APAP + NAC treated animals than control or APAP treated. Hepatocyte damage was scored in controls and animals treated with APAP, but not animals treated with APAP + NAC. Control animals all had a score of 0, as did animals which were sacrificed at 72 or 96 hours post APAP treatment. Scores were significantly higher in APAP treated animals across time points. Log transformed values for ALT, TBil and GSH are plotted in Figure 4.2.

Table 4.14 Biochemistry and hepatocyte damage scores for C57/BL-6 mice treated with 300 mg/kg paracetamol.

Time (h)	Group	Mean ± SD ALT (U/L)	q-value	Mean ± SD TBil (mg/dL)	q-value[a]	Mean ± SD total GSH (nmol/mg protein)	q-value[a]	Mean ± SD score for hepatocyte damage	q-value
3	control	34.7±11.57		0.15±0.03		50.4±3.71		0±0	
	APAP	986±342	<0.0001	0.7±0.06	<0.0001	8.13±1.55	<0.0001	2.67±0.48	<0.0001
6	control	26.7±1.81		0.14±0.01		54.6±8.35		0±0	
	APAP	3205±212	<0.0001	0.4±0.04	0.0232	6.73±1.5	<0.0001	2±0	<0.0001
	NAC	999±257	<0.0001 0.0005†	0.32±0.07	0.1240 0.3712†	76.3±7.65	0.1139 <0.0001†	na	
24	control	33.1±20.1		0.2±0.08		49.5±13.6		0±0	
	APAP	3677±817	<0.0001	0.29±0.03	0.3712	40.8±7.82	0.2341	2±0.41	<0.0001
	NAC	235±100	0.0007 <0.0001†	0.29±0.08	0.3712 0.7286†	83.2±6.28	0.0217 0.0016†	na	
48	control	23±4.09		0.22±0.01		72.8±10.4		0±0	
	APAP	1204±935	<0.0001	0.55±0.23	0.0232	70.8±16.8	0.2886	1±0.18	<0.0001
72	control	18.3±0.55		0.26±0.04		73.4±3.2		0±0	
	APAP	65±6.7	0.0027	0.26±0.03	0.7286	94.2±16.6	0.1866	0±0	
96	APAP	58.7±9.32	0.0055	0.47±0.02	0.1102	60.3±9.36	0.1866	0±0	

[a]q-values were calculated using one-way ANOVA with FDR corrected multiple comparisons comparing APAP and APAP+NAC treated animals with control. Control n = 4, APAP n = 6 (n = 5 for GSH) NAC n = 5.† = APAP + NAC versus APAP alone
Abbreviations: ALT: alanine aminotransferase; ANOVA: Analysis of variance; APAP: paracetamol; FDR: false discovery rate; GSH: reduced glutathione; NAC: n-acetyl-cysteine; SD: standard deviation.

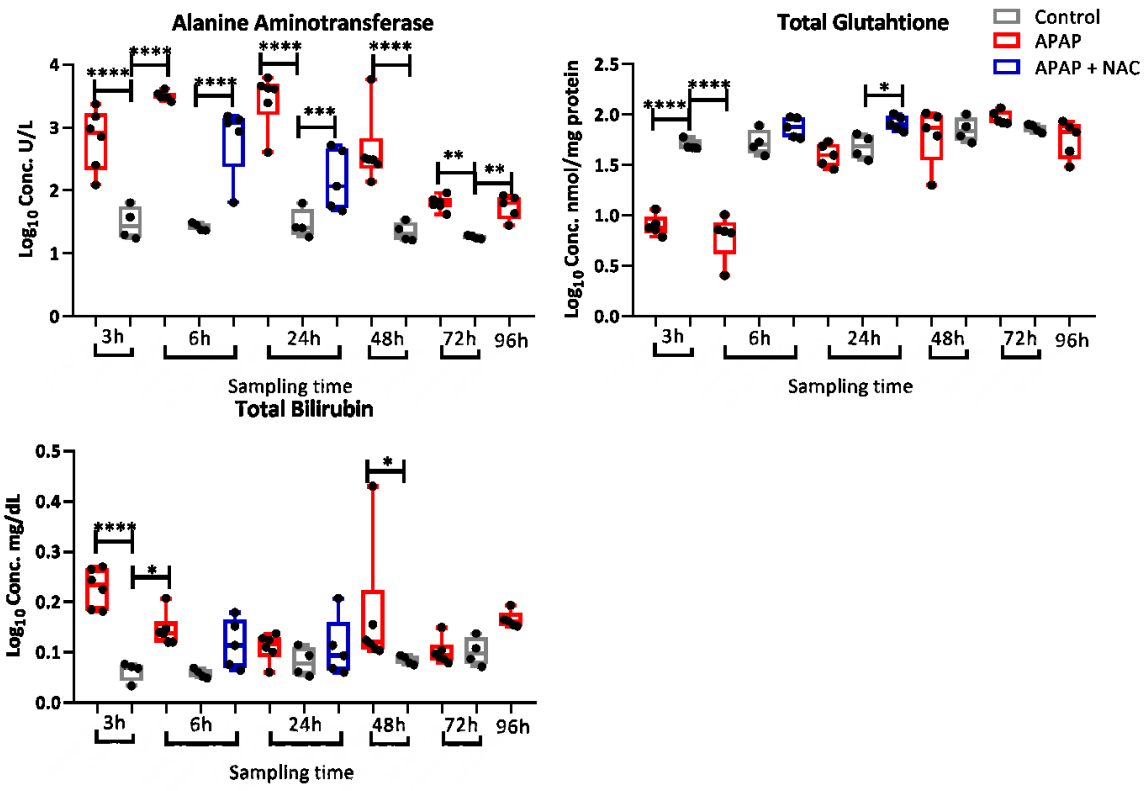


Figure 4.2 Clinical chemistry measurements analysed by One-way ANOVA, FDR corrected p values (q), q<0.03 (*), q<0.002 (**), q<0.0002 (***), q<0.0001 (****)
Abbreviations: ANOVA: Analysis of variance; APAP: paracetamol; FDR: false discovery rate; NAC: n-acetyl-cysteine.

4.3.2 Circulating metabolites

4.3.2.1 Analytical precision, accuracy and matrix effects of APAP method

Samples taken from mice at 3 and 6 hours were analysed alongside a full validation run as described in Chapter 2, all calibration curves and QCs were within the acceptance criteria. Samples from later time points were analysed using a more concentrated sample preparation method and so this was evaluated for accuracy, precision and matrix effects and recovery. In Table 4.15, the linearity and the percentage of the curve that met acceptance criteria, percentage of QCs that met acceptance criteria and CVs and percentage bias at each QC level are shown. The results highlighted in orange show that CV or bias were outside the original acceptance criteria (15%, 20% at LLOQ), but were below 20% (30 % at LLOQ) and were deemed acceptable in this analysis. Those highlighted in red were outside these new acceptance criteria or had fewer than 67% acceptable curve or QC points. Two LLOQs were analysed meaning that for analytes where the LLOQ failed, LLOQ2 could be used as the new LLOQ, and

therefore the analyte was deemed to meet acceptance criteria if all QCs above this were acceptable. APAP-S had a number of QC failures but was deemed acceptable as CVs and bias were below 20%.

The matrix effects and recoveries using the new sample preparation are recorded in Table 4.16. Matrix effects were minimal, and generally below 20% with the exception of APAP-S, but this matrix effect was only marginally higher than 20%. The results were consisent at the HQC and LQC. Recoveries were also close to 100% at the HQC and LQC for all analytes. In calculating recovery at the HQC there were only four acceptable responses due to an instumentation issue, as recoveries were not IS normalised. APAP-OMe was the only analyte for which matrix effects could not be IS normalised, and was the only analyte to have a matrix effect CV >20%.

Table 4.15 Summary of APAP method application to mouse serum: concentrated sample preparation method.

		APAP	APAP-C	APAP-G	APAP-GSH	APAP-NAC	APAP-S	APAP-OMe
Curve	r2	0.988	0.996	0.994	0.988	0.994	0.994	0.974
	% Pass	89	89	89	78	89	89	84
LLOQ	% Pass	67	0	50	67	33	0	0
	% Bias	24.9	59.7	30.0	33.2	31.2	53.2	43.7
	% CV	23.4	16.8	20.3	23.1	14.5	21.0	16.1
LLOQ2	% Pass	83	17	83	100	83	50	83
	% Bias	0.650	19.4	1.28	6.42	0.917	16.7	6.1
	% CV	14.1	10.6	14.7	11.5	14.1	15.4	13.2
LQC	% Pass	100	67	83	83	67	50	83
	% Bias	1.95	14.1	5.17	4.92	-0.70	18.7	0.1
	% CV	10.2	9.8	7.9	13.1	16.0	16.1	10.7
MQC	% Pass	100	100	83	83	83	100	67
	% Bias	-2.20	3.12	5.70	2.00	1.62	5.53	-13.3
	% CV	5.96	8.33	8.31	7.81	9.16	4.10	22.0
HQC	% Pass	100	100	83	100	100	100	67
	% Bias	-0.250	1.13	6.85	1.25	-2.93	1.07	-14.4
	% CV	7.33	1.34	11.02	4.88	5.44	1.23	25.5
ULOQ	% Pass	100	100	83	83	83	100	83
	% Bias	-0.92	1.02	-3.52	-1.10	-4.38	-0.03	0.53
	% CV	9.91	6.85	10.03	8.71	8.61	5.66	10.4
Total QCs	% Pass	92	64*	78	86	75	67	64*

The percentage of each QC meeting acceptance criteria (% pass), CV of QCs and mean bias from expected concentration are displayed. Linearity is expressed as r^2 value of calibration curve. Red colour: CV≥20% (30% LLOQ); orange colour: CV≥15% (20% LLOQ)
Abbreviations: APAP: paracetamol; APAP-C: paracetamol-cysteinyl conjugate; APAP-G: paracetamol glucuronide; APAP-OMe: 3-methoxy paracetamol; APAP-NAC: paracetamol n-acetylcysteine conjugate; APAP-S: paracetamol sulfate; APAP-SG: paracetamol glutathione conjugate; CV: coefficient of variance; HQC: high quality control; LLOQ: lower limit of quantification; LQC: low quality control; MQC: mid quality control; PAP-G: p-aminophenol glucuronide; QC: quality control; ULOQ: upper limit of quantification.

Table 4.16 Summary of matrix effects and recovery at LQC and HQC when APAP method was applied to mouse serum: concentrated sample preparation.

Analyte	HQC				LQC			
	MF % n=6	CV	Recovery % n=4	CV	MF % n=4	CV	Recovery % n=6	CV
APAP	-10.3	4.50	102	16.7	-6.19	10.9	105	8.4
APAP-NAC	-11.7	5.80	105	12.3	5.86	16.9	99.5	18.8
APAP-C	-10.6	7.01	106	10.3	-3.05	13.0	105	11.7
APAP-G	5.49	10.3	101	13.4	15.9	9.76	102	11.7
APAP-GSH	-13.9	4.22	105	8.1	-9.71	6.84	105	19.7
APAP-S	-21.5	6.34	103	11.5	-20.2	8.78	102	10.3
APAP-OMe	-13.0*	23.5	106	15.7	-13.0*	14.9	99.4	10.5

Red colour: CV≥20% (30% LLOQ); orange colour: CV≥15% (20% LLOQ)
Abbreviations: APAP: paracetamol; APAP-C: paracetamol-cysteinyl conjugate; APAP-G: paracetamol glucuronide; APAP-OMe: 3-methoxy paracetamol; APAP-NAC: paracetamol n-acetylcysteine conjugate; APAP-S: paracetamol sulfate; APAP-SG: paracetamol glutathione conjugate; CV: coefficient of variance; HQC: high quality control; LLOQ: lower limit of quantification; low quality control; MF: matrix factor; MQC: mid quality control; PAP-G: p-aminophenol glucuronide; QC: quality control; ULOQ: upper limit of quantification.

4.3.2.2 Circulating APAP metabolism changes

Concentrations of circulating APAP and its metabolites are shown in Figure 4.3Figure 4.2. From 24 hours after APAP dosing in general there were no quantifiable metabolites remaining in the circulation or in the hepatic tissue extracts. Kruskal-wallis analysis with FDR correction was used to compare results at 6 hours and at 24 hours for animals treated with APAP and APAP+NAC. APAP-G concentrations were significantly lower in serum samples at both 6 and 24 hours in APAP+NAC treated mice compared to APAP alone treated. At 24 hours APAP-S and APAP-GSH concentrations were significantly higher in the serum of mice treated with APAP + NAC compared to APAP.

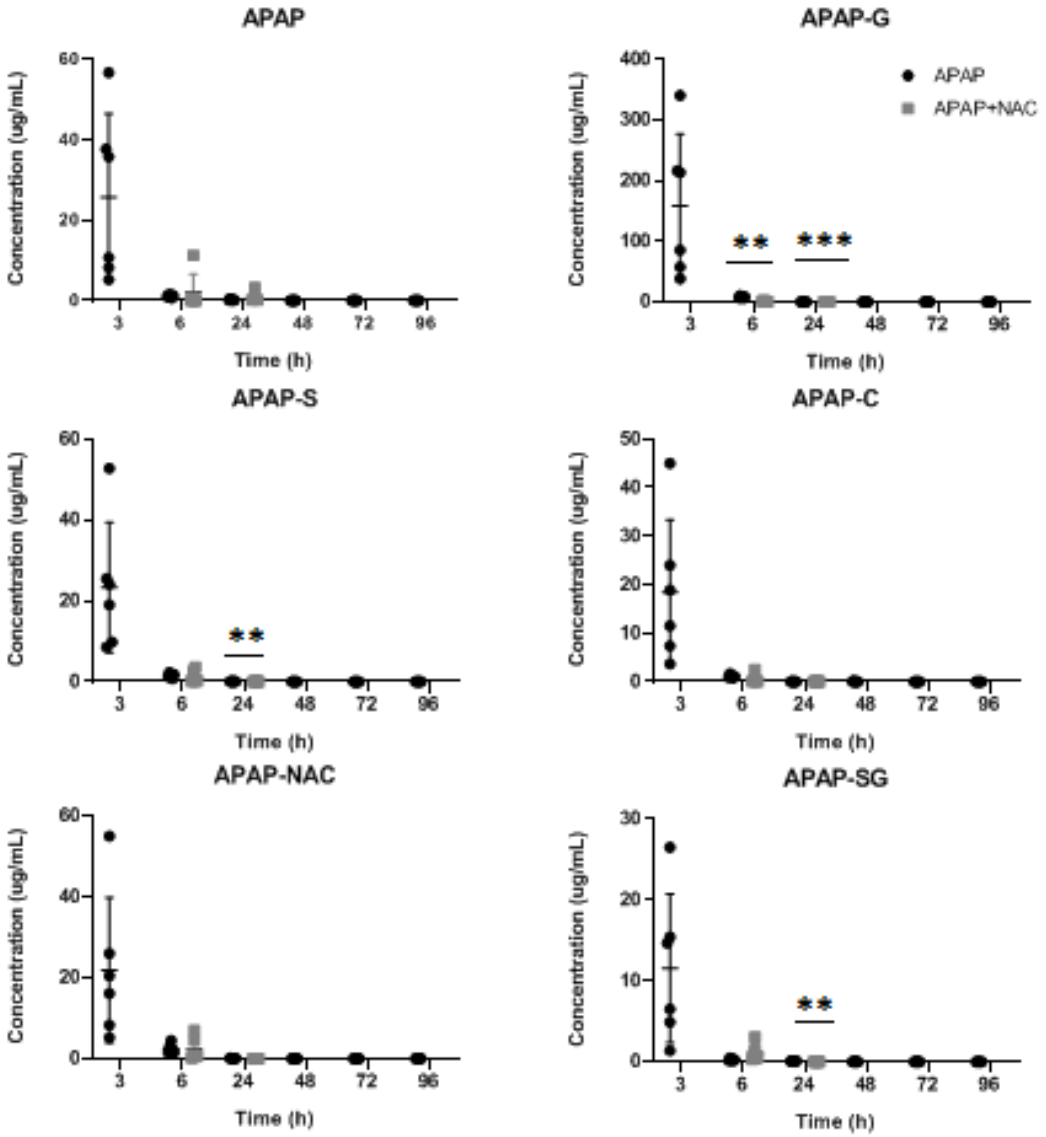


Figure 4.3. Concentrations of APAP and metabolites measured in serum samples from mice treated with APAP at 300mg/kg i.p. or with APAP followed by NAC. Analysed by Kruskal-Wallis of three groups followed by FDR correction, adjusted p values 0.03 (*), 0.002 (**), 0.0002
Abbreviations: APAP: paracetamol; APAP-C: paracetamol-cysteinyl conjugate; APAP-G: paracetamol glucuronide; APAP-OMe: 3-methoxy paracetamol; APAP-NAC: paracetamol n-acetylcysteine conjugate; APAP-S: paracetamol sulfate; APAP-SG: paracetamol glutathione conjugate; FDR: false discovery rate; NAC: n-acetylcysteine; PAP-G: p-aminophenol glucuronide.

4.3.2.3 Circulating GSH metabolism changes

The GSH method has previously undergone validation for serum (Isobelle Grant Thesis, and Chapter 3), so for the application of the assay to mouse serum an LQC, MQC and HQC were analysed as part of the analytical run. Results were used for any metabolites for which >67% of the overall curve and QCs met acceptance criteria and metabolite concentrations measured in the serum were within

analytical range. A number of metabolites could not be measured accurately in the serum due to the analyte being below the limit of quantification or detection in the samples, including γ-glu-cys, homocysteine, homocysteine, cysteic acid and 2-AB. Curves were not linear and QCs did not meet acceptance criteria for GSH, glycine, serine and betaine. Results for analytes which could be measured are summarised in Table 4.17 below.

Table 4.17 The linearity and percentage meeting acceptance criteria for calibration curves, QCs at each level and, the total percentage of QCs meeting acceptance criteria, for glutathione pathway assay applied to mouse serum.

Analyte	Linearity, r^2	% Curve	% LQC	% MQC	% HQC	% Total QCs
Choline	0.997	86	100	100	100	100
Cystathionine	0.999	86	100	100	100	100
Cysteine	0.994	86	100	100	100	100
Cystine	0.992	100.0	100	67	100	88.9
Glutamate	0.987	79	33	100	100	78
Glutamine	0.994	100.0	100	100	100	100
GSSG	0.997	86	67	100	100	88.9
Homoserine	0.99	86	100	100	100	100
Hypotaurine	0.991	86	100	100	100	100
Methionine	0.996	100.0	100	100	100	100
OA	0.9	71	67	67	67	67
5-OP	0.997	100.0	100	100	100	100
SAH	0.996	100.0	100	100	100	100
SAMe	0.994	79	100	100	100	100
Taurine	0.998	100.0	100	100	100	100

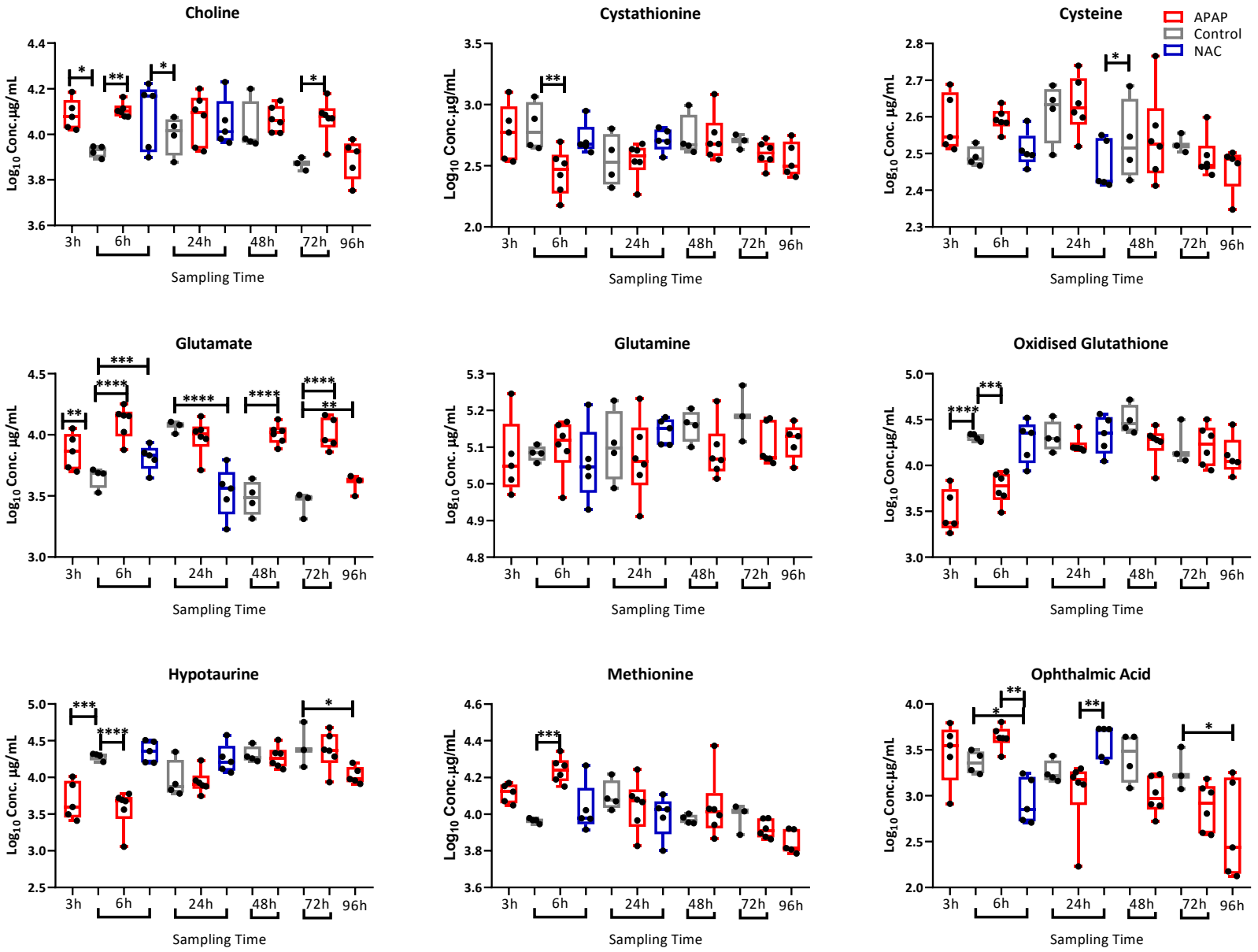
Abbreviations: GSSG: oxidised glutathione; HQC: high quality control; LQC: low quality control: MQC: mid quality control; OA: Ophthalmic acid; 5-OP: 5-oxoproline; QC: quality control; SAH: s-adenosyl homocysteine; SAMe: s-adenosyl methionine.

There were no control serum samples available from the study for the 3-hour time point, so 3- and 6-hour APAP treated samples were compared with control and APAP+NAC samples at 6 hours, similarly samples from 96 hours were compared to 72-hour controls. The concentrations of 5-OP, choline, glutamate, taurine and methionine were significantly increased compared to controls and APAP + NAC treated animals at early time points pre-24 hours. OA concentrations were not increased significantly compared to controls but were significantly elevated compared to the concentration in serum from animals treated with APAP+NAC, which had lower OA concentrations than in controls. Circulating hypotaurine, cystathionine, SAH, SAMe and GSSG were significantly decreased in APAP-only treated

animals compared to control and APAP + NAC treated animals at early time points. At 24 hours a number of the metabolites had recovered to control concentrations, there were some changes in APAP + NAC treated animals, where 5-OP and OA were both elevated in compared to control or APAP-only treated animals, and cysteine and glutamate were decreased. At later time points, 5-OP, glutamine and choline were elevated compared to controls, while hypotaurine and OA were decreased. Taurine was significantly decreased compared to controls at 6 hours, having been previously elevated. Cysteine concentrations were decreased in the serum of APAP+NAC treated animals at 24 hours post treatment. Results are shown in Figure 4.4**.**

4.3.2.4 Circulating APAP/APAP metabolites and GSH-pathway-related metabolites summary

In order to understand whether the concentration of these metabolites had a relationship with liver damage, Pearson correlation coefficients were calucalted for APAP and GSH metabolites with hepatic GSH, ALT, TBil or hepatocyte damage scores. Pearson r coefficients and respective p-values are displayed in Table 4.18. Any significant ($p<0.05$) correlations were assessed for strength of correlation, $r<0.3$ was considered negligible, $0.3<r>0.5$ was considered weak, $0.5<r>0.7$ was considered moderate and $r\geq0.7$ was considered to be a strong correlation. Correlations were significant for all APAP metablites for each of the markers of liver injury. APAP-C and APAP-NAC were both strongly correlated with ALT and hepatocyte damage scores and moderately with TBil, which was also correlated with APAP-S. Hepatic GSH concentration was negatively correlated with all the APAP metablites, and was most strongly correlated with APAP-SG and APAP.


Choline
Cystathionine
Cysteine
APAP
Control
NAC
Glutamate
Glutamine
Oxidised Glutathione
Hypotaurine
Methionine
Ophthalmic Acid
Log10 Conc.µg/mL
Log10 Conc. µg/mL
3h
6h
24h
48h
72h
96h
Sampling Time

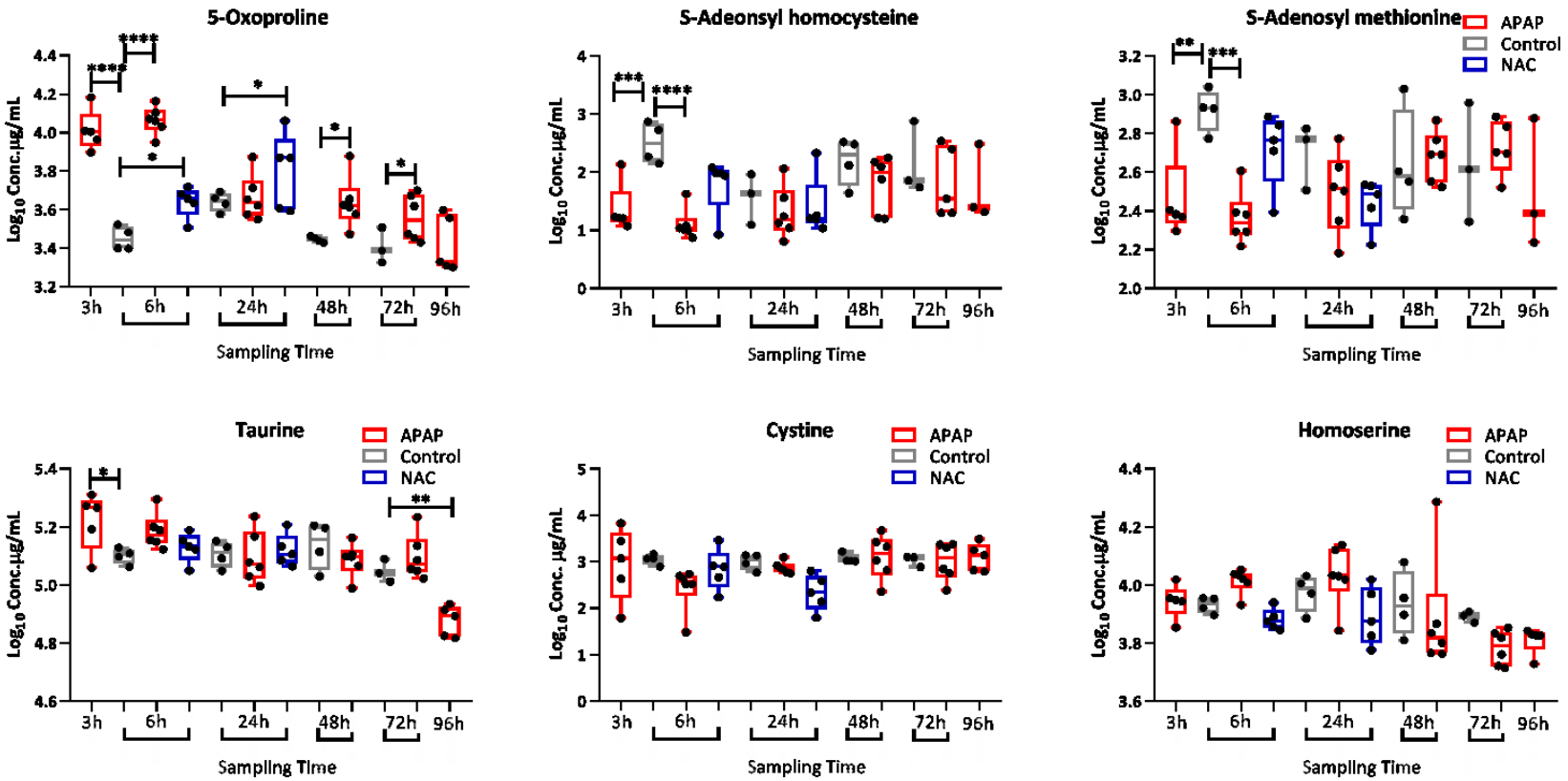


Figure 4.4 GSH-related metabolites measured in serum from mice treated with APAP, Vehicle or APAP+ NAC and sacrificed at time points from 3 to 96 hours post APAP treatment. Analysed by one-way ANOVA followed by FDR correction, adjusted p (q) values, adjusted p values 0.03 (*), 0.002 (**), 0.0002 (***), <0.0001 (****).
Abbreviations: APAP: paracetamol; GSH: reduced glutathione; NAC: n-acetylcysteine.

ALT was weakly negatively correlated with GSSG and glutamine and positively correlated with cysteine, methionine and choline concentrations. The strongest correlations with ALT were a moderate negative correlation with hypotaurine and moderate positive correlation with 5-OP. Total bilirubin was weakly negatively correlated with the amounts of hypotaurine and positively with 5-OP and was moderately negatively correlated with GSSG. Total hepatic GSH concentration was weakly negatively correlated with methionine, cysteine and 5-OP and positively with GSSG. In fact, GSH was most strongly correlated with hypotaurine. Hepatocyte damage scores were significantly but weakly positively correlated with choline and taurine, and negatively with cystine. There were moderate negative correlations with GSSG and hypotaurine and a moderate positive correlation with methionine and cysteine and a strong positive correlation with 5-OP. The putative biomarker OA showed no correlation with any of the standard clinical measures of APAP-induced liver damage.

Table 4.18 Pearson correlation coefficients for metabolites measured in serum with key biomarkers, only metabolites with at least 1 significant correlation and r>0.45 are included in the table.

Analyte	ALT	p-value	TBil	p-value	GSH	p-value	Score for hepatocyte damage	p-value
APAP	0.564	<0.0001	0.454	0.0009	-0.749	<0.0001	0.694	<0.0001
APAP-C	0.729	<0.0001	0.647	<0.0001	-0.638	<0.0001	0.818	<0.0001
APAP-G	0.636	<0.0001	0.599	<0.0001	-0.716	<0.0001	0.737	<0.0001
APAP-NAC	0.771	<0.0001	0.630	<0.0001	-0.647	<0.0001	0.828	<0.0001
APAP-S	0.682	<0.0001	0.623	<0.0001	-0.711	<0.0001	0.747	<0.0001
APAP-SG	0.646	<0.0001	0.566	<0.0001	-0.771	<0.0001	0.783	<0.0001
Choline	0.548	<0.0001	ns	ns	ns	ns	0.430	0.002
Cysteine	0.439	0.002	ns	ns	-0.458	0.002	0.519	0.0001
GSSG	-0.452	0.001	-0.607	<0.0001	0.484	0.001	-0.510	0.0002
Hypotaurine	-0.614	<0.0001	-0.487	0.0004	0.712	<0.0001	0.644	<0.0001
Methionine	0.466	0.001	ns	ns	-0.529	0.0002	0.651	<0.0001
5-OP	0.643	<0.0001	0.349	0.014	-0.502	0.001	0.713	<0.0001

Abbreviations: ALT: alanine aminotransferase; APAP: paracetamol; APAP-C: paracetamol-cysteinyl conjugate; APAP-G: paracetamol glucuronide; APAP-NAC: paracetamol n-acetylcysteine conjugate; APAP-S: paracetamol sulfate; APAP-SG: paracetamol glutathione conjugate; GSSG: oxidised glutathione; 5-OP: 5-oxoproline; GSH: glutathione; TBil: total bilirubin.

4.3.3 Hepatic metabolism

4.3.3.1 APAP method suitability for application to hepatic extracts

The APAP method had not previously been applied to liver extracts and in order to assess the robustness of the assay in application to tissue extracts, a full set of QCs were analysed as part of the analytical run and a summary of the reproducibility and bias from expected values is shown in Table 4.19. All the QCs were within acceptance criteria for the run with the exception of ULOQ 4 which had a 50% reduced value across all analytes; therfore the ULOQ has a CV above 20%. All analytes had curves which were linear and had an r^2 value over 0.99. Two points on the curve were excluded across all analtyes as these did not meet acceptance criteria, it is likely this is due to a sample preparation error as the error was systematic across all analytes.

Table 4.19 Summary of linearity displayed as r2 value of calibration curve and number of acceptable points on curve, the CV of the QCs and mean % bias form the expected concentration.

		APAP	APAP-C	APAP-G	APAP-SG	APAP-NAC	APAP-S
Linearity	**r2**	0.999	0.999	0.994	0.999	0.997	0.995
	% Pass	78	78	83	78	78	78
LLOQ	**CV**	4.08	4.22	8.18	1.41	6.10	19.7
	Bias %	-5.76	-9.54	-13.6	-6.28	-14.6	17.6
LQC	**CV**	2.28	7.21	4.22	2.89	6.54	12.0
	Bias %	-2.55	-2.58	-9.93	-4.5	-1.65	-0.875
MQC	**CV**	1.66	2.77	1.95	1.46	2.20	5.43
	Bias %	-0.55	0.275	-4.73	-1.75	-0.075	-1.8
HQC	**CV**	0.58	2.06	3.52	1.33	2.17	5.24
	Bias %	0.24	2.46	-3.5	0.6	-0.14	-3.7
ULOQ	**CV**	24.5	26.1	26.5	24.6	26.1	27.3
	Bias %	-7.82	-5.5	-8.12	-9.18	-6.72	-7.64

Abbreviations: APAP: paracetamol; APAP-C: paracetamol-cysteinyl conjugate; APAP-G: paracetamol glucuronide; APAP-NAC: paracetamol n-acetylcysteine conjugate; APAP-S: paracetamol sulfate; APAP-SG: paracetamol glutathione conjugate; CV: coefficient of variance; HQC: high quality control; LLOQ: lower limit of quantification; LQC: low quality control; MQC: mid quality control; ULOQ: upper limit of quantification.

As indicated pooled QCs were prepared and over-spiked with the HQC of each analyte and these were analysed throughout the run. The mean concentration and CV for each analyte are displayed in Table 4.20. Concentrations remained consistent and CVs were low. The mean difference in concentration between the pooled and over-spiked QCs were compared to the HQC nominal concentration and the percentage bias from this is displayed in Table 4.20. The bias was very low and therfore it appears matrix effects did not affect the analysis of tissue samples.

Table 4.20 Mean concentration of pooled QCs and pooled QCs over-spiked with the HQC.

Analyte	Pooled QC n=3		Over-spiked QC n=3		% Bias
	Mean Conc. ng/mL	CV	Mean Conc. ng/mL	CV	
APAP	9.10	1.10	91.0	1.57	-2.33
APAP-S	4.83	5.97	86.4	9.21	-2.00
APAP-C	8.50	3.11	93.0	2.37	-5.67
APAP-G	28.5	7.42	438	1.79	-2.45
APAP-GSH	25.9	2.41	436	1.95	-2.48
APAP-NAC	13.3	0.44	430	2.80	-4.08

Abbreviations: APAP: paracetamol; APAP-C: paracetamol-cysteinyl conjugate; APAP-G: paracetamol glucuronide; APAP-NAC: paracetamol n-acetylcysteine conjugate; APAP-S: paracetamol sulfate; APAP-SG: paracetamol glutathione conjugate; CV: coefficient of variance; QC: quality control.

4.3.3.2 APAP metabolism changes in hepatic extracts

APAP metabolites measured in hepatic extracts are shown in Figure 4.5. There were no significant differences in the APAP metabolites measured in APAP or APAP+NAC treated mice. There were no detectable APAP metabolites after 24 hours from APAP treatment.

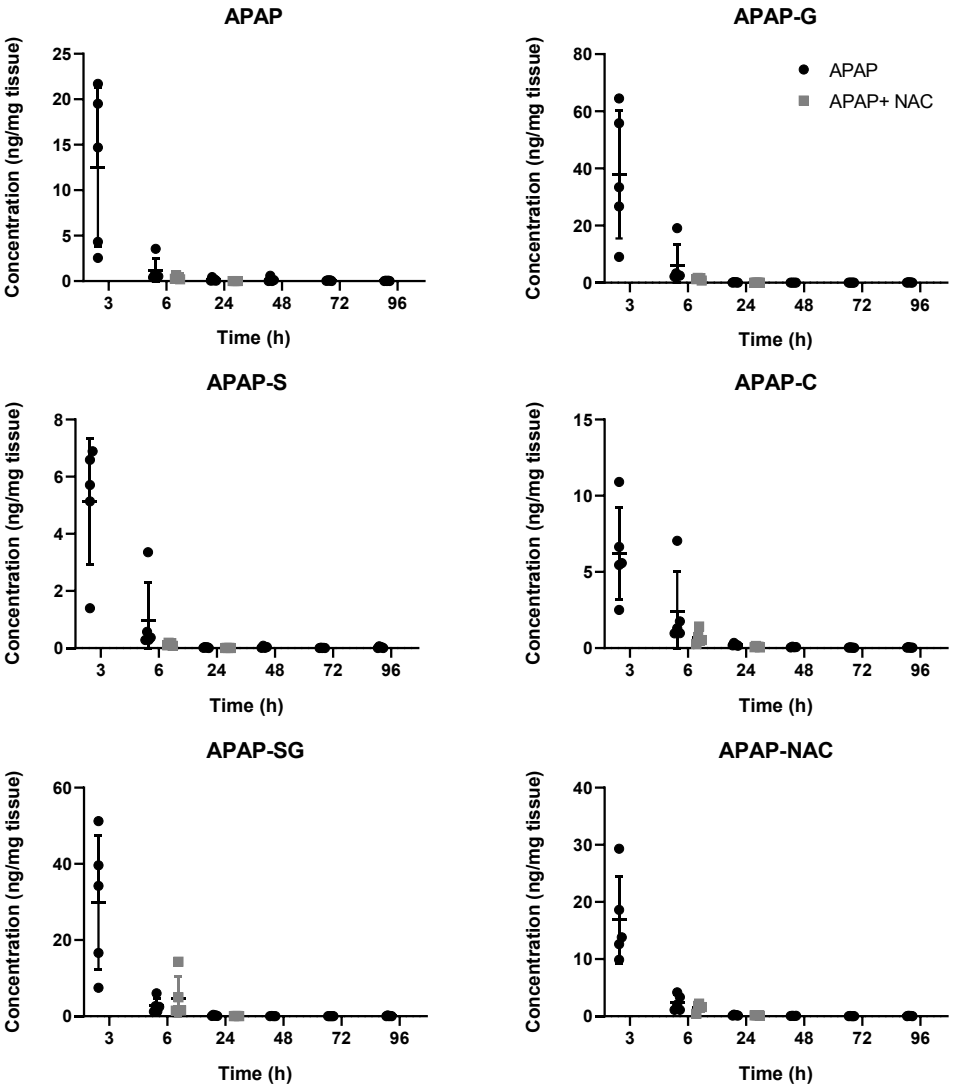


Figure 4.5. Concentrations of APAP and metabolites measured in dried hepatic extracts from mice treated with APAP at 300mg/kg ip or with APAP followed by NAC.

4.3.3.3 GSH method suitability for application to hepatic extracts

As displayed in Table 4.21, the assay was more effective at measuring some metabolites than others, and analytes highlighted in red either could not be quantified due to analytical issues, or there was no measurable metabolite in the tissue extract samples in the run. Analytes for which curves or QCs failed to meet acceptance criteria at either the low or high end of the standard curve but were linear and QCs passed within the truncated range, are highlighted in orange. Also highlighted in orange are any analytes that could be detected in tissue extract samples, but some samples were below the range of quantification, or truncated range determined by curves and QCS.

In addition, pooled QCs and over-spiked pooled QCs were analysed as part of the liver extract analytical run. The pooled QCs and the over-spiked QCs were injected at 6 equally spaced times through the analytical run. The over-spiked QCs had standards at nominal concentrations added depending on the range of the calibration curve each was analysed against. The mean concentrations of both the pooled QCs and over-spiked pooled QCs are shown in Table 4.22 along with CVs for both, which should ideally be below 20%. All the pooled QCs were reproducible except for glycine, and the over-spiked QCs were reproducible with the exception of glycine and cysteic acid. The differences between the concentration of the over-spiked QCs and pooled QCs were compared to the concentration of the standard spiked into the samples (*i.e*. "expected difference"). The mean bias from the expected concentration is also displayed in Table 4.22 and results less than -20% or greater than 20% suggest a matrix effect with ion suppression or enhancement causing the difference in concentration to be greater or less than expected.

There appeared to be ion enhancement with glycine and cys-gly, and these were also the analytes which had least reproducible QCs, while OA had a smaller ion enhancement effect. Cysteine and betaine suffered an ion suppression effect, while GSH concentration was over 100% lower than expected, however this was due to saturation of the detector and GSH could not be measured at concentrations over 2000 ng/mL.

Analyte	Linearity R^2	% Meeting Acceptance Criteria (20% or 30% at LLOQ)							Range of Analyte in Tissue extracts	Acceptable Range of curve	RT range
		Calibration curve	LLOQ	LQC	MQC	HQC	ULOQ	Total QCs			
2-AB	na	na	na	na	na	na	na	na	na	na	na
betaine	0.991	81	83	89	78	100	0	74	102-1111	10-500	1.34-1.39
choline	0.996	81	100	89	78	67	100	85	100-274	10-250	0.66-0.7
cys-gly	0.987	88	0	56	89	89	17	56	bld	50-2000	1.2-1.32
cystathionine	0.995	63	100	89	78	78	100	87	4.5-41.5	10-250	6.47-6.51
cysteic acid	0.99	81	17	100	78	67	0	56	bld	25-1000	5.17-6.19
cysteine	0.998	100	100	89	78	44	67	69	6.2-840	20-2000	1.94-2.01
cystine	0.999	94	100	67	56	44	67	64	0-24.8	20-2000	6.45-6.65
glutamate	0.992	69	50	100	78	89	100	85	221-1493	20-2000	2.32-2.4
glutamine	0.999	75	100	89	67	67	0	67	248-1936	200-5000	2.95-3.07
glycine	0.972	42	0	78	100	0	0	46	644-10435	500-20000	2.78-2.99
y-glu-cys	0.995	94	83	100	100	100	100	97	0.2-30.4	10 -1000	2.24-2.3
GSH	0.999	63	83	100	100	0	0	59	49.6-2108	200-2000	2.9-3.08
GSSG	0.997	75	83	89	56	33	33	59	0.3-9521	200-20000	6.66-7.04
homocysteine	0.997	94	100	100	100	78	83	92	bld	10-1000	1.35-1.51
homocystine	0.992	94	100	100	89	67	100	97	0.6-2	10-1000	5.89-6.2
homoserine	0.977	88	83	100	100	78	0	77	42.2-111	20-1000	2.26-2.35
hypotaurine	0.998	100	83	100	100	67	83	87	26.5-112	20-2000	3.58-3.6
methionine	0.996	63	100	89	78	78	100	87	37.9-114	20-500	1.21-1.3
OA	0.998	94	83	100	78	78	100	87	12.8-710	10-1000	2.74-2.81
5-OP	0.998	88	0	100	78	67	83	69	23.1-173	50-2000	0.83-0.84
SAH	0.998	94	83	100	78	78	100	87	0-58.7	10-1000	5-5.33
SAMe	0.998	100	100	89	67	44	67	69	17.9-241	10-1000	6.16-6.24
serine	0.988	100	100	89	89	67	100	87	149-383	200-20000	3.06-3.29
taurine	0.995	100	100	89	78	67	100	85	1368-7125	200-20000	2.61-2.63

Table 4.21 Effectiveness of the assay when applied to mouse hepatic extracts, including linearity (r2), the percentage of calibration curve points and QCs meeting acceptance criteria, the actual range over which analyte were present in the tissue extracts and the accurate range of the method, and the range of retention times in the run. Red highlighting indicates analytes did not meet acceptance criteria and/or all concentrations were outside analytical range, orange indicates a truncated range was used, and/or some results were outside the acceptable analytical range. Abbreviations: 2-AB: 2-amino butyrate; bld: below limit of detection; cys-gly: cysteinyl-glycine; y-glu-cys: gamma glutamyl cysteine; GSH: glutathione; GSSG: oxidised glutathione; HQC: high quality control; LLOQ: lower limit of quantification; LQC: low quality control; MQC: mid quality control; na: not applicable; OA: ophthalmic acid; 5-OP: 5-oxoproline; QC: quality control; RT: retention time; SAH: s-adenosyl homocysteine; SAMe: s-adenosyl methionine; ULOQ: upper limit of quantification.

Table 4.22 Mean areas of pooled QCs and over-spiked QCs with CVs, and the mean difference between the pooled and over-spiked QC and the percentage difference from the concentration of standard added in application of glutathione pathway assay to mouse tissue.

	Analyte	Mean Pooled QC (ng/mL)	CV	Mean Over-spiked (ng/mL)	CV	Mean measured difference in conc. ng/mL	Expected difference conc. ng/mL	Mean bias from expected (%)
"High Curve"	glutamine	1497	2.84	4970	4.97	4051	4000	1.28
	glycine	3509	29.4	8362	32.5	5662		41.5
	GSH	1957	3.74	1796	5.13	-188		-105
	serine	749	3.59	3888	11.7	3662		-8.46
	taurine	4797	3.38	8380	2.18	4180		4.51
"Mid Curve"	cysteine	98.0	1.22	597	5.21	166	400	-58.5
	cys-gly	23.7	0.00	166	2.94	583		45.7
	cystine	65.8	0.98	456	19.1	455		13.8
	glutamate	844	8.01	1175	4.93	386		-3.55
	homoserine	124	8.89	457	8.64	389		-2.80
	hypotaurine	113	5.68	422	7.39	361		-9.81
	methionine	118	7.60	445	5.22	382		-4.55
	5-OP	147	4.91	489	2.02	399		-0.37
"Low Curve"	betaine	502	14.8	583	5.16	95	200	-52.6
	choline	198	3.00	369	2.13	199		-0.53
	cystathionine	38.9	3.78	192	8.98	179		-10.5
	cysteic acid	30.0	0.00	210	22.4	210		5.01
	homocysteine	33.4	0.367	218	6.24	216		7.83
	homocystine	26.9	0.31	184	2.91	183		-8.33
	OA	153	3.55	371	5.73	255		27.5
	SAMe	129	2.09	300	2.11	200		-0.25
	y-glu-cys	38.8	1.95	202	5.83	190		-4.78

Abbreviations: 2-AB: 2-amino butyrate; bld: below limit of detection; cys-gly: cysteinyl-glycine; y-glu-cys: gamma glutamyl cysteine; GSH: glutathione; OA: ophthalmic acid; 5-OP: 5-oxoproline; QC: quality control; RT: retention time; SAH: s-adenosyl homocysteine; SAMe: s-adenosyl methionine.

The pooled and over-spiked QCs were plotted on different graphs based on whether they were measured against the “low”, “mid” or “high” range calibration curve. Pooled QCs are shown in Figure 4.6A to Figure 4.8A, over-spiked QCs are displayed in Figure 4.6B to Figure 4.8B. Taking into account the curve and QCs, linearity, range of metabolites, potential matrix effects, peak shapes and retention times, and a lack of consistency in pooled QC concentrations, the following analytes were not included in further statistical analysis: 2-AB, cys-gly, cysteic acid, glycine, GSSG, and homocysteine.

For analytes where there were some issues, data were reviewed on a case by case basis. For samples where GSH was saturated, the ULOQ was imputed as the concentration. For any samples where an analyte fell below the LLOQ but were within 30% of the LLOQ, this was imputed. If the value was lower than this, it was imputed as 0.

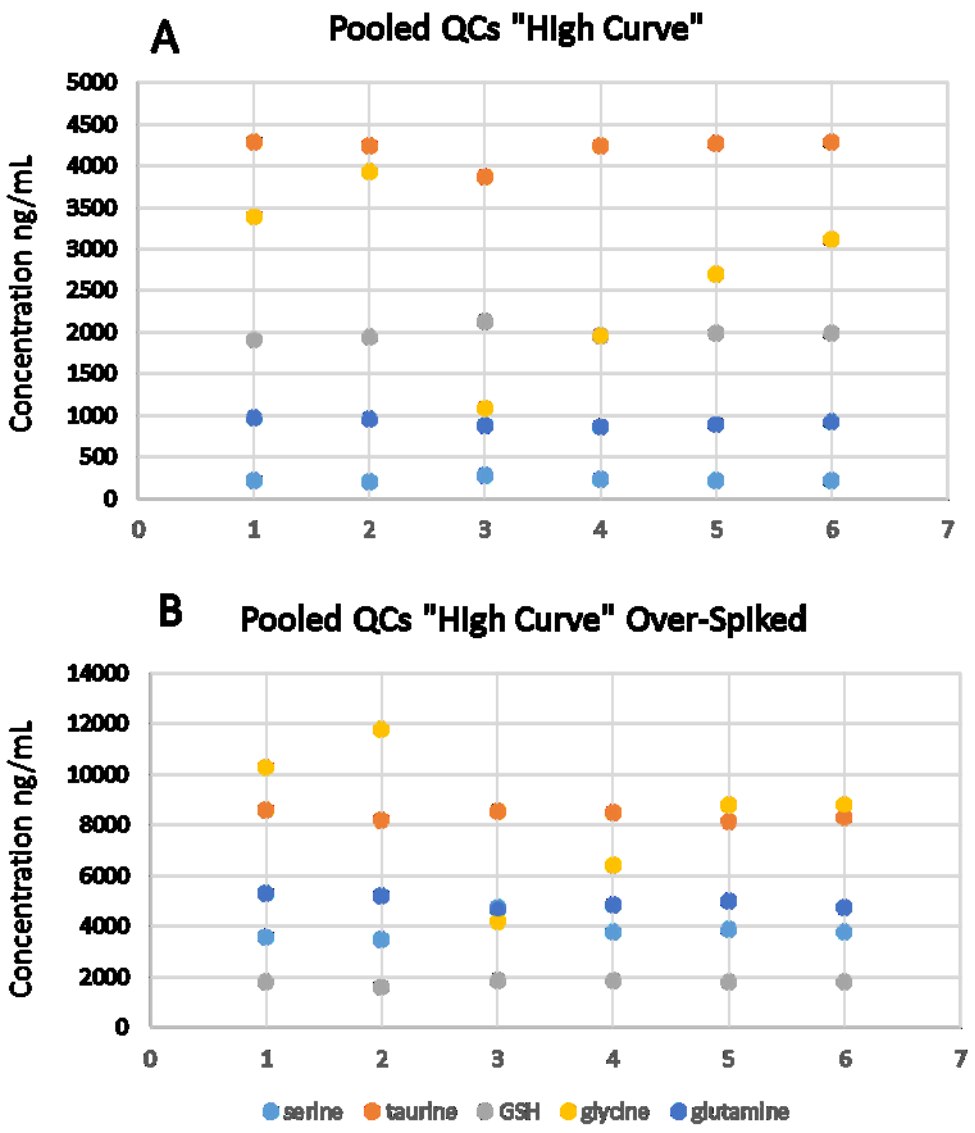


Figure 4.6. Concentrations of A) Pooled QCs and B) Over-spiked QCs for analytes measured against the "High" curve, which were analysed at regular intervals throughout the run (n=6) Abbreviations: GSH: glutathione; QC: quality control.

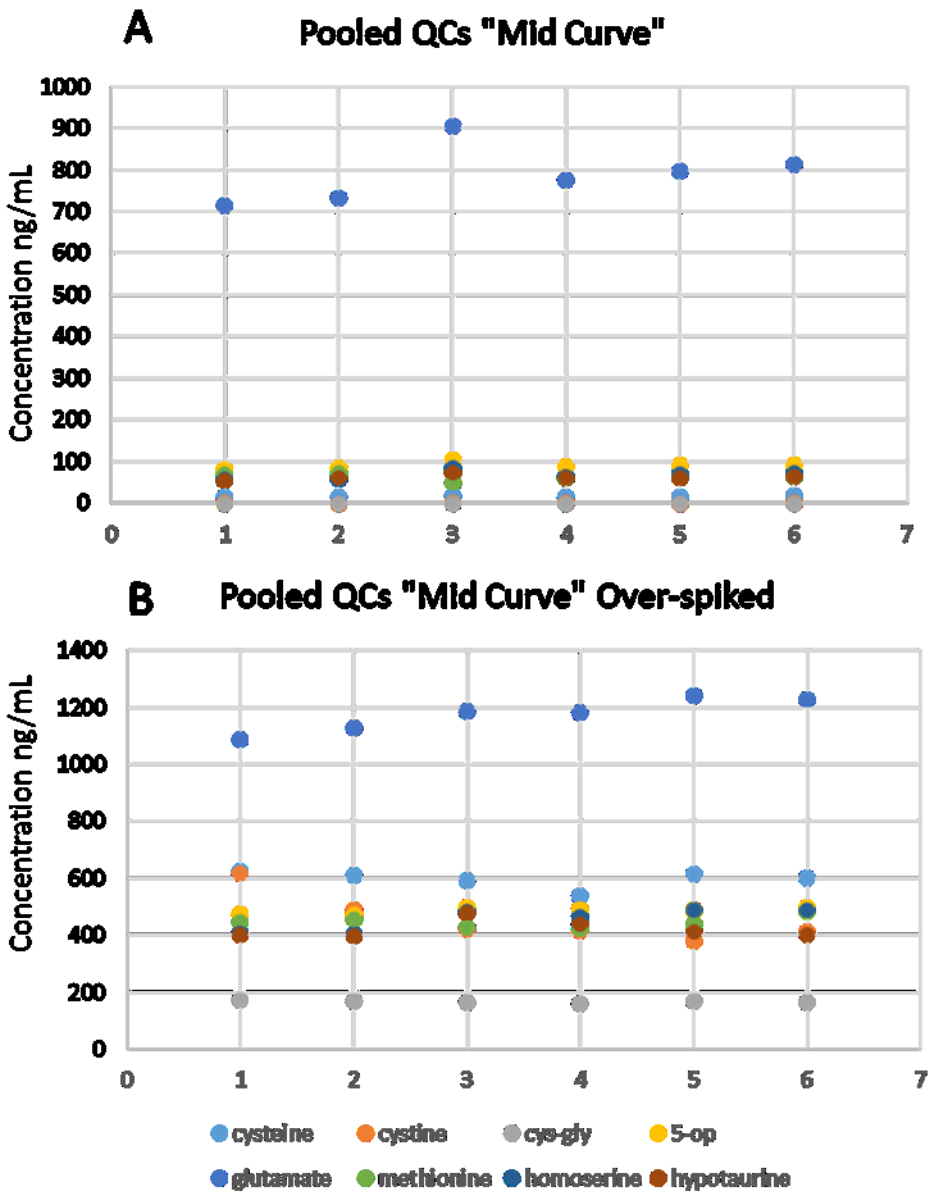


Figure 4.7. Concentrations of A) Pooled QCs and B) Over-spiked QCs for analytes measured against the "Mid" curve, which were analysed at regular intervals throughout the run (n=6)
Abbreviations: cys-gly: cysteinyl-glycine; 5-OP: 5-oxoproline; QC: quality control

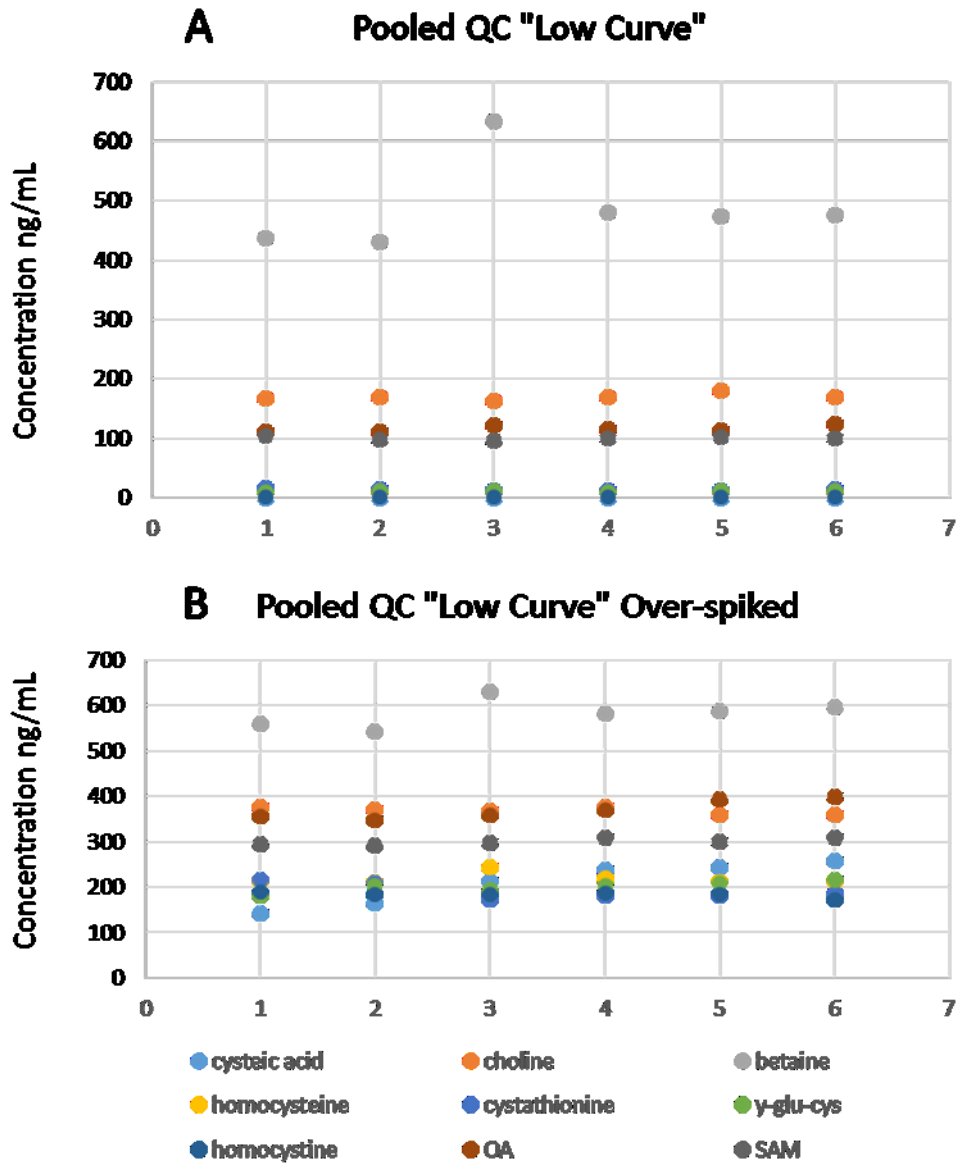
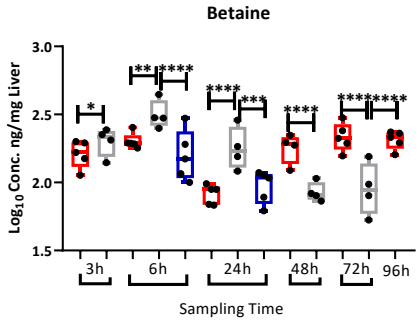
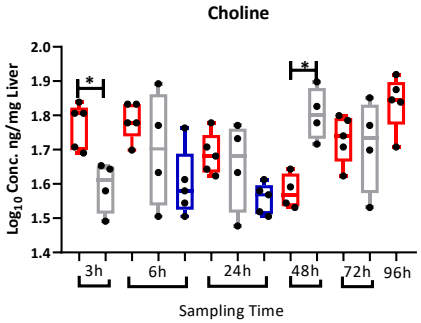


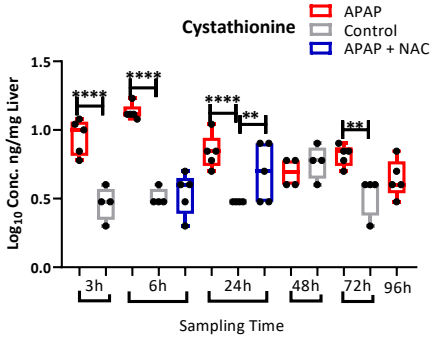
Figure 4.8. Concentrations of A) Pooled QCs and B) Over-spiked QCs for analytes measured against the "low" curve, which were analysed at regular intervals throughout the run (n=6) Abbreviations: y-glu-cys: gamma glutamyl cysteine; QC: quality control; SAM: s-adenosyl methionine.

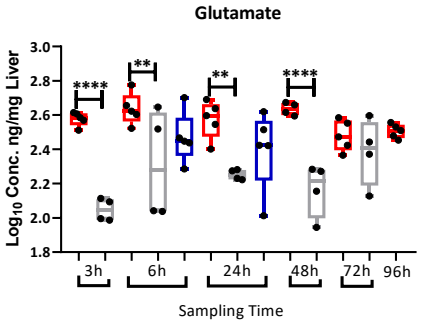
4.3.3.4 Hepatic changes to GSH metabolism

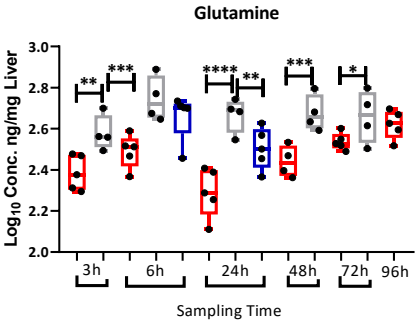
As shown in Figure 4.9 below, metabolites were individually analysed using univariate statistical methods. There were a number of significant changes in metabolite concentrations in hepatic aqueous extracts particularly at the 3- and 6-hour time points. In the hepatic extracts from mice treated with APAP-only, hypotaurine, glutamine, GSH, SAMe and γ-glu-cys concentrations were significantly decreased compared to controls and APAP + NAC mice. 5-OP, cystathionine, methionine, OA and glutamate concentrations were elevated in hepatic extracts from APAP-dosed mice compared to the controls and APAP + NAC treated animals. Betaine concentrations were decreased in the livers of both APAP and APAP + NAC treated groups compared to control mice at 6 and 24 hours, concentrations in the APAP treated mice were then increased compared to controls at later time points. Choline concentrations were significantly increased compared to controls at 3 hours but decreased at 48 hours. Methionine concentrations appear to return to control concentrations by 24 hours but become elevated again in APAP treated animals at 72 and 96 hours post dose. OA concentrations were decreased at late time points having been previously elevated. Serine concentrations were only elevated in APAP treated animals at 96 hours post dose. 5-OP, hypotaurine and GSH were only altered in concentrations at early time points, whereas other metabolites concentrations remained altered until the end of the experiment. There were no changes detected to the amounts of cysteine or taurine for APAP-dosed mice compared to the controls at any time point.

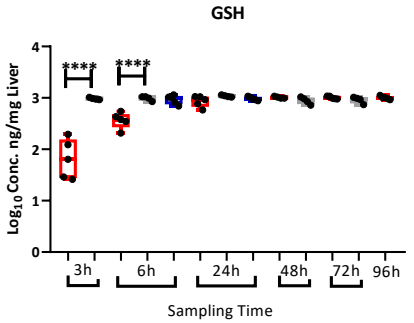

Betaine
Log10 Conc. ng/mg Liver
Sampling Time
3h
6h
24h
48h
72h
96h

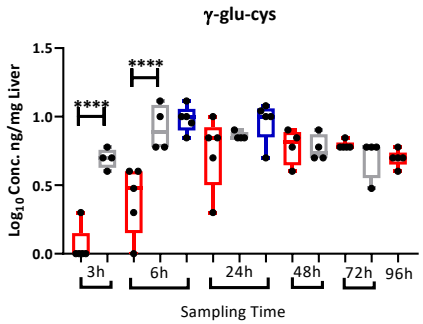

Choline
Log10 Conc. ng/mg Liver
Sampling Time
3h
6h
24h
48h
72h
96h

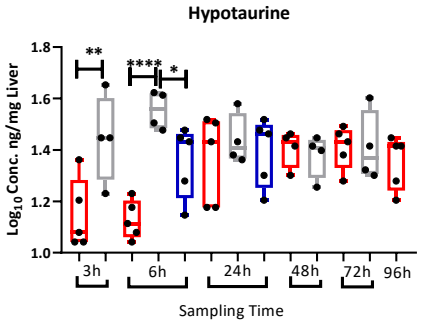

Cystathionine
APAP
Control
APAP + NAC
Log10 Conc. ng/mg Liver
Sampling Time
3h
6h
24h
48h
72h
96h

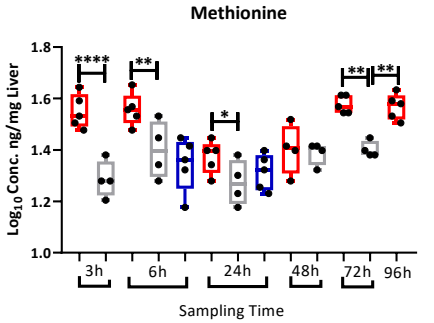

Glutamate
Log10 Conc. ng/mg Liver
Sampling Time
3h
6h
24h
48h
72h
96h


Glutamine
Log10 Conc. ng/mg Liver
Sampling Time
3h
6h
24h
48h
72h
96h


GSH
Log10 Conc. ng/mg Liver
Sampling Time
3h
6h
24h
48h
72h
96h


γ-glu-cys
Log10 Conc. ng/mg Liver
Sampling Time
3h
6h
24h
48h
72h
96h


Hypotaurine
Log10 Conc. ng/mg Liver
Sampling Time
3h
6h
24h
48h
72h
96h


Methionine
Log10 Conc. ng/mg Liver
Sampling Time
3h
6h
24h
48h
72h
96h

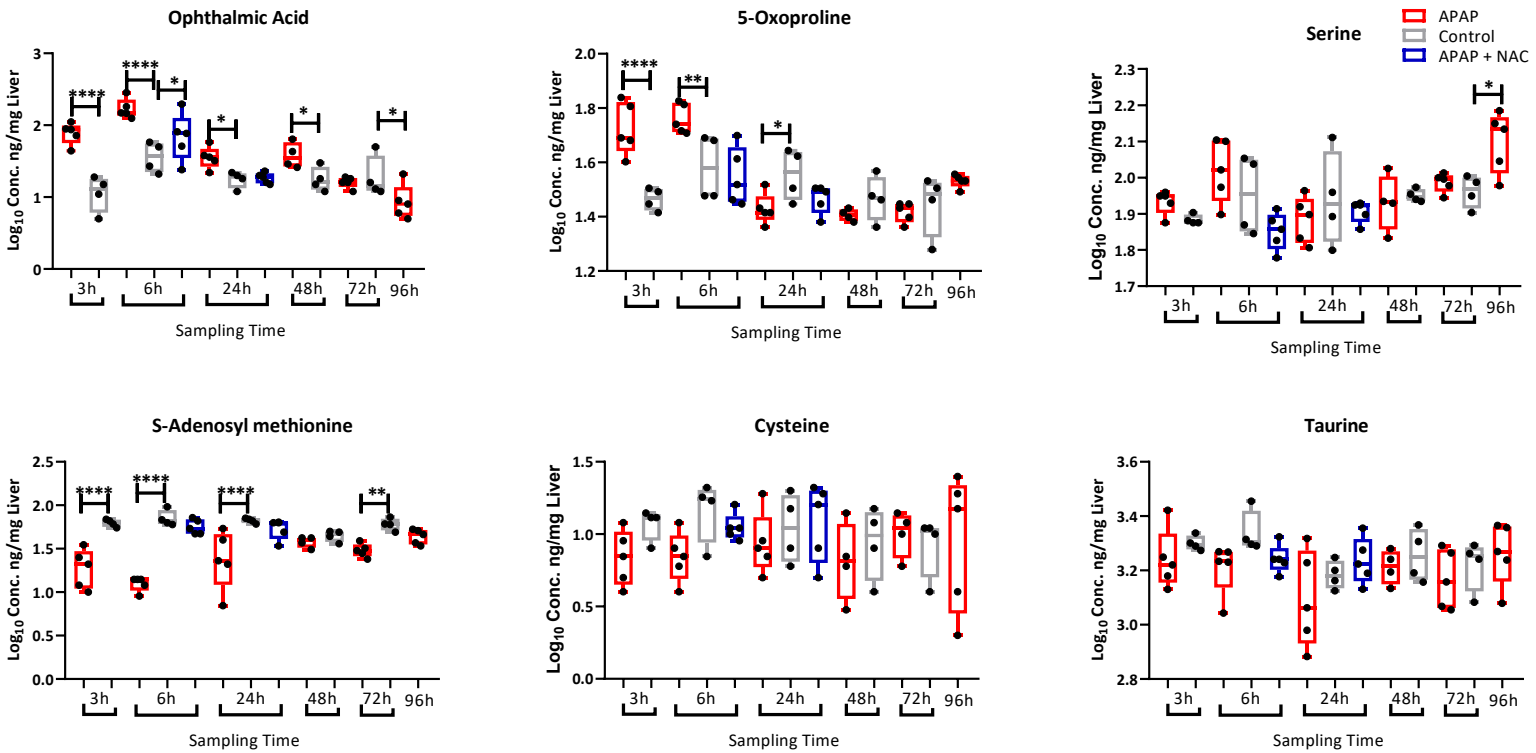


Figure 4.9. Metabolites measured in liver extracts from mice treated with APAP, Vehicle or APAP + NAC and sacrificed at time points from 3 to 96 hours post treatment. Time-points with 2 groups analysed by one-way ANOVA followed by FDR correction, adjusted p values 0.03 (*), 0.002 (**), 0.0002 (***), <0.0001 (****).
Abbreviations: APAP: paracetamol; γ-glu-cys: gamma-glutamyl cysteine; GSH: reduced glutathione; NAC: n-acetylcysteine.

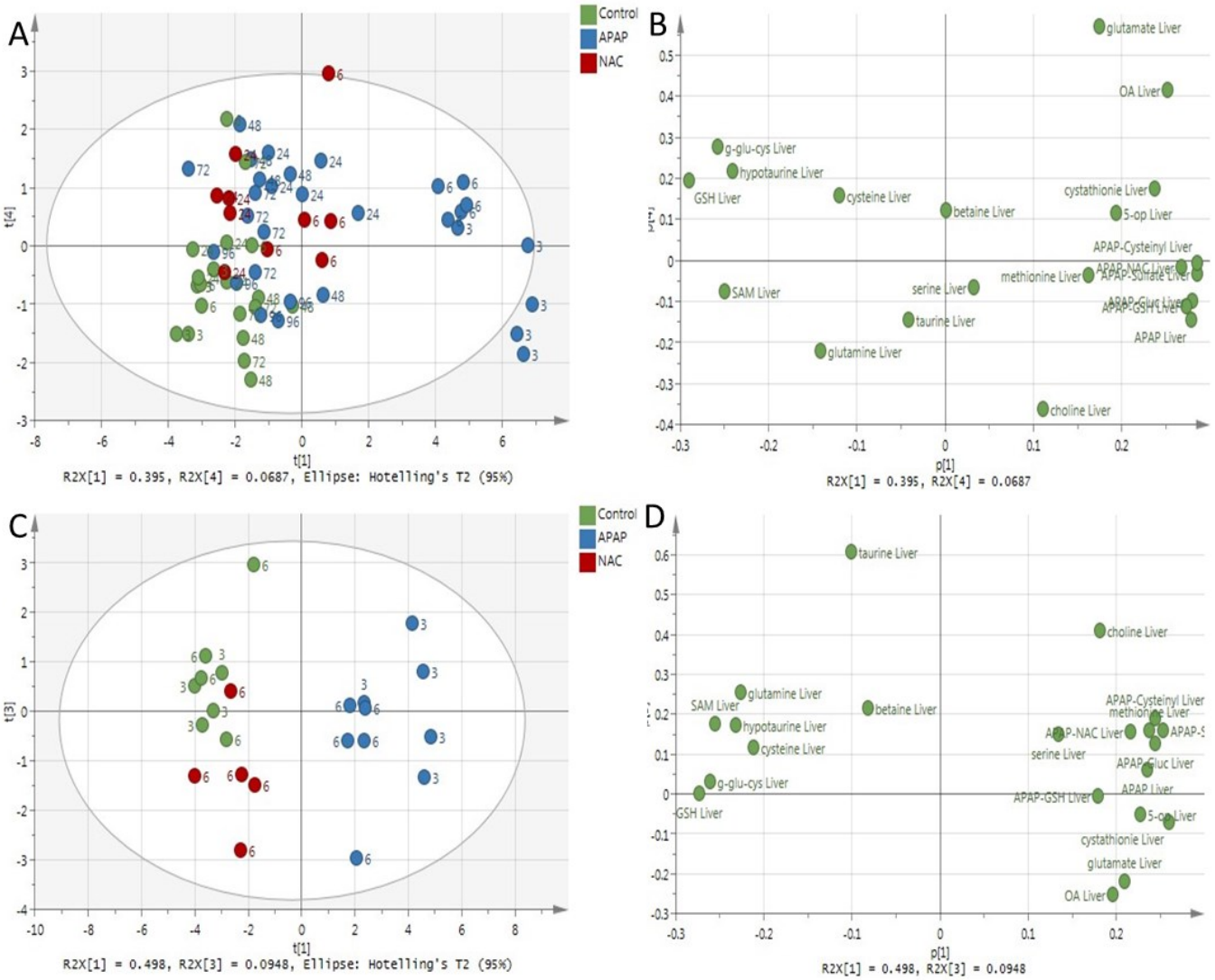


Figure 4.10. Each point on the plots A & C represents a mouse and is coloured according to treatment and labelled with the time point of sampling, each point on plots B & D represents a metabolite. A) PCA scores plot and B) Loadings plot for all metabolites measured in liver extracts. C) PCA scores plot and B) Loadings plot for all metabolites measured in hepatic extracts at 3 and 6 hours only.
Abbreviations: APAP: paracetamol; cys-gly: cysteinyl-glycine; y-glu-cys: gamma glutamyl cysteine; GSH: glutathione; GSSG: oxidised glutathione; NAC: n-acetylcysteine; OA: ophthalmic acid; 5-OP: 5-oxoproline PCA: principal components analysis; SAH: s-adenosyl homocysteine; SAM: s-adenosyl methionine.

4.3.3.5 Hepatic results summary

Principal components analysis (PCA) was performed on hepatic data following log transformation ($\log_{10}(X+1)$) and UV scaling. Animals sacrificed at 3 and 6 hours post APAP treatment were most different to controls and were tightly clustered by time point, while controls, APAP + NAC and 24 hour plus APAP animals were clustered together, as shown in Figures 4.10 A and B. APAP samples from 3 and 6 hours were analysed with controls and 6h NAC samples, there was a very clear separation between APAP and NAC/Control samples in the first component. Metabolites which were driving separation in the 1st components included drug metabolites, 5-

OP, cystathionine, methionine, OA and glutamate increases in the APAP group, and decreases in cysteine, glutamine, GSH, γ-glu-cys, hypotaurine and SAMe, as shown in Figures 4.10 C and D.

4.4 Discussion

The key aims of this work were to investigate the changes to GSH biosynthesis-related metabolites, including those in the methionine and gamma-glutamyl cycles and trans-sulfuration pathways, in mice treated with APAP 300mg/kg, compared to controls and to those treated subsequently with NAC. Using biomarkers and hepatic GSH concentration as measured by traditional methods as comparators, correlations between these GSH metabolites and APAP metabolites measured in serum were measured, in order to determine if there were any relationships between circulating metabolites and liver injury and assess the suitability of circulating endogenous and xenobiotic metabolites as biomarkers for both GSH depletion and liver damage.

4.4.1 Key findings

The APAP metabolism assay can be effectively applied to samples containing APAP and its major metabolites at low concentration by reducing the sample dilution factor, there were minimal matrix effects and curves and QCs were acceptable. The APAP assay can also be applied effectively to tissue extracts, although a full validation has yet to be carried out and it is more difficult to gain fully quantitative results from liver extracts. The GSH pathway assay was applied successfully to hepatic extracts, with fewer matrix effects than are found when the method is applied to serum as discussed in Chapter 3.Results of the GSH assay study showed that 5-OP concentrations were significantly increased compared to control and APAP+ NAC treated animals in hepatic extracts and serum following APAP treatment. Circulating 5-OP was strongly positively correlated with markers of liver injury, providing evidence that circulating 5-OP is a biomarker for APAP-induced liver injury. The alternative biomarker OA was increased in hepatic extracts but its early concentrations in serum did not correlate with liver injury markers. Hypotaurine was significantly decreased in serum and hepatic extracts with APAP treatment compared to control and APAP+NAC animals, and was correlated with liver damage and GSH depletion. APAP-C and APAP-NAC were the APAP metabolites most strongly correlated with liver injury markers.

4.4.2 Summary of results

There were a number of changes to GSH related metabolism in mice treated with APAP at 3 and 6 hours post dosing, in both serum and aqueous liver extracts. Most notably, there were increased methionine and 5-OP concentrations, and decreased concentrations of hypotaurine in both serum and hepatic extracts. In the hepatic extracts, there were also changes in some key GSH biosynthetic precursors, including glutamate, cysteine and γ-glu-cys. For the majority of GSH metabolites the elevated or decreased concentrations were significantly different to animals also treated with NAC, and using PCA analysis to visualise the separation, it was clear that APAP + NAC mice were statistically similar to controls, as were APAP-alone treated animals from 24 hours onwards as metabolic homeostasis was restored. Table 4.23 summarises the metabolic changes in GSH metabolites over the time course of the experiment.

APAP appeared to be cleared slightly more rapidly from the APAP+NAC treated mice, as concentrations of some circulating APAP metabolites were lower in APAP+NAC treated animals. APAP-C and APAP-NAC correlated most strongly with ALT and hepatocyte damage, but APAP and APAP-G correlated most strongly with hepatic GSH depletion.

Table 4.23 Summary of changes in both hepatic extracts and serum in APAP and APAP + NAC treated mice compared to controls.

Analyte	Matrix	3h APAP	6h APAP	6h NAC	24h APAP	24h NAC	48h APAP	72h APAP	96h APAP
Betaine	*Serum*								
	Liver								
Choline	*Serum*								
	Liver								
Cystathionine	*Serum*								
	Liver								
Cysteine	*Serum*								
	Liver								
γ-Glu-cys	*Serum*								
	Liver								
Glutamate	*Serum*								
	Liver								
Glutamine	*Serum*								
	Liver								
GSH	*Serum*								
	Liver								
GSSG	*Serum*								
	Liver								
Hypotaurine	*Serum*								
	Liver								
Methionine	*Serum*								
	Liver								
OA	*Serum*								
	Liver								
5-OP	*Serum*								
	Liver								
SAH	*Serum*								
SAMe	*Serum*								
	Liver								
Serine	*Serum*								
	Liver								
Taurine	*Serum*								
	Liver								

RED=significantly increased, BLUE=significantly decrease, depth of colour shows q-value significance, 0.03-0.0001.

Abbreviations: APAP: paracetamol; y-glu-cys: gamma glutamyl cysteine; GSH: glutathione; GSSG: oxidised glutathione; NAC: n-acetylcysteine; OA: ophthalmic acid; 5-OP: 5-oxoproline PCA: principal components analysis; SAH: s-adenosyl homocysteine; SAMe: s-adenosyl methionine.

4.4.3 GSH assay discussion

The GSH-assay results show that methionine is increased in both hepatic extracts and serum at 3-6 hours post APAP treatment, it is not increased in NAC treated samples, or at 24 or 48 hours post dose but increases again at 72 hours post treatment. This could suggest that in the cases where NAC treatment was not given, the cell was increasing methionine synthesis to maintain methionine concentrations and was limiting processes such as protein synthesis and methylation, in order to synthesise depleted cysteine for the cell (McLean et al. 1989). Methionine elevations have been reported in other mouse models of GSH depletion (Soga et al. 2006), and during liver regeneration (Jung et al. 2013). The decreased concentrations of hepatic SAMe and circulating SAMe and SAH may also suggest that methionine was not being converted to SAMe via MAT enzymes, as this phenomenon was also seen in a previous study in the same mouse strain, and MAT I, II and III gene expression was significantly decreased in APAP treated animals, and the MAT activity was only higher at 2 hours and not 4 hours post treatment (Brown et al. 2010). This study similarly found that NAC treatment after APAP prevented the SAMe decreases (Brown et al. 2010). Therefore, it seems possible that APAP treatment leads to decreased MAT activity and therefore decreased SAMe concentrations which may have an impact on DNA methylation (Purohit et al. 2007). Following this, cellular metabolism may switch to using all the available cysteine for the biosynthesis of GSH, hence reducing concentrations of downstream sulfur-containing metabolites, which causes decreases to both circulating and hepatic hypotaurine concentrations (Eriksson et al. 2015; Kyriakides 2016). There was a slight increase in serum taurine at 3 hours post dose but there were no hepatic changes, and there was a more significant taurine serum depletion at 96 hours post treatment. Alterations to taurine concentrations and to bile acid conjugations have been seen previously in the rat (Yamazaki et al. 2013). The cell appears to also upregulate the enzymes involved in GSH biosynthesis, GCL and GS, which appears to cause an accumulation of 5-OP and glutamate, and an increase in OA, while there is depleted hepatic GSH and γ-glutamyl-cysteine. The OA increase is likely due to 2-amino butyrate replacing cysteine as a substrate resulting for GCL, in OA biosynthesis (Griffith and Meister 1979; Meister 1991). Changes to betaine and choline were similar between APAP and APAP + NAC treatment mice, which may be due to their role in methionine synthesis. The decreased betaine concentrations could be due to attempts by the cell

to synthesise methionine and could depend on BHMT expression and activity. In order to fully understand the metabolism results of this study, gene expression, protein expression and enzyme activity would ideally be measured to understand how the changes in metabolite concentration relate to metabolic changes. The key changes to GSH metabolism APAP treated mice at early time points are summarised in Figure 4.11.

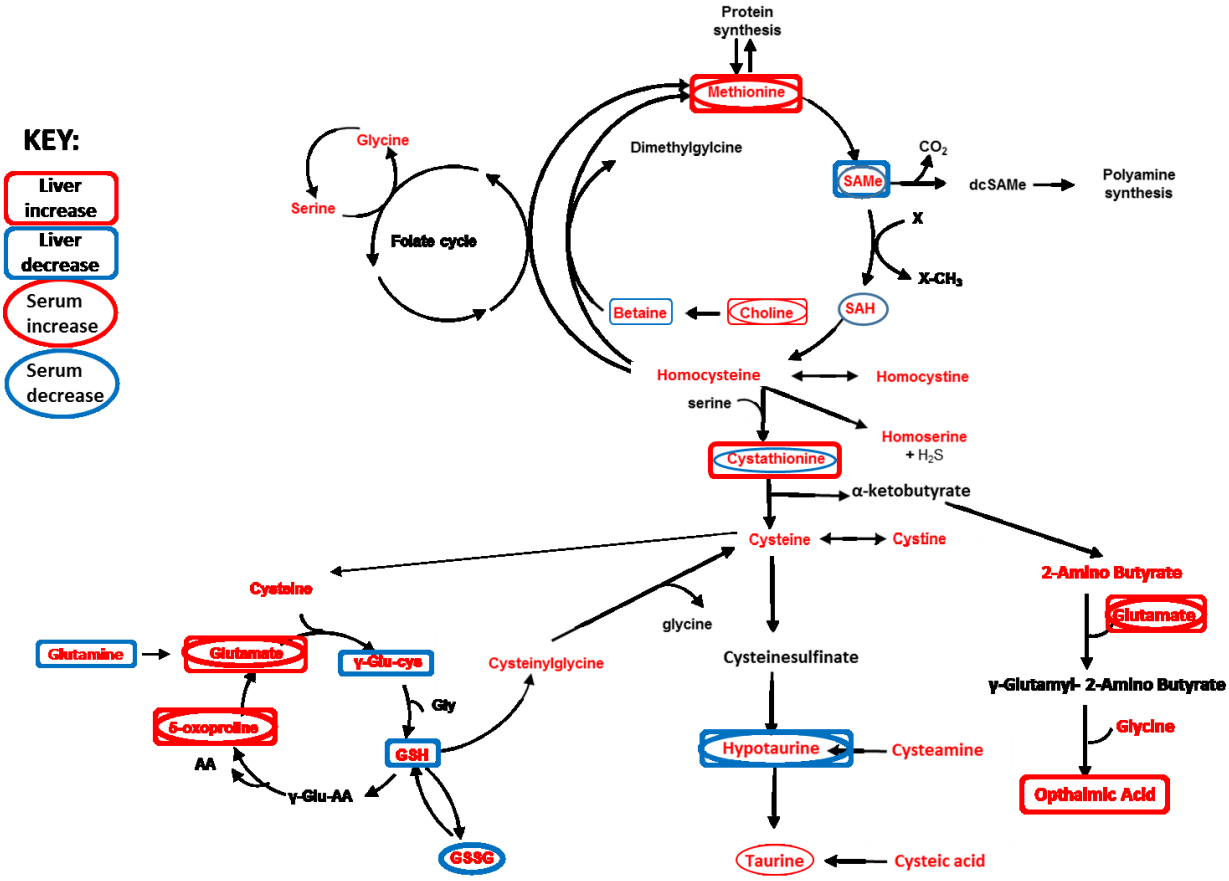


Figure 4.11. Overview of the GSH metabolism pathway and the metabolism changes seen following APAP treatment at early time points (3-6h.)
APAP compared to control RED=significantly increased, BLUE=significantly decreased. Oval shapes represent results from serum and Oblong represent results from liver extracts. Thickness of shape outline represents strength of q value, i.e. thickest shape outline=q<0.0001.

4.4.4 APAP metabolism discussion

Based on the UHPLC -MS-based assay there were differences in some APAP metabolites in APAP and APAP + NAC treated mice, which suggests that NAC may have an impact on how APAP is metabolised due to increasing cellular sulfur which may prevent saturation of sulfation and hence providing a source of GSH to detoxify NAPQI. However, there were no significant differences in APAP-CYP-derived metabolites measured in either

the serum or liver between APAP and APAP + NAC treated groups at 6 hours post treatment. In contrast there were significantly decreased concentrations of serum APAP-SG at 24 hours post treatment in APAP + NAC samples, and the concentrations of all metabolites were lower in these samples. The decrease in hepatic concentrations of APAP-S at 24 hours post dose in the APAP+NAC group was also significant, and APAP-G concentrations were also decreased in NAC-treated mice at both at 6 and 24 hours. APAP and its metabolites were difficult to quantify in the mouse from 24 hours post dose onwards, as APAP is rapidly metabolised in the mouse. It appeared in general that APAP was cleared more quickly in the NAC treated animals, as these mice had lower metabolite concentrations by 24 hours post dose, and the much lower concentration of APAP-G at 6 hours. To understand any key differences in metabolism between the two treatment groups it would have been preferable to have further time points prior to, and between, the 3 and 6h time points, especially for quantification of APAP metabolites in NAC treated animals prior to NAC treatment. APAP metabolites APAP-C and APAP-NAC were most strongly positively correlated with ALT, TBil and hepatocyte damage score in the mice treated with APAP. They were however, least strongly correlated with hepatic GSH as measured using a fluorescence-based assay, and APAP-SG and un-metabolised APAP were most strongly negatively correlated. This fits the hypothesis that APAP-C in particular could be potential biomarker of APAP induced liver injury.

4.4.5 Conclusions and future work

This work has provided evidence that the UHPLC-MS/MS assays described in Chapters 2 and 3 can successfully be applied to tissue extracts and mouse serum. The GSH pathway assay was shown to be more effective in liver extracts than in serum, as the matrix effects caused by phospholipids in serum were not present in the hepatic extracts. As suggested in Chapter 3, removal of the phospholipids using e.g., SPE, may well be worth exploring in order to improve the GSH-pathway assay.

The hypothesis that there would be changes in concentrations of key sulfur-containing metabolites was shown to be correct, and the study provided further evidence that 5-OP increases represent a biomarker for APAP-induced liver injury. This study also showed that NAC treatment altered changes to GSH and related metabolites of interest at 6 hours post APAP administration. There may be differences to APAP metabolism

following NAC treatment, such as lower glucuronidation, which tentatively could be suggested to be due to increased cellular sulfur availability.

There were a large number of changes to the GSH related metabolites of interest over the whole time course of this experiment, future work will involve measuring the gene expression and activity of key enzymes in the pathway, particularly CDO, MAT, GS, GCL, CSE, CGL, MS and BHMT, to provide a clearer understanding of the metabolic changes to the methionine and γ-glutamyl cycles and trans-sulfuration pathway following APAP administration, and the differences when NAC treatment is provided. Other pathways of interest could be changes to trans-methylation, polyamine synthesis and the folate cycle. The mechanism of taurine biosynthesis following hypotaurine depletion would also be of interest in this model.

5 APAP metabolism and related toxicity in a porcine model of acute liver failure

5.1 Introduction

In the work presented in this chapter, a combination of approaches including global metabolic profiling with ^{1}H-NMR spectroscopy, followed by confirmation of circulating APAP metabolites and potential GSH depletion biomarkers using the targeted UHPLC-MS/MS methods previously developed were applied to a porcine ALF model.

5.1.1 Hypotheses

The first hypothesis was that APAP metabolism in the pig may differ from that of human and other animal models, as had been suggested previously from early literature.

The second hypothesis was that APAP metabolism, based on the production of methaemoglobin, led to the production of large amounts of *p*-aminophenol, which would cause toxic outcomes different to those reported in human APAP toxicity.

5.1.2 Aims

- To understand the metabolism of APAP in the pig and how this relates to the previously described toxicity, including hepatic necrosis, kidney damage and methaemoglobineamia.
- To profile the metabolome of the pig using ^{1}H-NMR spectroscopy of tissues and biofluids in order to understand APAP metabolism and the endogenous metabolism changes seen in relation to this toxicity.
- To apply the sensitive, targeted UHPLC-MS/MS assay as described in Chapter 2, in order to accurately quantify concentrations of circulating APAP metabolites over the course of the experiment.
- To apply further analytical methods to understand the relationship, if any, between porcine APAP metabolism and the GSH pathway related metabolism using the UHPLC-MS/MS methodology described in Chapter 3.

5.1.3 Background and rationale

APAP metabolism and related toxicity in humans and model species has been discussed in depth in the previous chapters of this Thesis. In order to investigate paracetamol metabolism and toxicity in a porcine model of APAP induced ALF, biofluids and hepatic extracts were analysed using both global profiling with ^{1}H-

NMR spectroscopy, and targeted quantification of metabolites of interest using UHPLC-MS/MS. Samples were collected by external collaborators at University College London as part of a larger study to assess efficacy of a medical device for the clinical treatment of ALF. Pigs were used to model clinical ALF due to their large size and organ similarity to humans, and to allow the set up to replicate the clinical situation (Lee et al. 2013). APAP overdose is a leading cause of clinical ALF, which is associated with high mortality, and often liver transplantation is the only available treatment option. The University College London Liver Dialysis Device (UCL-LDD) was being developed in order to prolong life in ALF while patients await liver transplantation (Lee et al. 2013). The porcine model of ALF had been previously published in detail and was shown to be reproducible and clinically relevant (Baker et al. 2015; Lee et al. 2012, 2013). As shown in these previous studies, hourly APAP treatment for up to 20 hours led to onset of ALF in the pigs. Animals were able to survive for up to 20 hours after ALF, before suffering multi-organ failure including liver and kidney failure, leading to cardiorespiratory arrest, or meeting other criteria to represent 'death' including high blood lactate and acidosis (Baker et al. 2015; Lee et al. 2015). During the treatment with APAP, blood percentage methaemoglobin increased leading to development of methaemoglobinemia in some animals, and as such this study had taken the approach of maintaining APAP blood concentrations below 300 mg/L in order to keep methaemoglobin concentrations below a fatal level (Lee et al. 2013). The cause of methaemoglobinaemia in these pigs had not been previously investigated.

Little has been published on the metabolism of APAP in the pig however, in some early work it was reported that pigs had a lower sulfation capacity than humans (Capel et al. 1972). A number of reports have discussed the enzymatic similarities and differences between human and the pig, and reports have suggested that the gastrointestinal tract and kidney related drug metabolism are likely to show most metabolic differences (Helke et al. 2016; Thorn et al. 2012). The phenomenon of methaemoglobinaemia after administration of paracetamol at doses higher than 200-300 mg/L has been previously reported in the pig, with studies aiming to keep the dose below this threshold in order to reduce methaemoglobin formation (He et al. 2017; Newsome et al. 2010; Thiel et al. 2011).

Porcine drug metabolism and toxicity has become an increasingly relevant topic in toxicology, as the pig and minipig have become popular choices as second species for pre-clinical studies other than non-human primate or dog (Helke et al. 2016).

5.2 Materials and methods

5.2.1 Animal model and study design

The methodology for the animal handling and dosing has been described in detail elsewhere and is summarised below in Figure 5.1**.** (Lee et al. 2015). Briefly, 22 female Landrace cross Large White Pigs (26-36kg) were randomised into 3 groups: APAP plus UCL-LDD (APAP-UCL-LDD; *n*=9), APAP plus Control Device (APAP-CD; *n*=9) or control plus CD (control-CD; *n*=4). Animals were maintained under total intravenous anaesthesia with intermittent positive pressure ventilation and underwent intensive care monitoring and management. In order to induce ALF, APAP was administered via an oroduodenal tube in an aqueous suspension at an initial concentration of 250mg/kg, APAP serum concentrations were maintained above 300 mg/L with maintenance APAP doses of 0.5-4g hourly. Dosing of APAP continued until the animal reached 'ALF' as defined as an INR of >3. Two hours after onset of ALF, treatment with either the UCL-LDD or a control device (CD) was initiated until death. 'Death' was defined as non-recoverable cardiorespiratory arrest or when two of the following criteria were reached: haematocrit <10%; blood potassium >5.5 mmol/L; blood lactate >10 mmol/L; blood pH <7.25; partial pressure of oxygen in arterial blood (P_aO_2) <60 mmHg. An albumin infusion protocol was developed based on the pilot study (Lee et al. 2013). Human serum albumin (20%) was infused at onset of APAP dosing at 1.6g albumin/h increasing to 16g/h at 12h APAP dosing finally increasing to 20g/h at ALF. Control animals were infused with 1.6g albumin/h throughout the study. Albumin infusion was stopped if the serum albumin concentration was greater than 20g/L. Two units of porcine fresh frozen plasma were given at 'ALF' in both groups. All animals were maintained throughout the study with an I.V. infusion of 'Viamin 14', a solution containing glucose, alanine, arginine, aspartic acid, cysteine, glutamic acid, glycine, histidine, isoleucine, leucine, lysine, methionine, phenylalanine, proline, serine, threonine, tryptophan, tyrosine, valine, glacial acetic acid. In addition, intravenous fluid therapy was administered according to set protocols including compound sodium lactate, 0.9% sodium chloride, 8.4% sodium bicarbonate, 6% hydroxyethyl starch 130/0.4

and potassium chloride. Serum and plasma sampling were conducted every 4 hours and the following parameters measured in serum: serum APAP (mg/L), urea (mmol/L), Creatinine (µmol/L), Total Bilirubin (µmol/L), AST (U/L), ALP (U/L), Albumin (g/L). Arterial blood gas monitoring pre and post ALF included lactate mmol/L and percentage methaemoglobin and were taken hourly. Anaesthetic monitor data were taken every 15 minutes, haematology was taken every 4 hours. Liver biopsies were taken at time 0 h, 12 h and study endpoint. Kidney samples were taken at study endpoint. Urine samples were taken at 4-hour intervals throughout the study. Full methods are provided in previous reports (Baker et al. 2015; Lee et al. 2015; Lee et al. 2013).

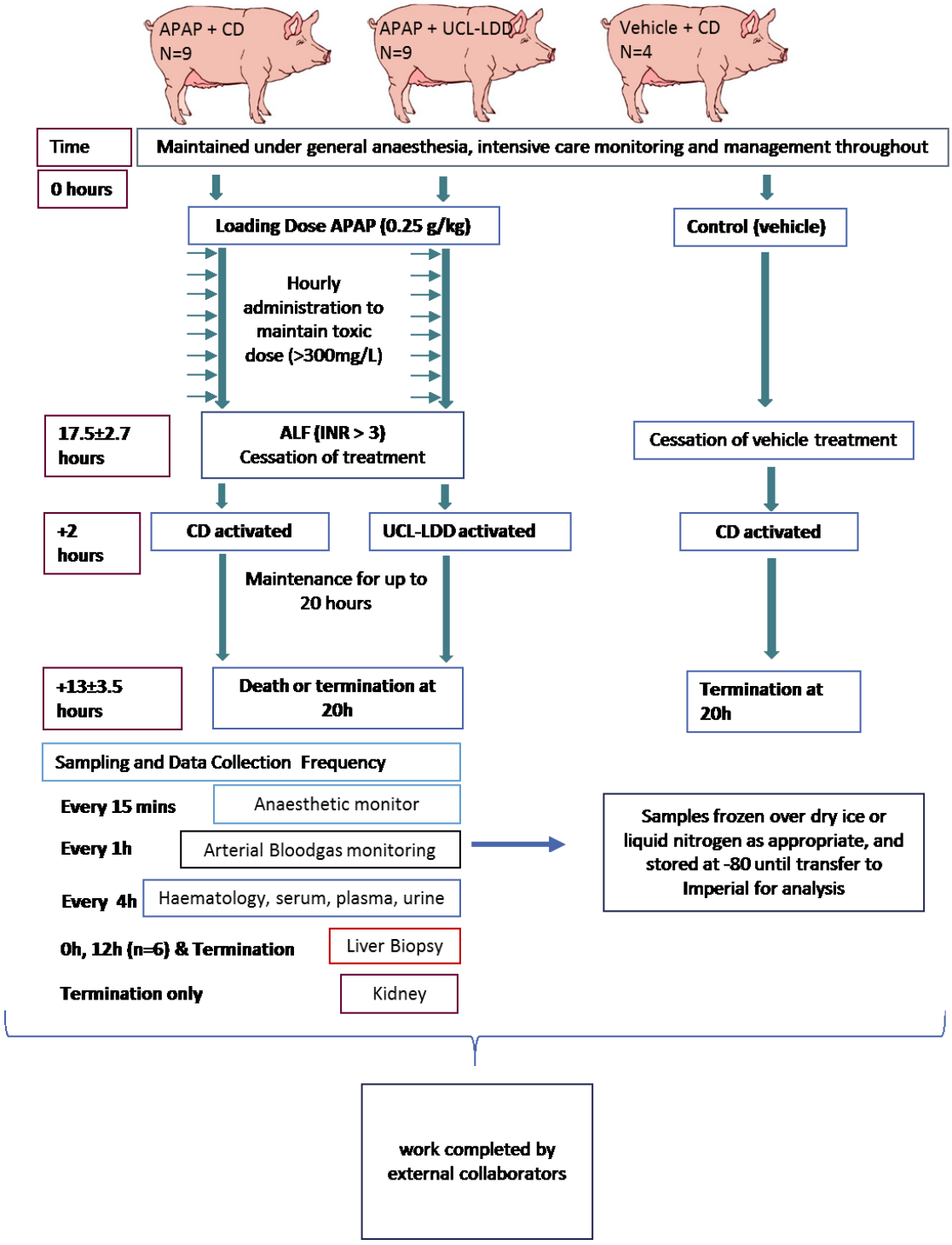


Figure 5.1 Overview of study design, timings and sampling as undertaken by external collaborators at University College London, prior to sample shipping to Imperial College London for analysis. Abbreviations: ALF: acute liver failure; APAP: paracetamol; CD: control device; INR: International Normalised Ratio; UCL-LDD: UCL Liver Dialysis Device

5.2.2 ^{1}H-NMR spectroscopy of aqueous tissue extracts, plasma and urine

Each sample type was prepared differently as summarised in Figure 5.2and described in detail below, before being mixed with the relevant ^{1}H-NMR spectroscopy buffers for analysis.

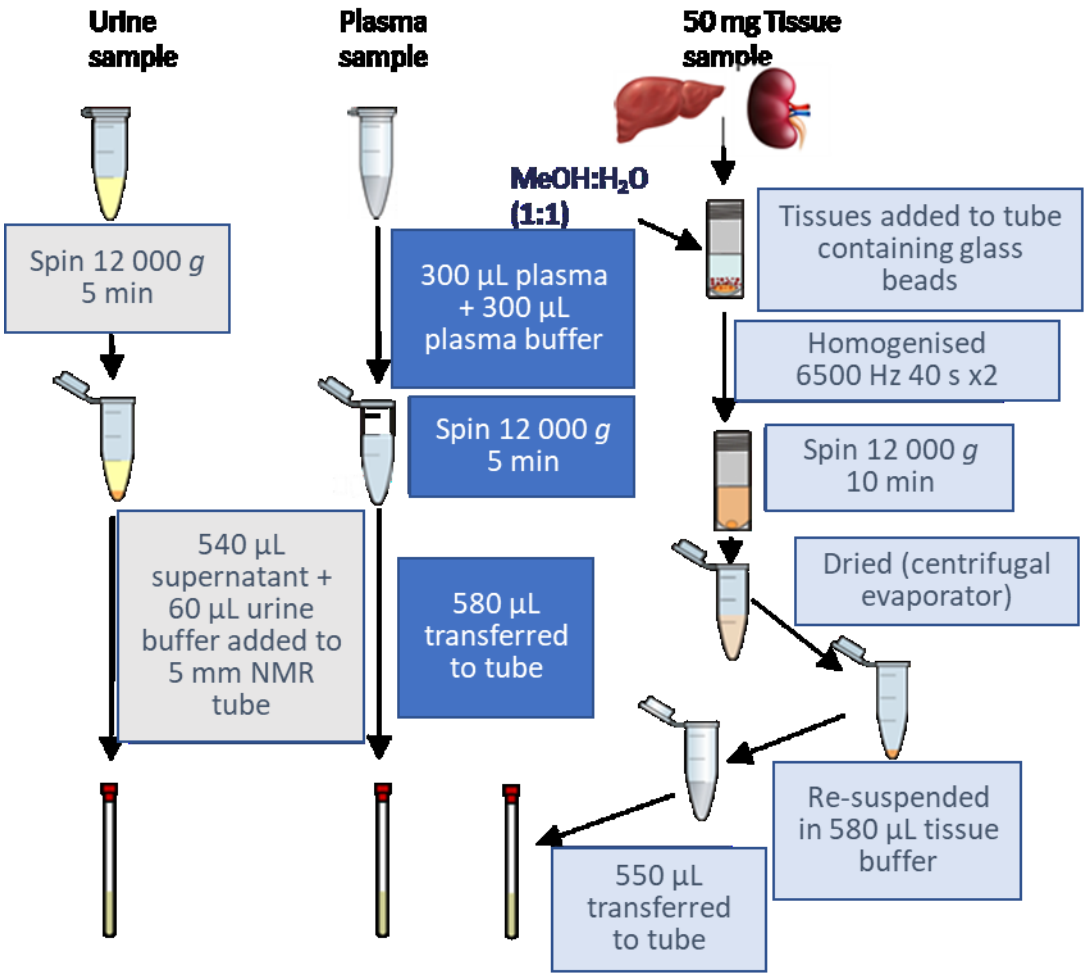


Figure 5.2 Overview of sample preparation and analysis for 1H-NMR spectroscopy. Abbreviations: NMR: nuclear magnetic resonance.

5.2.2.1 Preparation of Plasma Samples for ^{1}H-NMR Spectroscopic analysis

Plasma samples were prepared as described elsewhere (Dona et al. 2014). Briefly, 300 µL of each plasma sample were added to 300 µL plasma buffer and centrifuged for 5 min at 12 000 *g*, after which 580 µL of supernatant were taken and placed in a 5 mm glass NMR tube for analysis.

Preparation of Urine samples for analysis

Urine samples were prepared as described elsewhere (Dona et al. 2014). Briefly, 600 µL of each urine sample was centrifuged at 12,000 *g* for 5 min at 4°C. Supernatants (540 µL) were transferred to 5 mm NMR tubes containing urine buffer (60 µL).

5.2.2.2 Preparation of aqueous tissue extracts

Kidney extractions for ^{1}H-NMR spectroscopic analysis were performed as described elsewhere (Beckonert et al. 2007; Want et al. 2013). Briefly, 1.5 mL ice-cold methanol/water (1:1, v/v) and kidney tissues (mean weight 68.5±6.7 mg) were placed into bead beater tubes. Samples were homogenised using a bead beater (Precylls24, Bertin) using two cycles of 6500 Hz for 40 s with samples cooled on dry-ice in-between cycles. Samples were then centrifuged at 10,000 *g* for 10 min. (4°C) with 1 mL of supernatant transferred to Eppendorf tubes for concentration in a centrifugal evaporator (Eppendorf Concentrator Plus) (45°C overnight). Dried supernatants were reconstituted in 580µL pH 7.4 tissue buffer prepared in D_2O containing 0.5mM 3-(trimethylsilyl)-[2,2,3,3-2 H4]-propionic acid sodium salt (TSP), vortexed for 90 s and centrifuged at 12,000 *g* for (5 min. 4°C). Supernatants (550 µL) were transferred to 5 mm NMR tubes (HP-507, Norell) which were inserted into an automated sample handling carousel (Bruker Biospin, Germany). Liver extracts were prepared using a similar approach to that used for kidney samples described above however, the volume of tissue buffer was adjusted (20:1, v/w) to the tissue weight (mean 50.6±7.6 mg).

5.2.2.3 ^{1}H-NMR spectroscopy of plasma samples

CPMG pulse sequence (Beckonert et al. 2007). The D_2O and TSP present in the buffer provided a field frequency lock and chemical shift reference compound ($\delta^{1}H$=0.00), respectively. 32 Transients were collected into 73 K data points using a spectral width of 18028.85 Hz. All experiments had a relaxation delay of 4 s and an acquisition time of 2.73 s.

5.2.2.4 ^{1}H-NMR spectroscopy of urine and tissue extract samples

^{1}H NMR spectra for urine were acquired on a Bruker Avance-600 spectrometer, using a 4 mm BBI probe (Bruker), operating at 600.1MHz ^{1}H frequency and at a temperature of 300 K. A standard one-dimensional solvent suppression pulse sequence was used to acquire the free induction decay (FID; relaxation delay-90° pulse-4 µs delay-90° pulse-mixing time-90° pulse-acquire FID (Beckonert et al. 2007) The D_2O and TSP present

in the buffer provided a field frequency lock and chemical shift reference compound (δ^1H=0.00), respectively. For liver extracts and urine 128 transients were collected whilst for kidney extracts the number was increased to 256. The data from all of these experiments were collected into 65,000 data points using a spectral width of 12,019.2 Hz, relaxation delay of 4 s and an acquisition time of 2.73 s**.**

5.2.3 ^{1}H-NMR spectral data processing

All ^{1}H NMR spectra were initially processed in TopSpin (v3.1, Bruker), where a line-broadening factor of 0.3Hz was applied prior to Fourier transformation (FT). Spectra were automatically phased, baseline-corrected and referenced to TSP (δ=0.00) for urine and tissue extracts, whilst plasma spectra were referenced to the α-glucose anomeric proton resonance at 5.23 ppm. Using an in-house script, ^{1}H-NMR data were imported to MATLAB (R2016b, MathWorks). TSP and water resonances were removed, before applying probabilistic quotient normalisation for urine and tissue spectra (Dieterle et al. 2006). For urine and plasma spectra, peaks were manually aligned using in-house scripts (Veselkov et al. 2009). Endogenous metabolite assignments were performed using Statistical TOtal Correlation Spectroscopy (STOCSY) (Cloarec et al. 2005), J-resolved Spectroscopy (JRES), spectral database and literature (Kyriakides 2016; Merrifield et al. 2011; Nicholson et al. 2002). APAP metabolites were assigned using STOCSY (see Figure 5.3 below), JRES, and literature (Bales et al. 1988; Gartland et al. 1990; Kyriakides 2016) PAP-G was identified using a standard spike of the compound shown in Figure 5.4.

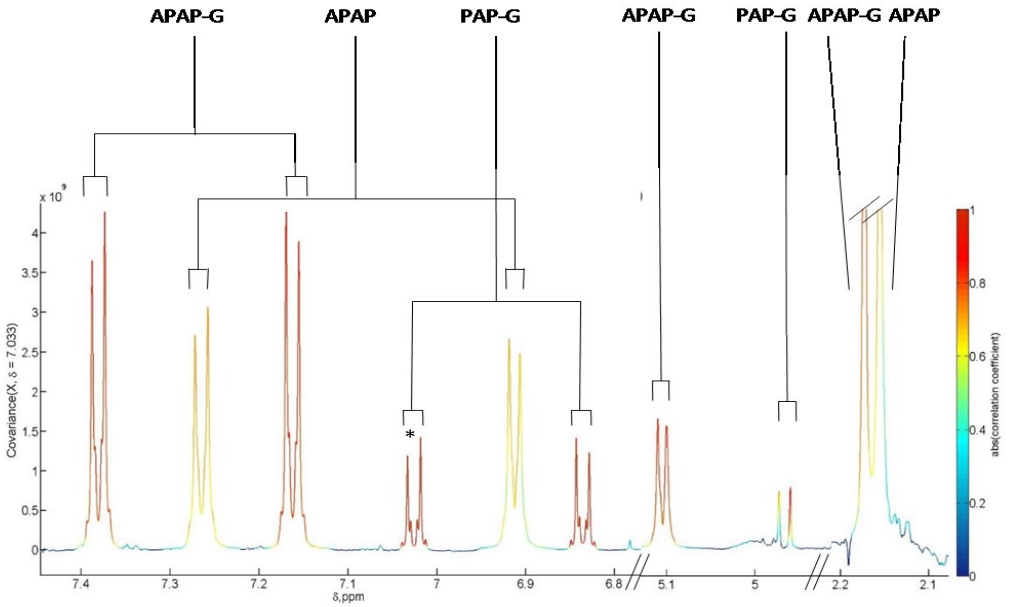


Figure 5.3 Representative figure of STOCSY driven from PAP-G labelled above
**indicates resonance from which STOCSY is driven. Darker red suggests stronger metabolite correlation according to colour scale on right hand side of figure.*
Abbreviations: APAP: paracetamol; APAP-G: paracetamol glucuronide; PAP-G: para-aminophenol glucuronide; ppm: parts per million; STOCSY: Statistical TOtal Correlation Spectroscopy.

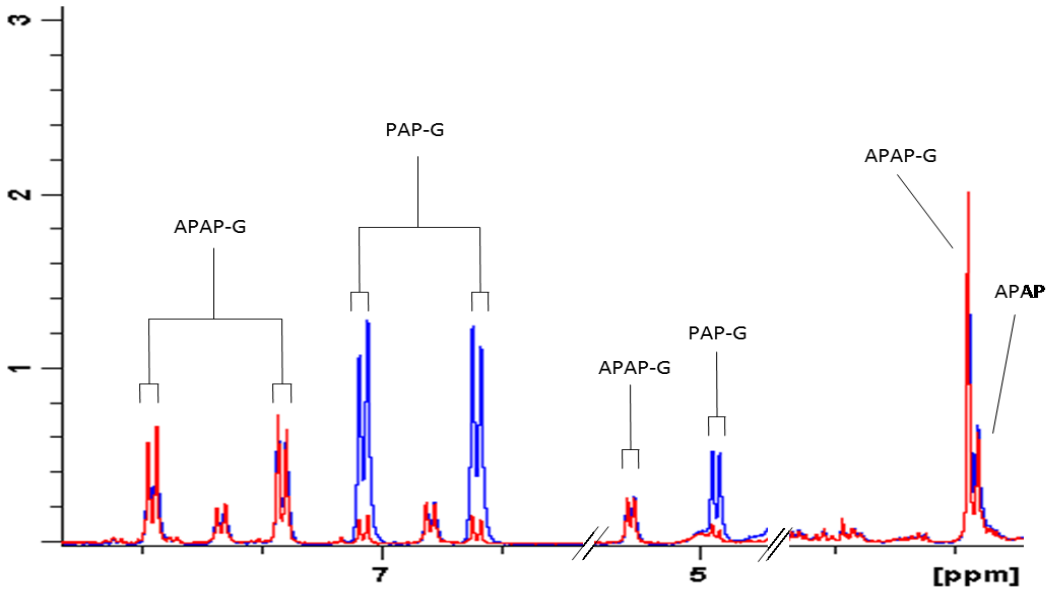


Figure 5.4 Overlaid spectra of a plasma sample analysed before and after addition of PAP-G standard. Original spectrum in red, PAP-G-spiked plasma represented by blue spectrum.
Abbreviations: APAP: paracetamol; APAP-G: paracetamol glucuronide; PAP-G: p-aminophenol glucuronide; ppm: parts per million.

5.2.4 APAP UHPLC-MS/MS method analysis of plasma

The APAP method was performed as described in detail in Chapter 2. Briefly, calibration curve and QC samples were prepared at ranges listed in Table 5.1 and Table 5.2 for the curve and QCs respectively. Internal standards were prepared to give the final concentrations displayed in

Table 5.3. As described previously, for standard curve and QC samples 50 µL of each standard curve or QC stock solution was added to 5 µL of pooled control porcine plasma, followed by 35 µL of MeOH and 10 µL of IS stock solution. Porcine plasma samples for analysis were prepared by diluting 5 µL of plasma with 85 µL of MeOH and 10 µL of IS stock solution. Samples were stored at -20°C for 20 minutes to precipitate proteins, then centrifuged for 10 min at 10, 000 *g*, after which 20 µL of the supernatant was taken and diluted with 980 µL water for analysis and transferred into glass vials. Analysis was performed as described in detail in Chapter 2, using the chromatographic separation and mass spectrometry parameters described previously. Mass spectrometry conditions are summarised in Table 5.4**.**

Table 5.1 Concentration ranges for APAP and metabolites in application of APAP method to porcine plasma.

Calibration Curve Ranges / ng/mL					
APAP, PAP-G	**APAP-G**	**APAP-S**	**APAP-C**	**APAP-SG**	**APAP-NAC**
16	22.5	2.75	0.44	0.58	-
24	33.8	4.12	0.67	0.88	0.84
40	56.3	6.87	1.11	1.46	1.40
60	84	10.3	1.67	2.19	2.10
90	127	15.5	2.50	3.28	3.16
150	211	25.8	4.173	5.47	5.26
250	352	42.9	6.94	9.12	8.77
500	703	85.9	13.9	18.2	17.5

Abbreviations: APAP: paracetamol; APAP-C: paracetamol-cysteinyl conjugate; APAP-G: paracetamol glucuronide; APAP-NAC: paracetamol n-acetylcysteine conjugate; APAP-S: paracetamol sulfate; APAP-SG: paracetamol glutathione conjugate; PAP-G: p-aminophenol glucuronide.

Table 5.2 Final QC concentrations for APAP and metabolites in application of APAP method to porcine plasma.

QC Concentration in ng/mL						
QC	APAP-G	APAP, PAP-G	APAP-S	APAP-SG	APAP-C	APAP-NAC
ULOQ	703	500	85.9	18.2	13.9	17.5
High	562	400	68.7	14.6	11.1	14.0
Mid	141	100	17.2	3.65	2.78	3.51
Low	67.5	48	8.24	1.75	1.33	1.68
LLOQ	22.5	16	2.75	0.58	0.44	0.84

Abbreviations: APAP: paracetamol; APAP-C: paracetamol-cysteinyl conjugate; APAP-G: paracetamol glucuronide; APAP-NAC: paracetamol n-acetylcysteine conjugate; APAP-S: paracetamol sulfate; APAP-SG: paracetamol glutathione conjugate; PAP-G: p-aminophenol glucuronide.

Table 5.3 Final measured concentrations of each deuterated internal standard in porcine sample analysis.

Internal Standard	Final Concentration
APAP-d_3	200 ng/mL
APAP-S-d_3	40 ng/mL
APAP-G-d_3	300 ng/mL
APAP-C-d_5	12 ng/mL
APAP-NAC-d_5	12 ng/mL

Abbreviations: APAP: paracetamol; APAP-C: paracetamol-cysteinyl conjugate; APAP-G: paracetamol glucuronide; APAP-NAC: paracetamol n-acetylcysteine conjugate; APAP-S: paracetamol sulfate.

Table 5.4 UHPLC-MS/MS conditions for analytes and internal standards measured for the APAP assay in porcine plasma.

Compound	Parent ion (m/z)	Product ions (m/z)	Cone voltage (V)	Collision voltage (V)	Dwell time (s)	Retention Time (min)
APAP	152.10	65.00 92.88 110.06	30	26 22 16	0.02	2.92
APAP-d_3	155.07	110.99	30	20	0.089	2.90
APAP-C	271.03	96.094 139.99 182.06	34	36 24 16	0.02	2.52
APAP-C-d_5	276.22	142.81 186.84	34	26 12	0.02	2.49
APAP-S	232.07	110.09 152.10	30	22 12	0.02	2.18
APAP-S-d_3	235.02	111.022 155.053	30	22 14	0.02	2.16
APAP-G	328.13	110.008 152.09	20	34 14	0.02	1.80
APAP-G-d_3	353.20	353.20 369.14	42	16 26	0.02	1.78
APAP-NAC	335.14	152.028 206.053	6	16 18	0.08	4.98
APAP-NAC-d_5	340.20	152.024 211.059	34	18 16	0.08	4.95
APAP-SG	457.24	139.99 328.11	30	36 14	0.089	3.85
PAP-G	308.33	181.04 199.05	2	12 12	0.025	0.39

Abbreviations: APAP: paracetamol; APAP-C: paracetamol-cysteinyl conjugate; APAP-G: paracetamol glucuronide; APAP-NAC: paracetamol n-acetylcysteine conjugate; APAP-S: paracetamol sulfate; APAP-SG: paracetamol glutathione conjugate; PAP-G: p-aminophenol glucuronide.

5.2.5 Glutathione pathway UHPLC-MS/MS method analysis of plasma

The GSH assay was applied to porcine serum, and samples were prepared as described for mouse serum in Chapter 3 and 4. In brief, metabolites were analysed against 3 curves, a “low”, “mid” and “high” range curve based on their expected ranges in samples. IS were used to correct for ion suppression or enhancements where commercially available. The analytes in each curve and the ULOQ of each is, with associated IS and its concentration in samples are displayed in Table 5.5. Serial dilution of the ULOQ standards gave calibration curve ranges and QCs, the concentrations of which for the “low”, “medium” and “high” range curves are displayed in Table 5.6 and Table 5.7 for curves and QCs respectively. Samples for analysis were prepared by

diluting 20 µL of porcine plasma with 10 µL IS in H_2O + 0.2% FA and 70 µL 80:20 MeCN:H_2O + 0.2% FA. These mixtures were kept at -20°C for 20 minutes to precipitate proteins and were then centrifuged at 10 000 *g* for 10 minutes, after which 80 µL of the solution was transferred to total recovery vials for analysis. Pooled QCs and over-spiked QCs were produced by taking six 20 µL aliquots of pooled plasma sample, three of these were prepared as normal samples, and 3 were mixed with 10 µL IS stock and over-spiked with 10 µL of the HQC stock, before 60 µL CH_3CN was added prior to protein precipitation.

Table 5.5 Standard ULOQ and IS concentration for the three curves concentration levels which were prepared and mixed for sample analysis

"High" curve (ULOQ 20 µg/mL)		"Mid" Curve (ULOQ 2 µg/mL)		"Low" Curve (ULOQ 1 µg/mL)	
Glutamine	Glutamine-d_5	5-OP	5-OP-d_5	Cystathionine	Cystathionine-d_4
Glycine	Glycine-$^{13}C^{15}N$	Cys-gly	Cystine-d_6	Choline	Choline-d_4
Serine	Serine-d_3	Glutamate	Glutamate-d_3	Homocysteine	Homocysteine-d_4
Taurine	Taurine-d_4	Hypotaurine	Hypotaurine-d_4	SAMe	SAMe-d_3
GSSG	GSSG-$^{13}C_4{}^{15}N_2$	Methionine	Methionine -$^{13}C^{15}N$	Homocystine	Homocystine-d_8
		Cysteine	Cysteine-$^{13}C_3{}^{15}N$	G-glu-cys	
		Homoserine		GSH	
		Cystine		Cysteic acid	
				Betaine	
				OA	
				2-amino-butyrate	
				SAH	

Abbreviations: G-glu-cys: gamma-glutamyl cysteine; GSH: reduced glutathione; GSSG: oxidised glutathione; IS: internal standard; OA: Ophthalmic acid; 5-OP: 5-oxoproline; QC: quality control; SAH: s-adenosyl homocysteine; SAMe: s-adenosyl methionine; ULOQ: upper limit of quantification.

Table 5.6 Calibration range used for standards in the "low", "mid" and "high" QC ranges.

Standard number	**Final concentration of curve (µg/mL)**		
	"High"	**"Mid"**	**"Low"**
7	20	2	1
6	10	1	0.5
5	5	0.5	0.2
4	2	0.2	0.2
3	1	0.2	0.05
2	0.5	0.05	0.02
1	0.2	0.02	0.01

Abbreviations: QC: quality control

Table 5.7 Final concentration of the QCs at the for each high, mid and low curve calibration curves

QC	Final Conc. QC (ng/mL)		
	High	**Mid**	**Low**
HQC	8000	800	400
MQC	2000	200	100
LQC	600	60	30

Abbreviations: HQC: high quality control; LQC: low quality control; MQC: mid quality control; QC: quality control

5.2.6 Univariate statistical analysis

Prism 8.0 was used for univariate analysis of integrated ^{1}H-NMR spectral resonances. Kruskal-Wallis with multiple comparison with FDR multiple test correction (two-stage linear step-up procedure of Benjamini, Krieger and Yekutieli) was used to compare between three or more groups and Mann-Whitney was used for comparison between two groups. Initially statistical comparisons were made between three groups at each time point of Control, APAP + CD and APAP + UCL-LDD. There was no statistical significance between the two APAP-treated groups, so these were combined for future further analysis. For GSH pathway UHPLC-MS/MS results, data were $\log_{10}$ transformed before being analysed using one-way ANOVA followed by FDR corrected multiple comparisons.

5.3 Results

5.3.1 Survival, histopathological and biochemical characterisation of the model

Following administration of APAP, ALF was recorded at a median time of 17.5±2.7 h (range 12-23 h) with a median total administered dose of 48.5 g (31.5-68.5 g.) Median survival time from ALF APAP animals was 13±3.5 hours, with a range from 8 h to 20 h (All animals surviving were terminated at 20 h post ALF). Post mortem histopathological analysis of liver specimens showed acute centrilobular to midzonal hepatocyte degeneration and necrosis in all APAP treated animals, but not in control animals. Post mortem histopathological analysis of renal specimens showed tubular epithelial cell swelling and protein loss in all APAP treated animals, but not in control animals. Serum creatinine was significantly higher in APAP treated animals at the onset of ALF, compared to control animals, while serum albumin concentrations were significantly lower than control animals at onset of ALF (Figure 5.5). A number of other biomarkers were measured including bilirubin, ALP, AST and urea, of which the mean values are displayed in Table 5.8, and the results for individual animals with median and interquartile range for each time point in Figure 5.5 Summary

of parameters measured to characterise the ALF model.. APAP treated animals showed hematotoxicity, with significantly increased blood concentrations of methaemoglobin (MetHb) and lactate and significant increases in prothrombin time (21 ± 1.3 s at 0 h; 80 ± 19 s at ALF). MetHb concentrations increased with APAP dosing and decreased upon cessation of dosing at ALF and were highly variable, ranging from 0.5% to 13.7% in animals dosed with APAP at ALF onset. Intracranial pressure (ICP) increased in APAP treated animals over the course of the experiment, while in control animals ICP remained more constant, although the difference between treated and control groups was not statistically significant.

Table 5.8 Results of clinical chemistry tests on serum taken from pigs at 4 hours intervals up to ALF, and 4 hourly intervals from ALF until death.

Time	Urea mmol/L		Creatinine µmol/L		TBil µmol/L		AST U/L		ALP U/L		Albumin g/L	
	A	C	A	C	A	C	A	C	A	C	A	C
0h	4±1	4±1	65±9	56±9	2±1	3±2	39±13	43±13	203±36	184±70	31±3	34±2
4h	4±1	4±0.4	67±7	58±11	4±1	5±2	49±16	47±12	160±27	160±56	24±3	30±3
8h	4±1	3±1	73±8	53±9	6±1	6±2	54±15	53±28	154±28	129±36	22±4	29±3
12h	4±1	3±0.5	75±9	61±11	6±2	4±2	51±17	61±12	132±28	133±51	18±4	29±1
16h	4±1	3±0.3	95±24	65±12	9±1	6±1	34±11	45±21	85±28	135±45	21±2	29±6
ALF	4±1	3±0.3	114±24	66±9	5±1	6±2	31±11	62±13	62±28	133±42	13±2	30±6
ALF+ 4h	4±1	3±0.4	107±20	61±16	5±1	9±4	44±12	97±19	51±14	107±27	16±2	30±6
ALF+ 8h	3±1	3±0.8	103±18	49±22	6±1	7±6	45±16	79±28	51±19	91±23	17±3	27±7
ALF+ 12h	3±1	2±0.6	104±20	45±15	6±2	6±3	52±19	86±19	68±46	98±25	19±5	29±4
ALF+ 16h	3±1	2±0.8	102±13	35±16	9±2	6±2	88±35	71±10	77±22	85±23	24±4	28±3
ALF+ 20h	3±1	2±0.6	101±9	41±10	10±2	6±1	124±27	70±9	100±39	88±23	26±5	31±2

A=APAP treated (n=18) C=control (n=4)
Abbreviations: ALF: acute liver failure; ALP: Alkaline phosphatase; APAP: paracetamol; AST: aspartate aminotransferase; TBil: Total bilirubin.

Samples of organs were analysed for tissue damage and scored for damage on a scale of 1-4. Livers showed signs of acute centrilobular to midzonal hepatocellular dissociation, degeneration and necrosis. There was also parenchymal haemorrhage in the affected areas. Kidney samples from APAP treated animals were shown to have diffuse clear vascular swelling of tubular epithelium with accompanying mild to moderate protein droplets within tubular lumens. Scores for hepatocyte and kidney damage for each individual are shown in Table 5.9**.**

Table 5.9 Histopathology scores for liver and kidney for individual animals.
Scored from 0-4 for severity (0=no injury, 4=Severe injury) Abbreviations: APAP: paracetamol

Treatment Group	Animal	Liver pre-treatment	Liver 12 h biopsy	Liver post mortem	Kidney
APAP	RV31	0		2	1
	RV32	0		1	1
	RV33	0		3	2
	RV34	0		1	1
	RV35	0		3	1
	RV36	0		2	1
	RV37	0	1	2	1
	RV38	0	0	3	1
	RV40	0		3	1
	RV41	0		3	1
	RV42	1		1	1
	RV43	0		1	0
	RV45	0		2	0
	RV46	0		3	1
	RV47	0		2	1
	RV48	0		3	1
	RV50	0		1	1
	RV52	0	0	3	1
Control	RV39	0	0	0	0
	RV44	0		0	0
	RV49	0	0	1	0
	RV51	0	0	0	0

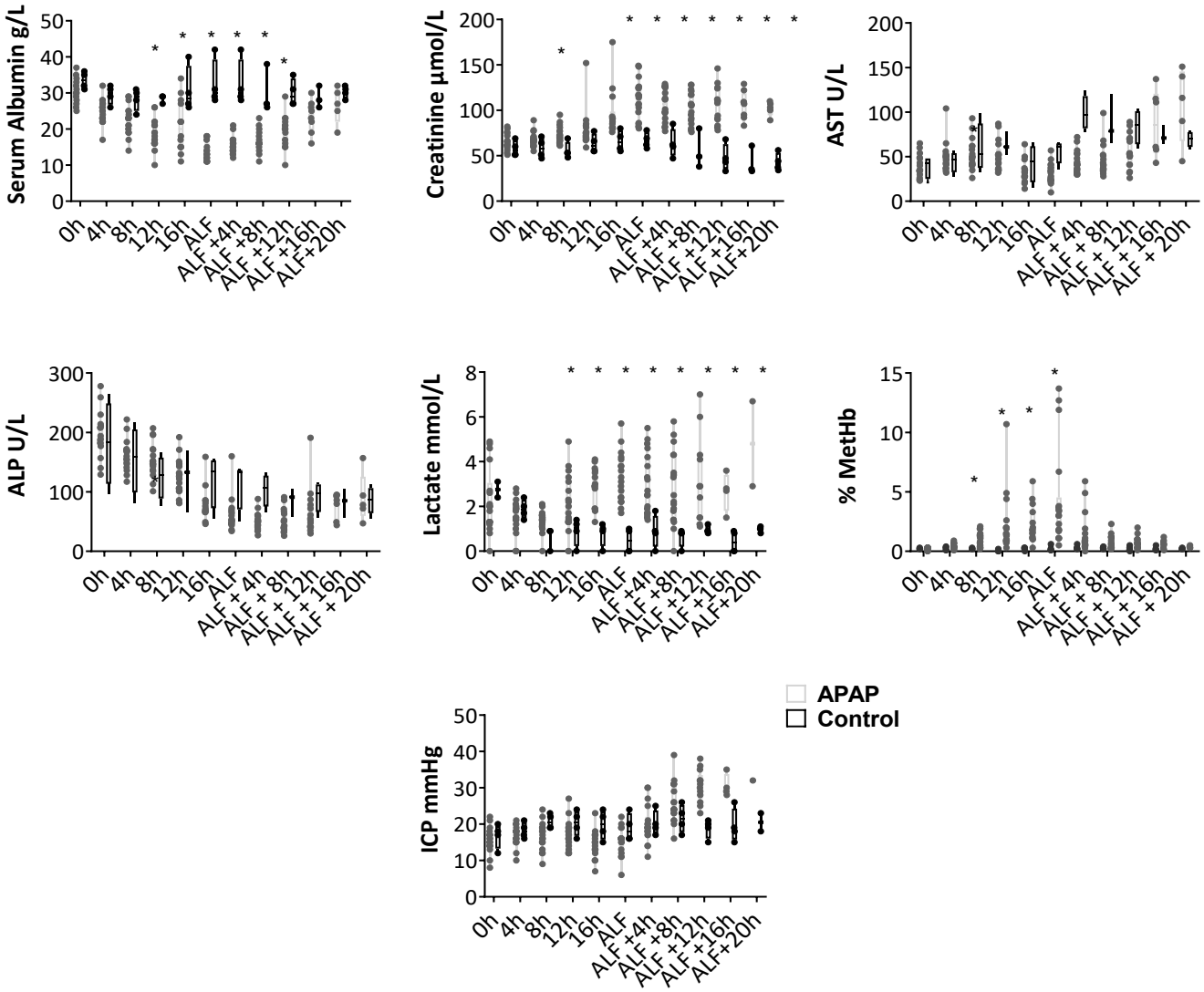


Figure 5.5 Summary of parameters measured to characterise the ALF model.
Each is plotted for individual animals at 4 hourly intervals up to ALF. Boxes display median and inter-quartile range and the whiskers show the full range. Asterisks (*) indicate that data from APAP treated animals was significantly different to controls at that time point with a q value <0.05 after FDR correction, following Kruskal-Wallis with multiple comparisons.
Abbreviations: ALP: Alkaline phosphatase; APAP: paracetamol; AST: aspartate aminotransferase; FDR: false discovery rate; ICP: intracranial pressure; MetHb: methaemoglobin.

5.3.2 ^{1}H-NMR Spectroscopy of tissue extracts and biofluids

5.3.2.1 Identification and integration of metabolites

Representative ^{1}H-NMR spectra from APAP-treated and Control samples from each matrix are shown below. Plasma samples at ALF are displayed in Figure 5.6, urine in Figure 5.7, liver extracts in Figure 5.8 and kidney extracts in Figure 5.9. The ppm spectral regions assigned and integrated for individual metabolites are listed

in Table 5.10 to Table 5.13 for plasma, urine, liver and kidney extracts. Spectra from all matrices, but kidney extracts and urine in particular, showed convoluted signals between 3 to 4 ppm, from overlapped sugar and amino acid resonances, which complicated the assignment of individual resonances and prevented the integration of peaks in this region.

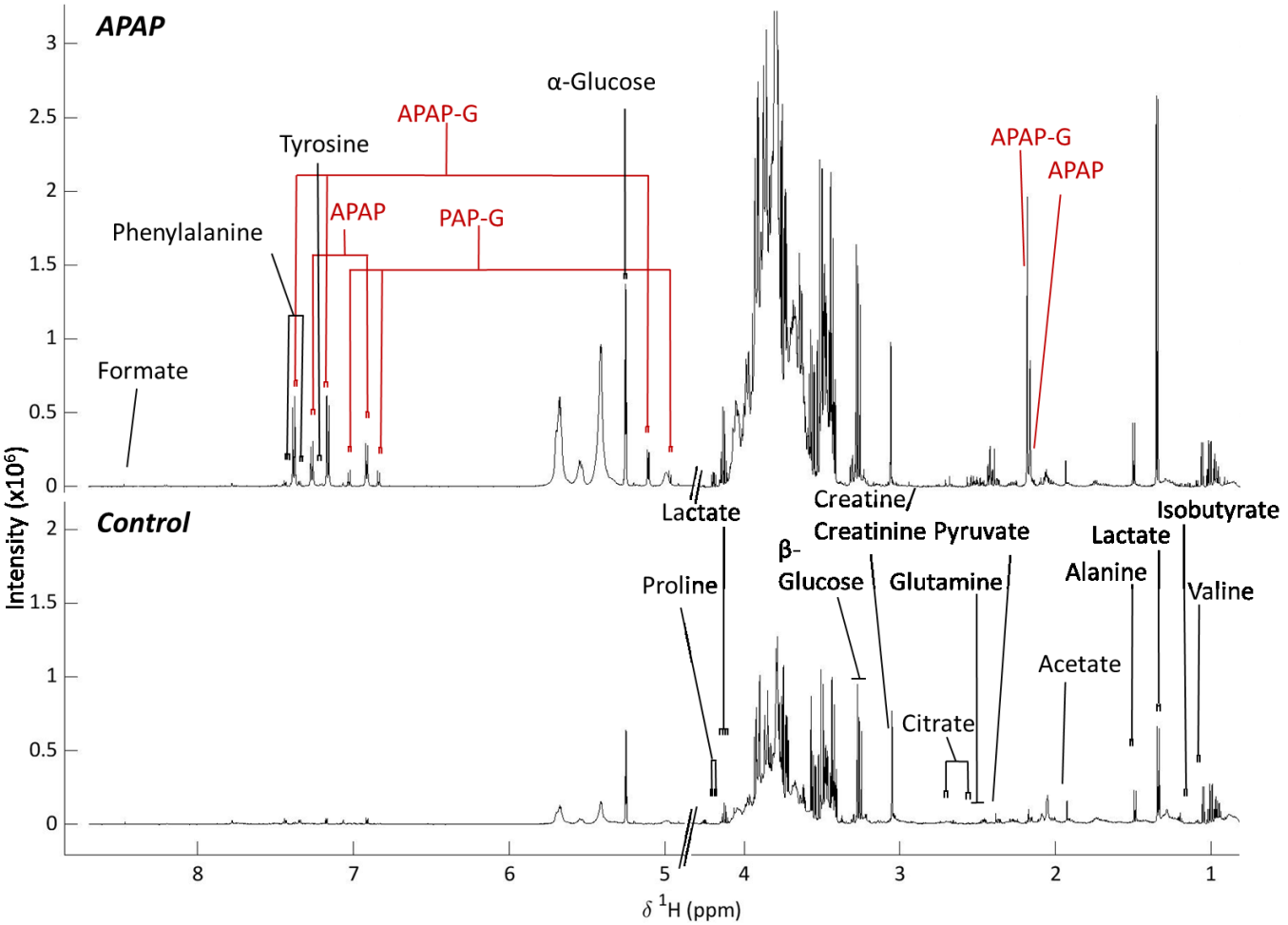


Figure 5.6 Representative 1H-NMR spectra of porcine plasma at the ALF timepoint in an APAP treated and Control animal with key endogenous and drug metabolite resonances labelled.

Abbreviations: ALF: acute liver failure; APAP: paracetamol; APAP-G: paracetamol glucuronide; NMR: nuclear magnetic resonance; PAP-G: p-aminophenol glucuronide; ppm: parts per million.

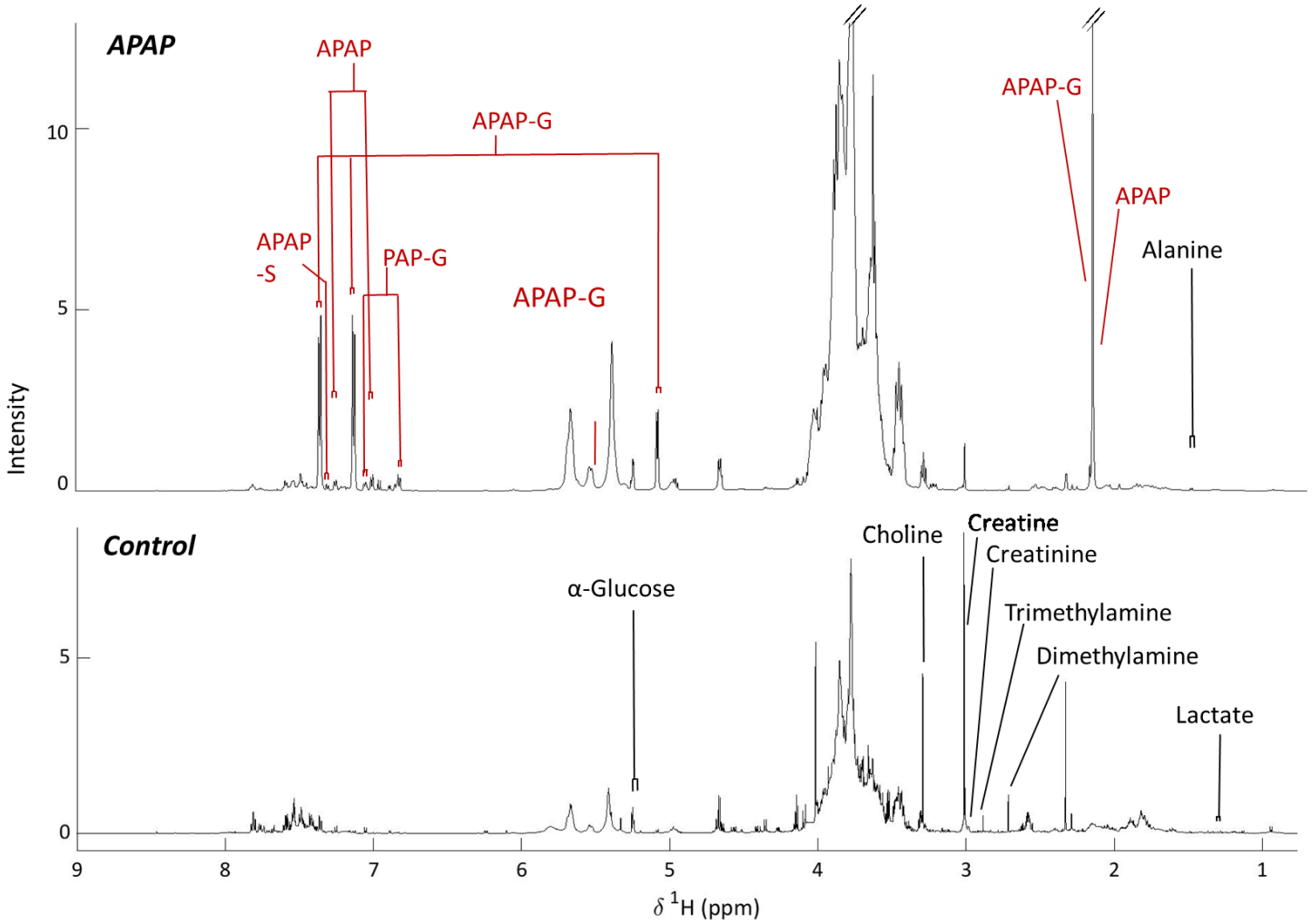


Figure 5.7 Representative 1H-NMR spectra of porcine urine at the ALF timepoint in an APAP treated and Control animal with key endogenous and drug metabolite resonances labelled.

Abbreviations: ALF: acute liver failure; APAP: paracetamol; APAP-G: paracetamol glucuronide; NMR: nuclear magnetic resonance; PAP-G: p-aminophenol glucuronide; ppm: parts per million.

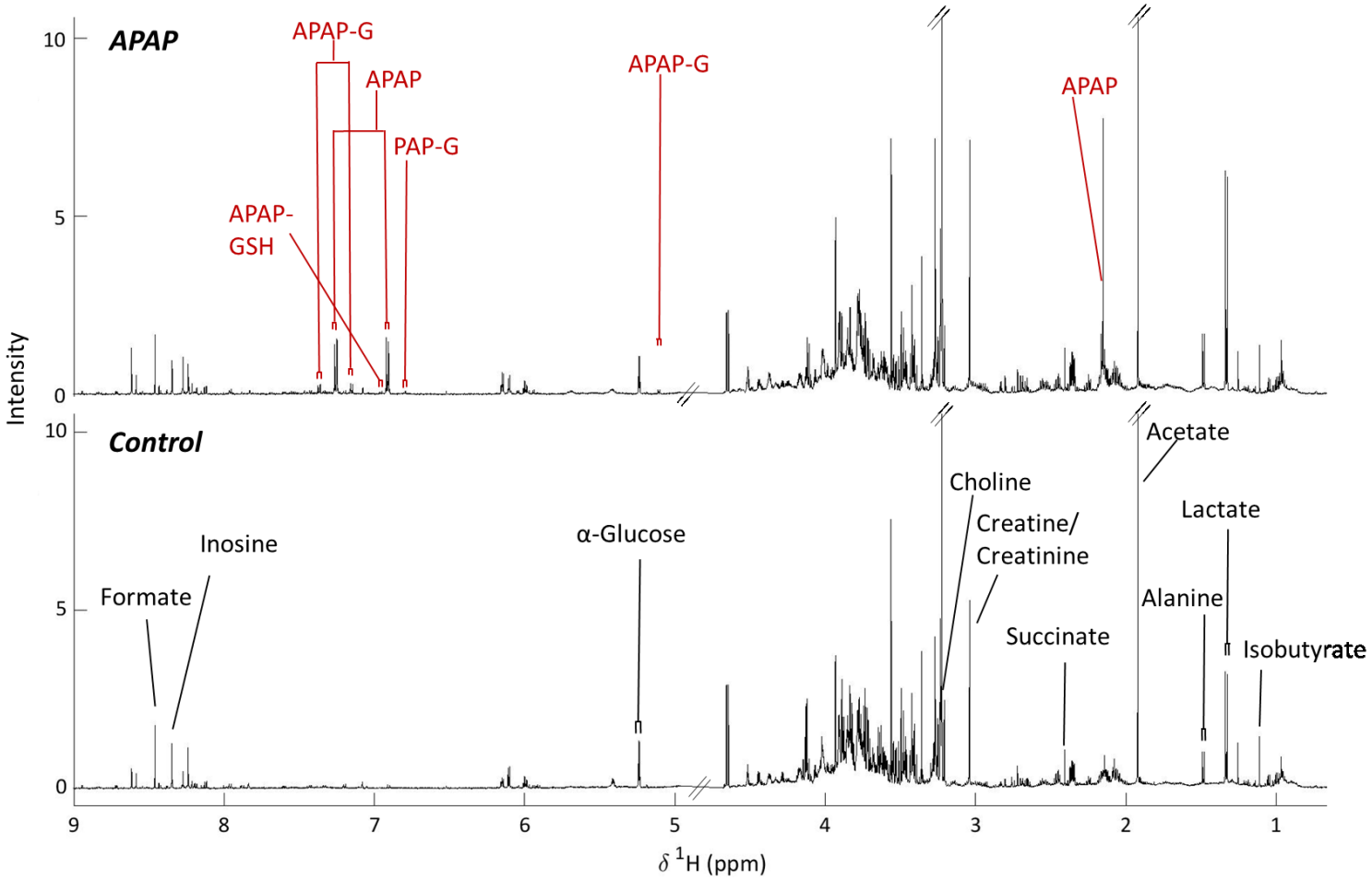


Figure 5.8 Representative 1H-NMR spectra of porcine liver at the ALF timepoint in an APAP treated and Control animal with key endogenous and drug metabolite resonances labelled.

Abbreviations: ALF: acute liver failure; APAP: paracetamol; APAP-G: paracetamol glucuronide; APAP-GSH: paracetamol glutathione conjugate; NMR: nuclear magnetic resonance; PAP-G: p-aminophenol glucuronide; ppm: parts per million.

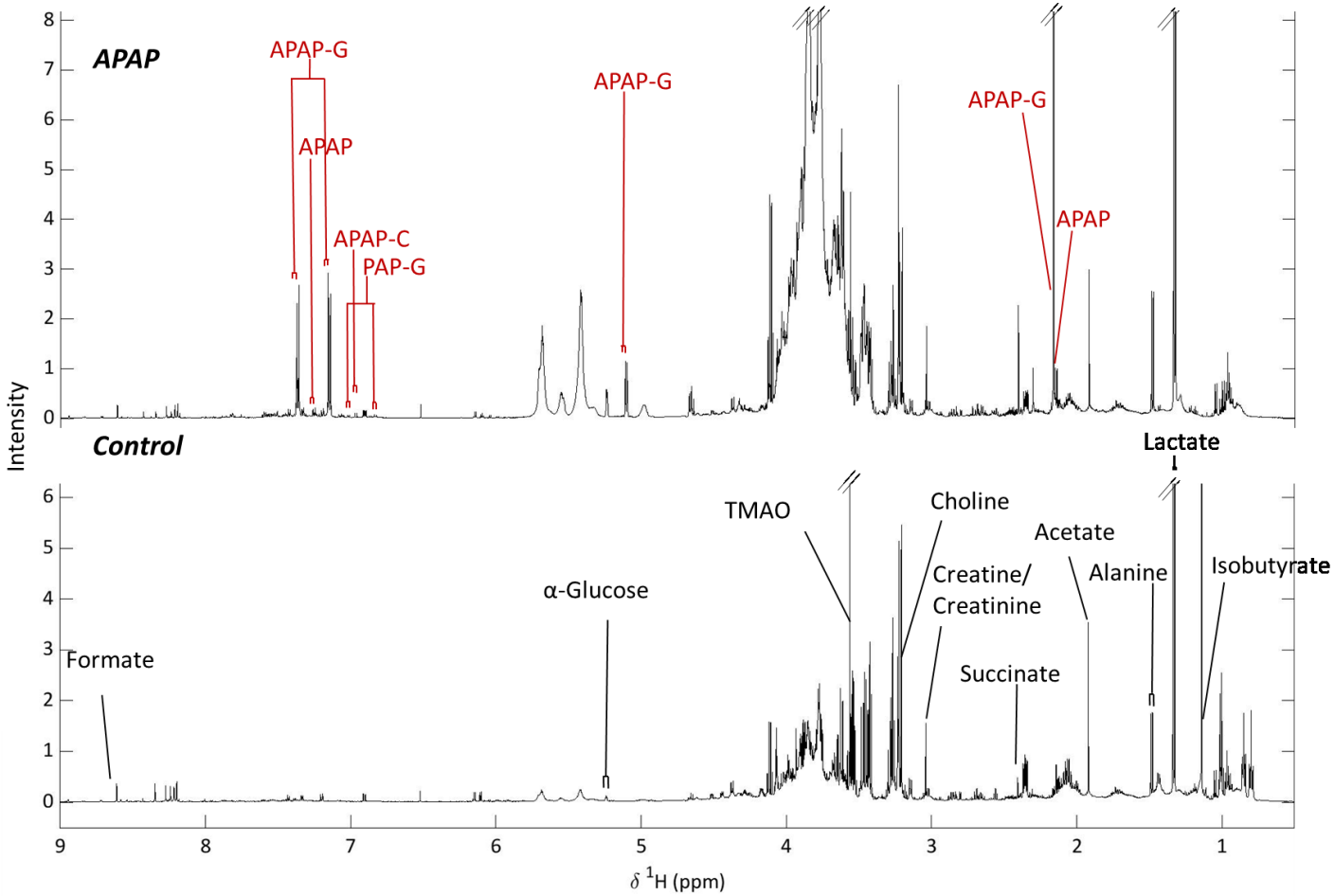


Figure 5.9 Representative 1H-NMR spectra of porcine kidney extracts at the ALF timepoint in an APAP treated and Control animal with key endogenous and drug metabolite resonances labelled.
Abbreviations: ALF: acute liver failure; APAP: paracetamol; APAP-G: paracetamol glucuronide; NMR: nuclear magnetic resonance; PAP-G: p-aminophenol glucuronide; ppm: parts per million; TMAO; trimethylamine N-oxide.

Table 5.10 Assigned representative resonances for endogenous and APAP metabolites in plasma, with multiplicity and functional group of proton represented

Plasma			
Endogenous metabolites			
Metabolite	**ppm region**	**Multiplicity**	**Functional group**
Acetate	1.92-1.93	s	βCH_3
Alanine	1.47-1.50	d	βCH_3
Citrate	2.5-2.57	d	1/2γCH
Creatine/creatinine	3.04-3.06	s/s	$N\text{-}CH_3$
Formate	8.44-8.48	s	HCOOH
α-glucose	5.22-5.28	d	C1H
Glutamine	2.44-2.47	m	γCH_3
Isobutyrate	1.13-1.14	d	CH_3
Lactate	4.09-4.15	q	αCH
Phenylalanine	7.42-7.46	m	C3H/C6H
Proline	4.17-4.21	dd	αCH
Pyruvate	2.38-2.39	s	CH_3
Tyrosine	7.19-7.22	d	C2H/C6H
Valine	1.03-1.06	d	γCH_3
APAP metabolites			
APAP	7.24-7.29	d	C2H/C6H
APAP-G	7.14-7.18	d	C3H/C5H
PAP-G	6.82-6.86	d	C3H/C5H

Abbreviations: APAP: paracetamol; APAP-G: paracetamol glucuronide; d: doublet; m: multiplet; PAP-G: p-aminophenol glucuronide; s: singlet.

Table 5.11 Assigned resonances for endogenous and APAP metabolites in urine, with multiplicity and functional group of proton represented.

Urine			
Endogenous metabolites			
Metabolite	**ppm region**	**Multiplicity**	**Functional group**
Alanine	1.46-1.50	d	βCH_3
Choline	3.26-3.26	s	$N\text{-}(CH_3)_3$
Creatine	2.99-3.02	s	$N\text{-}CH_3$
Creatinine	3.02-3.04	s	$N\text{-}CH_3$
Dimethylamine	2.71-2.72	s	CH_3
α-glucose	5.23-5.27	d	C1H
Lactate	1.31-1.36	d	βCH_3
Trimethylamine	2.87-2.89	s	CH_3
TMAO	3.28-3.30	s	$N\text{-}(CH_3)_3$
APAP metabolites			
Metabolite	**ppm region**	**Multiplicity**	
APAP	6.86-6.92	d	C3H/C5H
APAP-C	6.93-6.98	d	C5H
APAP-G	7.08-7.15	d	C3H/C5H
APAP-S	7.29-7.32	d	C2H/C6H
PAP-G	6.80-6.85	d	C3H/C5H

Abbreviations: APAP: paracetamol; APAP-C: paracetamol cysteinyl conjugate; APAP-G: paracetamol glucuronide; APAP-S: paracetamol sulfate; d: doublet; PAP-G: p-aminophenol glucuronide; s: singlet; TMAO; trimethylamine N-oxide.

Table 5.12 Assigned resonances for endogenous and APAP metabolites in soluble aqueous liver extracts, with multiplicity and functional group of proton represented.

Liver			
Endogenous metabolites			
Metabolite	**ppm region**	**Multiplicity**	**Functional group**
Acetate	1.91-1.93	s	βCH_3
Alanine	1.47-1.50	d	βCH_3
Choline	3.20-3.21	s	$N\text{-}(CH_3)_3$
Creatine	3.03-3.05	s	$N\text{-}CH_3$
Formate	8.45-8.48	s	HCOOH
α-glucose	5.22-5.26	d	C1H
Inosine	8.33-8.35	s	C8H
Isobutyrate	1.13-1.16	d	CH_3
Lactate	1.31-1.35	d	βCH_3
Succinate	2.4-2.41	s	CH_2
TMAO	3.26-3.27	s	$N\text{-}(CH_3)_3$
APAP metabolites			
APAP	7.24-7.27	d	C2H/C6H
APAP-G	7.14-7.16	d	C3H/C5H
APAP-SG	6.95-6.97	d	C5H
PAP-G	6.79-6.80	d	C3H/C5H

Abbreviations: APAP: paracetamol; APAP-G: paracetamol glucuronide; APAP-S: paracetamol sulfate; APAP-SG: paracetamol glutathione conjugate; d: doublet; PAP-G: p-aminophenol glucuronide; s: singlet; TMAO; trimethylamine N-oxide.

Table 5.13 Assigned resonances for endogenous and APAP metabolites in soluble aqueous liver extracts, with multiplicity and functional group of proton represented.

Kidney			
Endogenous metabolites			
Metabolite	**ppm region**	**Multiplicity**	**Functional group**
acetate	1.90 - 1.94	s	βCH_3
alanine	1.47 - 1.49	d	βCH_3
choline	3.19 - 3.21	s	$N\text{-}(CH_3)_3$
creatine	3.03 - 3.05	s	$N\text{-}CH_3$
α-Glucose	5.22 - 5.26	d	C1H
lactate	1.26 - 1.39	d	βCH_3
succinate	2.39 - 2.41	s	CH_2
TMAO	3.26 - 3.27	s	$N\text{-}(CH_3)_3$
APAP metabolites			
APAP	7.24 - 7.27	d	C2H/C6H
APAP-C	6.95 - 6.98	d	C5H
APAP-G	7.11 - 7.18	d	C3H/C5H
PAP-G	7.00 - 7.03	d	C2H/C6H

Abbreviations: APAP: paracetamol; APAP-C: paracetamol cysteinyl conjugate; APAP-G: paracetamol glucuronide; d: doublet; PAP-G: p-aminophenol glucuronide; s: singlet; TMAO; trimethylamine N-oxide.

5.3.2 APAP metabolism

5.3.2.1 Plasma

In plasma, APAP, its glucuronide and PAP-G could be detected in the ^{1}H-NMR spectra. The most abundant metabolite was APAP-glucuronide which was at higher concentrations than the parent throughout most of the experiment, while PAP-G was the only other metabolite that could be detected, at a lower concentration relative to parent (Figure 5.10).

5.3.2.2 Urine

In urine samples APAP and its glucuronide, sulfate, and cysteine conjugates, as well as PAP-G were detected in the ^{1}H-NMR spectra obtained from APAP treated, but not control animals. There were a number of resonances seemingly due to drug metabolites at lower concentrations, and other overlapping peaks in the aromatic region which made integration and assignments of all drug metabolites difficult. The major metabolite detected was APAP-G, which was present in the largest amounts throughout the experiment, followed by APAP for the first 12h after the commencement of drug administration, after which PAP-G was seen to provide the second most abundant APAP metabolite. Two further conjugated metabolites, APAP-S and APAP-C were observed in urine samples at relatively low intensities (Figure 5.10).

5.3.2.3 Soluble aqueous tissue extracts

In the renal extracts APAP-G was the most abundant metabolite detected, followed by unchanged APAP and APAP-C, with PAP-G detected in trace amounts. Similarly to urine there seemed to be a number of drug related metabolites at low concentrations which were difficult to assign and integrate. In the hepatic extracts obtained at 12h post the start of drug administration, unchanged APAP had the highest abundance, followed by APAP-G and APAP-GSH. PAP-G was also present, at low intensities, in these samples (Figure 5.10).

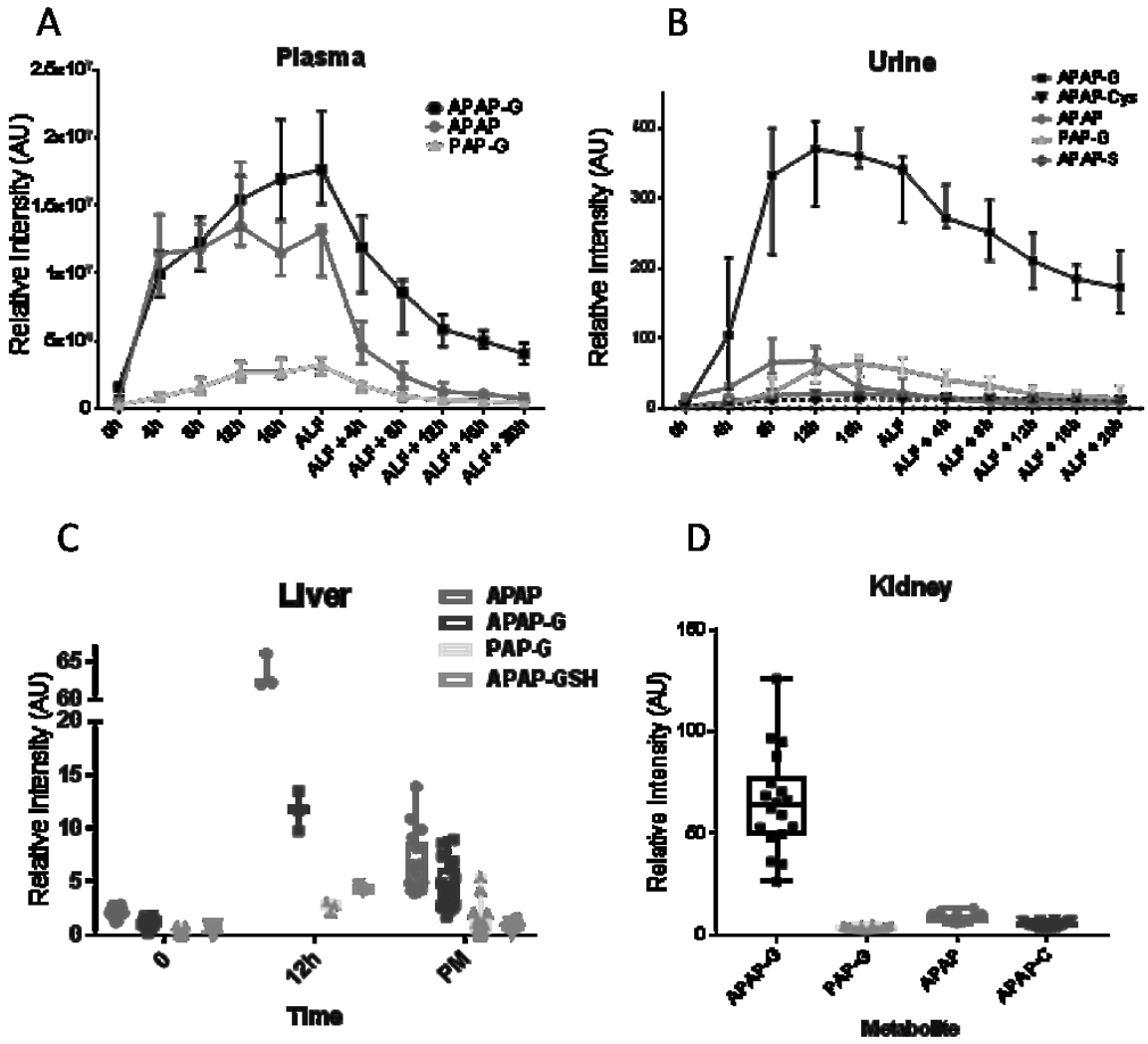


Figure 5.10 APAP and metabolites measured by ^{1}H-NMR spectroscopy in biofluids and tissue extracts. A) Plasma: median concentration and interquartile range of APAP and 2 metabolites identified in plasma over the time course of the experiment (n=18).
B) Urine: Median concentration and interquartile range of APAP and 4 metabolites identified in samples across the time course of the experiment (n=12)
C) Liver aqueous extracts: APAP plus 3 metabolites identified in samples taken at predose (n=17), 12 hours (n=3) and at post-mortem (n=17) Boxes represent median and interquartile range while whiskers represent the full range, all data points are shown.
D) Kidney aqueous extracts: APAP and 3 metabolites identified in samples taken post mortem (n=18). Boxes represent median and interquartile ranges while whiskers represent the full range, all data points are shown.
Abbreviations: APAP: paracetamol; APAP-Cys: paracetamol cysteinyl conjugate; APAP-G: paracetamol glucuronide; APAP-GSH: paracetamol glutathione conjugate; APAP-S: paracetamol sulfate; ALF: acute liver failure; AU: arbitrary units; PAP-G: p-aminophenol glucuronide.

5.3.3 Endogenous metabolism changes

Results of changes to endogenous metabolism are summarised in Table 5.14.

5.3.3.1 Plasma

In the ^{1}H-NMR spectra generated from plasma samples 14 metabolites were identified, and area integrated, including valine, isobutyrate, alanine, acetate, pyruvate, glutamine, citrate, proline, lactate, glucose, tyrosine,

phenylalanine and formate, shown in the representative spectra in Figure 5.6. In addition, overlapped resonances for creatine and creatinine were also noted as a combined metabolite integral. Following up to 8 hours of APAP treatment glutamine was significantly decreased in concentration in the plasma of drug treated animals, while tyrosine concentrations were increased. From 16 hours post commencement of APAP administration the amount of pyruvate detected in plasma was significantly increased in drug treated animals, plasma glucose and lactate and concentrations were significantly increased from the onset of ALF, while citrate was increased in APAP treated animals compared to controls from 4 hours after the onset of ALF. Glutamine concentrations in the APAP treated animals increased in the latter stages of ALF. Figure 5.11shows all the metabolites measured and integrated in plasma.

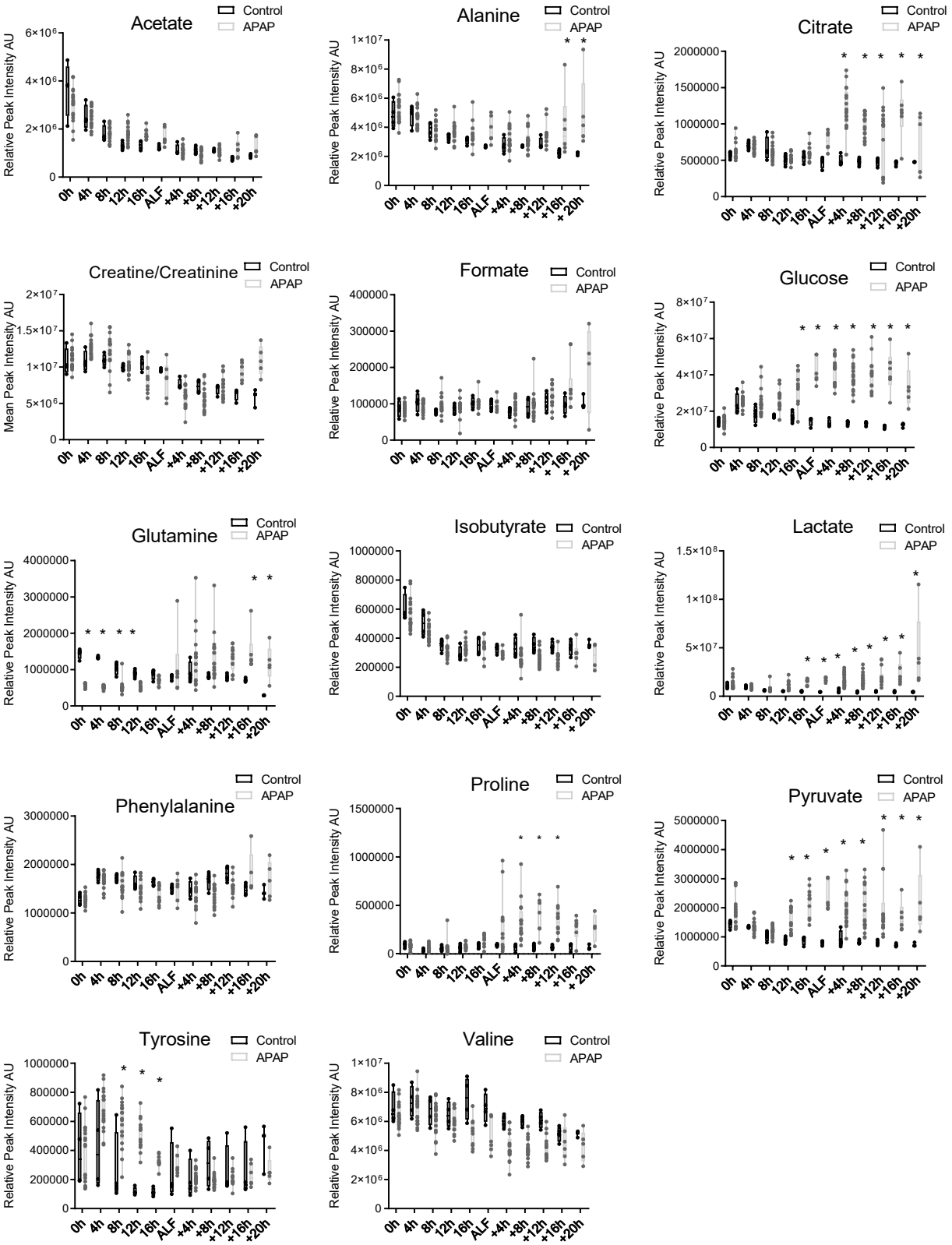


*Figure 5.11 Endogenous metabolism changes in plasma. Kruskal-Wallis with FDR corrected multiple comparisons. * q<0.05.*
Abbreviations: ALF: acute liver failure; APAP: paracetamol; AU: arbitrary units; FDR: false discovery rate.

5.3.3.2 Urine

In the ^{1}H-NMR spectra generated from urine samples, 9 endogenous metabolites were identified and integrated, these were choline, creatine, creatinine, glucose resonances, lactate, phosphocholine, dimethylamine, trimethylamine and trimethylamine N-oxide (TMAO), the most abundant of which can be seen in Figure 5.12. During APAP treatment, but prior to the onset of ALF, there were significant decreases in choline, creatine and creatinine concentrations and also a significant increase in the amount of lactate detected. In APAP-treated animals post ALF, quantities of trimethylamine and dimethylamine were significantly decreased whilst those of glucose were significantly increased compared to controls. Alanine concentrations were apparently higher than in controls following ALF however, this difference was not statistically significant.

5.3.3.3 Aqueous soluble tissue extracts

In hepatic extracts, no significant differences were observed at 0h or 12h, succinate, creatine, inosine and isobutyrate were significantly increased in the APAP treated animals post mortem as shown in Figure 5.13. There was also an apparent increase in alanine concentration the liver extracts of in APAP-treated animals post-mortem, but this was not statistically significant. In kidney extracts, 10 metabolites were identified and integrated. Glucose, succinate and alanine were significantly increased in the APAP-treated animals, compared to control at post mortem.

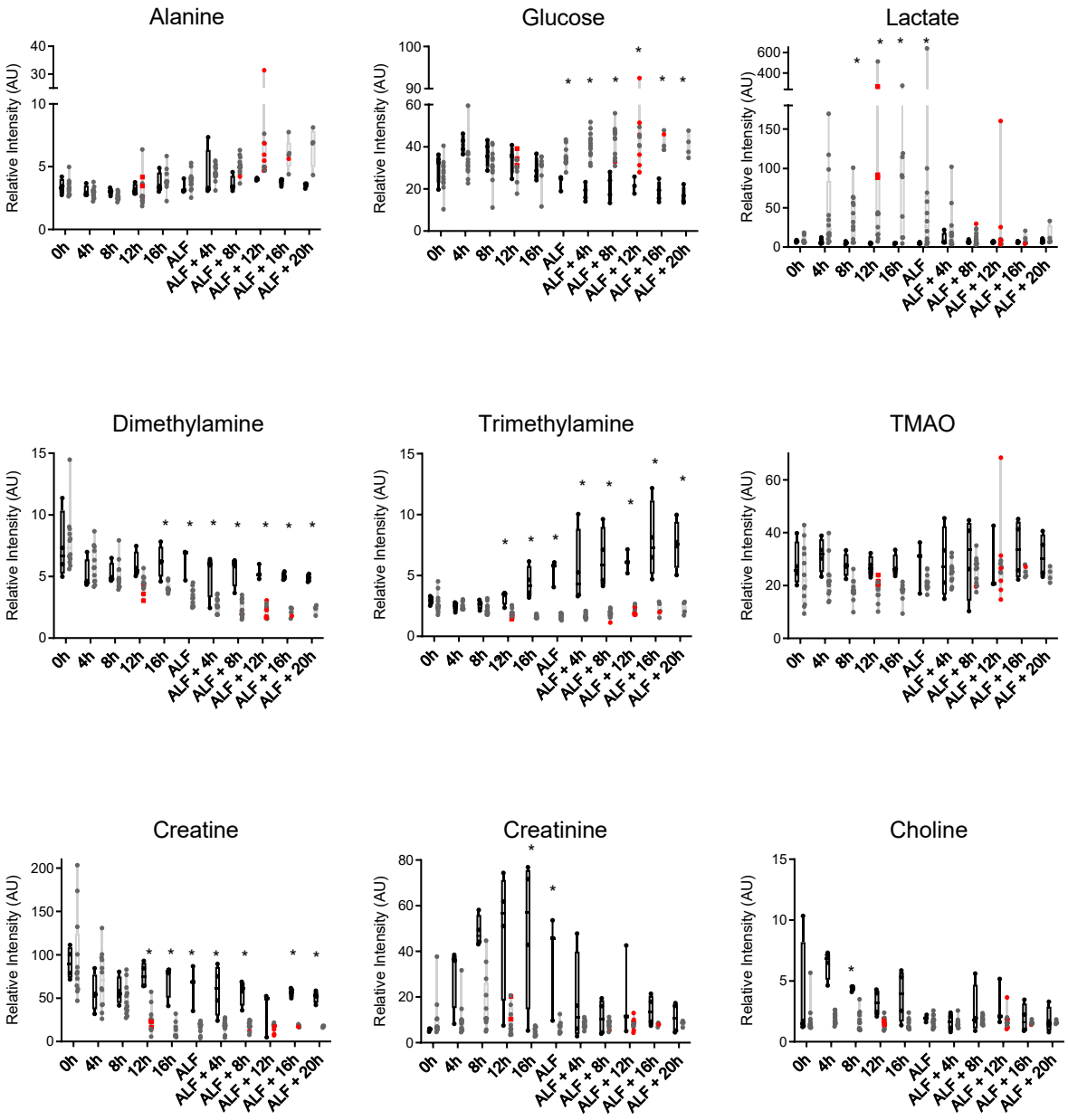


*Figure 5.12 Endogenous metabolism changes in urine. Kruskal-Wallis with FDR corrected multiple comparisons. * q<0.05. Red colour represents final time point for that animal prior to ALF or prior to death. Abbreviations: ALF: acute liver failure; APAP: paracetamol; AU: arbitrary units; FDR: false discovery rate; TMAO: trimethylamine N-oxide.*

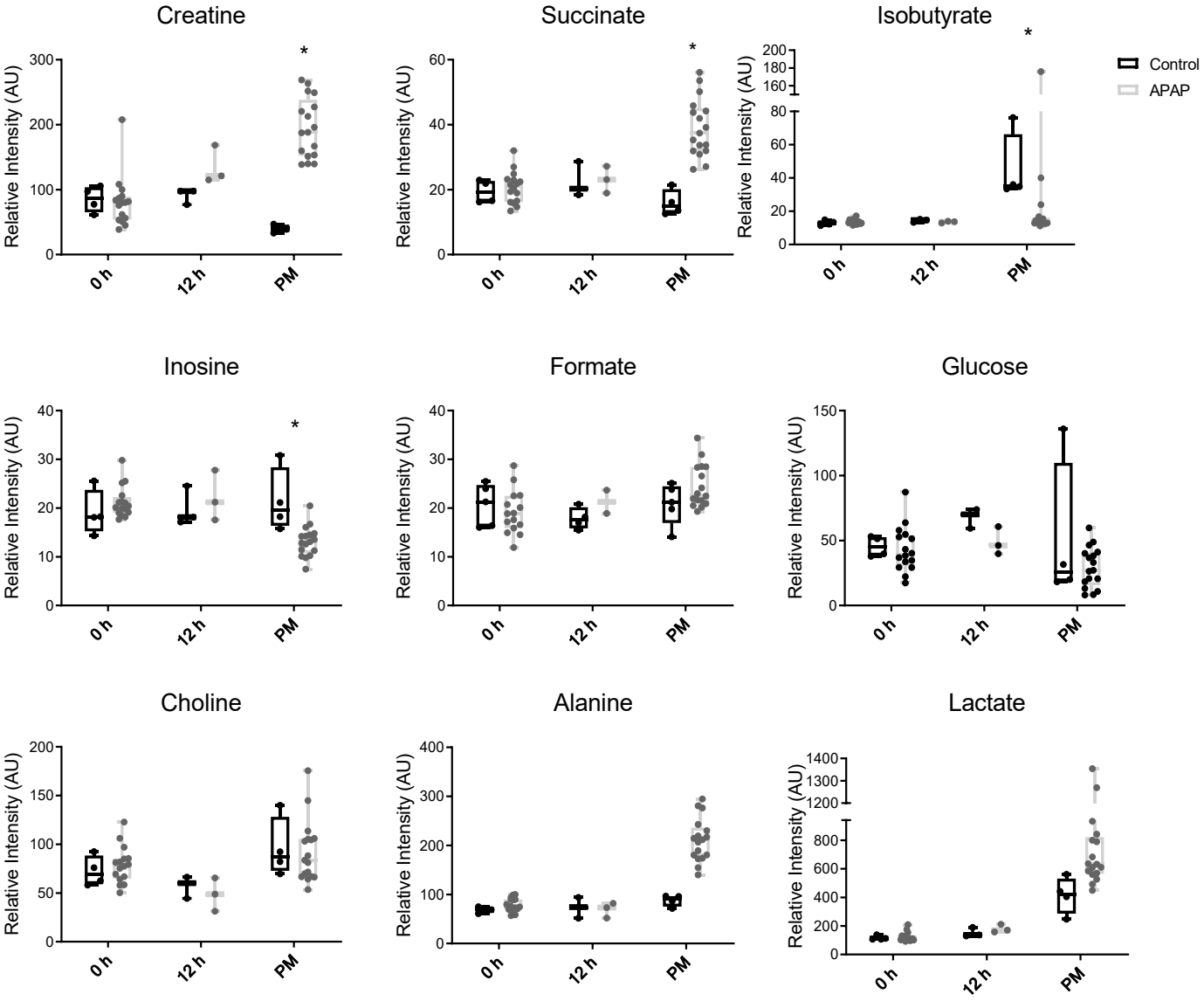


*Figure 5.13 Endogenous metabolism changes in liver extracts from pigs treated with paracetamol, at 0 h, 12 h and post-mortem. Kruskal-Wallis with FDR corrected multiple comparisons. * q<0.05. Abbreviations: AU: arbitrary units; FDR: false discovery rate; PM: post-mortem*

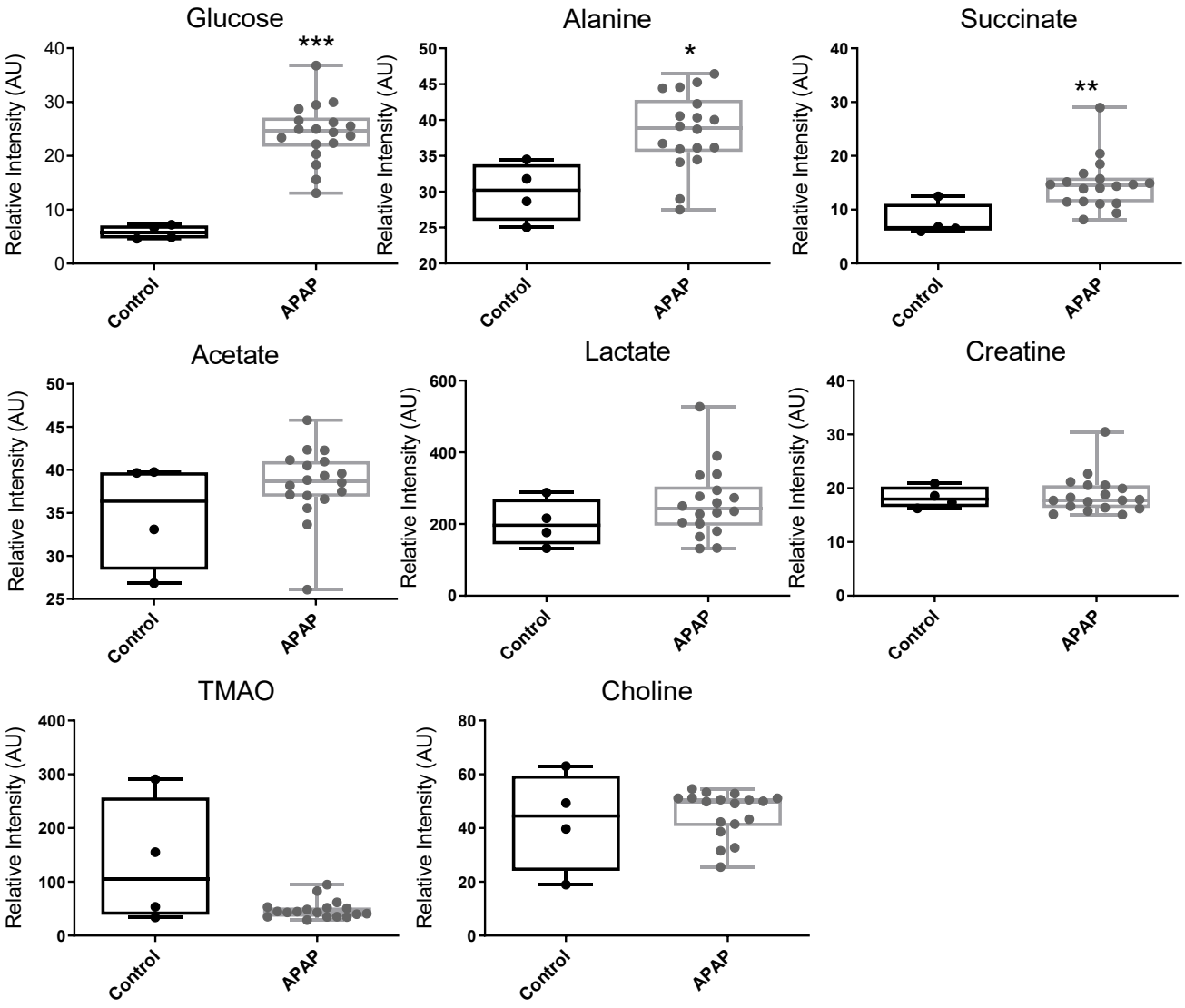


Figure 5.14 Significant changes to endogenous metabolites in kidney extracts from pigs treated with paracetamol, at 0 h and post-mortem.
*Mann-Whitney **p<0.01 ***p<0.001*
Abbreviations: APAP: paracetamol; AU: arbitrary units; PM: post-mortem; TMAO: trimethylamine N-oxide.

Table 5.14 Summary of endogenous metabolism changes in the pig pre- and post- paracetamol induced ALF, as measured by 1H-NMR spectroscopy, across all matrices.

Sample Matrix	Metabolite Changes Pre-ALF	P value	Adjusted p value (q)	Metabolite Changes Post-ALF	P value	Adjusted p value (q)
Plasma	Pyruvate	0.0001	0.0002	Pyruvate	0.0005	0.0006
	Lactate	0.002	0.0012	Lactate	<0.0001	0.0002
	Glucose	0.0172	0.009	Glucose	<0.0001	<0.0001
	Glutamine	0.0002	0.0007	Glutamine	0.0018	0.0037
	Tyrosine	<0.0001	0.0002	Alanine	0.0047	0.308
				Citrate	<0.0001	0.0002
Urine	Dimethylamine	0.0637	0.0418	Dimethylamine	0.0012	0.0046
	Trimethylamine	<0.0001	0.0001	Trimethylamine	<0.0001	0.0001
	Choline	0.0025	0.0286	Glucose	<0.0001	0.0004
	Creatine	0.0003	0.0011	Creatine	0.0075	0.0073
	Creatinine	0.0006	0.0068			
	Lactate	0.0001	0.0012			
Liver	No significant changes			Creatine	<0.0001	<0.0001
				Isobutyrate	0.0117	0.0245
				Succinate	<0.0001	<0.0001
				Inosine	0.0088	0.0184
				Alanine†	0.0236	0.0743
				Lactate†	0.224	0.706
Kidney	No Data			Glucose	0.0003	Not Applicable
				Succinate	0.0074	
				Alanine	0.0104	

Q values calculated using FDR corrected Kruskal-Wallis. Red=metabolite increase Blue=Metabolite decrease †=changes not statistically significant
Abbreviations: ALF: acute liver failure; FDR: false discovery rate; NMR: nuclear magnetic resonance.

5.3.4 UHPLC-MS/MS analysis of plasma samples

5.3.4.1 APAP metabolism

APAP and its metabolites were separated by the chromatographic gradient as shown below in Figure 5.15, which shows the separation and relative peak height of each metabolite in a representative sample at 4 hours after APAP treatment began. Plasma concentrations of APAP and metabolites, quantified by UHPLC-MS/MS using stable isotope-labelled internal standards, or in the case of PAP-G monitored and semi-quantified relative to an external standard curve, showed that APAP-G was the major circulating metabolite. APAP itself had the second highest concentration throughout, with the second most abundant metabolite detected being PAP-G. Both APAP-S and APAP-C were also quantified, but were at relatively low concentrations, while APAP-GSH and APAP-NAC were not detected, as is shown in Figure 5.16.

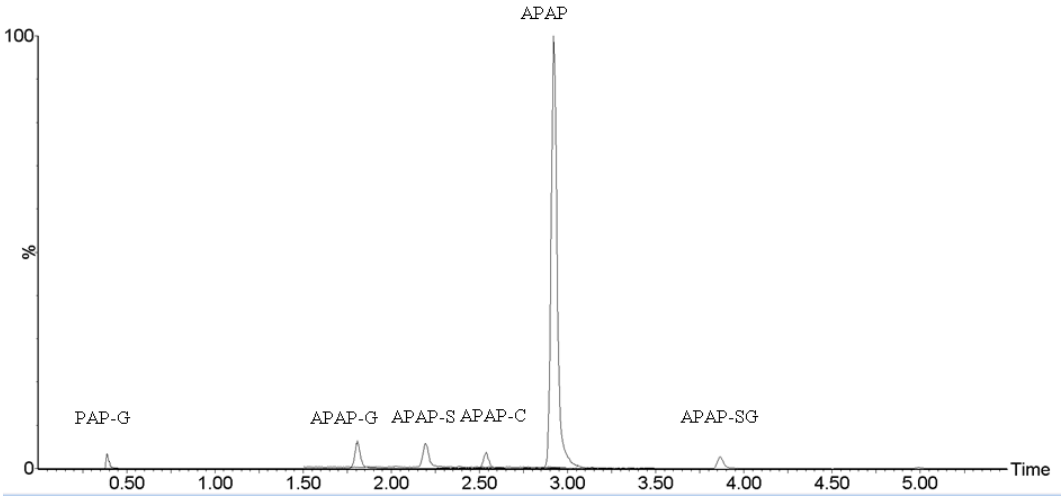


Figure 5.15 Representative total ion chromatogram of APAP metabolites in porcine plasma after 4 hours of dosing.
Abbreviations: APAP: paracetamol; APAP-C: paracetamol cysteinyl conjugate; APAP-G: paracetamol glucuronide; APAP-S: paracetamol sulfate; APAP-SG: paracetamol glutathione conjugate; PAP-G: p-aminophenol glucuronide.

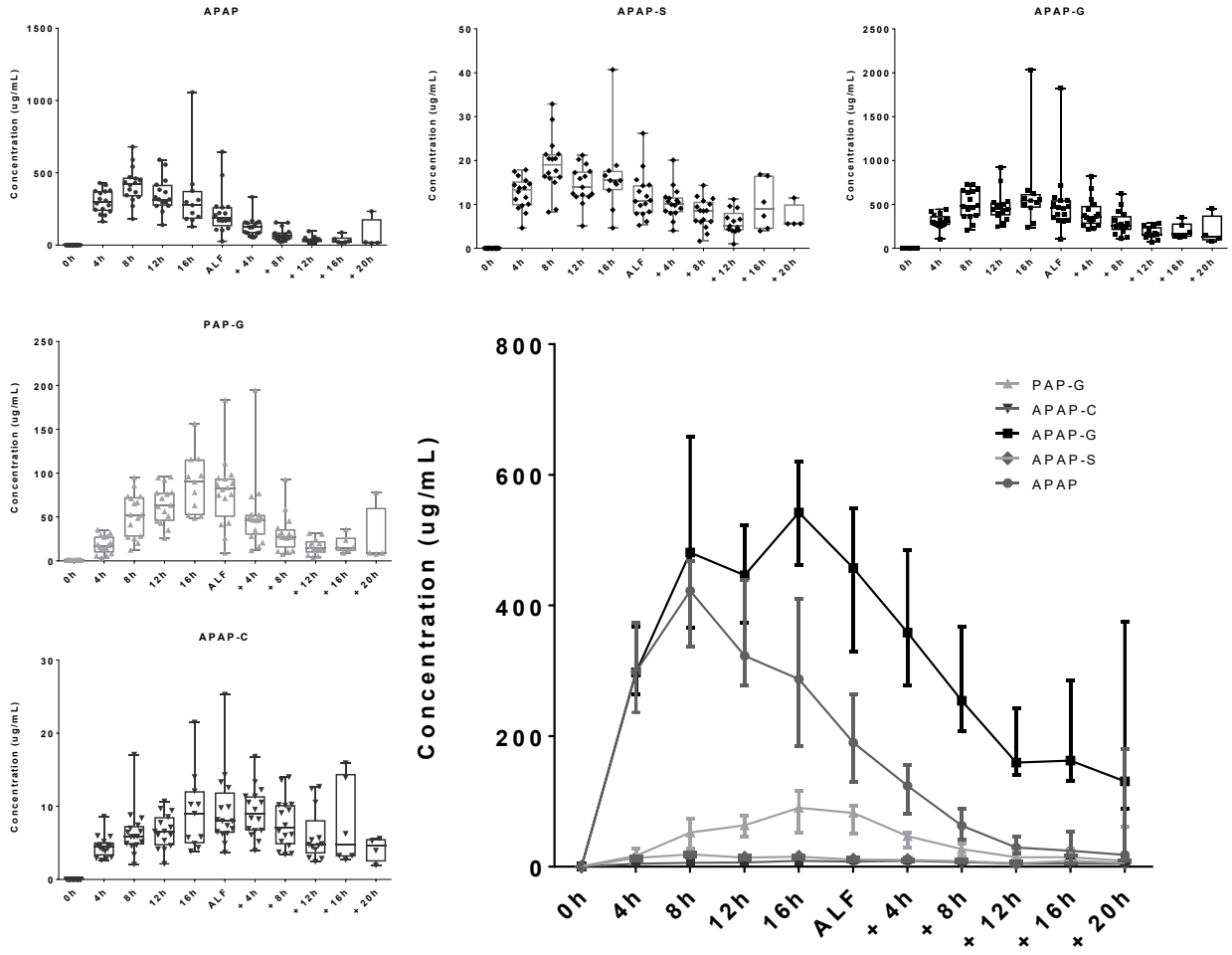


Figure 5.16 Metabolites quantified in plasma using the UHPLC-MS/MS method.
Abbreviations: ALF: acute liver failure; APAP: paracetamol; APAP-C: paracetamol cysteinyl conjugate; APAP-G: paracetamol glucuronide; APAP-S: paracetamol sulfate; PAP-G: p-aminophenol glucuronide; UHPLC-MS/MS: ultra-high-performance liquid chromatography coupled tandem mass spectrometry.

5.3.4.2 Glutathione metabolism

GSH and related biomarkers were measured in porcine plasma. As previously discussed in Chapter 4, this method is affected by matrix effects, which have not yet been assessed in plasma or porcine plasma, and these effects were particularly pronounced with this set of samples, and therefore only results from metabolites which had internal standards and that were detectable in the plasma are displayed in Figure 5.17. In Table 5.15, the analytes for which curves were linear and QCs met acceptance criteria are displayed. Of these analytes, homocysteine and homocystine were below the limit of detection in samples, other

metabolites (choline, methionine, GSSG) were affected by interference or matrix effects in the samples despite curves and QCs being linear and acceptable (curves and QC are prepared matrix free).

Table 5.15 Linearity and percentage of curves and QCs which met acceptance criteria for application of the glutathione method to porcine plasma.

Analyte	linearity	curve pass (%)	LQC (%)	MQC (%)	HQC (%)	Total (%)
choline	0.99	86	83	101	100	94
cystathionine	0.992	86	100	100	100	100
cystine	0.993	86	83	67	100	83
glutamine	0.995	100	67	100	100	89
GSSG	0.993	100	67	67	83	72
homocysteine	0.996	100	100	100	100	100
homocystine	0.996	100	100	100	100	100
hypotautine	0.981	79	50	100	67	72
methionine	0.995	100	0	100	100	67
5-oxoproline	0.994	93	83	100	100	94
SAMe	0.999	100	100	100	100	100
taurine	0.993	100	100	100	100	100

Abbreviations: HQC; high quality control; GSSG: oxidised glutathione; LQC: low quality control; MQC: mid quality control; QC: quality control; SAMe; s-adenosyl methionine

Pooled QCs and over-spiked QCs were analysed alongside samples and the mean concentration and CVs of these for analytes are given in Table 5.16, along with the mean percentage difference between the measured over-spiked concentration and the expected concentration. As all these analytes had internal standards, both the CVs and % bias from expected concentration should be 20% or less. The CV of the three repeated injections of the pooled QC are below 20% for all analytes except hypotaurine, although the CV was only slightly above at 21%, and this may be due to the concentration being towards the LLOQ of the standard curve. The overspiked QCs were more variable for cystathionine with a CV just over 30%. The bias over the over-spiked concentration from nominal concentration was not within 20% for 5-OP, SAMe or cystathionine which suggests there could be some kind of ion enhancement despite the presence of the IS for these analytes.

Table 5.16 Mean concentrations and CVs of pooled QCs and QCs over-spiked with 50% of the HQC, plus the mean percentage bias of the over-spiked concentration from the nominal concentration, for application of glutathione pathway assay to porcine plasma.

	Pooled QC mean conc. (ng/mL)	CV pooled QC	Over spiked QC mean conc. (ng/mL)	CV over-spiked QC	% Bias from nominal conc.
cystathionine	35	2.84	171	31.9	36.3
cystine	446	2.55	620	19.0	-12.8
glutamine	11189	9.91	12974	0.7	-10.8
hypotaurine	45	21.2	265	21.4	10.4
5-oxoproline	2682	1.05	2998	2.6	58.4
SAMe	137	6.45	275	8.2	38.3
taurine	2078	3.29	4196	0.3	5.87

Abbreviations: CV: coefficient of variance; QC: quality control; SAMe; s-adenosyl methionine.

5-OP concentrations were at or above the ULOQ for the control samples, and over the ULOQ for most of the APAP treated samples, so will not be fully quantitative. However, it was clear that there were large increases in 5-OP in plasma from APAP treated animals at all time-points from 4 hours onwards. SAMe concentrations were also increased from 4h onwards. Glutamine was increased only at the end point of the experiment, which reflects the increases seen post ALF in ^{1}H-NMR spectroscopy although the significant decreases pre-ALF were not seen with UHPLC-MS/MS. There were no significant changes to cysteine, cystathionine, hypotaurine or taurine following APAP administration in the pigs, or at ALF or death. Metabolite concentrations are summarised in Figure 5.17.

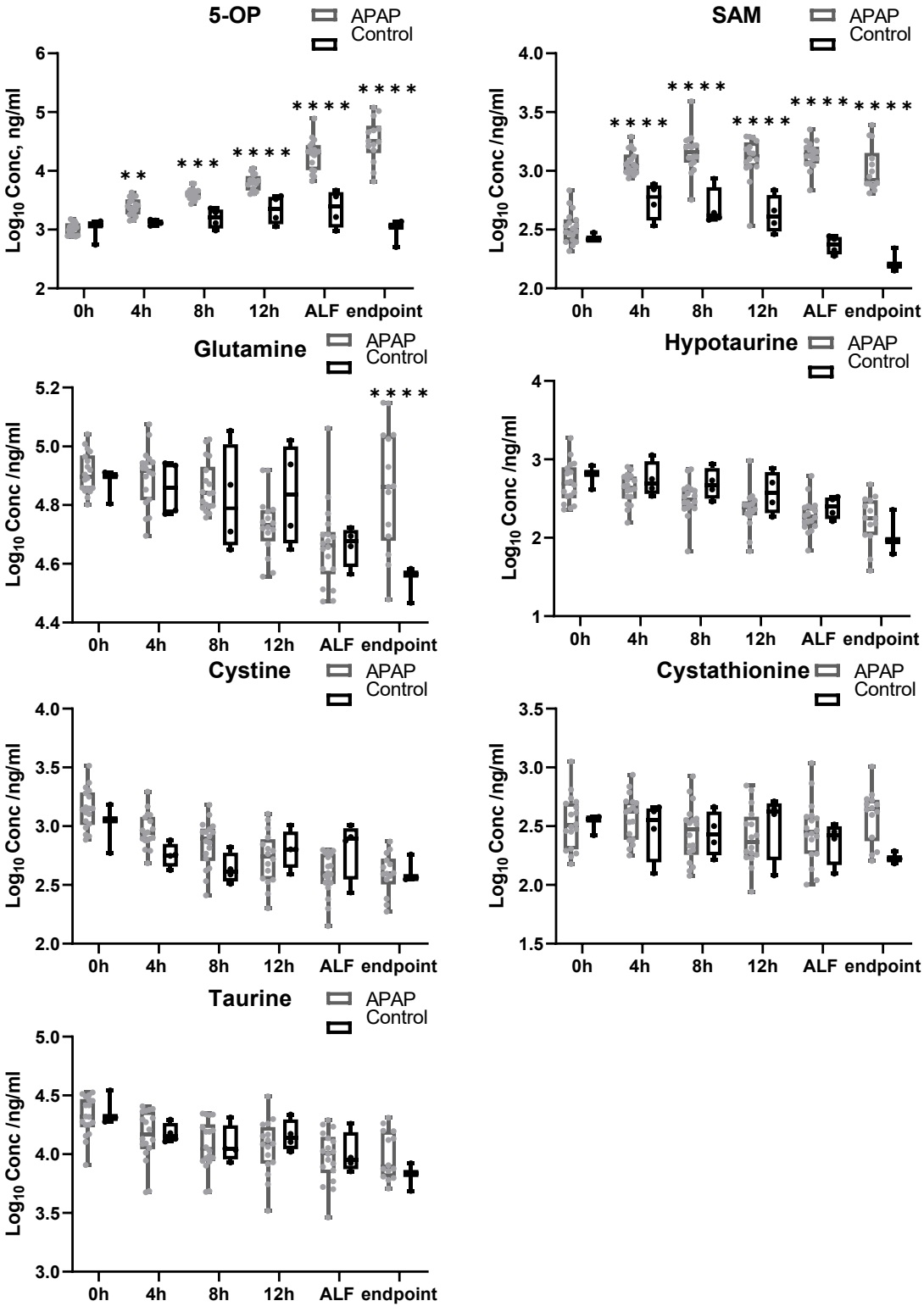


Figure 5.17 GSH metabolites measured in porcine plasma. Data were log transformed and analysed by One-Way ANOVA with FDR corrected multiple comparisons. q<0.03(*), q<0.002 (**), q<0.0001 (***), q<0.0001(****).
Abbreviations: ALF: acute liver failure; APAP: paracetamol; FDR: false discovery rate; 5-OP: 5-oxoproline; SAM: s-adenosyl methionine.

5.4 Discussion

5.4.1 Endogenous metabolite changes measured by NMR spectroscopy

There were endogenous changes in metabolism in the pig in response to APAP-induced toxicity which represented 3 main pathways; energy metabolism, amino acid metabolism and choline metabolism. The changes to energy metabolism are summarised in Figure 5.18**.**

Increased concentrations of a number of components of the citric acid cycle, such as succinate, have been previously reported in different animal models including the mouse and pig (Coen et al. 2003; Coen et al. 2004; Dabos et al. 2011; Kyriakides 2016). In the current model there were also increased concetrations of citrate. This coupled with the Pre-ALF increase in circulating lactate, pyruvate and alanine in plasma indicates that there was likely a hepatic switch to glycolysis early on after APAP treatment due to mitochondrial dysfunction. In accordance with previous studies in animals models, but contrary to the report by Dabos et al., an increase in glucose in the kidney was noted here, suggesting gluconeogenesis was upregulated in the kidney to compensate for the reduction in hepatic energy metabolism (Dabos et al. 2011). There was also significantly increased circulating glucose in the plasma from 16 hours of APAP treatment onwards, and significantly increased urinary glucose concentrations from ALF until death.

Glutamine was elevated at death in these animals as is often seen in humans with ALF, and glutamine has been proposed to be linked to hepatic encephalopathy as it breaks down to form toxic ammonia in the brain. A number of factors may contribute to increased glutamine, including muscle upregulation of glutamine synthase (Rao et al. 2012). Urinary decreases in TMA, DMA and TMAO concentrations may show alterations to the gut microbiota (Ussher et al. 2013).

Changes to creatine and creatinine in the cirulation, urine and liver have also been previously seen in APAP toxicity and ALF (Kyriakides 2016) in the mouse. Creatinine increases in serum and decreases in urine are commonly indicative of poor renal clearance. Creatinine is synthesised from creatine in the muscle and the increase in creatine may be due to a change in muscle energy metabolism (Wyss and Kaddurah-Daouk 2000). There was also a significant decrease in hepatic inosine; adult porcine erythrocytes are inefficient at using glucose as an energy source, and hepatic inosine has been suggested as a substitute for glucose (Watts et al. 1979). Inosine has been suggested to reduce methaemoglobin in-vitro in the pig compared to glucose;

methaemoglobin reductase activity was measured in porcine erythrocytes which were incubated with medium containing either glucose or inosine (Sartorelli et al. 1996).

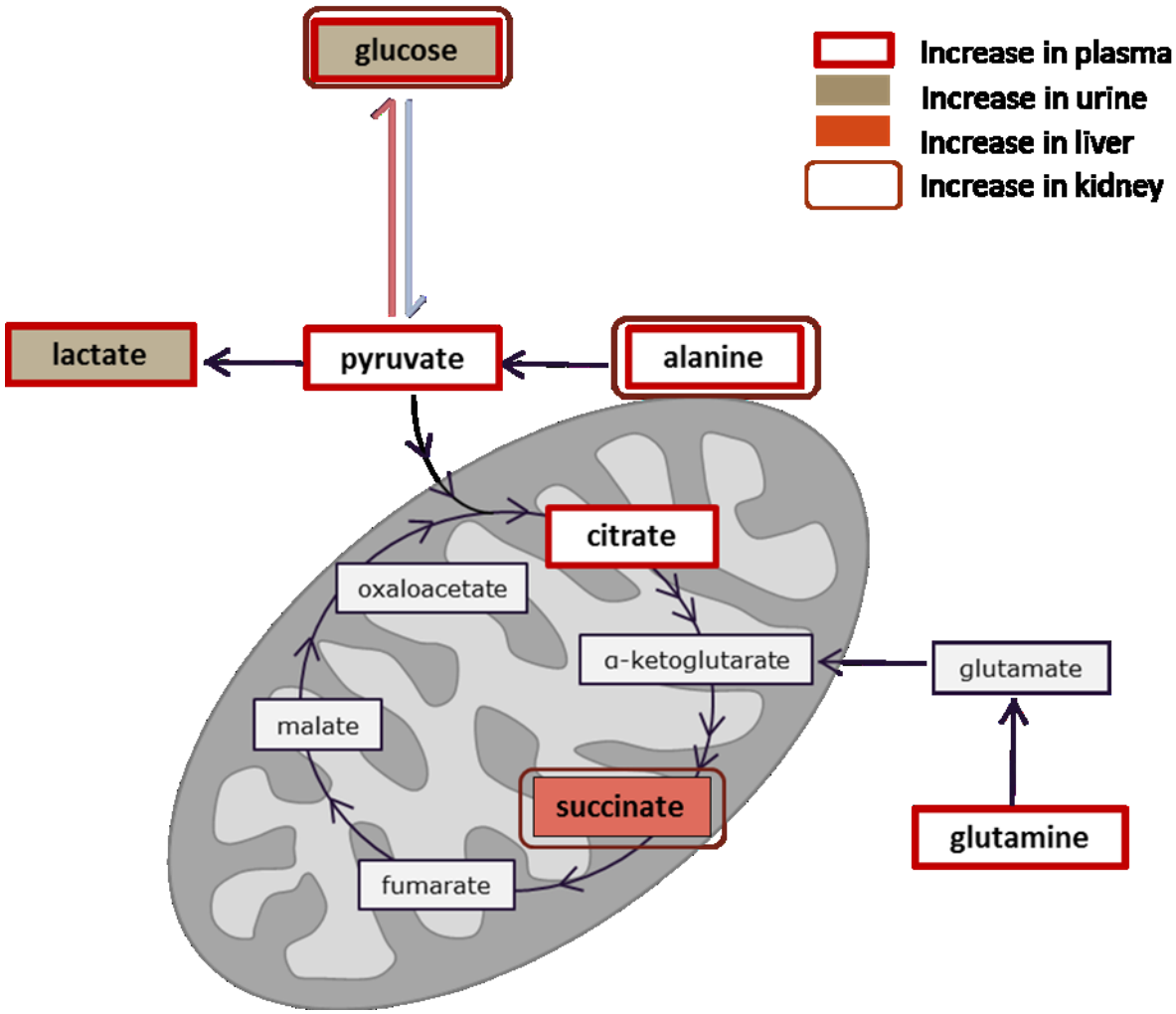


Figure 5.18 Diagram showing the key components of the TCA cycle within the mitochondria some of which were seen to change in one or more of the matrices and biofluids we investigated, including plasma, urine, liver and kidney extracts. The TCA cycle components have been colour coded to show in which of the matrices these components were increased in as per the key within the figure.
Abbreviations: TCA: tricarboxylic acid.

5.4.2 GSH metabolism changes measured by UHPL-MS/MS

Metabolites that could not be detected by NMR spectroscopy but were measured by the GSH method which changed significantly following APAP administration in the pig were 5-OP and SAMe. The increase in 5-OP concentration reflected what was seen in the mouse in Chapter 4, and also would be expected based on literature, as the pigs in this study were suffering with metabolic acidosis and 5-OP concentrations are often

increased in humans during APAP induced metabolic acidosis (Liss et al. 2013). It should be noted that 5-OP was significantly increased at a much earlier time point than ALF was developed in any animal, and therefore may be a good early biomarker of liver injury and metabolic acidosis. SAMe was decreased following APAP treatment in the livers and serum of the mouse model in Chapter 4 and previous reports suggest that MAT enzymes are down-regulated in the mouse following a single APAP dose (Brown et al. 2010). The increased circulating SAMe concentrations in this porcine model may suggest that in this model the MAT enzyme expression and activity was instead increased following repeated APAP administration in the pig, the mice were starved before APAP administration and SAMe did not increase where NAC was administered, therefore as the pigs were being supplied with the "viamin14" mix containing amino acids, they may have had ample methionine available and therefore be able to produce greater quantities of SAMe (Jung et al. 2008). In addition, a previous study has reported that in neonatal pigs, intestinal MAT is highly upregulated following sulfur amino acid deprivation, leading to increased SAMe concentrations (Bauchart-Thevret et al. 2009), so it is possible that intestinal SAMe could contribute to increased circulating SAMe. Unlike in the mouse model studied in Chapter 4, there were no differences in the circulating hypotaurine, cystathionine or taurine concentrations.

5.4.3 APAP metabolism and its relation to toxicity in the pig

Whilst APAP is widely used in veterinary practice in the pig, and some pharmacokinetic studies on APAP have been performed in minipigs (Suenderhauf et al. 2014), detailed metabolic studies on the biotransformation of APAP do not seem to have been undertaken (Helke et al. 2016). In terms of sulfation and glucuronidation, which represent the major conjugation reactions that APAP undergoes in humans, glucuronidation seems to predominate in the pig over sulfation which appears to represent only a minor route. Similar results were seen for the metabolism of *p*-cresol, a gut microbial metabolite of tyrosine (and a phenol with structural and metabolic similarities to APAP) with pig forming the glucuronide rather than sulfate metabolite, which dominates metabolism in man (Merrifield et al. 2011; Thorn et al. 2012). These observations are, in accordance with previous reports, that the pig has a reduced sulfation capacity compared to human (Capel et al. 1972). However, sulfation is not completely absent and low concentrations of the sulfate conjugate were

detected in the circulation. Interestingly, the second most abundant metabolite we measured in plasma and urine was PAP-G, which may have been formed from PAP following the N-deactylation of APAP.

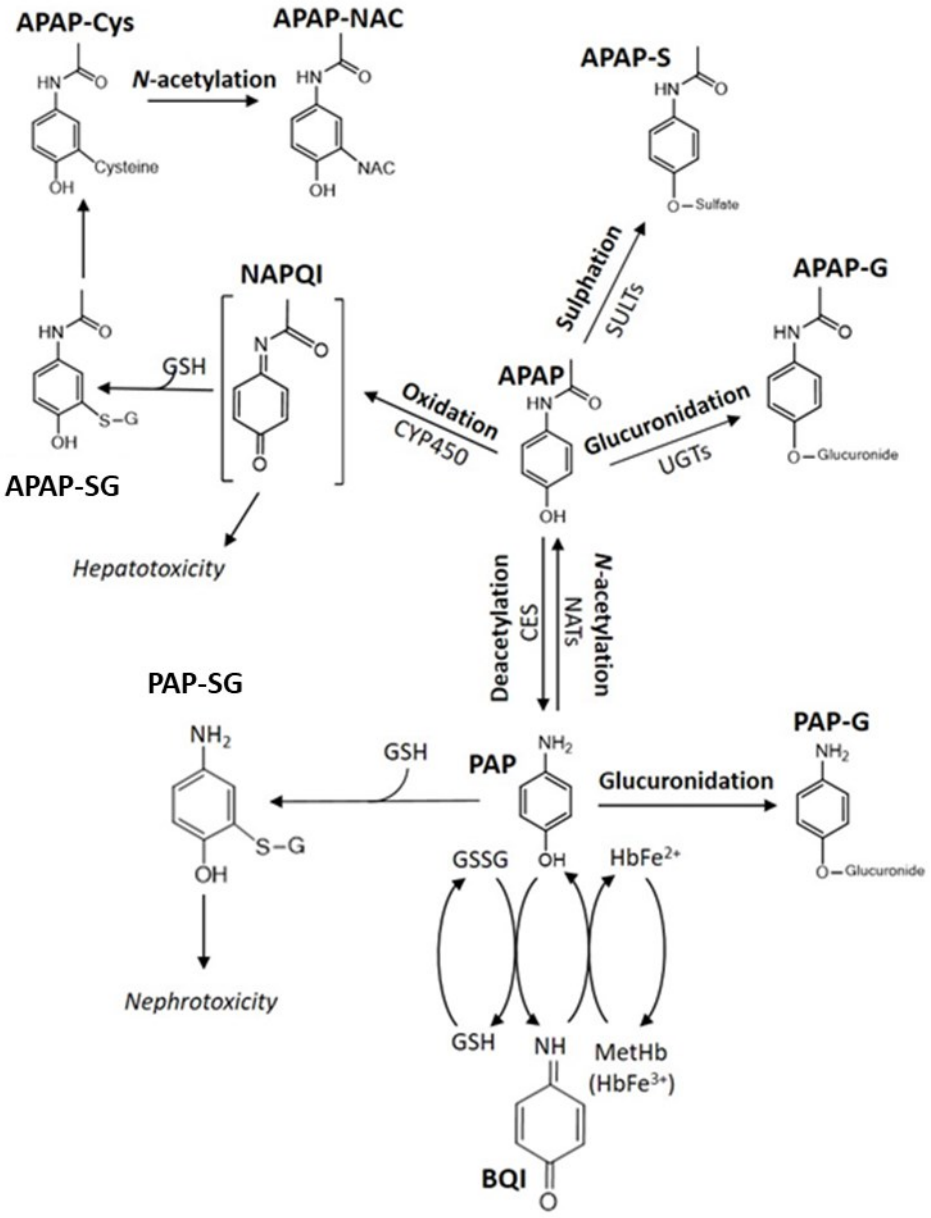


Figure 5.19 Proposed mechanism of APAP metabolism in the pig including the formation of PAP-G from PAP and the potential mechanism of metHb formation by PAP in red blood cells, and the formation of a PAP-GSH conjugate which may have a role in nephrotoxicity.
Abbreviations: APAP: paracetamol; APAP-C: paracetamol cysteinyl conjugate; APAP-G: paracetamol glucuronide conjugate ; APAP-NAC: paracetamol n-acetyl-cysteine conjugate; APAP-OMe: 3-methoxy paracetamol; APAP-S : paracetamol sulfate conjugate; APAP-SG: Paracetamol glutathione conjugate; BQI: benzoquinone imine; CES: Carboxyl esterase; CYP: Cytochrome p-450; MetHb: methaemoglobin; NAPQI: n-acetyl-p-benzoquinone imine; NAT: n-acetyl transferase; PAP: p-aminophenol; PAP-G: p-aminophenol glucuronide; PAP-SG: p-aminophenol glutathione conjugate; SULTs: sulfotransferase enzymes; UGT: UDP-glucuronosyl transferase

PAP-G was formed to a greater extent in the pig than in other species, presumably due to differences in the key drug metabolising enzymes responsible for both de- and re-acetylation of aromatic amides and amines such as APAP and PAP. The production of PAP provides a potential explanation for the methaemoglobin and nephro-toxicity observed in pigs dosed with APAP. Indeed the phenomenon of increased methaemoglobin on APAP dosing to pigs is something which has been widely reported in previous attempts to produce a large animal model of APAP-induced ALF (Hennebruns et al. 1988). More recent models, including the one reported here, have taken care to maintain the metHb below a threshold to ensure survival of the animals (Lee et al. 2013; Newsome et al. 2010; Thiel et al. 2011). However, despite monitoring of APAP concentration being used to maintain methaemoglobin no correlation between maximal APAP concentration and methaemoglobin has been seen (Newsome et al. 2010). Previously it has been suggested that the production of methaemoglobin in pigs administered APAP was the result of erythrocyte GSH depletion and poor glucose uptake (Hennebruns et al. 1988; Newsome et al. 2010). However, the well known association of aromatic amines, including PAP, with methaemoglobin formation (Harrison and Jollow 1987) provides a more obvious mechanism. PAP has previously been suggested as the cause of APAP induced methaemoglobinemia in cats and dogs (McConkey et al. 2009). In most species, N-acetylation reactions in the liver are catalysed by N-acetyl transferase (NAT) enzymes NAT1 and NAT2, while de-acetylation is catalysed by carboxylesterases (CES), including CES1 and CES2 and arylacetamide deacetylase in humans. However, the rates of these reactions vary significantly amongst species (Jones et al. 2016; McConkey et al. 2009; Watanabe et al. 2010). APAP has been shown to form PAP by *N*-deacetylation in man as a minor route of metabolism, and to a greater extent in rat with, in both cases, the majority being detoxified by being rapidly re-acetylated to APAP in a so called 'futile-deacetylation' reaction (Nicholls et al. 1995). The formation of methaemoglobin in the dog is attributed to a lack of either NAT1 or NAT2 enzymes and in cats to be due to their only expressing NAT1 (McConkey et al. 2009). C57BL/6 mice have been shown to be slow to deacetylate APAP, but rapid to re-acetylate and, whilst methaemoglobin was formed from APAP in NAT1/2 knockout mice, it was not comparable to the levels seen

in dogs or cats, suggesting the PAP accumulation is due not simply to deficiency in NAT2, but may also be related to the rate of de-acetylation of APAP (McConkey et al. 2009).

In addition to methaemoglobin, APAP administration to pigs in this study was associated with nephrotoxicity and the production of PAP represents a possible cause of this. For example, in rats, PAP has been reported to be a potent nephrotoxin (C. R. Green 1969 ; Gartland et al. 1990), primarily effecting the proximal tubules (Fowler et al. 1993; Fowler et al. 1994; Yang et al. 2007), causing both tubular dilation and necrosis. Similar pathological changes were observed here in the renal histopathology of the porcine model. The exact mechanism of PAP-induced nephrotoxicity is not fully understood; however, it has been postulated that the mechanism involves formation of the PAP-glutathionyl conjugate as PAP-GSH has been reported to be more nephrotoxic than PAP itself (Fowler et al. 1993; Fowler et al. 1991). Furthermore, PAP-GSH-induced nephrotoxicity has been reported to lead to glycosuria, which could explain the observed increase in urinary glucose levels seen in the current work (Fowler et al. 1991). cγ-glutamyltransferase (GGT) is predominantly localised in the brush border membrane of renal proximal tubules, the area susceptible to PAP and PAP-GSH mediated nephrotoxicity. Inhibition of GGT has been reported to be protective against PAP-GSH mediated nephrotoxicity (Fowler et al. 1994).

It is likely that both the methaemoglobin and renal toxicity seen in the pig in this study were caused by the de-acetylation of APAP to PAP. Following its formation PAP was further metabolized by the conjugation of a significant amount to the glucuronide conjugate. PAP-G was the only PAP metabolite detected suggesting that, like APAP, sulfation is a minor route for the metabolism of PAP, and it is unclear from this work whether or not reacetylation, to reform APAP, as observed in other species occurred to any extent. Further studies, utilising a labelled form of APAP in the acetyl moiety, would be required to confirm the extent of any futile deacetylation in the porcine model. Figure 5.19displays the proposed mechanism for APAP metabolism in the pig.

Lastly in terms of toxic effects of APAP in the pig, the detection of small amounts of APAP-C, a degradation product of APAP-GSH, in the urine and plasma provides evidence for the formation of the reactive metabolite

NAPQI from APAP and implies that this oxidative route of metabolism may be responsible for the heptoxicity seen in this model similar to that observed in clinical studies.

5.4.4 Conclusions

The pig is susceptible to hepatotoxicity and renal toxicity in response to paracetamol dosing over a period of 20 hours. The paracetamol-induced hepatotoxicity in the pig shows some histopathological similarity to that seen in humans, with a number of clinical similarites to APAP induced ALF including signs of hepatic encephalopy. In addition to hepatic toxicity, methaemoglobin formation, accompanied by some renal toxicity was identified. Both of the latter may be related to the formation of PAP, which is an obvious candidate for methaemoblin formation and is also a known renal toxin. Whilst PAP itself was not detected its formation was clearly evidenced by the relatively high concentrations of PAP-G detected in the liver, kidney, plasma and urine of these animals. The pig is thus possibly a poor model for toxicology studies for compounds which need to be cleared by sulfation, or which contain amide bonds which either are hydrolysed leading to toxic effects or mechanism of action, as the model showed low sulfation of APAP and deacetylation to PAP. Alternatively it may provide a useful model where amide bond hydrolysis is seen in drugs or environmental chemicals in humans, but not in standard toxicological animal models.

Despite differences in APAP metabolites and some GSH related metabolites compared to previous investigations presented in this Thesis, 5-OP concentrations were increased in this model following APAP adminnistration.

This provides promising evidence for the transaltional nature of 5-OP as a biomarker, which may be useful in clinical patients.

6 Application of UHPLC-MS/MS assays to serum from APAP overdose patients for identification of circulating biomarkers of glutathione depletion

6.1 Introduction

Throughout this thesis, advanced analytical strategies have been developed and applied to animal models of APAP overdose. These include two UHPLC-MS/MS assays which can be used to quantify or semi-quantify APAP and metabolites, and metabolites related to GSH biosynthesis and metabolism. It has been demonstrated that there are differences in APAP metabolism between the animal models (rat, mouse and pig) used in this research. In order to investigate the clinical relevance of these animal models, and the utility of the analytical methods in a clinical setting, both UHPLC-MS/MS assays were applied to serum from a selection of patients from the Markers and Paracetamol Poisoning (MAPP) cohort study. The effectiveness NAC in replenishing GSH and related metabolites has also been investigated in the research described in this thesis, and the purpose of the current work was to discover if measuring circulating GSH metabolites, in particular 5-OP, in patients on admission to hospital would help to determine which patients were at risk of liver injury and should receive NAC treatment. In addition, APAP metabolism has previously been suggested as a potential marker for patient stratification, in particular the circulating concentrations of APAP metabolites formed by CYP metabolism and subsequent glutathione conjugation, specifically APAP-C.

6.1.1 Hypothesis

It was hypothesised that upon presentation at hospital, circulating concentrations of GSH related metabolites, in particular 5-oxoproline and hypotaurine, as seen in the mouse model of APAP overdose, would correlate with the severity of liver injury as measured by ALT. In addition, concentrations of circulating APAP metabolites, formed via CYP metabolism, APAP-C and APAP-NAC, would differ with liver injury severity and the ratio of APAP-C to APAP-S could be used as an indicator of the likely severity of liver injury.

6.1.2 Aims

- To measure circulating APAP and its major metabolites using the UHPLC-MS/MS assay developed in Chapter 2 in serum from patients selected from the MAPP study.
- To also measure GSH biosynthesis related metabolites using the “GSH” UHPLC-MS/MS assay in serum from patients selected from the MAPP study.

- To compare how metabolites differ between 3 groups of patients as follows: 1. Patients without liver injury; 2. Patients with liver injury on hospital presentation; 3. Patients who presented without liver injury, but later developed it (liver injury determined by ALT concentration).
- To determine any relationships between either GSH-related or APAP metabolites or the severity of liver injury.

6.1.3 Background and rationale

As discussed previously, the current first line treatment for APAP overdose is NAC which is an effective treatment when administered within 8-10 hours post dose (Antoine and Dear 2016; Prescott et al. 1980). NAC is reported to replenish cellular cysteine stores in order to help the cell to biosynthesise GSH (Lauterburg et al. 1983; Prescott et al. 1977). The decision to initiate NAC treatment is currently based on a nomogram based primarily on serum APAP concentration and time from dose (Bateman 2015; Rumack et al. 1981). The UK guidelines on thresholds for NAC treatment were lowered in 2012, meaning the UK has amongst the lowest thresholds for NAC treatment globally and this has accounted for a 7% increase in hospital admissions (Bateman et al. 2014; Gosselin et al. 2013). However, many patients who meet criteria for NAC treatment would not go on to develop any liver injury and, in addition, there are still patients who do develop liver injury despite NAC treatment. Therefore, there is a need for new biomarker strategies for predicting patient risk of developing liver injury, and for understanding in which cases NAC treatment is appropriate and most effective. New potential biomarkers that have been explored for patient stratification include mir-122 and HMGB1, amongst others (Clarke et al. 2016). There have been recent attempts to assess both these new biomarkers, and APAP metabolites, for risk stratification of ALI in patients (Dear et al. 2018; Vliegenthart et al. 2015; Vliegenthart et al. 2017) and using strategies such as a systems biology approach to toxicity (Mason et al. 2018). A previous investigation into APAP metabolism in a different subset of patients from the MAPP study, and from another cohort study, found that APAP-C, APAP-NAC and APAP-SG were more predictive of liver injury than traditional biomarkers (Vliegenthart et al. 2017). In addition, 5-OP has been shown to be a potential biomarker in rodent models (Ghauri et al. 1993) and a systems biology model (Geenen et al. 2012). In Chapter 5 of this thesis, 5-OP was significantly increased in pigs following APAP overdose and this correlated with ALP.

In Chapter 4 of this Thesis, 5-OP was found to be increased following APAP administration in the mouse and correlated with ALT increases, while 5-OP was significantly lower in mice treated subsequently with NAC that APAP-alone, suggesting 5-OP may be a circulating biomarker for GSH depletion. 5-OP increases in urine have been reported in many cases of APAP overdose, and has been linked to metabolic acidosis, which has previously been reviewed by (Liss et al. 2013). It is possible that 5-OP has been underestimated as a potential biomarker for APAP induced liver injury, and for a potential cause of metabolic acidosis, due to a lack of effective and reproducible methods for its quantification. There have been methods described previously such as gas, and liquid chromatography coupled to mass spectrometry (Croal et al. 1998; Geenen et al. 2011a), and a recent capillary electrophoresis method has been developed for measuring 5-OP and APAP concurrently (Hlozek et al. 2017).

6.2 Methods

6.2.1 Study design and group selection

The MAPP cohort study was devised by researchers at the University of Edinburgh and enrolled patients from a number of hospitals in Scotland and England. Full written informed consent was obtained from every participant, and ethical approval was from the South East Scotland Research Ethics Committee and the East of Scotland Research Ethics Committee *via* the South East Scotland Human Bioresource. The study was carried out in compliance with the Declaration of Helsinki and Good Clinical Practice guidelines and reported according to the Standards for Reporting Diagnostic Accuracy.

The study design and patient recruitment and exclusion criteria are described in detail elsewhere (Dear et al. 2018). Briefly adults (≥16 years in Scotland, ≥18 years in England) with capacity to give consent were recruited from eight hospitals in the UK. The inclusion criteria were a history of paracetamol overdose that was judged to require NAC treatment as per UK guidelines, and a first blood sample obtained within 24 h of paracetamol ingestion. The exclusion criteria were detention under the Mental Health Act; documented cognitive impairment; inability to provide informed consent for any reason; or an unreliable overdose history.

For the research that is the subject of this thesis, a subset of presentation serum samples were taken from the original MAPP cohort of 985 patients in order to investigate whether any GSH or APAP metabolites could be

potential biomarkers for use in patient stratification. This could then be further investigated with a larger pool of patients, or in a study including healthy controls or patients with more severe liver injury. In this study, none of the patients required liver transplant, and there were no deaths. Patients were allocated to one of three groups based on outcome. “Group 1” (n=102) was described as “no liver injury” and consisted of patients who presented at hospital with ALT <50 U/L and INR <1.5, and these values remained below these thresholds for the length of hospital stay. “Group 2” (n=27) presented at hospital with ALT which was already elevated above 50 U/L, while “Group 3” (n=25) presented at hospital with ALT<50 U/L and INR<1.5 however, ALT concentrations then increased above the liver injury threshold during their stay in hospital, despite NAC treatment. Groupings of patients for the study is summarised in Figure 6.1 Four centres which had the most patients in Groups 2 and 3 were selected, and samples were taken from the Edinburgh (ED), Aberdeen (AB), St John’s (SJ) and St Thomas’ (ST) centres. Samples from each centre were taken using the same protocol. Due to smaller numbers of patients in Groups 2 and 3, all samples available from patients in these groups who took an acute overdose were analysed. There were a much larger number of patients in Group 1, therefore a selection was taken from this group from patients who took an acute dose to reflect the proportion of Group 2 and 3 patients from each centre. These were selected to be gender balanced from each centre, using a randomly generated number for each patient, and selecting alternate patients, Group 1 selections were as follows ED n=30; AB, SJ, ST n=24 per centre.

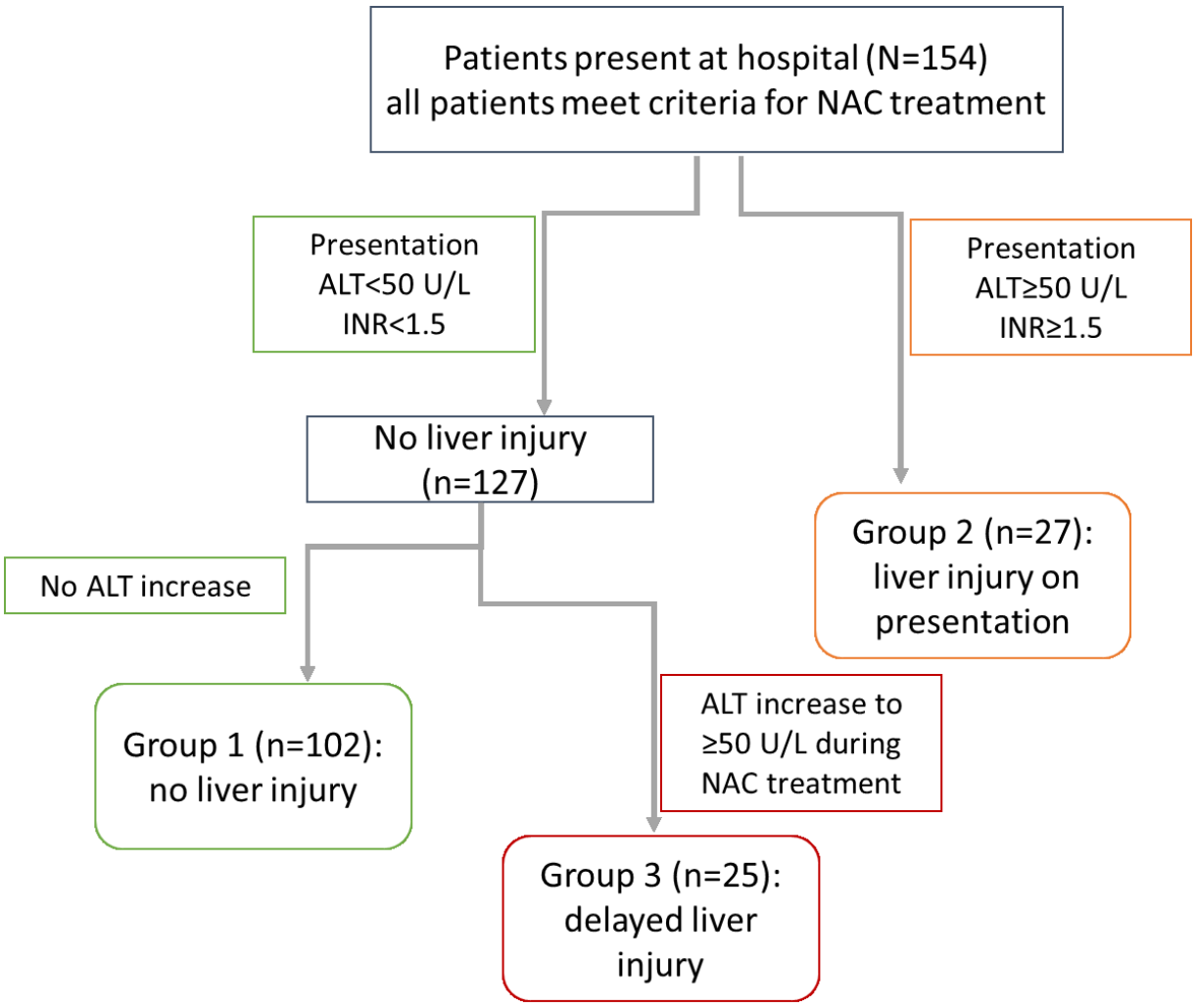


Figure 6.1 Summary of definitions for groups of patients in the sub-set of patients sampled for application of the paracetamol and glutathione pathway assays.
Abbreviations: ALT: alanine aminotransferase; INR: international normalised ratio; NAC: n-acetylcysteine.

Table 6.1 Overview of patient metadata from collaborators including patient information, APAP dose and timing and traditional biomarkers measured in the clinic.

Characteristic	Group 1 n=102	Group 2 n=27	Group 3 n=25
Age	29 (21-45)	29.5 (21-45)	37 (24-45)
Female N(%)	49(48)	17(63) p=0.002†	14(56)
APAP ingested (g)	15(8.25-19.5)	16(12.8-20) (n=24)	20(15.5-33.5) p=0.002†(n=23)
APAP mg/L	106(75-139)	69(27-96.5) p=0.0035†, p=0.003‡ (n=23)	132 (78-177) (n=24)
Time post OD (hours)	4(4-5)	13.5(5.75-19.5) P<0.0001†	5.25(4-12.8)
Presentation ALT (U/L)	17.5(13-28)	210(132-719) p<0.0001†‡	28(15-38)
Peak ALT (U/L)	18.5(14-31)	665(140-2258) p<0.0001†	567(232-1648) p<0.0001†
Presentation INR	1(1-1.1)	1.1(1-1.4) p=0.0013†	1.1(1-1.2) p=0.019†
Peak INR	1(1-1.1)	1.3(1.1-1.6) p<0.0001†	1.5(1.1-1.7) p<0.0001†
Creatinine	65(55-74)	69(60.5-82.5)	66(59-77)
Bilirubin	7(5.5-11)	15(8-34.3) p<0.0001†	12(8-19) p<0.0001†
Alkaline phosphatase	71(55-87.5) n=99	91(62-105)	83(73-102)

Group 1 = ALT<50 INR<1.5; Group 2 = Liver Injury; Group 3 = delayed liver injury with presentation ALT<50 but later increases. Groups compared with Kruskal-Wallis with FDR corrected multiple comparisons. Sex was compared with Chi^2 test. †statistically significant compared to group 1 ‡=statistically significant compared to group 3. P values presented are adjusted p-values (q)
Abbreviations: ALT: alanine aminotransferase; INR: international normalised ratio; APAP: paracetamol; NAC: n-acetylcysteine; OD: overdose.

Patient information for each group is displayed in Table 6.1. With the exception of Sex, all data are displayed as median (interquartile range.) Groups were compared with a Kruskal-Wallis test with FDR corrected multiple comparisons, and chi-squared test to compare Sex. Age was not significantly different between groups, Group 2 had a significantly higher proportion of females compared to Groups 1 and 3, while group 3 had a higher reported APAP ingested than group 1. There were some expected significant differences between the groups, for example Group 2 had significantly higher presentation ALT than Groups 1 and 3, and Groups 2 and 3 had significantly higher peak ALT and INR than group 1. Group 3 presentation INR was significantly higher than Group 1 but all values were under the 1.5 threshold for no liver injury as previously defined. Group 2 had a lower APAP concentration as measured in the clinic than either Groups 1 or 3.

6.2.2 Materials for UHPLC-MS/MS

All materials used for the UHPLC-MS/MS methods including solvents, standards and stable isotope labelled internal standards were as described previously in Chapters 2–5. For the APAP method blank human serum for calibration curve and QCs was purchased from Seralabs (BioIVT).

6.2.3 GSH UHPLC-MS/MS method and sample preparation

The chromatography and mass spectrometry for this method has been described in detail in Chapter 3. Samples were prepared as previously stated. Briefly, 20 µL serum samples were extracted with 180 µL of MeOH + 0.2% FA (v/v) containing internal standards. 180 µL of the clear supernatant was dried at room temperature under a stream of nitrogen gas. The sample pellets were re-suspended in 90 µL of 16:84 H_20:CH_3CN + 0.2% (v/v) FA. Calibration curve standards and QC samples were produced by combining each standard or QC stock solution with IS stock solution at a 1:1 ratio and 180 µL of these were added to 20 µL water before drying and reconstitution as per the samples. The analytes were analysed using three standard curves, the grouping of analytes and the IS used for each, where available, are shown in Table 6.2. The analytical ranges and QCs are as indicated in Table 6.3 and Table 6.4Stock solutions for IS and standards and QCs were prepared as described in detail in Chapter 3.3.

Pooled QCs were also prepared by mixing 5 µL aliquots of serum from all the patients in the study then taking 20 µL aliquots and preparing these as samples. Over-spiked QCs were also prepared by adding 90 µL of the MQC stock solution and 90µL of the IS stock solution to 20 µL aliquots of the pooled plasma. Three pooled QCs and over-spiked QCs were analysed throughout the run.

Table 6.2 Standards and IS for the "low", "mid" and "high" calibration curves, with the ULOQ concentration and the concentration of IS in the samples.

"High" curve (ULOQ 20 µg/mL)		**"Mid" Curve (ULOQ 2 µg/mL)**		**"Low" Curve (ULOQ 1 µg/mL)**	
Glutamine	**Glutamine-d_5**	**5-OP**	**5-OP-d_5**	**Cystathionine**	**Cystathionine-d_4**
Glycine	Glycine-$^{13}C^{15}N$	Cys-gly	Cystine-d_6	Choline	Choline-d_4
Serine	Serine-d_3	Glutamate	Glutamate-d_3	Homocysteine	Homocysteine-d_4
Taurine	Taurine-d_4	Hypotaurine	Hypotaurine-d_4	SAMe	SAM-d_3
GSSG	GSSG-$^{13}C_4{}^{15}N_2$	Methionine	Methionine -$^{13}C^{15}N$	Homocystine	Homocystine-d_8
		Cysteine	Cysteine-$^{13}C_3{}^{15}N$	G-glu-cys	
		Homoserine		GSH	
		Cystine		Cysteic acid	
				Betaine	
				OA	
				2-amino-butyrate	
				SAH	

Abbreviations: G-glu-cys: gamma-glutamyl cysteine; GSH: reduced glutathione; GSSG: oxidised glutathione; IS: internal standard; OA: Ophthalmic acid; 5-OP: 5-oxoproline; QC: quality control; SAH: s-adenosyl homocysteine; SAMe: s-adenosyl methionine; ULOQ: upper limit of quantification.

Table 6.3 Calibration range used for standards in the "low", "mid" and "high" QC ranges.

Standard no.	**Final Concentration of Curve (µg/mL)**		
	"High"	**"Mid"**	**"Low"**
7	20	2	1
6	10	1	0.5
5	5	0.5	0.2
4	2	0.2	0.2
3	1	0.2	0.05
2	0.5	0.05	0.02
1	0.2	0.02	0.01

Abbreviations: QC: quality control

Table 6.4 Final concentration of the QCs at the for each "high", "mid" and "low" curve calibration curves

QC	**Final Conc. QC (ng/mL)**		
	High	**Mid**	**Low**
HQC	8000	800	400
MQC	2000	200	100
LQC	600	60	30

Abbreviations: HQC: high quality control; LQC: low quality control; MQC: mid quality control; QC: quality control

6.2.4 APAP UHPLC-MS/MS method and sample preparation

The APAP assay liquid chromatography and mass spectrometry are described elsewhere in this Thesis in depth, including Chapter 2. Sample preparation is described in section 2.2.5 and human matrix-specific validation results in section 2.3.4. Standard curve and QC stock solutions were prepared as stated in Chapter 2, using the analytical ranges and QC concentrations as described in Table 2.8 and Table 2.9. QC samples were analysed alongside randomised samples in the analytical run. Deuterated internal standards were used for all analytes and were added to samples at 40% of the concentration of the ULOQ for APAP, APAP-G and APAP-S, and 60% of the ULOQ for APAP-C, APAP-NAC and APAP-SG. The IS stock solution was prepared in water as discussed in previous chapters. Standard curves and QCs were prepared by adding 50 µL of the curve or QC stock solution to 5 µL of blank serum, 10 µL of IS stock solution and 35 µL of MeOH. Samples were prepared by adding 10 µL of the IS stock solution and 85 µL of MeOH to 5 µL serum. All samples were then stored at -20°C for 20 minutes to precipitate proteins, before being centrifuged at 10 000g for 10 minutes, then 20 µL of the clear supernatant was diluted with 980 µL of H_2O and transferred to vials for analysis.

6.2.5 Statistics

All Mass Spectral data were processed from MassLynx using TargetLynx software and data were then exported into Excel for further analysis. For univariate and receiver operating characteristics (ROC) analysis, all data were log transformed with the addition of a constant $Log_{10}(X+1)$, in an attempt to normalise the data and for consistency across analysis. GraphPad Prism (La Jolla, CA) was used for univariate analysis including correlation analysis, ANOVA with FDR corrected multiple comparisons, and receiver operating characteristic (ROC) analysis.

6.3 Results

6.3.1 GSH method overview

Acceptance criteria for the GSH pathway method have been discussed previously (Chapters 3 & 4). QCs and points on the curve were acceptable if within 20% of their nominal concentration, with the exception of the LLOQ which must have been within 30%. To be acceptable within a given range, 67% of the QCs at that concentration level had to meet the acceptance criteria, and 67% of QCs overall. Ideally curves should have an $r^2 \geq 0.99$. Below, in Table 6.5, a summary of the linearity and the percentage of points on the curve and QCs

which met acceptance criteria are shown. The analytes highlighted in red either failed to meet run acceptance criteria and/or the metabolite was not detected in the samples. Analytes which could be detected in samples, but were below the limit of quantification for the majority of samples measured, or analytes which partially met acceptance criteria, are highlighted in orange. Over the course of a long analytical run, curves for analytes without IS generally failed to stay consistent when measured at the beginning and end of the run, and considering the matrix effects previously discussed, only analytes with IS were considered to be quantifiable.

Table 6.5 Overview of the effectiveness of the GSH assay in human serum.

Analyte	**R^2**	**% Curve pass**	**% LQC**	**% MQC**	**% HQC**	**Total % QC pass**
2-AB	Below LOD , curve not linear and curve and QCs fail					
Betaine	0.863	0	0	0	0	0
Choline	0.993	100	100	100	100	100
Cys-gly	Below LOD , curve not linear and curve and QCs fail					
Cystathionine	0.975	76	100	100	33	76
Cysteic Acid	0.978	53	0	67	83	53
Cysteine	0.991	59	20	83	67	59
Cystine	0.988	94	100	100	83	94
gamma-glu-cys	Below LOD , curve not linear and curve and QCs fail					
Glutamine	0.992	88	60	100	100	88
GSH	Below LOD , curve not linear and curve and QCs fail					
GSSG	0.994	94	80	100	100	94
Homocysteine	0.995	100	100	100	100	100
Homocystine	0.995	100	100	100	100	100
Homoserine	0.790	47	60	50	33	47
Hypotaurine	0.995	88	100	83	83	88
Methionine	0.973	76	60	83	83	76
5-OP	0.992	94	80	100	100	94
Ophthalmic Acid	0.976	71	60	67	83	71
SAH	0.991	82	80	83	83	82
SAMe	0.997	100	100	100	100	100
Serine	0.972	82	80	83	83	82
Taurine	0.997	100	100	100	100	100

Red=curve and QCs did not meet the acceptance criteria, analytes could not be detected in samples.
Orange=curve and QCs partially did not meet acceptance criteria, or the majority of the analyte was below the limit of quantification.
Abbreviations: G-glu-cys: gamma-glutamyl cysteine; GSH: reduced glutathione; GSSG: oxidised glutathione; IS: internal standard; LOD: limit of detection; OA: ophthalmic acid; 5-OP: 5-oxoproline; QC: quality control; SAH: s-adenosyl homocysteine; SAMe: s-adenosyl methionine; ULOQ: upper limit of quantification.

The pooled QC and over-spiked QC concentrations were evaluated for reproducibility throughout the analytical run, and the difference in concentration between the pooled QC and over-spiked QC, and the

deviation of this difference to the nominal over-spiked concentration calculated (displayed in Table 6.6). Of the three over-spiked QCs prepared, one was not analysed due to an injection error so the difference between the QC and over spiked QC could only be measured using 2 QCs and therefore will not be as accurate. CVs of the pooled QCs were over 20% for a number of the analytes as highlighted in red, likely in some cases due to the pooled QC being below or around the limit of quantification such as SAMe, homocysteine and cystathionine. There were also significant differences from the expected concentrations of some metabolites in the over-spiked QC, suggesting there were matrix effects and that these may not have been totally compensated for by IS, but further investigation is required to confirm this.

Table 6.6 Summary of pooled QCs reproducibility and the % difference between over-spiked QC concentration and expected concentration.

Analyte	Pooled QC		Over-spiked QC Mean % Bias
	Mean conc. ng/mL	CV	
Choline	503	14.6	17.0
Cystathionine	10.2	32.9	-56.7
Cysteine	192	82.3	-76.3
Cystine	205	21.9	-18.1
Glutamate	893	28.7	-105
Glutamine	10904	8.34	88.4
Homocysteine	6.45	47.1	-58.3
Hypotaurine	73.3	11.5	-42.4
Methionine	632	19.9	5.89
5-OP	563	15.9	5.25
SAH	4.07	17.8	-80.3
SAMe	11.2	45.8	-53.2
Serine	1430	35.8	-40.3
Taurine	2903	6.97	-11.1

Orange= 20%<CV>30% red=CV≥30%, or red=%Bias≥20, or %Bias≤-20
Abbreviations: CV: coefficient of variance; 5-OP: 5-oxoproline; QC: quality control; SAH: s-adenosyl homocysteine; SAMe: s-adenosyl methionine; ULOQ: upper limit of quantification.

It appears that the assay can reproducibly and accurately measure 5-OP, choline, glutamine, hypotaurine, serine, taurine and methionine, taking together the overall precision and accuracy of QCs and pooled QCs, and the analytical range of the analyte in these particular samples. It should be noted that there appeared to be an enhancement of the concentration of glutamate and a suppression of hypotaurine based on the over-spiked QC analysis.

6.3.2 APAP method overview

The APAP method was applied successfully for quantification of key APAP metabolites in MAPP serum as is displayed in Table 6.7. Linearity was acceptable with r^2 values above 0.99 for all analytes. Curve and QC bias form expected values also met acceptance criteria for the majority of analytes, with the exception of APAP-SG for which the bias of LQCs were in the range of 20-30%, however APAP-SG could not be detected in any samples so the results were not used for further analysis.

Table 6.7 Overview of linearity and number of points on the curve and QCs which meet acceptance criteria, for application of APAP method to MAPP samples.

Analyte	R^2	% Curve pass	% LQC	% MQC	% HQC	Total % QC pass
APAP-S	0.993	100	83	100	100	94
APAP	0.995	100	83	100	100	94
APAP-C	0.992	100	67	100	100	89
APAP-G	0.991	100	67	100	100	89
APAP-NAC	0.991	88	83	100	100	94
APAP-SG	0.994	100	0	100	100	67

Red=no detected metabolite.
Abbreviations: APAP: paracetamol; APAP-C: paracetamol-cysteinyl conjugate; APAP-G: paracetamol glucuronide; APAP-NAC: paracetamol n-acetylcysteine conjugate; APAP-S: paracetamol sulfate; APAP-SG: paracetamol glutathione conjugate; HQC: high quality control; LQC: low quality control; MQC: mid quality control; QC: quality control.

Of the metabolites analysed only 5-OP was significantly higher in patients with liver injury but there was no significant difference between Groups 2 and 3. The Pearson's correlation coefficient for 5-OP and Peak ALT concentration was calculated, there was a weak positive correlation, (r=0.372, 95% CI 0.226-0.502, p<0.0001). Linear regression analysis was also performed, the slope was 1.77 (95% CI 1.06-2.48, p<0.0001), however the R^2 value was 0.139, suggesting 5-OP was not very predictive of the variation in peak ALT (Figure 6.2).

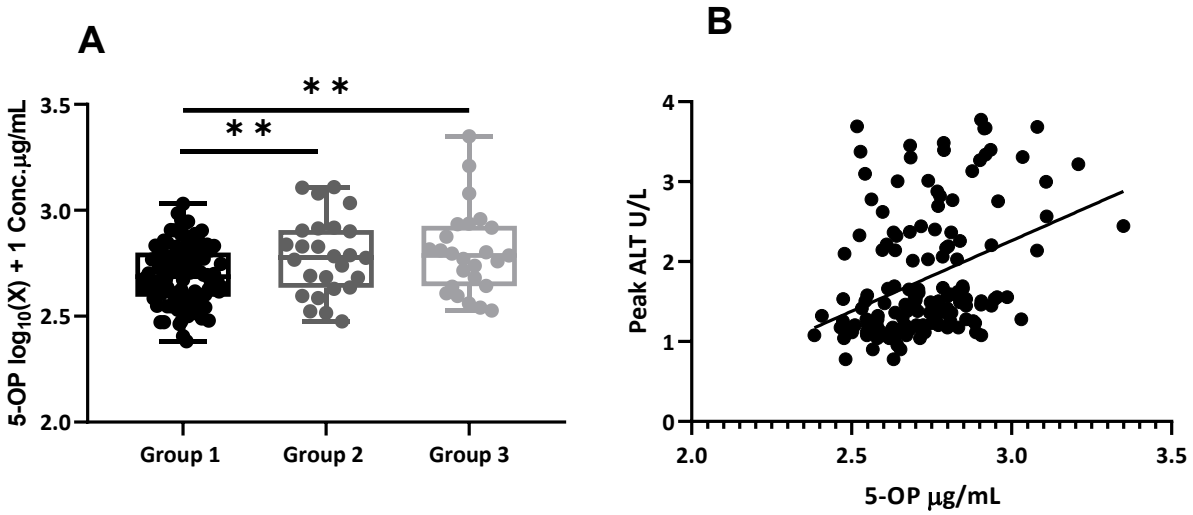


*Figure 6.2 A) differences in 5-OP concentrations in groups 1-3. Analysed using ANOVA and FDR multiple comparisons, **=p<0.002. B) Scatter plot of 5-OP vs. Peak ALT with fitted linear regression.*
Abbreviations: ANOVA: Analysis of variance; ALT: alanine aminotransferase; FDR: false discovery rate; 5-OP: 5-oxoproline.

6.3.3 APAP metabolism

There were some patients whose serum had no detectable APAP or metabolites at any time point, or for which there was an error in the injection of the sample, and therefore data were not available and were not used. As shown in Table 6.8, there were a higher proportion of patients in Group 2 with no measurable APAP or metabolites detectable. For any results which were below the LLOQ, but were less than 30% different from the LLOQ, the LLOQ was imputed and used for analysis.

Table 6.8 Exclusions made from analysis due to all, or the majority of, APAP metabolites being under the limit of quantification, or due to no metabolites being detected due to an analytical issue.

Group	N	n for data analysis	n excluded all analytes below limit of quantification	% Below limit of quantification	n excluded analytical issue
1	102	97	4	3.9%	1
2	27	20	5	19%	2
3	22	20	2	9.1%	0

In a previous pilot investigation with samples from the MAPP study, it was found that APAP metabolites formed by CYP metabolism as a proportion of metabolites, and as a proportion of APAP-S, were predictive of liver injury. As shown in Figure 6.3, there were significant differences in the log transformed concentrations of a number of APAP metabolites, APAP and APAP-G were significantly lower in Group 2 compared to Groups

1 and 3, APAP-S was not significantly different between groups, APAP-C and NAC were significantly increased in Group 3 compared to Groups 1 and 2, while APAP-C was also significantly higher in Group 2 than Group 1.

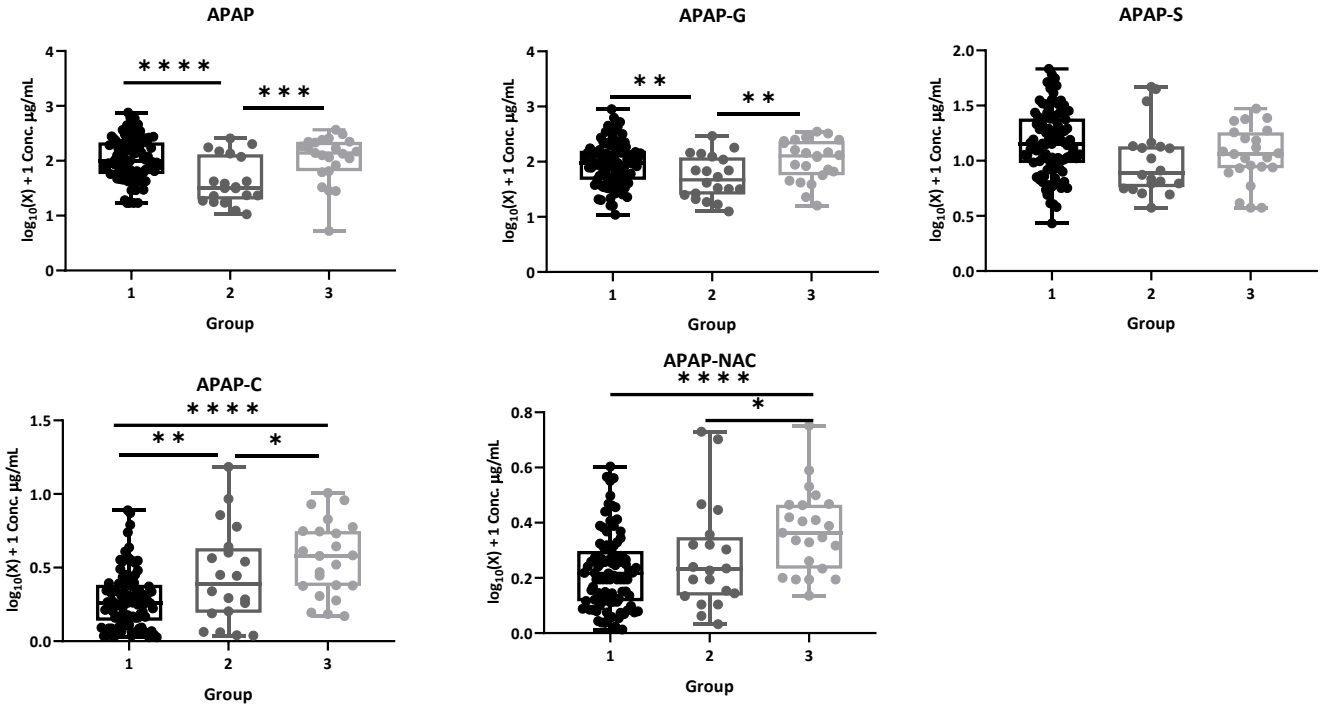


Figure 6.3 Differences in log transformed APAP metabolite concentrations in Groups 1-3. Analysed using ANOVA and FDR multiple comparisons p<0.03 (*), p<0.002 (**), p<0.0002 (***), p<0.0001 (****) Abbreviations: ANOVA: Analysis of variance; APAP: paracetamol; APAP-C: paracetamol-cysteinyl conjugate; APAP-G: paracetamol glucuronide; APAP-NAC: paracetamol n-acetylcysteine conjugate; APAP-S: paracetamol sulfate; APAP-SG: paracetamol glutathione conjugate; FDR: false discovery rate.

In order to account for differing doses and time to hospital admission, APAP metabolites were then analysed as a proportion of total metabolites and APAP-C and APAP-NAC were summed to give a "total CYP" metabolites hereby referred to "APAP-CYP" and this was also calculated as a proportion of the total metabolites in the individual, displayed in Figure 6.4. Following this, APAP-C was also calculated as a percentage of APAP-S, and this along with APAP-CYP as a proportion of total metabolites were analysed by correlation analysis and linear regression with ALT, and ROC analysis with Group 1 as control against Group 3.

Following normalisation to total metabolites, there was a still slight decrease in APAP measured in Group 2 compared to group 1. There were no significant differences in APAP-G as a proportion of metabolites between any of the groups. In contrast APAP-S was significantly increased in Group 2 compared to Group 1 and 3, while

APAP-S proportion was lowest in group 3. For the "CYP"-derived metabolites, individually and in combination, groups 2 and 3 formed a significantly higher proportion compared to Group 1.

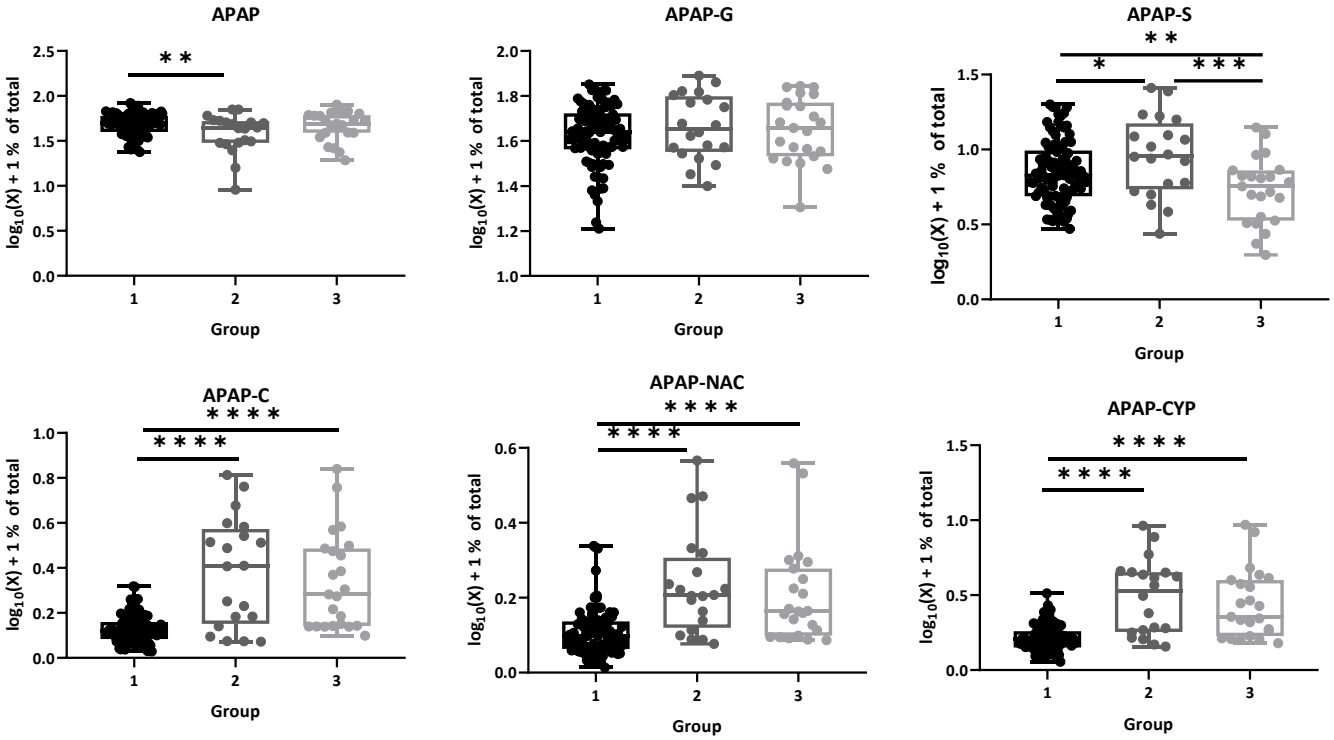


Figure 6.4 Differences in log transformed APAP metabolite concentrations as a proportion of total metabolites in Groups 1-3. Analysed using ANOVA and FDR multiple comparisons p<0.03 (*), p<0.002 (**), p<0.0002 (***), p<0.0001 (****)
Abbreviations: ANOVA: Analysis of variance; APAP: paracetamol; APAP-C: paracetamol-cysteinyl conjugate; APAP-G: paracetamol glucuronide; APAP-NAC: paracetamol n-acetylcysteine conjugate; APAP-S: paracetamol sulfate; APAP-SG: paracetamol glutathione conjugate; FDR: false discovery rate.

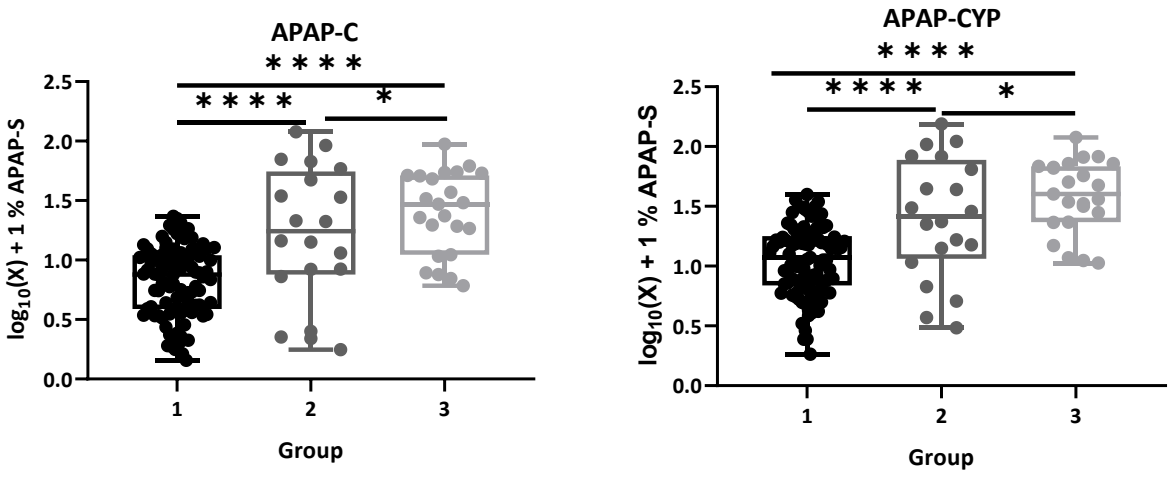


Figure 6.5 Differences in log transformed APAP-C and total APAP-CYP as a proportion of APAP-S in Groups 1-3. Analysed using Kruskal-Wallis and FDR multiple comparisons p<0.03 (*), p<0.002 (**), p<0.0002 (***), p<0.0001 (****)
Abbreviations: ANOVA: Analysis of variance; APAP-C: paracetamol-cysteinyl conjugate; APAP-CYP: paracetamol conjugates formed by cytochrome p450 metabolism; APAP-S: paracetamol sulfate FDR: false discovery rate.

In Figure 6.5, APAP-CYP and APAP-C are plotted as a proportion of APAP-S. Similarly to APAP-CYP as a proportion of total metabolites, Groups 2 and 3 had a significantly higher proportion of APAP metabolites than Group 1, however the use of APAP-S as the comparator also allows for a statistically significant separation of groups 2 and 3. Due to the similarity between the two results, it seemed plausible that just measuring APAP-C and APAP-S could provide a lot of information, and therefore this was taken forward for comparison with the percentage of APAP-CYP as a proportion of total APAP and metabolites.

In order to compare how the changes to APAP metabolism, including increasing APAP-CYP as a proportion of the total of APAP metabolites and APAP-C as a proportion of APAP-S, could explain ALT increases, both were plotted on a scatter plot and the relationship estimated. APAP-CYP/Total had a Pearson's correlation coefficient of r=0.705 (95% CI 0.611-0.78, p<0.0001) and the simple linear regression gave a slope of 3.00 (95% CI 2.492 to 3.507) and R square value of 4.97 (p<0.0001). Comparing just two metabolites, APAP-C and APAP-S the Pearson's coefficient r=0.600 (95% CI 0.482-0.696, p<0.0001). Linear regression gave a slope of 1.127 (95% CI 0.874-1.38) and an R square value of 0.36 (p<0.0001). Therefore, the proportion of CYP

metabolites present in the patient presentation sample was strongly positively correlated with peak ALT, and was able to explain around 50% of the variation in ALT. APAP-C/APAP-S was less strongly positively correlated with peak ALT. Both relationships are likely skewed by a much higher number of the patients in Group 1 compared to Groups 2 and 3, so there were fewer patients with ALT above 50

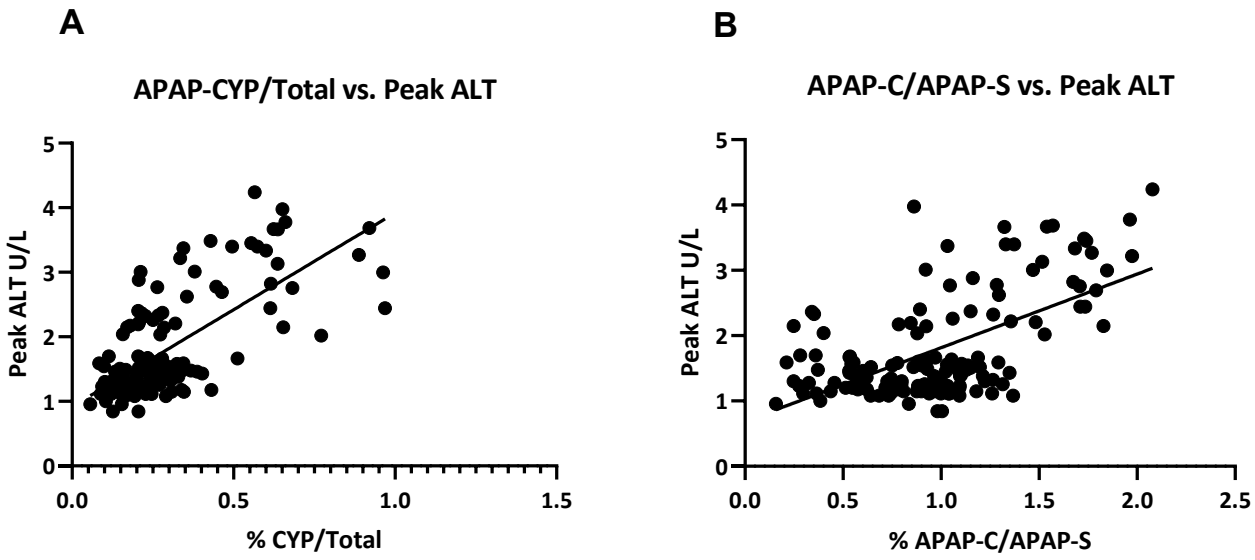


Figure 6.6 Scatter plots of A) APAP-CYP as a proportion of Total APAP and B) APAP-C as a proportion of APAP-S, with Peak ALT, fitted with a linear regression.
Abbreviations: ALT: alanine aminotransferase; APAP-C: paracetamol-cysteinyl conjugate; APAP-CYP: paracetamol conjugates formed by cytochrome p450 metabolism; APAP-S: paracetamol sulfate.

Groups 1 and 3 had statistically the same ALT concentration and APAP concentration in the presentation blood sample, and therefore these were not reliable biomarkers for predicting liver injury, therefore to estimate how predictive APAP metabolites measured using the UHPLC-MS/MS method were, ROC analysis was performed comparing %APAP-CYP/Total and %APAP-C/APAP-S with APAP and some traditional biomarkers.

6.3.4 Predictivity of suggested biomarkers

The proportion of APAP-CYP and APAP-C as a percentage of APAP-S were found to be the best predictors of late onset liver injury, whilst the ROC AUC for APAP itself was not significant. While ALT was significant it was much less sensitive at 90% specificity and described less of the variation between groups. Bilirubin was the most successful of the traditional biomarkers at predicting liver injury and was also statistically significantly

higher in Group 3 compared to Group 1, as shown in Table 6.9. However, the AUC and sensitivity were lower than with the APAP-CYP metabolites. Both APAP-CYP proportions were significantly predictive of the difference between groups 1 and 3, and therefore of the later onset of ALI despite initial low ALT on presentation. The %APAP-C/APAP-S had the highest ROC-AUC of 0.884, with a specificity of 0.739 at 90% specificity. 5-OP was the most predictive of the endogenous metabolites measured, however it was only slightly more predictive than presentation ALT.

Table 6.9 Summary of ROC-analysis comparing traditionally measured biomarkers with APAP concentration and APAP-CYP metabolism as a proportion of total metabolites, and APAP-C as a proportion of APAP-S. Sensitivity is given for 90% specificity.

Marker	ROC-AUC	95% confidence interval	P-value	Sensitivity	95% confidence interval
ALT	0.645	0.511-0.779	0.0258	0.280	0.143-0.476
APAP	0.534	0.406-0.662	0.610	0.04348	0.00223-0.210
APAP-C / APAP-S	0.884	0.799-0.968	<0.0001	0.739	0.535-0.875
APAP-CYP/ Total	0.838	0.747-0.930	<0.0001	0.609	0.408-0.778
Bilirubin	0.727	0.612-0.842	0.0005	0.480	0.300-0.665
5-OP	0.655	0.530-0.779	0.0169	0.28	0.143-0.476

Abbreviations: ALT: alanine aminotransferase; APAP-C: paracetamol-cysteinyl conjugate; APAP-CYP: paracetamol conjugates formed by cytochrome p450 metabolism; APAP-S: paracetamol sulfate; AUC: area under the curve; 5-OP: 5-oxoproline; ROC: receiver operating characteristic.

6.4 Discussion

6.4.1 GSH metabolism changes summary

Serum taken from human patients upon presentation at hospital following a reported APAP overdose, who were deemed to need NAC treatment following assessment using a nomogram methodology, was analysed using the GSH cycle UHPLC-MS/MS method. When comparing the endogenous metabolites using ANOVA between the 3 outcome groups, only 5-OP was increased significantly in patients who developed liver injury, compared to those that did not. ROC analysis showed that 5-OP may be a marginally better predictor of late onset liver injury when measured in a presentation blood sample compared to ALT or APAP concentration, but 5-OP was inferior to the APAP-CYP metabolites as a biomarker for patient stratification.

6.4.2 APAP metabolism changes summary

There were significant differences in APAP metabolism between the 3 outcome groups. Normalising the APAP metabolites to the total measured metabolites allowed for comparison, as both the APAP dose and time to

presentation varied. Concentrations of APAP itself were lower in the Group 2 patients, as was to be expected due to their statistically later arrival at hospital post overdose. APAP-S was decreased in the late onset liver injury patients but not Group 2 patients, suggesting that these patients may have reduced sulfation capacity, which could cause the more rapid depletion of GSH through NAPQI conjugation. Taking the CYP metabolites which could be measured, these were significantly increased in the liver injury groups, and were most increased in the late onset group. This difference between groups 2 and 3 is not likely to be due to the time to presentation difference in group 2, as the CYP metabolites are formed later, following the saturation of other metabolic reactions (sulfation and glucuronidation) and GSH depletion. Therefore, if due to time to presentation alone, the proportion of CYP metabolites would be expected to be higher in group 2 patients (Mazaleuskaya et al. 2015). Both APAP-C as a proportion of APAP-S and APAP-CYP as a proportion of total metabolites were shown to correlate with the peak ALT of the patient and were more predictive than traditional biomarkers such as ALT at prediction of late onset liver injury when analysed by ROC analysis.

6.4.3 Discussion of results

From the selection of patients made from this study, there were key differences in the presentation blood sample between patients who did and did not develop liver injury in APAP metabolite and 5-OP concentrations. Taking Groups 1 and 3, these were statistically indistinguishable based on the presentation ALT, APAP mg/L, time since overdose and reported APAP dose. The Group 3 patients did have elevated bilirubin and slightly elevated INR upon presentation, but these were not major contributors to the current guidelines for decision to commence NAC treatment (Bateman et al. 2014; Gosselin et al. 2013). For patients who later developed liver injury, APAP-S was lower, suggesting saturation of sulfation capacity and formation of the reactive metabolite NAPQI which binds to GSH forming APAP-CYP metabolites. Quantities of APAP-CYP-related metabolites were elevated in both liver injury groups, Groups 2 and 3, but more so in Group 3, suggesting this could be a specific biomarker for late onset ALI. The ratio of APAP-C to APAP-S was also predictive of the severity of liver injury, and in particular of late onset liver injury.

The likely depletion of GSH in these patients did not appear to translate to the significant differences between these groups in GSH metabolism related metabolites as was seen in the mouse (Chapter 4). 5-OP was

significantly higher in concentration in the serum of the liver injury patients, which further validates that 5-OP has potential to be a biomarker of APAP induced liver injury, a key hypothesis of this thesis. Differences in the diets, genetics and environments of individual patients may mean that the variability of the GSH-related metabolites was too great to detect changes which may be subtle between these groups. For example, a methionine rich diet may reduce impact on the GSH biosynthesis pathway compared to starvation and use of alcohol (McLean et al. 1989; Whitcomb and Block 1994). Previous studies have found that differences in background metabolism could predict APAP metabolism and toxicity in rats and humans (Clayton et al. 2009; Clayton et al. 2006). Ethnicity, gender and genetic polymorphisms may also have some impact on APAP metabolism on toxicity (Court et al. 2017; Critchley et al. 1986; Lee et al. 1992).

In this study no healthy controls were used and all patients had been deemed appropriate for NAC treatment, therefore it may be that GSH metabolites would be significantly altered in these liver injury patients compared to healthy controls, or if the study included patients with severe liver injury requiring liver transplant or resulting in fatality. The results suggest that 5-OP will have some value in patient stratification and further analysis could explore the utility of 5-OP when in combination with drug metabolite or other endogenous metabolites. APAP metabolites, particularly the CYP metabolites, seem to be potential candidates as alternative biomarkers for patient stratification, and the results of this study were very similar to a previous independent analysis of APAP metabolism in a different selection of patients from the MAPP study and The Scottish and Newcastle Antiemetic Pre-treatment for Paracetamol Poisoning study (SNAP) (Vliegenthart et al. 2017).

6.4.4 Conclusions, limitations and future directions

Analysis of the presentation serum samples from patients who required treatment with NAC following an APAP overdose was performed using the two UHPLC-MS/MS assays.

The key findings were:

- Circulating concentrations of APAP-CYP metabolites, and the APAP-C/APAP-S ratio, may be predictive of development of liver injury.

- 5-Oxoproline was significantly increased in patients with liver injury, providing further evidence that this may be a biomarker of liver injury following hepatic GSH depletion.

Limitations of this study include the fact that the sample size available for patients developing liver injury later, or presenting at hospital with liver injury, was limited by the small proportion of patients in these groups that presented at hospital. It was necessary to combine patients from a number of centres for this analysis, which may lead to some differences in sample collection and handling, however this is unlikely to have impacted on the APAP results as all analytes used SIL internal standards. Also, visualisation of the results using PCA did not show a separation by centre (data not shown). The nature of this study meant that backgrounds and patient histories could not be accounted for however, the purpose of this study was to replicate the clinical realities of decision making, based on only an initial blood sample, and 5-OP and APAP metabolites appeared to have utility for this. In order to understand GSH metabolism in humans, the use of healthy controls or inclusion of patients with severe injury would have allowed the comparison of GSH metabolic pathway metabolite profiles in these cases, and it is possible that the GSH pathway would have been more clearly perturbed between these groups. In addition, the patients could have been grouped by gender, ethnicity, body weight, diet, and alcohol use profile to reduce and potential impact of these factors on hepatic GSH. A future study in healthy individuals taking low dose paracetamol and comparison with patients with more severe liver injury could be developed for this purpose.

In terms of the analytical methods, the limitations previously discussed were also found in this application. The APAP assay had dynamic range issues as APAP-SG could not be accurately quantified and a number of APAP-NAC results were below the limit of quantification and had to be imputed based on the LLOQ. The method has been shown to be effective when serum is diluted by a lower dilution factor, and if CYP metabolites as a proportion of APAP-S are the only metabolites required, this assay could be easily applied to those metabolites alone by using a smaller dilution factor. If APAP and APAP-G are also required to be analysed, methods such as increasing the cone voltage and other analytical properties, or measuring the ^{13}C isotopes, could be investigated.

The GSH assay also still suffered from the probable phospholipid-induced matrix effects as discussed in Chapter 3, and these should be addressed for future applications of the assay. These effects mean that only the 14 metabolites for which valid SIL IS were available can be considered quantifiable, and within these some metabolites were not present at high enough concentrations in the serum for accurate determination. Effectively this reduced the metabolites which could realistically be used in analysis to below 10, and less than half of the metabolites the assay is designed to measure. It therefore seems that the assay should be developed to concentrate on key metabolites of interest, as only a few metabolites could be measured in the serum at the current ranges where the samples are already diluted as little as possible without further increasing matrix effects. A new sample preparation protocol using a solid phase extraction and drying steps to concentrate samples could be investigated, or the assay could be further refined for plasma/serum for the determination of the absolute concentration of around 10 key metabolites.

7 Conclusions

7.1 Key hypotheses and aims

The approach for the research described in this Thesis was to develop and apply advanced analytical strategies for the investigation of APAP metabolism and associated toxicity across a range of species and sample types, leading ultimately to application in human patients.

Specifically, the focus of this thesis was on GSH depletion and related metabolism changes, and an assessment of the effectiveness of 5-OP and OA as translational biomarkers for GSH depletion and the estimation of the extent of liver injury. It was hypothesised, based on previous studies *in- vitro* and in animal models, that 5-OP and OA may be translational biomarkers for liver injury following GSH depletion (Geenen et al. 2012; Soga et al. 2006), and this was tested by evaluating these in animal models and clinical APAP overdose. A "targeted" UHPLC-MS/MS method was developed previously to assess these biomarkers, and to understand the wider impact on GSH biosynthesis and related metabolism. This method presents an improvement on current methods for GSH related metabolite quantification as it covers a large range of metabolites and does not require a derivatisation step (Geenen et al. 2011a; Geenen et al. 2011b; Gil et al. 2018; Lafaye et al. 2005). This method included metabolites from the methionine cycle, trans-sulfuration pathway and gamma-glutamyl cycle, and sulfur containing metabolites of cysteine such as taurine and its precursor hypotaurine. This method was further developed here and evaluated for matrix effects and recoveries and was then applied to samples from animal models of APAP overdose.

In addition, the rate and routes of the metabolism of APAP has an impact on its toxicity, and therefore understanding APAP metabolism in animal models is important (Bales et al. 1984; Mazaleuskaya et al. 2015; Prescott 1980). APAP metabolite concentrations themselves may be circulating indicators of severity of liver injury (Vliegenthart et al. 2017). A UHPLC-MS/MS method was developed and validated for the quantification of APAP and its major metabolites in plasma and serum and applied to rat plasma.

Two further animal models of APAP overdose were studied in detail, a single non-fatal dose in mice, and a repeated dosing strategy in a porcine model of APAP-induced ALF. Both GSH-biosynthesis and APAP metabolite methods were applied to serum and liver extracts from the mouse model. In the pig ALF model,

urine, plasma and tissue samples were initially analysed using ^{1}H-NMR spectroscopy and circulating drug metabolite concentrations and GSH metabolism changes were then confirmed *via* the application of the UHPLC-MS/MS methods. Both methods were then applied to a presentation serum sample from non-fatal APAP overdose patients who required hospitalisation and NAC treatment.

7.2 Summary of key findings

- A rapid, reproducible, UHPLC-MS/MS method to quantify APAP its major metabolites has been successfully developed and validated for application to rat serum, with subsequent partial cross-validations to human, pig, and mouse serum and/or plasma.
- This method has then been applied to animal models and clinical samples showing that there is differential APAP metabolism between animal species and humans, which impact on its toxicity.
- Mouse APAP metabolism appeared to be most similar to human, with the glucuronide being the most abundant metabolite, and indeed was more concentrated than the parent drug in the samples analysed.
- The pig had the most differing APAP metabolism, with PAP-G being a major APAP metabolite. The detection of PAP-G, which was not detected in any other samples, is indicative of extensive N-deacetylation. The pig also demonstrated a very low sulfation capacity.
- Metabolites of APAP oxidative metabolism, and particularly circulating concentrations of the cysteine conjugate, were shown to be predictive of severity of liver injury in humans.
- In patients developing late onset liver injury despite NAC treatment, there were decreased APAP-S concentrations paired with increased APAP-C and APAP-NAC concentrations, suggesting that the key cause of toxicity is a depletion of cellular sulfur following saturation of sulfation capacity and increased oxidative metabolism.
- APAP-C and -NAC appeared to correlate most strongly with liver injury in the mouse, but this relationship was not clear in the pig, due to the differences in drug metabolism, with understanding further complicated by the multiple dose study design employed.

- The GSH method suffered from significant matrix effects and difficulties with the chromatography which made it difficult to quantify a number of the metabolites in serum. However, this method performed better when applied to liver aqueous extract samples.
- The result of applying the GSH method to different species was the identification of 5-OP as the key metabolite of interest. Thus, concentrations of 5-OP were increased in circulation in both animal models and in overdose patients, and this metabolite does indeed appear to be a translational biomarker of APAP overdose leading to liver damage.

7.3 Study Limitations

7.3.1 Methodological limitations

In terms of the method development, the main issues surround sample preparation techniques. For both GSH-pathway and APAP/metabolite methods, the sample preparation was designed to be rapid and simple, therefore, protein precipitation with organic solvents was used. For the APAP method, the small number of exogenous analytes made validation simpler as this could all be carried out in blank matrix, meaning matrix effects were investigated as part of the development (Chambers et al. 2007; van de Merbel 2008). In addition, the sample preparation included a large dilution step in water which seemed to reduce any potential effects of matrix, and samples were not prone to evaporation. As internal standards for all compounds became commercially available during the course of the research, it was possible to internally standardise for any matrix effects. However, one limitation of the study is that adding the analytes to only 5 µL of plasma or serum in the extraction solvent means that spiked in standards did not associate with the plasma proteins and then get extracted, to more accurately replicate real sample preparation. Experimentation to investigate this is underway but has proved to be associated with a number of practical difficulties. From the work undertaken so far, the most practical approach would have been to investigate the recoveries of each analyte spiked into serum or plasma sample in an appropriate solvent at less than 5% of the total final volume (as per FDA guidelines).

For the GSH-metabolite method the limitations relate to the fact that, as these are endogenous and no analyte-free matrix can be obtained, the initial development was carried out using water-based samples.

Whilst matrix effects are to be expected in LC-MS-based methods, and it is to be hoped that IS will compensate for these, such standards were not available for all analytes. Samples prepared in serum seemed to suffer from both ion enhancement and suppression, differing for each analyte. There were also chromatography issues such as sample-dependent changes to retention times in matrix versus matrix free samples. A clear recommendation arising from this work is that, whilst the method does seem applicable to tissues, it would be advisable to re-investigate sample preparation for plasma/serum using a range of alternative sample preparation techniques, and particularly removal of lipids using solid phase extraction before the application to samples of interest (Chambers et al. 2007).

7.3.2 Study design and sample collection

For the research reported in this thesis, the samples obtained were shared resources which were taken as part of larger studies which were generally designed by collaborators with different endpoints in mind. The porcine study in particular had a very complex study design which made results difficult to interpret. For the purpose of the hypotheses presented in this thesis, the key sampling points come before ALF, as one of the main aims was to identify early biomarkers to predict liver injury severity (Lee et al. 2013). An ideal study design would have consisted of a large single dose with more immediate sampling time points, as pigs had already received four doses of APAP by the time the first sample was taken. In addition, pigs were treated with titrated doses of APAP based on their serum APAP and MetHb concentrations, meaning direct comparisons between animals were complex. In some respects, the differing doses made this study more representative of the clinical situation. Tissue samples were only available from the majority of animals at post-mortem, after liver failure, and after up to 48 hours of anaesthesia, therefore it was difficult to assess metabolic changes in the tissues due to the potential implications of the extended sedation. In addition, the potential impact on APAP metabolism and toxicity of the sedative agents that pigs were treated with during the experiment were not accounted for.

The study undertaken in the mouse had a small sample size at each time point which was restrictive to the analysis which could be undertaken. As with the porcine model, the first available time point at 3 hours after the initial dose was too late to capture the early metabolism changes that might replicate a human being at

around 4 hours post dose, which was the average time of arrival at hospital after reported overdose. As the samples were a shared resource, aliquots of the 3-hour time point control serum were no longer available. In terms of the animals treated with NAC, if the study were to be developed specifically for studying early changes to GSH metabolism following APAP dosing, mice treated with Vehicle and then NAC would be included as a positive control, and a time point before NAC treatment should be included to show that the metabolites of interest were equally depleted in the animals treated with NAC. It would have been beneficial to take in-life sampling of blood from 1 hour onwards and to take termination samples at 6 hours.

For the clinical study, the most obvious limitation was the number of patients available which were in the liver injury groups, as this study focussed specifically on patients who presented at hospital early and were able to be treated with NAC. There were no healthy controls available, and it may be that there would have been extensive changes in the GSH related metabolites in all patients compared to healthy controls which could not be detected as all samples were from patients who had taken paracetamol. Other limitations included the fact that genetic, ethnic and dietary backgrounds of patients were not controlled for (Court et al. 2017).

7.4 Future Work

7.4.1 Method development and validation

The next steps will be to further optimise the GSH method by developing a new sample preparation protocol, which should help to reduce matrix effects and increase the accuracy and precision of the method. The method may also be reduced in scope to quantify only the key metabolites highlighted in this work to be of interest such as 5-OP, OA, SAMe, cystathionine, hypotaurine, taurine, methionine, cystine, cysteine, glutamine, glutamate, γ-glu-cys, GSH and GSSG. Following the improvement of sample preparation protocol, the chromatographic gradient will be altered to favour these metabolites. For the APAP method, further work should be done to fully quantify the recoveries of analytes when spiked individually into serum at less than 5% volume, and to evaluate individual matrix effects.

7.4.2 Understanding APAP toxicity and sulfur depletion more broadly

Firstly, the MAPP clinical study has many more samples available, although predominantly without liver injury, enabling a larger group of patients to be studied and samples analysed using the improved GSH method, and

also analysed with the APAP method, in order to perform multivariate modelling on large patient sample. In the absence of samples from healthy controls, the metabolites could be instead mapped for the individual patient during NAC treatment and up to hospital discharge, taking the final sample upon discharge as a baseline state of metabolism. Although, the results in Chapter 4 suggest the GSH metabolism may be altered at late time points as the liver recovers. It would also be interesting to model whether APAP metabolism is predictive in larger patient groups. 5-OP should also be measured in drug induced liver injury caused by other compounds which are known to deplete GSH by different mechanisms, in order to evaluate 5-OPs utility as a marker of all GSH-related drug induced liver injury.

For the porcine study, the GSH method could be applied to liver and kidney extracts to detect whether the increased circulating SAMe is linked with a concurrent decrease in the hepatic SAMe, and to try to detect GSH depletion. The impact of changes to methionine metabolism and SAMe, such as reduced DNA methylation capacity, could also be investigated further in both the porcine and mouse models using microarray and related techniques (Garcia-Gimenez et al. 2017). And as there is little prior literature on this particular breed of pig , and to further understand the formation of PAP or the reduced sulfation capacity (Capel et al. 1972), samples of liver and kidney could be analysed for gene and protein expression of key enzymes involved in APAP metabolism and methylation such as SULTS and NAT enzymes. Similarly, by taking liver samples from the mice the expression of several key enzymes involved in the GSH cycle could be measured and activities of enzymes also measured *in-vitro,* to fully understand how the enzymatic changes relate to the hepatic and circulating 5-OP increases.

Finally, to understand how metabolism of APAP in this breed of pig relates to mini-pig breeds (which are more commonly used in the lab) a small single dose study could be carried out in these pigs (Bode et al. 2010; Helke et al. 2016).

7.5 Conclusions

- 5-OP is a promising biomarker for APAP induced liver injury.
- 5-OP increases appear to be translational from mouse and pig to human.
- Circulating APAP metabolites formed through the formation of reactive intermediate NAPQI are predictive of severity of liver injury in patients.
- APAP metabolism is more varied between species, and the pig is a poor model species for investigation of APAP metabolism.

References and bibliography

Human Metabolome Database http://www.hmdb.ca/ Accessed 25th May 2017

Abdelghani R, Daray R, Kosztowski A, Brierre S (2015) Methemoglobinemia Secondary to Massive Acute Acetaminophen Toxicity. Chest 148(4) doi:10.1378/chest.2243445

Acharya M, Lau-Cam CA (2010) Comparison of the protective actions of N-acetylcysteine, hypotaurine and taurine against acetaminophen-induced hepatotoxicity in the rat. Journal of Biomedical Science 17 doi:10.1186/1423-0127-17-s1-s35

Al-Hourani K, Mansi R, Pettie J, Dow M, Bateman DN, Dear JW (2013) The predictive value of hospital admission serum alanine transaminase activity in patients treated for paracetamol overdose. Qjm-an International Journal of Medicine 106(6):541-546 doi:10.1093/qjmed/hct062

Alhourani HM, Kumar A, George LK, Sarwar T, Wall BM (2018) Recurrent Pyroglutamic Acidosis Related to Therapeutic Acetaminophen. American Journal of the Medical Sciences 355(4):387-389

Alpert AJ (1990) Hydrophilic-interaction chromatography for the separation of peptides, nucleic-acids and other polar compounds. Journal of Chromatography 499:177-196 doi:10.1016/s0021-9673(00)96972-3

An JH, Lee HJ, Jung BH (2012) Quantitative analysis of acetaminophen and its six metabolites in rat plasma using liquid chromatography/tandem mass spectrometry. Biomedical chromatography : BMC 26(12):1596-604 doi:10.1002/bmc.2737

Antoine DJ, Dear JW (2016) How to treat paracetamol overdose and when to do it. Expert Review of Clinical Pharmacology 9(5):633-635 doi:10.1586/17512433.2016.1154786

Antoine DJ, Dear JW, Lewis PS, et al. (2013) Mechanistic biomarkers provide early and sensitive detection of acetaminophen-induced acute liver injury at first presentation to hospital. Hepatology 58(2):777-787 doi:10.1002/hep.26294

Antoine DJ, Williams DP, Kipar A, et al. (2009) High-Mobility Group Box-1 Protein and Keratin-18, Circulating Serum Proteins Informative of Acetaminophen-Induced Necrosis and Apoptosis In Vivo. Toxicological Sciences 112(2):521-531 doi:10.1093/toxsci/kfp235

Armenian P, Gerona RR, Blanc PD, Wu AHB, Mookherjee S (2012) 5-oxoprolinemia causing elevated anion gap metabolic acidosis in the setting of acetaminophen use. Journal of Emergency Medicine 43(1):54-57 doi:10.1016/j.jemermed.2011.06.017

Aruoma OI, Halliwell B, Hoey BM, Butler J (1988) The antioxidant action of taurine, hypotaurine and their metabolic precursors. Biochemical Journal 256(1):251-255 doi:10.1042/bj2560251

Baker LA, Lee KCL, Jimenez CP, et al. (2015) Circulating microRNAs Reveal Time Course of Organ Injury in a Porcine Model of Acetaminophen-Induced Acute Liver Failure. Plos One 10(5) doi:10.1371/journal.pone.0128076

Bales JR, Bell JD, Nicholson JK, et al. (1988) Metabolic profiling of body-fluids by proton nmr - self-poisoning episodes with paracetamol (acetaminophen). Magnetic Resonance in Medicine 6(3):300-306 doi:10.1002/mrm.1910060308

Bales JR, Sadler PJ, Nicholson JK, Timbrell JA (1984) Urinary-excretion of acetaminophen and its metabolites as studied by proton nmr-spectroscopy. Clinical Chemistry 30(10):1631-1636

Bateman DN (2015) Paracetamol poisoning: beyond the nomogram. British Journal of Clinical Pharmacology 80(1):45-50 doi:10.1111/bcp.12604

Bateman DN, Carroll R, Pettie J, et al. (2014) Effect of the UK's revised paracetamol poisoning management guidelines on admissions, adverse reactions and costs of treatment. British Journal of Clinical Pharmacology 78(3):610-618 doi:10.1111/bcp.12362

Bauchart-Thevret C, Stoll B, Chacko S, Burrin DG (2009) Sulfur amino acid deficiency upregulates intestinal methionine cycle activity and suppresses epithelial growth in neonatal pigs. American Journal of Physiology-Endocrinology and Metabolism 296(6):E1239-E1250 doi:10.1152/ajpendo.91021.2008

Beckonert O, Coen M, Keun HC, et al. (2010) High-resolution magic-angle-spinning NMR spectroscopy for metabolic profiling of intact tissues. Nature Protocols 5(6):1019-1032 doi:10.1038/nprot.2010.45

Beckonert O, Keun HC, Ebbels TMD, et al. (2007) Metabolic profiling, metabolomic and metabonomic procedures for NMR spectroscopy of urine, plasma, serum and tissue extracts. Nature Protocols 2(11):2692-2703 doi:10.1038/nprot.2007.376

Benjamini Y, Krieger AM, Yekutieli D (2006) Adaptive linear step-up procedures that control the false discovery rate. Biometrika 93(3):491-507 doi:10.1093/biomet/93.3.491

Bessems JGM, Vermeulen NPE (2001) Paracetamol (acetaminophen)-induced toxicity: Molecular and biochemical mechanisms, analogues and protective approaches. Critical Reviews in Toxicology 31(1):55-138 doi:10.1080/20014091111677

Bode G, Clausing P, Gervais F, et al. (2010) The utility of the minipig as an animal model in regulatory toxicology. Journal of Pharmacological and Toxicological Methods 62(3):196-220 doi:10.1016/j.vascn.2010.05.009

Bonfiglio R, King RC, Olah TV, Merkle K (1999) The effects of sample preparation methods on the variability of the electrospray ionization response for model drug compounds. Rapid Communications in Mass Spectrometry 13(12):1175-1185 doi:10.1002/(sici)1097-0231(19990630)13:12<1175::aid-rcm639>3.0.co;2-0

Boobis AR, Tee LBG, Hampden CE, Davies DS (1986) Freshly isolated hepatocytes as a model for studying the toxicity of paracetamol. Food and Chemical Toxicology 24(6-7):731-736 doi:10.1016/0278-6915(86)90172-9

Botta D, Shi S, White CC, et al. (2006) Acetaminophen-induced liver injury is attenuated in male glutamate-cysteine ligase transgenic mice. Journal of Biological Chemistry 281(39):28865-28875 doi:10.1074/jbc.M605143200

Bradford MM (1976) Rapid and sensitive method for quantitation of microgram quantities of protein utilizing principle of protein-dye binding. Analytical Biochemistry 72(1-2):248-254 doi:10.1016/0003-2697(76)90527-3

Bray GP, Tredger JM, Williams R (1992) S-adenosylmethionine protects against acetaminophen hepatotoxicity in 2 mouse models. Hepatology 15(2):297-301 doi:10.1002/hep.1840150220

Brown JM, Ball JG, Hogsett A, Williams T, Valentovic M (2010) Temporal study of acetaminophen (APAP) and S-adenosyl-L-methionine (SAMe) effects on subcellular hepatic SAMe levels and methionine adenosyltransferase (MAT) expression and activity. Toxicology and Applied Pharmacology 247(1):1-9 doi:10.1016/j.taap.2010.04.018

Buszewski B, Noga S (2012) Hydrophilic interaction liquid chromatography (HILIC)-a powerful separation technique. Analytical and Bioanalytical Chemistry 402(1):231-247 doi:10.1007/s00216-011-5308-5

C. R. Green KNH, and J. D. Tange (1969) Kidney Lesions Induced in Rats by P-aminophenol. The British Medical Journal 1(5637):162-164

Capel ID, French MR, Milburn MV, Smith RL, Williams RT (1972) The fate of (14C)phenol in various species. Xenobiotica 2(1):25-35

Carr HY, Purcell EM (1954) Effects of Diffusion on Free Precession in Nuclear Magnetic Resonance Experiments. Physical Review 94(3):630-638

Chambers E, Wagrowski-Diehl DM, Lu ZL, Mazzeo JR (2007) Systematic and comprehensive strategy for reducing matrix effects in LC/MS/MS analyses. Journal of Chromatography B-Analytical Technologies in the Biomedical and Life Sciences 852(1-2):22-34 doi:10.1016/j.jchromb.2006.12.030

Chen C, Krausz KW, Idle JR, Gonzalez FJ (2008) Identification of novel toxicity-associated metabolites by metabolomics and mass isotopomer analysis of acetaminophen metabolism in wild-type and Cyp2e1-null mice. Journal of Biological Chemistry 283(8):4543-4559 doi:10.1074/jbc.M706299200

Chen WQ, Koenigs LL, Thompson SJ, et al. (1998) Oxidation of acetaminophen to its toxic quinone imine and nontoxic catechol metabolites by baculovirus-expressed and purified human cytochromes P450 2E1 and 2A6. Chemical Research in Toxicology 11(4):295-301 doi:10.1021/tx9701687

Chen Y, Yang Y, Miller ML, et al. (2007) Hepatocyte-specific Gclc deletion leads to rapid onset of steatosis with mitochondrial injury and liver failure. Hepatology 45(5):1118-1128 doi:10.1002/hep.21635

Chou JY (2000) Molecular genetics of hepatic methionine adenosyltransferase deficiency. Pharmacology & Therapeutics 85(1):1-9 doi:10.1016/s0163-7258(99)00047-9

Clarke JI, Dear JW, Antoine DJ (2016) Recent advances in biomarkers and therapeutic interventions for hepatic drug safety - false dawn or new horizon? Expert Opinion on Drug Safety 15(5):625-634 doi:10.1517/14740338.2016.1160057

Clayton TA, Baker D, Lindon JC, Everett JR, Nicholson JK (2009) Pharmacometabonomic identification of a significant host-microbiome metabolic interaction affecting human drug metabolism. Proceedings of the National Academy of Sciences of the United States of America 106(34):14728-14733 doi:10.1073/pnas.0904489106

Clayton TA, Lindon JC, Cloarec O, et al. (2006) Pharmaco-metabonomic phenotyping and personalized drug treatment. Nature 440(7087):1073-1077 doi:10.1038/nature04648

Cloarec O, Dumas ME, Craig A, et al. (2005) Statistical total correlation spectroscopy: An exploratory approach for latent biomarker identification from metabolic H-1 NMR data sets. Analytical Chemistry 77(5):1282-1289 doi:10.1021/ac048630x

Coen M, Lenz EM, Nicholson JK, Wilson ID, Pognan F, Lindon JC (2003) An integrated metabonomic investigation of acetaminophen toxicity in the mouse using NMR spectroscopy. Chemical Research in Toxicology 16(3):295-303 doi:10.1021/tx0256127

Coen M, Ruepp SU, Lindon JC, et al. (2004) Integrated application of transcriptomics and metabonomics yields new insight into the toxicity due to paracetamol in the mouse. Journal of Pharmaceutical and Biomedical Analysis 35(1):93-105 doi:10.1016/j.jpba.2003.12.019

Cook SF, King AD, van den Anker JN, Wilkins DG (2015) Simultaneous quantification of acetaminophen and five acetaminophen metabolites in human plasma and urine by high-performance liquid chromatography-electrospray ionization-tandem mass spectrometry: Method validation and application to a neonatal pharmacokinetic study. Journal of Chromatography B-Analytical Technologies in the Biomedical and Life Sciences 1007:30-42 doi:10.1016/j.jchromb.2015.10.013

Corcoran GB, Racz WJ, Smith CV, Mitchell JR (1985) Effects of n-acetylcysteine on acetaminophen covalent binding and hepatic-necrosis in mice. Journal of Pharmacology and Experimental Therapeutics 232(3):864-872

Corcoran GB, Wong BK (1986) Role of glutathione in prevention of acetaminophen-induced hepatotoxicity by n-acetyl-l-cysteine invivo - studies with n-acetyl-d-cysteine in mice. Journal of Pharmacology and Experimental Therapeutics 238(1):54-61

Court MH, Duan SX, Von Moltke LL, et al. (2001) Interindividual variability in acetaminophen glucuronidation by human liver microsomes: Identification of relevant acetaminophen UDP-glucuronosyltransferase isoforms. Journal of Pharmacology and Experimental Therapeutics 299(3):998-1006

Court MH, Greenblatt DJ (2000) Molecular genetic basis for deficient acetaminophen glucuronidation by cats: UGT1A6 is a pseudogene, and evidence for reduced diversity of expressed hepatic UGT1A isoforms. Pharmacogenetics 10(4):355-369 doi:10.1097/00008571-200006000-00009

Court MH, Zhu ZH, Masse G, et al. (2017) Race, Gender, and Genetic Polymorphism Contribute to Variability in Acetaminophen Pharmacokinetics, Metabolism, and Protein-Adduct Concentrations in Healthy African-American and European-American Volunteers. Journal of Pharmacology and Experimental Therapeutics 362(3):431-440 doi:10.1124/jpet.117.242107

Critchley J, Nimmo GR, Gregson CA, Woolhouse NM, Prescott LF (1986) Inter-subject and ethnic-differences in paracetamol metabolism. British Journal of Clinical Pharmacology 22(6):649-657 doi:10.1111/j.1365-2125.1986.tb02953.x

Croal BL, Glen ACA, Kelly CJG, Logan RW (1998) Transient 5-oxoprolinuria (pyroglutamic aciduria) with systemic acidosis in an adult receiving antibiotic therapy. Clinical Chemistry 44(2):336-340

Dabos KJ, Whalen HR, Newsome PN, et al. (2011) Impaired gluconeogenesis in a porcine model of paracetamol induced acute liver failure. World Journal of Gastroenterology 17(11):1457-1461 doi:10.3748/wjg.v17.i11.1457

Dahlin DC, Miwa GT, Lu AYH, Nelson SD (1984) N-acetyl-para-benzoquinone imine - a cytochrome-p-450-mediated oxidation-product of acetaminophen. Proceedings of the National Academy of Sciences of the United States of America-Biological Sciences 81(5):1327-1331 doi:10.1073/pnas.81.5.1327

Dalton TP, Dieter MZ, Yang Y, Shertzer HG, Nebert DW (2000) Knockout of the mouse glutamate cysteine ligase catalytic subunit (Gclc) gene: Embryonic lethal when homozygous, and proposed model for moderate glutathione deficiency when heterozygous. Biochemical and Biophysical Research Communications 279(2):324-329 doi:10.1006/bbrc.2000.3930

Das J, Ghosh J, Manna P, Sil PC (2010) Acetaminophen induced acute liver failure via oxidative stress and JNK activation: Protective role of taurine by the suppression of cytochrome P450 2E1. Free Radical Research 44(3):340-355 doi:10.3109/10715760903513017

de Lima Marson FA, Bertuzzo CS, Ribeiro AF, Ribeiro JD (2014) Polymorphisms in the glutathione pathway modulate cystic fibrosis severity: a cross-sectional study. Bmc Medical Genetics 15 doi:10.1186/1471-2350-15-27

Dear JW, Clarke JI, Francis B, et al. (2018) Risk stratification after paracetamol overdose using mechanistic biomarkers: results from two prospective cohort studies. Lancet Gastroenterology & Hepatology 3(2):104-113 doi:10.1016/s2468-1253(17)30266-2

Dettmer K, Aronov PA, Hammock BD (2007) Mass spectrometry-based metabolomics. Mass Spectrometry Reviews 26(1):51-78 doi:10.1002/mas.20108

Di Girolamo A, O'Neill WM, Wainer IW (1998) A validated method for the determination of paracetamol and its glucuronide and sulphate metabolites in the urine of HIV+/AIDS patients using wavelength-switching UV detection. Journal of Pharmaceutical and Biomedical Analysis 17(6-7):1191-1197 doi:10.1016/s0731-7085(98)00084-3

Dieterle F, Ross A, Schlotterbeck G, Senn H (2006) Probabilistic quotient normalization as robust method to account for dilution of complex biological mixtures. Application in H-1 NMR metabonomics. Analytical Chemistry 78(13):4281-4290 doi:10.1021/ac051632c

Dona AC, Jimenez B, Schafer H, et al. (2014) Precision High-Throughput Proton NMR Spectroscopy of Human Urine, Serum, and Plasma for Large-Scale Metabolic Phenotyping. Analytical Chemistry 86(19):9887-9894 doi:10.1021/ac5025039

Du K, Williams CD, McGill MR, Jaeschke H (2014) Lower susceptibility of female mice to acetaminophen hepatotoxicity: Role of mitochondrial glutathione, oxidant stress and c-jun N-terminal kinase. Toxicology and Applied Pharmacology 281(1):58-66 doi:10.1016/j.taap.2014.09.002

E. Dominy J, Jr., Simmons CR, Hirschberger LL, Hwang J, Coloso RM, Stipanuk MH (2007) Discovery and characterization of a second mammalian thiol dioxygenase, cysteamine dioxygenase. Journal of Biological Chemistry 282(35):25189-25198 doi:10.1074/jbc.M703089200

Eckstein JA, Ammerman GM, Reveles JM, Ackermann BL (2008) Analysis of glutamine, glutamate, pyroglutamate, and GABA in cerebrospinal fluid using ion pairing HPLC with positive electrospray LC/MS/MS. Journal of Neuroscience Methods 171(2):190-196 doi:10.1016/j.jneumeth.2008.02.019

Eksi YE, Karaali ZE, Incekara K, Ergen HA (2014) MYELOPEROXIDASE AND GLUTAMATE-CYSTEINE LIGASE POLYMORPHISMS IN TYPE 2 DIABETES MELLITUS: A PRELIMINARY STUDY. Journal of Medical Biochemistry 33(2):156-161 doi:10.2478/jomb-2013-0022

Eriksson S, Prigge JR, Talago EA, Arner ESJ, Schmidt EE (2015) Dietary methionine can sustain cytosolic redox homeostasis in the mouse liver. Nature communications 6:6479-6479 doi:10.1038/ncomms7479

FDA (2018) Bioanalytical Method Validation Guidance for Industry. doi:https://www.fda.gov/downloads/drugs/guidances/ucm070107.pdf

Fisher MB, VandenBranden M, Findlay K, et al. (2000) Tissue distribution and interindividual variation in human UDP-glucuronosyltransferase activity: relationship between UGT1A1 promoter genotype and variability in a liver bank. Pharmacogenetics 10(8):727-739 doi:10.1097/00008571-200011000-00007

Flint RB, Mian P, van der Nagel B, Slijkhuis N, Koch BCP (2017) Quantification of Acetaminophen and Its Metabolites in Plasma Using UHPLC -MS: Doors Open to Therapeutic Drug Monitoring in Special Patient Populations. Therapeutic Drug Monitoring 39(2):164-171 doi:10.1097/ftd.0000000000000379

Forte AJ, Wilson JM, Slattery JT, Nelson SD (1984) The formation and toxicity of catechol metabolites of acetaminophen in mice. Drug Metabolism and Disposition 12(4):484-491

Fowler LM, Foster JR, Lock EA (1993) Effect of ascorbic-acid, acivicin and probenecid on the nephrotoxicity of 4-aminophenol in the fischer-344 rat. Archives of Toxicology 67(9):613-621 doi:10.1007/bf01974068
Fowler LM, Foster JR, Lock EA (1994) Nephrotoxicity of 4-amino-3-s-glutathionylphenol and its modulation by metabolism or transport inhibitors. Archives of Toxicology 68(1):15-23 doi:10.1007/bf03035706
Fowler LM, Moore RB, Foster JR, Lock EA (1991) NEPHROTOXICITY OF 4-AMINOPHENOL GLUTATHIONE CONJUGATE. Human & Experimental Toxicology 10(6):451-459 doi:10.1177/096032719101000615
Furey A, Moriarty M, Bane V, Kinsella B, Lehane M (2013) Ion suppression; A critical review on causes, evaluation, prevention and applications. Talanta 115:104-122 doi:10.1016/j.talanta.2013.03.048
Gama MR, Silva RGD, Collins CH, Bottoli CBG (2012) Hydrophilic interaction chromatography. Trac-Trends in Analytical Chemistry 37:48-60 doi:10.1016/j.trac.2012.03.009
Garcia-Gimenez JL, Roma-Mateo C, Perez-Machado G, Peiro-Chova L, Pallardo FV (2017) Role of glutathione in the regulation of epigenetic mechanisms in disease. Free Radical Biology and Medicine 112:36-48 doi:10.1016/j.freeradbiomed.2017.07.008
Gartland KPR, Eason CT, Bonner FW, Nicholson JK (1990) Effects of biliary cannulation and buthionine sulfoximine pretreatment on the nephrotoxicity of para-aminophenol in the fischer-344 rat. Archives of Toxicology 64(1):14-25 doi:10.1007/bf01973371
Geenen S, du Preez FB, Reed M, et al. (2012) A mathematical modelling approach to assessing the reliability of biomarkers of glutathione metabolism. European Journal of Pharmaceutical Sciences 46(4):233-243 doi:10.1016/j.ejps.2011.08.017
Geenen S, du Preez FB, Snoep JL, et al. (2013) Glutathione metabolism modeling: A mechanism for liver drug-robustness and a new biomarker strategy. Biochimica Et Biophysica Acta-General Subjects 1830(10):4943-4959 doi:10.1016/j.bbagen.2013.04.014
Geenen S, Guallar-Hoyas C, Michopoulos F, et al. (2011a) HPLC-MS/MS methods for the quantitative analysis of 5-oxoproline (pyroglutamate) in rat plasma and hepatic cell line culture medium. Journal of Pharmaceutical and Biomedical Analysis 56(3):655-663 doi:10.1016/j.jpba.2011.06.001
Geenen S, Michopoulos F, Kenna JG, Kolaja KL, Westerhoff HV, Wilson I (2011b) HPLC-MS/MS methods for the quantitative analysis of ophthalmic acid in rodent plasma and hepatic cell line culture medium. Journal of Pharmaceutical and Biomedical Analysis 54(5):1128-1135 doi:10.1016/j.jpba.2010.11.038
Ghauri FYK, McLean AEM, Beales D, Wilson ID, Nicholson JK (1993) Induction of 5-oxoprolinuria in the rat following chronic feeding with n-acetyl 4-aminophenol (paracetamol). Biochemical Pharmacology 46(5):953-957 doi:10.1016/0006-2952(93)90506-r
Giannini EG, Testa R, Savarino V (2005) Liver enzyme alteration: a guide for clinicians. Canadian Medical Association Journal 172(3):367-379 doi:10.1503/cmaj.1040752
Gibson JD, Pumford NR, Samokyszyn VM, Hinson JA (1996) Mechanism of acetaminophen-induced hepatotoxicity: Covalent binding versus oxidative stress. Chemical Research in Toxicology 9(3):580-585 doi:10.1021/tx950153d
Gicquel T, Aubert J, Lepage S, Fromenty B, Morel I (2013) Quantitative Analysis of Acetaminophen and its Primary Metabolites in Small Plasma Volumes by Liquid ChromatographyTandem Mass Spectrometry. Journal of Analytical Toxicology 37(2):110-116 doi:10.1093/jat/bks139
Gil A, van der Pol A, van der Meer P, Bischoff R (2018) LC-MS analysis of key components of the glutathione cycle in tissues and body fluids from mice with myocardial infarction. Journal of Pharmaceutical and Biomedical Analysis 160:289-296 doi:10.1016/j.jpba.2018.08.001
Gosselin S, Hoffman RS, Juurlink DN, Whyte I, Yarema M, Caro J (2013) Treating acetaminophen overdose: thresholds, costs and uncertainties. Clinical Toxicology 51(3):130-133 doi:10.3109/15563650.2013.775292
Grant I (2015) PhD Thesis. A UHPLC -MS Based Exploration of the Xenobiotic and Endogenous Metabolic Phenotypes of Pre-Clinical Models of Hepatotoxicity.
Gray N, Zia R, King A, et al. (2017) High-Speed Quantitative UHPLC -MS Analysis of Multiple Amines in Human Plasma and Serum via Precolumn Derivatization with 6-Aminoquinolyl-N-hydroxysuccinimidyl Carbamate: Application to Acetaminophen-Induced Liver Failure. Analytical Chemistry 89(4):2478-2487 doi:10.1021/acs.analchem.6b04623

Griffith OW, Meister A (1979) Glutathione - interorgan translocation, turnover, and metabolism. Proceedings of the National Academy of Sciences of the United States of America 76(11):5606-5610 doi:10.1073/pnas.76.11.5606
Grillo MA, Colombatto S (2008) S-adenosylmethionine and its products. Amino Acids 34(2):187-193 doi:10.1007/s00726-007-0500-9
Guan XM, Hoffman B, Dwivedi C, Matthees DP (2003) A simultaneous liquid chromatography/mass spectrometric assay of glutathione, cysteine, homocysteine and their disulfides in biological samples. Journal of Pharmaceutical and Biomedical Analysis 31(2):251-261 doi:10.1016/s0731-7085(02)00594-0
Hagiya Y, Kamata S, Mitsuoka S, et al. (2015) Hemizygosity of transsulfuration genes confers increased vulnerability against acetaminophen-induced hepatotoxicity in mice. Toxicology and Applied Pharmacology 282(2):195-206 doi:10.1016/j.taap.2014.11.015
Hammermeister DE, Serrano J, Schmieder P, Kuehl DW (2000) Characterization of dansylated glutathione, glutathione disulfide, cysteine and cystine by narrow bore liquid chromatography/electrospray ionization mass spectrometry. Rapid Communications in Mass Spectrometry 14(6):503-508 doi:10.1002/(sici)1097-0231(20000331)14:6<503::aid-rcm901>3.0.co;2-9
Harrill AH, Ross PK, Gatti DM, Threadgill DW, Rusyn I (2009) Population-Based Discovery of Toxicogenomics Biomarkers for Hepatotoxicity Using a Laboratory Strain Diversity Panel. Toxicological Sciences 110(1):235-243 doi:10.1093/toxsci/kfp096
Harrison JH, Jollow DJ (1987) Contribution of aniline metabolites to aniline-induced methemoglobinemia. Molecular Pharmacology 32(3):423-431
Hayes KC, Sturman JA (1981) TAURINE IN METABOLISM. Annual Review of Nutrition 1:401-425 doi:10.1146/annurev.nu.01.070181.002153
He GL, Feng L, Cai L, et al. (2017) Artificial liver support in pigs with acetaminophen-induced acute liver failure. World Journal of Gastroenterology 23(18):3262-3268 doi:10.3748/wjg.v23.i18.3262
Heard KJ, Green JL, James LP, et al. (2011) Acetaminophen-cysteine adducts during therapeutic dosing and following overdose. Bmc Gastroenterology 11 doi:10.1186/1471-230x-11-20
Helke KL, Nelson KN, Sargeant AM, et al. (2016) Pigs in Toxicology: Breed Differences in Metabolism and Background Findings. Toxicologic Pathology 44(4):575-590 doi:10.1177/0192623316639389
Hennebruns D, Artwohl J, Broelsch C, Kremer B (1988) Acetaminophen-induced acute hepatic-failure in pigs - controversial results to other animal-models. Research in Experimental Medicine 188(6):463-472 doi:10.1007/bf01852004
Henry J, Volans G (1984) ABC of poisoning - analgesics II. paracetamol. British Medical Journal 289(6449):907-908 doi:10.1136/bmj.289.6449.907
Hewavitharana AK, Lee S, Dawson PA, Markovich D, Shaw PN (2008) Development of an HPLC-MS/MS method for the selective determination of paracetamol metabolites in mouse urine. Analytical Biochemistry 374(1):106-111 doi:10.1016/j.ab.2007.11.011
Hlozek T, Krizek T, Tuma P, Bursova M, Coufal P, Cabala R (2017) Quantification of paracetamol and 5-oxoproline in serum by capillary electrophoresis: Implication for clinical toxicology. Journal of Pharmaceutical and Biomedical Analysis 145:616-620 doi:10.1016/j.jpba.2017.07.024
Hogestatt ED, Jonsson BAG, Ermund A, et al. (2005) Conversion of acetaminophen to the bioactive N-acylphenolamine AM404 via fatty acid amide hydrolase-dependent arachidonic acid conjugation in the nervous system. Journal of Biological Chemistry 280(36):31405-31412 doi:10.1074/jbc.M501489200
Huang Y, Louie A, Yang QY, et al. (2013) A simple LC-MS/MS method for determination of kynurenine and tryptophan concentrations in human plasma from HIV-infected patients (vol 5, pg 1397, 2013). Bioanalysis 5(12):1602-1602
Huang ZZ, Chen CJ, Zeng ZH, et al. (2001) Mechanism and significance of increased glutathione level in human hepatocellular carcinoma and liver regeneration. Faseb Journal 15(1):19-21 doi:10.1096/fj.00-0445fje

Ito S, Tsukada K (2002) Matrix effect and correction by standard addition in quantitative liquid chromatographic-mass spectrometric analysis of diarrhetic shellfish poisoning toxins. Journal of Chromatography A 943(1):39-46 doi:10.1016/s0021-9673(01)01429-7
Jaeschke H, McGill MR (2015) Cytochrome P450-derived versus mitochondrial oxidant stress in acetaminophen hepatotoxicity. Toxicology Letters 235(3):216-217 doi:10.1016/j.toxlet.2015.04.002
James LP, Mayeux PR, Hinson JA (2003) Acetaminophen-induced hepatotoxicity. Drug Metabolism and Disposition 31(12):1499-1506 doi:10.1124/dmd.31.12.1499
Jemnitz K, Veres Z, Monostory K, Kobori L, Vereczkey L (2008) Interspecies differences in acetaminophen sensitivity of human, rat, and mouse primary hepatocytes. Toxicology in Vitro 22(4):961-967 doi:10.1016/j.tiv.2008.02.001
Jensen LS, Valentine J, Milne RW, Evans AM (2004) The quantification of paracetamol, paracetamol glucuronide and paracetamol sulphate in plasma and urine using a single high-performance liquid chromatography assay. Journal of Pharmaceutical and Biomedical Analysis 34(3):585-593 doi:10.1016/s0731-7085(03)00573-9
Jones R, Marschmann M, Keller M, et al. (2016) Shedding light on minipig drug metabolism - elevated amide hydrolysis in vitro. Xenobiotica 46(6):483-494 doi:10.3109/00498254.2015.1089452
Jung YS, Kim SJ, Kwon DY, Jun DS, Kim YC (2013) Significance of alterations in the metabolomics of sulfur-containing amino acids during liver regeneration. Biochimie 95(8):1605-1610 doi:10.1016/j.biochi.2013.04.015
Jung YS, Kim SJ, Kwon DY, Kim YC (2008) Comparison of the effects of buthioninesulfoximine and phorone on the metabolism of sulfur-containing amino acids in rat liver. Biochemical and Biophysical Research Communications 368(4):913-918 doi:10.1016/j.bbrc.2008.02.005
Jurkowska H, Stipanuk MH, Hirschberger LL, Roman HB (2015) Propargylglycine inhibits hypotaurine/taurine synthesis and elevates cystathionine and homocysteine concentrations in primary mouse hepatocytes. Amino Acids 47(6):1215-1223 doi:10.1007/s00726-015-1948-7
Karmen A, Wroblewski F, LaDue JS (1955) Transaminase activity in human blood. Journal of Clinical Investigation 34(1)
Katakami N, Kaneto H, Matsuoka T-a, et al. (2014) Accumulation of oxidative stress-related gene polymorphisms and the risk of coronary heart disease events in patients with type 2 diabetes - An 8-year prospective study. Atherosclerosis 235(2):408-414 doi:10.1016/j.atherosclerosis.2014.05.936
Kaur G, Leslie EM, Tillman H, et al. (2015) Detection of Ophthalmic Acid in Serum from Acetaminophen-Induced Acute Liver Failure Patients Is More Frequent in Non-Survivors. Plos One 10(9) doi:10.1371/journal.pone.0139299
Kawabata K-i, Kobayashi T, Fujioka D, et al. (2011) Association of Polymorphism in Glutamate-Cysteine Ligase Modifier Subunit Gene with Idiopathic Dilated Cardiomyopathy. Circulation 124(21)
Kebarle P, Verkerk UH (2009) Electrospray: From ions in solution to ions in the gas phase, what we know now. Mass Spectrometry Reviews 28(6):898-917 doi:10.1002/mas.20247
Kensler TW, Wakabayash N, Biswal S (2007) Cell survival responses to environmental stresses via the Keap1-Nrf2-ARE pathway. Annual Review of Pharmacology and Toxicology 47:89-116 doi:10.1146/annurev.pharmtox.46.120604.141046
Kerai MDJ, Waterfield CJ, Kenyon SH, Asker DS, Timbrell JA (1998) Taurine: Protective properties against ethanol-induced hepatic steatosis and lipid peroxidation during chronic ethanol consumption in rats. Amino Acids 15(1-2):53-76 doi:10.1007/bf01345280
Kobayashi S, Lee J, Takao T, Fujii J (2017) Increased ophthalmic acid production is supported by amino acid catabolism under fasting conditions in mice. Biochemical and Biophysical Research Communications 491(3):649-655 doi:10.1016/j.bbrc.2017.07.149
Kotb M, Geller AM (1993) Methionine adenosyltransferase - structure and function. Pharmacology & Therapeutics 59(2):125-143 doi:10.1016/0163-7258(93)90042-c
Kyriakides M (2016) Comparative metabonomic analysis of hepatotoxicity induced by acetaminophen and its less toxic meta-isomer. Archives of Toxicology doi:DOI 10.1007/s00204-015-1655-x

Lafaye A, Labarre J, Tabet JC, Ezan E, Junot C (2005) Liquid chromatography - Mass spectrometry and N-15 metabolic labeling for quantitative metabolic profiling. Analytical Chemistry 77(7):2026-2033 doi:10.1021/ac048657g

Lambert IH, Kristensen DM, Holm JB, Mortensen OH (2015) Physiological role of taurine - from organism to organelle. Acta Physiologica 213(1):191-212 doi:10.1111/apha.12365

Lammers LA, Achterbergh R, Pistorius MCM, Romijn JA, Mathot RAA (2017) Quantitative Method for Simultaneous Analysis of Acetaminophen and 6 Metabolites. Therapeutic Drug Monitoring 39(2):172-179 doi:10.1097/ftd.0000000000000373

Lauterburg BH, Corcoran GB, Mitchell JR (1983) Mechanism of action of n-acetylcysteine in the protection against the hepatotoxicity of acetaminophen in rats in-vivo. Journal of Clinical Investigation 71(4):980-991 doi:10.1172/jci110853

Lee HS, Ti TY, Koh YK, Prescott LF (1992) Paracetamol elimination in chinese and indians in singapore. European Journal of Clinical Pharmacology 43(1):81-84 doi:10.1007/bf02280759

Lee KCL, Baker LA, Stanzani G, et al. (2015) Extracorporeal liver assist device to exchange albumin and remove endotoxin in acute liver failure: Results of a pivotal pre-clinical study. Journal of Hepatology 63(3):634-642 doi:10.1016/j.jhep.2015.04.020

Lee KCL, Jimenez CP, Alibhai H, et al. (2013) A reproducible, clinically relevant, intensively managed, pig model of acute liver failure for testing of therapies aimed to prolong survival. Liver International 33(4):544-551 doi:10.1111/liv.12042

Lee SST, Buters JTM, Pineau T, FernandezSalguero P, Gonzalez FJ (1996) Role of CYP2E1 in the hepatotoxicity of acetaminophen. Journal of Biological Chemistry 271(20):12063-12067 doi:10.1074/jbc.271.20.12063

Lee WM (2012a) Acute Liver Failure. Seminars in Respiratory and Critical Care Medicine 33(1):36-45 doi:10.1055/s-0032-1301733

Lee WM (2012b) Recent developments in acute liver failure. Best Practice & Research in Clinical Gastroenterology 26(1):3-16 doi:10.1016/j.bpg.2012.01.014

Linden JC, Lawhead CL (1975) LIQUID-CHROMATOGRAPHY OF SACCHARIDES. Journal of Chromatography 105(1):125-133 doi:10.1016/s0021-9673(01)81096-7

Liss DB, Paden MS, Schwarz ES, Mullins ME (2013) What is the clinical significance of 5-oxoproline (pyroglutamic acid) in high anion gap metabolic acidosis following paracetamol (acetaminophen) exposure? Clinical Toxicology 51(9):817-827 doi:10.3109/15563650.2013.844822

Liu L, Klaassen CD (1996) Different mechanism of saturation of acetaminophen sulfate conjugation in mice and rats. Toxicology and Applied Pharmacology 139(1):128-134 doi:10.1006/taap.1996.0151

Lu SC (2009) Regulation of glutathione synthesis. Molecular Aspects of Medicine 30(1-2):42-59 doi:10.1016/j.mam.2008.05.005

Lu SC (2013) Glutathione synthesis. Biochimica Et Biophysica Acta-General Subjects 1830(5):3143-3153 doi:10.1016/j.bbagen.2012.09.008

Mackenzie PI, Bock KW, Burchell B, et al. (2005) Nomenclature update for the mammalian UDP glycosyltransferase (UGT) gene superfamily. Pharmacogenetics and Genomics 15(10):677-685 doi:10.1097/01.fpc.0000173483.13689.56

Maher S, Jjunju FPM, Taylor S (2015) Colloquium: 100 years of mass spectrometry: Perspectives and future trends. Reviews of Modern Physics 87(1):113-135 doi:10.1103/RevModPhys.87.113

Makin AJ, Wendon J, Williams R (1995) A 7-year experience of severe acetaminophen-induced hepatotoxicity (1987-1993). Gastroenterology 109(6):1907-1916 doi:10.1016/0016-5085(95)90758-0

Mason CL, Leedale J, Tasoulis S, Jarman I, Antoine DJ, Webb SD (2018) Systems Toxicology Approach to Identifying Paracetamol Overdose. Cpt-Pharmacometrics & Systems Pharmacology 7(6):394-403 doi:10.1002/psp4.12298

Mast C, Dardevet D, Papet I (2018) Impact of medication on protein and amino acid metabolism in the elderly: the sulfur amino acid and paracetamol case. Nutrition Research Reviews 31(2):179-192 doi:10.1017/s0954422418000021

Masubuchi Y, Nakayama J, Watanabe Y (2011) Sex difference in susceptibility to acetaminophen hepatotoxicity is reversed by buthionine sulfoximine. Toxicology 287(1-3):54-60 doi:10.1016/j.tox.2011.05.018
Matuszewski BK, Constanzer ML, Chavez-Eng CM (2003) Strategies for the assessment of matrix effect in quantitative bioanalytical methods based on HPLC-MS/MS. Analytical Chemistry 75(13):3019-3030 doi:10.1021/ac020361s
Mazaleuskaya LL, Sangkuhl K, Thorn CF, FitzGerald GA, Altman RB, Klein TE (2015) PharmGKB summary: pathways of acetaminophen metabolism at the therapeutic versus toxic doses. Pharmacogenetics and Genomics 25(8):416-426 doi:10.1097/fpc.0000000000000150
McConkey SE, Grant DM, Cribb AE (2009) The role of para-aminophenol in acetaminophen-induced methemoglobinemia in dogs and cats. Journal of Veterinary Pharmacology and Therapeutics 32(6):585-595 doi:10.1111/j.1365-2885.2009.01080.x
McConnachie LA, Mohar I, Hudson FN, et al. (2007) Glutamate cysteine ligase modifier subunit deficiency and gender as determinants of acetaminophen-induced hepatotoxicity in mice. Toxicological Sciences 99(2):628-636 doi:10.1093/toxsci/kfm165
McGill MR (2016) The past and present of serum aminotransferases and the future of liver injury biomarkers. Excli Journal 15:817-828 doi:10.17179/excli2016-800
McGill MR, Jaeschke H (2013) Metabolism and Disposition of Acetaminophen: Recent Advances in Relation to Hepatotoxicity and Diagnosis. Pharmaceutical Research 30(9):2174-2187 doi:10.1007/s11095-013-1007-6
McGill MR, Jaeschke H (2014) Mechanistic biomarkers in acetaminophen-induced hepatotoxicity and acute liver failure: from preclinical models to patients. Expert Opinion on Drug Metabolism & Toxicology 10(7):1005-1017 doi:10.1517/17425255.2014.920823
McGill MR, Sharpe MR, Williams CD, Taha M, Curry SC, Jaeschke H (2012a) The mechanism underlying acetaminophen-induced hepatotoxicity in humans and mice involves mitochondrial damage and nuclear DNA fragmentation. Journal of Clinical Investigation 122(4):1574-1583 doi:10.1172/jci59755
McGill MR, Williams CD, Xie Y, Ramachandran A, Jaeschke H (2012b) Acetaminophen-induced liver injury in rats and mice: Comparison of protein adducts, mitochondrial dysfunction, and oxidative stress in the mechanism of toxicity. Toxicology and Applied Pharmacology 264(3):387-394 doi:10.1016/j.taap.2012.08.015
McKay RT (2011) How the 1D-NOESY Suppresses Solvent Signal in Metabonomics NMR Spectroscopy: An Examination of the Pulse Sequence Components and Evolution. Concepts in Magnetic Resonance Part A 38A(5):197-220 doi:10.1002/cmr.a.20223
McLean AEM, Armstrong GR, Beales D (1989) Effect of d-methionine or l-methionine and cysteine on the growth inhibitory effects of feeding 1-percent paracetamol to rats. Biochemical Pharmacology 38(2):347-352 doi:10.1016/0006-2952(89)90048-8
Meiboom S, Gill D (1958) Modified Spin Echo Method for Measuring Nuclear Relaxation Times. The Review of Scientific Instruments 29(8)
Meister A (1991) glutathione deficiency produced by inhibition of its synthesis, and its reversal - applications in research and therapy. Pharmacology & Therapeutics 51(2):155-194 doi:10.1016/0163-7258(91)90076-x
Merrifield CA, Lewis M, Claus SP, et al. (2011) A metabolic system-wide characterisation of the pig: a model for human physiology. Molecular Biosystems 7(9):2577-2588 doi:10.1039/c1mb05023k
Mitchell JR, Jollow DJ, Potter WZ, Davis DC, Gillette JR, Brodie BB (1973a) Acetaminophen-induced hepatic necrosis .1. Role of drug-metabolism. Journal of Pharmacology and Experimental Therapeutics 187(1):185-194
Mitchell JR, Jollow DJ, Potter WZ, Gillette JR, Brodie BB (1973b) Acetaminophen-induced hepatic necrosis .4. Protective role of glutathione. Journal of Pharmacology and Experimental Therapeutics 187(1):211-217
Myher JJ, Kuksis A, Pind S (1989) Molecular-species of glycerophospholipids and sphingomyelins of human-plasma - comparison to red blood-cells. Lipids 24(5):408-418 doi:10.1007/bf02535148

Nakamura S, Sugiyama S, Fujioka D, Kawabata K, Ogawa H, Kugiyama K (2003) Polymorphism in glutamate-cysteine ligase modifier subunit gene is associated with impairment of nitric oxide-mediated coronary vasomotor function. Circulation 108(12):1425-1427 doi:10.1161/01.cir.0000091255.63645.98

New LS, Chan ECY (2008) Evaluation of BEH C-18, BEH HILIC, and HSS T3 (C-18) column chemistries for the UHPLC -MS-MS analysis of glutathione, glutathione disulfide, and ophthalmic acid in mouse liver and human plasma. Journal of Chromatographic Science 46(3):209-214 doi:10.1093/chromsci/46.3.209

Newsome PN, Henderson NC, Nelson LJ, et al. (2010) Development of an invasively monitored porcine model of acetaminophen-induced acute liver failure. Bmc Gastroenterology 10 doi:10.1186/1471-230x-10-34

Newton JF, Pasino DA, Hook JB (1985) Acetaminophen nephrotoxicity in the rat - quantitation of renal metabolic-activation invivo. Toxicology and Applied Pharmacology 78(1):39-46 doi:10.1016/0041-008x(85)90302-3

Nicholls AW, Caddick S, Wilson ID, Farrant RD, Lindon JC, Nicholson JK (1995) HIGH-RESOLUTION NMR SPECTROSCOPIC STUDIES ON THE METABOLISM AND FUTILE DEACETYLATION OF 4-HYDROXYACETANILIDE (PARACETAMOL) IN THE RAT. Biochemical Pharmacology 49(8):1155-1164 doi:10.1016/0006-2952(95)98513-9

Nicholls AW, Farrant RD, Shockcor JP, et al. (1997) NMR and HPLC-NMR spectroscopic studies of futile deacetylation in paracetamol metabolites in rat and man. Journal of Pharmaceutical and Biomedical Analysis 15(7):901-910 doi:10.1016/s0731-7085(96)01950-4

Nicholson JK, Connelly J, Lindon JC, Holmes E (2002) Metabonomics: a platform for studying drug toxicity and gene function. Nature Reviews Drug Discovery 1(2):153-161 doi:10.1038/nrd728

Nicholson JK, Foxall PJD, Spraul M, Farrant RD, Lindon JC (1995) 750-mhz h-1 and h-1-c-13 nmr-spectroscopy of human blood-plasma. Analytical Chemistry 67(5):793-811 doi:10.1021/ac00101a004

Ostapowicz G, Fontana RJ, Schiodt FV, et al. (2002) Results of a prospective study of acute liver failure at 17 tertiary care centers in the United States. Annals of Internal Medicine 137(12):947-954 doi:10.7326/0003-4819-137-12-200212170-00007

Patten CJ, Thomas PE, Guy RL, et al. (1993) Cytochrome-p450 enzymes involved in acetaminophen activation by rat and human liver-microsomes and their kinetics. Chemical Research in Toxicology 6(4):511-518 doi:10.1021/tx00034a019

Pegg AE (2009) Mammalian Polyamine Metabolism and Function. Iubmb Life 61(9):880-894 doi:10.1002/iub.230

Periat A, Kohler I, Thomas A, et al. (2016) Systematic evaluation of matrix effects in hydrophilic interaction chromatography versus reversed phase liquid chromatography coupled to mass spectrometry. Journal of Chromatography A 1439:42-53 doi:10.1016/j.chroma.2015.09.035

Perkins JD (2006) Acetaminophen sets records in the United States: Number 1 analgesic and number 1 cause of acute liver failure - Acetaminophen-induced acute liver failure: Results of a United States multicenter, prospective study. Larson AM, Polson J, Fontana RJ, Davern TJ, Lalani E, Hynan LS, Reisch JS, Schiodt FV, Ostapowicz G, Shakil AO, Lee WW, Acute Liver Failure Study Group. Hepatology 2005;42 : 1364-1372. Liver Transplantation 12(4):682-683 doi:10.1002/lt.20735

Potter WZ, Davis DC, Mitchell JR, Jollow DJ, Gillette JR, Brodie BB (1973) Acetaminophen-induced hepatic necrosis .3. Cytochrome p-450-mediated covalent binding in-vitro. Journal of Pharmacology and Experimental Therapeutics 187(1):203-210

Prescott LF (1980) Kinetics and metabolism of paracetamol and phenacetin. British Journal of Clinical Pharmacology 10:S291-S298

Prescott LF, Ballantyne A, Park J, Adriaenssens P, Proudfoot AT (1977) Treatment of paracetamol (acetaminophen) poisoning with n-acetylcysteine. Lancet 2(8035):432-434

Prescott LF, Illingworth RN, Critchley J, Proudfoot AT (1980) Intravenous n-acetylcysteine - still the treatment of choice for paracetamol poisoning. British Medical Journal 280(6206):46-47 doi:10.1136/bmj.280.6206.46-b

Purohit V, Abdelmalek MF, Barve S, et al. (2007) Role of S-adenosylmethionine, folate, and betaine in the treatment of alcoholic liver disease: summary of a symposium. American Journal of Clinical Nutrition 86(1):14-24
Pushpakiran G, Mahalakshmi K, Anuradha CV (2004) Taurine restores ethanol-induced depletion of antioxidants and attenuates oxidative stress in rat tissues. Amino Acids 27(1):91-96 doi:10.1007/s00726-004-0066-8
Qu J, Chen W, Luo G, et al. (2002) Rapid determination of underivatized pyroglutamic acid, glutamic acid, glutamine and other relevant amino acids in fermentation media by LC-MS-MS. Analyst 127(1):66-69 doi:10.1039/b108422b
Queiros C, Salvador P, Ventura A, Lopes D (2017) Methemoglobinemia After Paracetamol Ingestion: A Case Report. Acta Medica Portuguesa 30(10):753-756 doi:10.20344/amp.8722
Raggi MA, Mandrioli R, Casamenti G, Musiani D, Marini M (1998) HPLC determination of glutathione and other thiols in human mononuclear blood cells. Biomedical Chromatography 12(5):262-266 doi:10.1002/(sici)1099-0801(199809/10)12:5<262::aid-bmc744>3.0.co;2-j
Rao KVR, Jayakumar AR, Norenberg MD (2012) Glutamine in the pathogenesis of acute hepatic encephalopathy. Neurochemistry International 61(4):575-580 doi:10.1016/j.neuint.2012.01.012
Rolleman EJ, Hoorn EJ, Didden P, Zietse R (2008) Guilty as charged: unmeasured urinary anions in a case of pyroglutamic acidosis. Netherlands Journal of Medicine 66(8):351-353
Roman HB, Hirschberger LL, Krijt J, Valli A, Kozich V, Stipanuk MH (2013) The Cysteine Dioxgenase Knockout Mouse: Altered Cysteine Metabolism in Nonhepatic Tissues Leads to Excess H2S/HS- Production and Evidence of Pancreatic and Lung Toxicity. Antioxidants & Redox Signaling 19(12):1321-1336 doi:10.1089/ars.2012.5010
Rosa FT, Freitas EC, Deminice R, Jordao AA, Marchini JS (2014) Oxidative stress and inflammation in obesity after taurine supplementation: a double-blind, placebo-controlled study. European Journal of Nutrition 53(3):823-830 doi:10.1007/s00394-013-0586-7
Rubin JB, Hameed B, Gottfried M, Lee WM, Sarkar M, Acute Liver Failure Study G (2018) Acetaminophen-induced Acute Liver Failure Is More Common and More Severe in Women. Clinical Gastroenterology and Hepatology 16(6):936-946 doi:10.1016/j.cgh.2017.11.042
Rumack BH, Peterson RC, Koch GG, Amara IA (1981) Acetaminophen overdose - 662 cases with evaluation of oral acetylcysteine treatment. Archives of Internal Medicine 141:380-385 doi:10.1001/archinte.141.3.380
Saito C, Zwingmann C, Jaeschke H (2010) Novel Mechanisms of Protection Against Acetaminophen Hepatotoxicity in Mice by Glutathione and N-Acetylcysteine. Hepatology 51(1):246-254 doi:10.1002/hep.2.3267
Sartorelli P, Paltrinieri S, Agnes F, Baglioni T (1996) Role of inosine in prevention of methaemoglobinaemia in the pig: In vitro studies. J Vet Med Ser A-Zentbl Vet Med Reihe A-Physiol Pathol Clin Med 43(8):489-493 doi:10.1111/j.1439-0442.1996.tb00479.x
Scaffidi P, Misteli T, Bianchi ME (2002) Release of chromatin protein HMGB1 by necrotic cells triggers inflammation. Nature 418(6894):191-195 doi:10.1038/nature00858
Soga T, Baran R, Suematsu M, et al. (2006) Differential metabolomics reveals ophthalmic acid as an oxidative stress biomarker indicating hepatic glutathione consumption. Journal of Biological Chemistry 281(24):16768-16776 doi:10.1074/jbc.M601876200
Stabler SP, Marcell PD, Podell ER, Allen RH (1987) Quantitation of total homocysteine, total cysteine, and methionine in normal serum and urine using capillary gas-chromatography mass-spectrometry. Analytical Biochemistry 162(1):185-196 doi:10.1016/0003-2697(87)90026-1
Stipanuk MH (2004) Sulfur amino acid metabolism: Pathways for production and removal of homocysteine and cysteine. Annual Review of Nutrition 24:539-577 doi:10.1146/annurev.nutr.24.012003.132418
Stipanuk MH, Ueki I (2011) Dealing with methionine/homocysteine sulfur: cysteine metabolism to taurine and inorganic sulfur. Journal of Inherited Metabolic Disease 34(1):17-32 doi:10.1007/s10545-009-9006-9

Suenderhauf C, Tuffin G, Lorentsen H, Grimm HP, Flament C, Parrott N (2014) Pharmacokinetics of Paracetamol in Gottingen Minipigs: In Vivo Studies and Modeling to Elucidate Physiological Determinants of Absorption. Pharmaceutical Research 31(10):2696-2707 doi:10.1007/s11095-014-1367-6

Tailor P, Raman T, Garganta CL, et al. (2005) Recurrent high anion gap metabolic acidosis secondary to 5-oxoproline (pyroglutamic acid). American Journal of Kidney Diseases 46(1):E4-E10 doi:10.1053/j.ajkd.2005.03.021

Tan QY, Zhu RH, Li HD, Wang F, Yan M, Dai LB (2012) Simultaneous quantitative determination of paracetamol and its glucuronide conjugate in human plasma and urine by liquid chromatography coupled to electrospray tandem mass spectrometry: Application to a clinical pharmacokinetic study. Journal of Chromatography B-Analytical Technologies in the Biomedical and Life Sciences 893:162-167 doi:10.1016/j.jchromb.2012.02.027

Tang DQ, Zou L, Yin XX, Ong CN (2016) HILIC-MS for metabolomics: An attractive and complementary approach to RPLC-MS. Mass Spectrometry Reviews 35(5):574-600 doi:10.1002/mas.21445

Tee LBG, Davies DS, Seddon CE, Boobis AR (1987) Species-differences in the hepatotoxicity of paracetamol are due to differences in the rate of conversion to its cytotoxic metabolite. Biochemical Pharmacology 36(7):1041-1052 doi:10.1016/0006-2952(87)90412-6

Theodoridis G, Gika HG, Wilson ID (2011) Mass spectrometry-based holistic analytical approaches for metabolite profiling in systems biology studies. Mass Spectrometry Reviews 30(5):884-906 doi:10.1002/mas.20306

Theodoridis GA, Gika HG, Want EJ, Wilson ID (2012) Liquid chromatography-mass spectrometry based global metabolite profiling: A review. Analytica Chimica Acta 711:7-16 doi:10.1016/j.aca.2011.09.042

Thiel C, Thiel K, Etspueler A, et al. (2011) A Reproducible Porcine Model of Acute Liver Failure Induced by Intrajejunal Acetaminophen Administration. European Surgical Research 46(3):118-126 doi:10.1159/000323411

Thorn HA, Yasin M, Dickinson PA, Lennernas H (2012) Extensive intestinal glucuronidation of raloxifene in vivo in pigs and impact for oral drug delivery. Xenobiotica 42(9):917-928 doi:10.3109/00498254.2012.683497

Thulin P, Nordahl G, Gry M, et al. (2014) Keratin-18 and microRNA-122 complement alanine aminotransferase as novel safety biomarkers for drug-induced liver injury in two human cohorts. Liver International 34(3):367-378 doi:10.1111/liv.12322

Thummel KE, Lee CA, Kunze KL, Nelson SD, Slattery JT (1993) Oxidation of acetaminophen to n-acetyl-p-aminobenzoquinone imine by human cyp3a4. Biochemical Pharmacology 45(8):1563-1569 doi:10.1016/0006-2952(93)90295-8

Trepanier LA, Cribb AE, Spielberg SP, Ray K (1998) Deficiency of cytosolic arylamine N-acetylation in the domestic cat and wild felids caused by the presence of a single NAT1-like gene. Pharmacogenetics 8(2):169-179 doi:10.1097/00008571-199804000-00009

Trepanier LA, Ray K, Winand NJ, Spielberg SP, Cribb AE (1997) Cytosolic arylamine N-acetyltransferase (NAT) deficiency in the dog and other canids due to an absence of NAT genes. Biochemical Pharmacology 54(1):73-80 doi:10.1016/s0006-2952(97)00140-8

Triantafyllou E, Pop OT, Possamai LA, et al. (2018) MerTK expressing hepatic macrophages promote the resolution of inflammation in acute liver failure. Gut 67(2):333-347 doi:10.1136/gutjnl-2016-313615

Ussher JR, Lopaschuk GD, Arduini A (2013) Gut microbiota metabolism of L-carnitine and cardiovascular risk. Atherosclerosis 231(2):456-461 doi:10.1016/j.atherosclerosis.2013.10.013

van de Merbel NC (2008) Quantitative determination of endogenous compounds in biological samples using chromatographic techniques. Trac-Trends in Analytical Chemistry 27(10):924-933 doi:10.1016/j.trac.2008.09.002

van den Berg RA, Hoefsloot HCJ, Westerhuis JA, Smilde AK, van der Werf MJ (2006) Centering, scaling, and transformations: improving the biological information content of metabolomics data. Bmc Genomics 7 doi:10.1186/1471-2164-7-142

Vermeulen NPE, Bessems JGM, Vandestraat R (1992) Molecular aspects of paracetamol-induced hepatotoxicity and its mechanism-based prevention. Drug Metabolism Reviews 24(3):367-407 doi:10.3109/03602539208996298
Vertzoni MV, Archontaki HA, Galanopoulou P (2003) Development and optimization of a reversed-phase high-performance liquid chromatographic method for the determination of acetaminophen and its major metabolites in rabbit plasma and urine after a toxic dose. Journal of Pharmaceutical and Biomedical Analysis 32(3):487-493 doi:10.1016/s0731-7085(03)00246-2
Veselkov KA, Lindon JC, Ebbels TMD, et al. (2009) Recursive Segment-Wise Peak Alignment of Biological H-1 NMR Spectra for Improved Metabolic Biomarker Recovery. Analytical Chemistry 81(1):56-66 doi:10.1021/ac8011544
Vliegenthart ADB, Antoine DJ, Dear JW (2015) Target biomarker profile for the clinical management of paracetamol overdose. British Journal of Clinical Pharmacology 80(3):351-362 doi:10.1111/bcp.12699
Vliegenthart ADB, Kimmitt RA, Seymour JH, et al. (2017) Circulating Acetaminophen Metabolites Are Toxicokinetic Biomarkers of Acute Liver Injury. Clinical Pharmacology & Therapeutics 101(4):531-540 doi:10.1002/cpt.541
Wallace HM, Fraser AV, Hughes A (2003) A perspective of polyamine metabolism. Biochemical Journal 376:1-14 doi:10.1042/bj20031327
Wang K, Zhang SL, Marzolf B, et al. (2009) Circulating microRNAs, potential biomarkers for drug-induced liver injury. Proceedings of the National Academy of Sciences of the United States of America 106(11):4402-4407 doi:10.1073/pnas.0813371106
Want EJ, Masson P, Michopoulos F, et al. (2013) Global metabolic profiling of animal and human tissues via UHPLC -MS. Nature Protocols 8(1):17-32 doi:10.1038/nprot.2012.135
Watanabe A, Fukami T, Takahashi S, et al. (2010) arylacetamide deacetylase is a determinant enzyme for the difference in hydrolase activities of phenacetin and acetaminophen. Drug Metabolism and Disposition 38(9):1532-1537 doi:10.1124/dmd.110.033720
Watanabe M, Osada J, Aratani Y, et al. (1995) MICE DEFICIENT IN CYSTATHIONINE BETA-SYNTHASE - ANIMAL-MODELS FOR MILD AND SEVERE HOMOCYST(E)INEMIA. Proceedings of the National Academy of Sciences of the United States of America 92(5):1585-1589 doi:10.1073/pnas.92.5.1585
Waters E, Wang JH, Redmond HP, Wu QD, Kay E, Bouchier-Hayes D (2001) Role of taurine in preventing acetaminophen-induced hepatic injury in the rat. American Journal of Physiology-Gastrointestinal and Liver Physiology 280(6):G1274-G1279
Watts RP, Brendel K, Luthra MG, Kim HD (1979) Inosine from liver as a possible energy-source for pig red blood-cells. Life Sciences 25(18):1577-1582 doi:10.1016/0024-3205(79)90440-5
Whitcomb DC, Block GD (1994) Association of acetaminophen hepatotoxicity with fasting and ethanol use. Jama-Journal of the American Medical Association 272(23):1845-1850 doi:10.1001/jama.272.23.1845
Wieckowska A, Zein NN, Yerian LM, Lopez AR, McCullough AJ, Feldstein AE (2006) In vivo assessment of liver cell apoptosis as a novel biomarker of disease severity in nonalcoholic fatty liver disease. Hepatology 44(1):27-33 doi:10.1002/hep.21223
Wilson ID, Nicholson JK, Castro-Perez J, et al. (2005) High resolution "Ultra performance" liquid chromatography coupled to oa-TOF mass spectrometry as a tool for differential metabolic pathway profiling in functional genomic studies. Journal of Proteome Research 4(2):591-598 doi:10.1021/pr049769r
Wyss M, Kaddurah-Daouk R (2000) Creatine and creatinine metabolism. Physiological Reviews 80(3):1107-1213
Yamazaki M, Miyake M, Sato H, et al. (2013) Perturbation of bile acid homeostasis is an early pathogenesis event of drug induced liver injury in rats. Toxicology and Applied Pharmacology 268(1):79-89 doi:10.1016/j.taap.2013.01.018

Yang A, Trajkovic D, Illanes O, Ramiro-Ibanez F (2007) Clinicopathological and tissue indicators of para-aminophenol nephrotoxicity in Sprague-Dawley rats. Toxicologic Pathology 35(4):521-532 doi:10.1080/01926230701338933

Yang H-T, Chien Y-W, Tsen J-H, Chang C-C, Chang J-H, Huang S-Y (2009) Taurine supplementation improves the utilization of sulfur-containing amino acids in rats continually administrated alcohol. Journal of Nutritional Biochemistry 20(2):132-139 doi:10.1016/j.jnutbio.2008.01.009

Yu H, Barrass N, Gales S, et al. (2015) Metabolism by conjugation appears to confer resistance to paracetamol (acetaminophen) hepatotoxicity in the cynomolgus monkey. Xenobiotica 45(3):270-277 doi:10.3109/00498254.2014.973000

Zaher H, Buters JTM, Ward JM, et al. (1998) Protection against acetaminophen toxicity in CYP1A2 and CYP2E1 double-null mice. Toxicology and Applied Pharmacology 152(1):193-199 doi:10.1006/taap.1998.8501

Zimmerman HJ (1968) The spectrum of hepatotoxicity. Perspect Biol Med 12(1)

Zwingmann C, Bilodeau M (2006) Metabolic insights into the hepatoprotective role of N-acetylcysteine in mouse liver. Hepatology 43(3):454-463 doi:10.1002/hep.21075